Understanding the Effects of Processing on the Properties of Perfluoroalkoxy (PFA)

Cassandra Natalie Zara TODD

Submitted for the Degree of

Master of Philosophy

Faculty of Engineering and Informatics

University of Bradford

2016

For my Grandparents, who have always believed in my potential

Abstract

Cassandra Natalie Zara TODD

Understanding the Effects of Processing on the Properties of Perfluoroalkoxy (PFA)

Keywords: Perfluoroalkoxy, Transfer Moulding, Processing, Fluoropolymers

The effect of processing on the properties of three transfer moulding grades of perfluoroalkoxy was investigated. There is anecdotal evidence to suggest exposure to high shear rates and residence time at processing temperature detrimentally affect the polymer, however there is a lack of information published in this area. This work set out to provide a better understanding of the material behaviour under various processing conditions.

A bespoke capillary rheometer was used to determine flow characteristics at various temperatures between 5-400s^{-1}. The materials were found to be shear thinning, with the virgin grades exhibiting Newtonian behaviour at low shear rates. The viscosity of the carbon black filled PFA was found to have a higher viscosity than the virgin materials, despite it having a higher Melt Flow Rate.

Spectroscopy was found to be unsuitable for investigation of polymer containing carbon black due to laser heating. However changes due to residence time at processing temperature in the virgin material could be detected using statistical analysis of Near Infrared spectra. Whether the mechanical properties of the virgin material changed following exposure to high shear rates or residence time varied on manufacturer, with Dyneon 6502TZ appearing to be more process stable than Chemours 350TJ. This information can be used to optimise the transfer moulding process, and assist in meeting the requirements of the Chemical Processing Industry for larger and more complex lined piping components.

Acknowledgements

This work was conducted as part of an Innovate UK Knowledge Transfer Partnership, and was financially supported by Innovate UK and CRP Ltd.

I would like to thank the following people for their help and contributions:

Dr Adrian Kelly and Dr Tim Gough for their advice and guidance throughout the project.

Nigel Price and David MacGregor of CRP Ltd for their support of the work and providing the opportunity for my professional development.

Glen Thompson and Ken Howell of The University of Bradford, and Dave Duncan of CRP Ltd for their technical assistance and patience.

Andrew Kenney of Innovate UK and Melanie Powell of The University of Bradford, for their support and facilitation of the project.

My parents for their encouragement and perseverance in proof reading my work.

Lewis for his outstanding patience, consistently reminding me of my capability and providing me with daily laughs.

Table of Contents

ABSTRACT I
ACKNOWLEDGEMENTS II
TABLE OF CONTENTS III
NOTATION VII
ABBREVIATIONS VIII

CHAPTER 1 INTRODUCTION

1.1 General Introduction 1
1.1.1 Perfluoroalkoxy Material 1
1.1.2 Transfer Moulding 3
1.2 Aim 7
1.3 Scope 8

CHAPTER 2 BACKGROUND

Introduction 10
2.1 Overview of Fluoropolymers 12
2.1.1 Properties 12
2.1.2 Applications 16
2.2 Processing of Melt Processable Fluoropolymers 19
2.2.1 Extrusion 20
2.2.2 Injection Moulding 21
2.2.3 Transfer Moulding 22
2.2.4 Key Process Parameters 23
2.2.4.1 Change in Melt Flow Rate 23
2.2.4.2 Critical Shear Rate 23
2.2.4.3 Rate of Cooling 24
2.3 Rheology 25
2.3.1 Rheometry 26
2.3.1.1 Melt Flow Rate Testing 27
2.3.1.2 Capillary Rheometry 28
2.4 Summary 31

CHAPTER 3 EXPERIMENTAL EQUIPMENT AND MATERIALS

Introduction 32
3.1 Capillary Rheometer 32
3.1.1 Mechanical Design 32
3.1.1.1 Overview 32
3.1.1.2 Messphysik Tensometer 34
3.1.1.3 Blockprogramming Control Software 35
3.1.2 Instrumentation 35
3.1.2.1 Melt Pressure and Temperature Measurement 35
3.1.2.2 Integrated Tensometer Load Cell 37
3.1.2.3 Extensometer 37
3.1.3 Data Acquisition System 37
3.1.3.1 Hardware 37
3.1.3.2 Software 38
3.1.4 Validation Study 39
3.1.4.1 Experimental Detail 39
3.1.4.2 Results 40
3.1.4.3 Conclusion 43
3.1.5 Experimental Methods 43
3.2 Melt Flow Rate Testing 46
3.3 Tensometer 49
3.4 Differential Scanning Calorimetry 51
3.5 Spectroscopy 55
3.5.1 Fourier Transform Infrared 56
3.5.2 Near Infrared 59
3.5.3 Raman 60
3.6 Materials 62
3.6.1 Preparation of Samples 62
3.6.1.1 Constant Shear 62
3.6.1.2 Residence Time 64
3.6.1.3 Processed Material 66
3.6.1.4 Tensile Testing 67
3.6.1.5 Cooling Rates 69

CHAPTER 4 RESULTS

Introduction 70
4.1 Base Comparison of Grades 70
4.1.1 Determination of Viscosity 70
4.1.2 Tensile Testing 73
4.1.3 DSC 75
4.1.4 Spectroscopy 77
4.2 Effect of Temperature 79
4.2.1 Melt Flow Rate Testing 79
4.2.2 Viscosity 80
4.3 Effect of Residence Time 84
4.3.1 Melt Flow Rate Testing 85
4.3.2 Viscosity 85
4.3.3 Tensile Testing 88
4.3.4 DSC 91
4.3.5 Near Infrared Spectroscopy 95
4.4 Effect of Shear 99
4.4.1 Viscosity 99
4.4.2 Tensile Testing 101
4.4.3 DSC 104
4.5 Effect of Processing 108
4.5.1 Viscosity 108
4.5.2 Melt Flow Rate Testing 109
4.5.3 DSC 110
4.5.4 Near Infrared Spectroscopy 118
4.6 Effect of Cooling Rate 121
4.6.1 Tensile Testing 121
4.6.2 DSC 124
4.6.3 Raman Spectroscopy 126

CHAPTER 5 DISCUSSION

5.1 Introduction 131
5.2 Suitability of Analytical Techniques 131
5.3 Determination of Basic Properties 134

5.4 Effect of Temperature 135
5.5 Effect of Residence Time 137
5.6 Effect of Shear 139
5.7 Effect of Processing 139
5.8 Effect of Cooling Rate 142
5.9 Summary 143

CHAPTER 6 CONCLUSIONS AND FURTHER WORK

6.1 Conclusions 144
6.2 Future Work 146

REFERENCES 147

APPENDICES

Appendix A Material Data Sheets
Appendix B Data Manipulation
Appendix C Fourier Transform Infrared Spectroscopy
Appendix D 5MPCA Melt Flow Rate Indexer Calibration Certificate

Notation

A	Area
a	Width of the transition from $0s^{-1}$ and the start of the power-law region
F	Force
G	Modulus
h	Height
K	Power law viscosity coefficient
L	Length of capillary die
n	Power law index
ΔP	Pressure drop
P_L	Long capillary die pressure drop
P_O	Orifice capillary die pressure drop
Q	Volumetric flow rate
R	Radius of capillary die
u	Displacement
v	Velocity
$\dot{\gamma}$	Shear strain rate
γ	Shear strain
$\dot{\varepsilon}$	Extensional strain rate
ε	Extensional strain
η	Shear viscosity
η_0	Viscosity at zero shear rate
η_E	Extensional viscosity
λ	Relaxation time
σ	Tensile stress
τ	Shear stress

Abbreviations

ASTM	American Society for Testing and Materials
BS	British Standards
CPI	Chemical Processing Industry
CSV	Comma Separated Variable
DSC	Differential Scanning Calorimetry
ECTFE	Ethylene Chlorotrifluoroethylene
ESC	Environmental Stress Cracking
ETFE	Ethylene Tetrafluoroethylene
FEP	Fluorinated Ethylene Propylene
FT	Fourier Transform
FTIR	Fourier Transform Infrared Spectroscopy
ISO	International Standards Organisation
LDPE	Low Density Polyethylene
MFR	Melt Flow Rate
MVR	Melt Volume Rate
NIR	Near Infrared Spectroscopy
PCTFE	Polychlorotrifluoroethene
PFA	Perfluoroalkoxy
PTFE	Polytetrafluoroethylene
PVDF	Polyvinylidene Fluoride
TFE	Tetrafluoroethylene

Chapter 1

Introduction

1.1 General Introduction

In any process, knowledge of material behaviour under various conditions is crucial. Whilst there are numerous publications regarding fluoropolymers in general (Gangal, 1989, Drobny, 2001 and Ebnesajjad, 2013); there is little available in terms of information specific to processing these materials.

The research within this MPhil is very closely linked to the subject of a Knowledge Transfer Partnership (KTP) between the University of Bradford and Corrosion Resistant Products (CRP) based in Littleborough. CRP manufactures piping products lined with a fluoropolymer material that prevents the corrosion of the metal pipe structure from a range of fluids (e.g. hydrochloric acid, sulphuric acid). The Company have partnered with the IRC in Polymer Engineering group at Bradford to support the ability to manufacture larger and more complex products using the transfer moulding process and perfluoroalkoxy (PFA) material. A better understanding of the phenomenological observations will provide an opportunity to address more complex lined products.

Currently, the material suppliers are able to provide a range of material properties and processing guidelines. However, the depth of information is limited in respect of the direct relevance to the particular conditions and products manufactured by CRP. The aim of this work is to generate data on the effect of various processing conditions on three transfer moulding grades of PFA. This information can then be used to optimise the transfer moulding process.

1.1.1 Perfluoroalkoxy Material

Perfluoroalkoxy was developed for commercial use in 1972 by DuPont (Utracki, 1998) and shares the trade name Teflon™ with fluorinated ethylene propylene (FEP) and the more commonly recognised polytetrafluoroethylene (PTFE). These polymers are all fully fluorinated members of the fluoropolymer family, they are perfluorinated. This means that all the hydrogen atoms have been

replaced with fluorine, whereas partially fluorinated polymers contain both C-F and C-H bonds. The replacement of some or all of the hydrogen atoms with fluorine leads to the polymer exhibiting some outstanding properties in terms of chemical inertness and thermal stability.

Perfluoropolymers		**Partially Fluorinated Polymers**	
PTFE	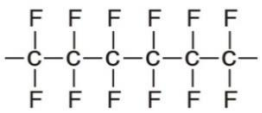	PVF	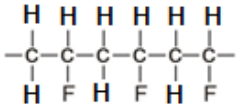
PFA	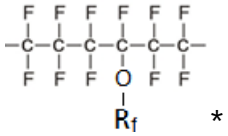	PVDF	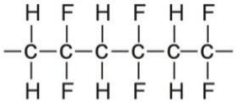
FEP	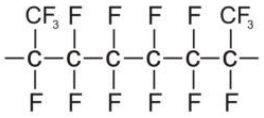	ETFE	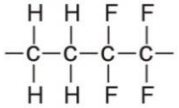
PCTFE	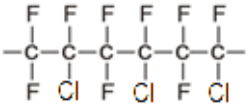	ECTFE	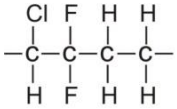

Figure 1.1: Structures of fluoropolymers. *R_f is a perfluorinated group containing carbon and fluorine

The carbon fluorine bond is often hailed as the strongest single bond in organic chemistry, and is responsible for the high thermal stability and chemical resistance of fluoropolymers. For a more detailed understanding of the carbon fluorine bond the interested reader is directed to a tutorial review by O'Hagan (2008). Another contributing factor to the chemical inertness of fluoropolymers is non-polarity, which is also responsible for the low dissipation factor and dielectric constant (Imbalzano, 1995).

The chemical resistance of fluoropolymers makes them suitable for use in hazardous fluid handling systems. Teng (2012) lists the main application of PFA as being chemically resistant components, namely in the chemical processing industry, with particular reference to the high purity requirements of semiconductor manufacture. The relatively low mechanical strength of the material is not an issue; the metalwork of the fitting provides the support, whilst the fluoropolymer liner delivers the chemical integrity. The tensile strength of

WCB grade carbon steel casting is specified as 70-95MPa in ASTM A216 (2014), compared to the tensile strength of PFA 350 listed by DuPont (2013) as 28MPa at 23°C, reducing to 14MPa at 250°C.

A key factor relating to fluoropolymer lined pipe is permeation, as such there are several articles in this area. These are written by fluoropolymer manufacturers themselves; Imbalzano, Washburn and Mehta (1991) and Buxton et al. (1993), and by others involved in the use of fluoropolymers; Extrand and Monson (2006), Monson et al. (2009) and Moon et al. (2011). A review of these will be included in the background information discussed in Chapter 2.

CRP manufacture both PTFE and PFA lined piping components. PTFE has an extremely high molecular weight of between 10^6 and 10^7 (DuPont, 2011). Molecular weight is essentially used as an indication of the length of polymer chains, so a high molecular weight means the polymer chains are long. Long polymer chains are more likely to become entangled, making it extremely viscous. PTFE cannot be processed using traditional methods due to its extremely high melt viscosity of approximately 1×10^{10} Pa.s (Kontopoulou, 2012 and Whelan, 1994). As a result of this, PTFE liners are limited in the geometries they take. Various methods of processing PTFE have been developed, however as this is not the focus of this work the interested reader is directed to texts such as Ebnesajjad (2000) and DuPont (2011). The viscosity of PFA is lower than that of PTFE, enabling it to be processed as a true thermoplastic material. Commonly this is in the form of injection moulding or transfer moulding. Transfer moulding is relatively uncommon compared to injection moulding, and a description of the process follows.

1.1.2 Transfer Moulding

Tooling is attached to the metalwork to be lined, forming a cavity for the PFA. The fitting, complete with tooling, is heated above the melt temperature of the polymer to improve the flow of molten polymer through the cavity. The polymer is injected into the cavity formed by the tooling. A hold pressure is applied to ensure full packing of the liner, as the shrinkage of PFA is significant. The fitting is cooled prior to removal of the tooling.

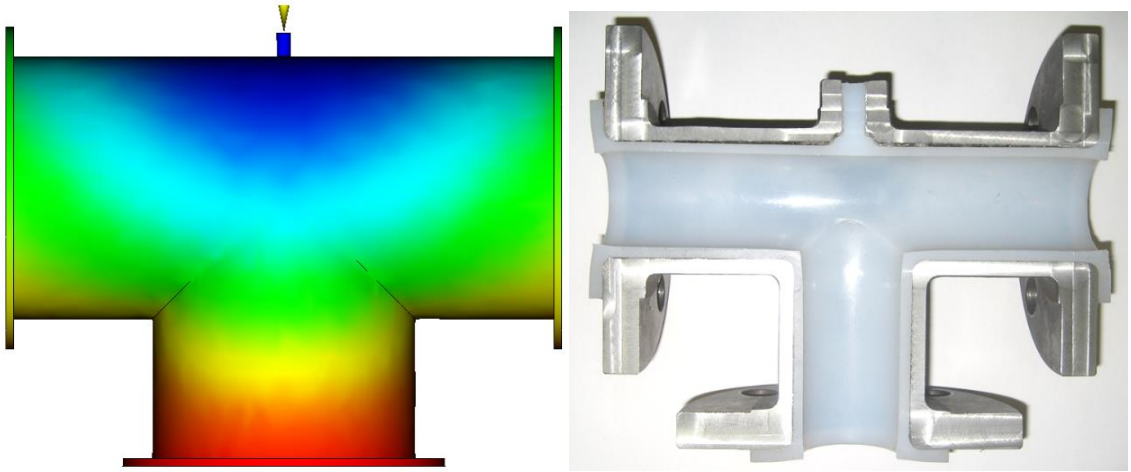

Figure 1.2: Model showing filling of a fitting created on Autodesk Simulation Moldflow (left) and photo of a fitting sectioned to show the liner (right)

The injection pressures used in transfer moulding are similar to those of injection moulding (DuPont, 1992), however due to the highly viscous nature of PFA, the rates of injection in transfer moulding are quite slow compared to injection moulding of commodity polymers. Transfer moulding cycles are significantly longer than those of injection moulding, which result in a relatively low throughput. Injection moulding machines are effective when producing high volumes of certain products to balance the high costs of machinery and tooling. However the flexibility of the transfer moulding process makes it ideal for manufacturing a wide range of components, enabling the various demands of the fluid processing industry to be met.

To obtain a successful component, the polymer must completely fill the mould cavity without voids, so it is important to optimise the flow conditions of the material. PFA is extremely viscous compared to other melt processable polymers, and with a pressure driven injection, the rate of injection of PFA depends on its viscosity.

Viscosity is the resistance to flow of a material, and is highly dependent on temperature and shear. Considering the effect of temperature first; generally the viscosity decreases with increased temperature. This can be observed in everyday situations: if honey is kept in the fridge it is relatively thick, if it is heated it becomes runny.

Shear refers to the application of a force parallel to the cross section of a body, and can be explained through use of a diagram:

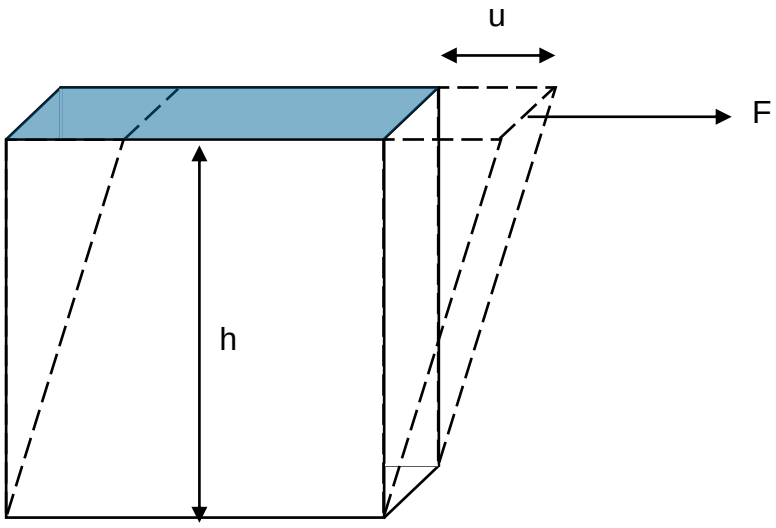

Figure 1.3: Shear flow

The displacement of the top layer relative to the bottom layer is the shear strain (γ)

$$\gamma = \frac{u}{h}$$

The shear stress (τ) is the magnitude of the force applied over the cross sectional area (shaded)

$$\tau = \frac{F}{A}$$

Shear rate ($\dot{\gamma}$) is the change in shear strain with respect to time, and therefore depends on the speed (v) at which the top layer is moving

$$\dot{\gamma} = \frac{v}{h}$$

In the context of this project, the polymer is sheared as it is pushed through an orifice, whether it is through the nozzle in the transfer moulding process itself, or through the die of a capillary rheometer. Increasing the rate of injection increases the shear rate the polymer is exposed to.

Many materials are ‘shear thinning’, so the viscosity of the material decreases with increased shear rate. A common example is toothpaste: squeezing it from the tube applies a shearing force, causing it to flow through the nozzle and onto

the toothbrush. When the shearing forces are removed the toothpaste regains its original viscosity and sits on the bristles.

The effects of temperature and shear on viscosity are important in processing because as viscosity decreases there is less resistance to flow. If the polymer flows easily the likelihood of fully filling the cavity increases, leading to a greater quantity of successfully moulded components. There are additional benefits in optimising the process conditions to minimise resistance to flow, such as lower injection pressures, reducing the wear on machinery and tooling.

This work sets out to generate data on the viscosity of PFA at various temperatures and shear rates, as there is a lack of published information available. This information can then be used to optimise the transfer moulding process.

In addition to the viscosity of PFA, other key areas to consider are the effects on the material properties due to processing conditions. Despite exhibiting some remarkable properties in terms of resistance to ultraviolet (UV) light, which can often be a cause of degradation in polymers, fluoropolymers are still susceptible to thermal degradation. This can either be due to exposure to exceptionally high temperature for a brief phase, or through extended periods of time above melt temperature. There are various recommendations against holding PFA at elevated temperatures for extended periods to prevent degradation of the polymer, but again there is little available in terms of published data to support this.

PFA is a poor thermal conductor, so investigation of residence time at elevated temperature is a key activity in balancing the temperature gradients against the effects on the material properties due to thermal degradation.

Degradation often results in undesirable changes in the material properties, whether it be visual i.e. colour change, or mechanical e.g. a reduction in the tensile properties of the material. These changes in characteristics often lead to unacceptable product quality, therefore obtaining data in this area is of high importance.

Another parameter of interest is the rate of injection. Several articles (DuPont, 1992, Dyneon, 2013 and Solvay, 2014) recommend processing PFA below its

critical shear rate, so as to avoid damaging it, however none explain what is meant by the term ‘damage’.

The critical shear rate of a polymer is defined as the onset of melt fracture (Whelan, 1994). This is the rate at which the flow is disturbed leading to surface defects, and in many polymers leads to stick slip, sharkskin and eventually gross melt fracture. Given the uses of PFA in wire coating the recommendation to process below this rate is understandable and valid, as a poor surface would presumably be a cause for rejection. However when a polymer is packed into a cavity under pressure during transfer moulding, the surface appearance of the extrudate is unlikely to cause concern. Once again, there is no data available to support the idea that processing above the critical shear rate is structurally damaging, so research in this area is necessary.

It is possible to use characterisation techniques to detect small changes in the polymer. Samples exposed to various conditions can then be used to attribute the changes seen in the material properties to individual processing parameters. Methods investigated in this project include: Melt Flow Rate (MFR), Differential Scanning Calorimetry (DSC) and various forms of spectroscopy: Fourier Transform Infrared (FTIR), Near Infrared (NIR) and Raman. A description of the equipment and the theory is provided in Chapter 3.

1.2 Aim

The overarching purpose of this work was to increase the level of scientific understanding of the effects of processing on the properties of perfluoroalkoxy.

Specific project aims were to:

1. Explore the suitability of different analytical methods for identifying the condition of PFA due to various process variables
2. Determine the influence on viscosity of:
    a. temperature
    b. shear
    c. residence time at temperature
3. Ascertain whether exposing PFA to high shear rates damages the polymer

4. Quantify the change in material properties as a result of the residence time at processing temperature
5. Examine the consequence of the rate of cooling on the structure and the mechanical properties of PFA
6. Investigate the correlation between the results generated from Melt Flow Rate testing and the viscosity data obtained from the capillary rheometer for samples of PFA exposed to the same conditions

1.3 Scope

Chapter 2 provides relevant information as a background to the research conducted. It comprises an overview of fluoropolymers and methods of processing, with specific emphasis on PFA and transfer moulding.

The equipment and materials used to conduct the experimental work in this study are discussed in Chapter 3. The design and validation of a bespoke capillary rheometer are explained, along with the instrumentation and data acquisition system used. The techniques used to assess changes in the polymers due to various processing conditions are detailed, and include: MFR testing, DSC and various forms of spectroscopy: Fourier Transform Infrared (FTIR), Near Infrared (NIR) and Raman. An overview of the materials used in the study is given, with details of the methods of preparation of the various samples required for the study also included.

Chapter 4 contains the results of the analytical techniques used to determine the effect of processing on the material properties of PFA. Basic material information was generated on the polymers in their unprocessed form to provide a baseline from which to compare data. Rheometric data was used to determine how temperature and shear rate affect the flow properties of each of the materials. The results from spectroscopic studies, DSC and tensile testing show the effect of exposing the polymers to high temperatures for long periods of time, and of processing at high shear rates on the properties of the material. Investigations of material subjected to transfer moulding process conditions and of the 350TJ grade of PFA exposed to various cooling rates are also presented. Comparison of the grades shows the differences between the materials, and demonstrates the requirement for this type of information to aid optimisation of processes.

A summary of the key results with regard to the original project aims is presented in Chapter 5. The outcomes from the analysis of the effect of each of the processing conditions investigated are discussed, and the methods used are reviewed in terms of their suitability.

The overall conclusions of the project are given in Chapter 6, accompanied by recommendations of areas for additional investigation.

Chapter 2

Background

Introduction

Corrosion Resistant Products (CRP) manufacture fluoropolymer lined piping components. The chemical inertness of the fluoropolymer makes the liner suitable for carrying corrosive fluids, negating the requirement for expensive exotic metals. The company was established in 1983 and has a wealth of practical experience in paste extrusion of PTFE and transfer moulding of PFA. In order to further their current understanding of fluoropolymers, CRP have partnered with the IRC in Polymer Engineering at the University of Bradford.

Figure 2.1: Examples of CRP's product range; PTFE bellows (left) and PFA reducing tee (right)

The aim of this project was to better understand how processing history may influence important material properties. The key variables investigated were the impact of temperature and shear on viscosity, and the effect of the level of shear and residence time at processing temperature on the properties of the material. To relate these back to the process, manufacturing activities were also monitored. The improved insight of the impact of transfer moulding process conditions on material properties is expected to improve the company's ability to manufacture larger and more complex products in order to meet growing customer demands.

This chapter provides relevant information to help put the research contained in this MPhil into context. An overview of fluoropolymers is given accompanied by their typical applications, with a particular focus on the key properties for lined piping and uses in the Chemical Processing Industry (CPI). The materials and methods of processing are covered, with a specific emphasis on transfer moulding and the parameters that must be considered.

Fluoropolymers do not seem to have been widely researched, and much of the information specific to fluoropolymers has been generated by the manufacturers themselves. Documents regarding transfer moulding are scarce and there is a lack of published information linking material characteristics of fluoropolymers to processing conditions. This highlights the necessity of the work conducted in this project.

A significant amount of the articles on fluoropolymers have been published as technical information by the fluoropolymer manufacturers or end users themselves. Earlier publications, particularly by DuPont, contained sufficient information to give the reader a good basic scientific understanding of the properties and applications of fluoropolymers. The focus of these documents seemed to lie more in promoting the technical understanding of the material, rather than the opportunity for marketing.

Despite, or potentially due to, the lack of information published on fluoropolymers there are a couple of areas of controversy. The key contentious issue that will be explored further is of the permeation performance of PTFE and PFA lined pipe. However, regarding the processing of PFA there is agreement in terms of the acceptable change in material properties due to thermal degradation, and the limits on rate of injection. There is general consensus regarding the acceptable change in Melt Flow Rate (MFR) as an indication of the level of degradation of PFA. A maximum allowable increase of 20% is quoted in a number of articles as being the limit at which the mechanical properties of the PFA begin to be compromised. The absence of data presented to support this reflects the level of technical information regarding processing of PFA. Another area of agreement lies in the importance of processing below the critical shear rate of the polymer, so as to avoid damaging it. Several articles echo this recommendation, however none explain what is meant by the term

‘damage’. Whelan (1994) defines the critical shear rate of a polymer as the onset of melt fracture. Melt fracture refers to the surface distortion resulting from the disturbed flow, which in many polymers gives rise to stick slip, sharkskin and gross melt fracture. As PFA is commonly used in wire coating applications, the recommendation to process below the rate at which flow is disturbed is sensible, as distorted surfaces would lead to rejected product. However the disturbed flow of the polymer is unlikely to cause concern in transfer moulding as the PFA is packed into the mould cavity under pressure. There has been a paper published in this area by Rosenbaum, Hatzikiriakos and Stewart (1995) which is discussed in more depth in the section regarding processing of fluoropolymers in the main body of the chapter.

2.1 Overview of Fluoropolymers

A significant proportion of the information available regarding fluoropolymers is provided by Ebnesajjad (2000), (2002), (2013) and Ebnesajjad and Khaladkar (2004). Ebnesajjad worked with DuPont in the fluoroproducts division for nearly 24 years according to FluoroConsultants Group (2015) and Elsevier (2015). As a result a significant amount of the information contained in these books is based on private or company communications which often cannot be accessed in order to verify the information.

2.1.1 Properties

The properties of fluoropolymers are widely quoted and can be found in the general texts discussed, however some articles, such as Imbalzano (1995) provide fuller explanations. The earlier DuPont publications appear to be more be focused on educating the user as they contain a higher level of technical detail.

PFA is comprised of tetrafluoroethylene (TFE) and a perfluoroalkyl vinyl ether (PAVE), most often perfluoropropyl vinyl ether (PPVE), however perfluoroethyl vinyl ether (PEVE) and perfluoromethyl vinyl ether (PMVE) can be used. The structures of these comonomers are provided in the table below.

Comonomer	Structure
Perfluoromethyl vinyl ether (PMVE)	$CF_2CF – O – CF_3$
Perfluoroethyl vinyl ether (PEVE)	$CF_2CF – O – CF_2 – CF_3$
Perfluoropropyl vinyl ether (PPVE)	$CF_2CF – O – CF_2 – CF_2 – CF_3$

Table 2.1: Structures of comonomers used in PFA (McKeen, 2009)

According to Ebnesajjad (2015), these PAVE comonomers have a pendent group which serves to reduce the crystallinity of the TFE; as polymerised PFA has a crystallinity of approximately 70% ± 5%. The PPVE content of PFA is only around 2-4 wt% as it is the most effective of the comonomers in reducing the crystallinity due to the larger pendent group (Banks et al., 1994). Teng (2012) links the presence of the PPVE to the lower melt viscosity and melt temperature of PFA compared to PTFE. PFA has a melt temperature of between 305-315°C, whereas the first melt temperature of PTFE is approximately 342°C, reducing to around 327°C after sintering. Ebnesajjad (2015) states that PFA has a first order transition at -5°C and three second order transitions at -100°C, -90°C and -30°C, however details of these transitions are not provided.

Imbalzano, Washburn and Mehta (1991) briefly explain permeation and discuss factors affecting permeation in polymers. The main message of the article is that fluoropolymers are more resistant to permeation than other polymers, with the article concluding “with few exceptions, the differences in permeability among fluoropolymers have little bearing on the end-use performance of fluoropolymer lined piping or equipment”. A graph shows the transmission rate of water vapour to decrease as the thickness of the FEP film increases. Unfortunately no data points are shown so there is uncertainty around the fit of the curve. Similarly the graph showing the permeability with temperature of PTFE, ECTFE and PVDF is poorly labelled, with no conditions stated (i.e. pressure, thickness etc.), however the graph is used to illustrate the point well. The article states the basics of Environmental Stress Cracking (ESC) with short explanations, and as an introduction to the subject is useful. Unfortunately there is no evidence provided to support any of the information given. The thickest films considered are just under 2.3mm, so whilst this is thicker than the samples described in more recent papers it is still difficult to draw any conclusions for thicker lined piping applications.

Extrand and Monson (2006) conducted work on the permeation of hydrogen, oxygen and nitrogen through samples made from the LP series of PFAs produced by DuPont. They found hydrogen permeated faster than nitrogen or oxygen and attributed it to the smaller size of the molecule. A key finding is that for films thicker than 0.25mm the permeability, diffusion and solubility coefficients do not change in response to different upstream pressures and thickness (this implies the rate of permeation is proportional to the thickness of the sample). The experimental detail is well documented, with details of the process used to measure permeation, as well as the DSC temperature profile used and the data generated to determine the level of crystallinity of the samples. A range of thicknesses of film were used to investigate the effect of thickness on rate of permeation. The work is more relevant to the semiconductor industry rather lined pipe applications as it concentrates on the effect of thickness on permeation of thin films (less than 1mm thick). The authors recognise the literature regarding fluoropolymers concerns mainly mechanical and thermal attributes, and that there is another gap in the research concerning permeation.

Having established that the permeability, diffusion and solubility coefficients do not change in response to different upstream pressures and thickness in samples thicker than 0.25mm, Monson, Moon and Extrand (2009) focus on the effect of varying the level of crystallinity of the samples on the permeation resistance. The authors identify the requirement for investigation into the effect of the architecture of the polymer and processing have on permeation. The authors' central point is that the method of cooling makes just as significant an impact upon the level of permeation resistance as the choice of polymer. The PTFE-filled PFA grades showed a higher crystallinity and improved resistance to permeation. The PFA with higher comonomer content was found to give a lower crystallinity, and a reduction in permeation performance was observed. The authors of this study go so far as to say the cooling process used had more significance on the rates of permeation than the architecture of the polymer chains. The paper is in agreement with other more general texts, that samples cooled more slowly demonstrate better permeation resistance to those that are cooled rapidly. The observation that the permeation resistance can be

determined by rate of cooling as much as choice of polymer also agrees with other texts, and it is a refreshing change to see data to support this claim.

Moon and Extrand (2011) highlight two of the most common process media as hydrochloric acid and ammonium hydroxide, and address the issue of cross contamination and corrosion. The active ingredient in both of these fluids is dissolved gas, therefore the focus of the work is on the permeation resistance of two grades of DuPont PFA against hydrogen chloride and ammonia gas. The study found a determining factor of permeation rate is molecular size, particularly when there is little interaction between the permeant and the polymer. However transport properties could not be justified based singularly on the size of the permeant molecules. The study found the permeation coefficients to be 30-80% reduced for hydrogen chloride than ammonia under various processing conditions. For all samples the rate of permeation was found to be proportional to the applied upstream pressure, and inversely proportional to thickness. As found previously, for various samples the value of the permeability coefficient was found to remain constant with varying pressure; and the permeability coefficients of the ice quenched samples were more than double those of the slow cooled samples. The authors postulated that the amorphous regions within the polymer allow the hydrochloric acid to dissolve and permeate. The slow cooled samples of both polymers were found to have similar crystallinity and permeation coefficients, whereas the difference was marked in the ice quenched samples. This is attributed to the difference in molecular weight, as a greater molecular weight reduces the ability of the polymer to crystallise. Diffusion and permeation occur more rapidly with smaller molecules, so it was expected ammonia would diffuse and permeate quicker than hydrogen chloride. Conversely ammonia was found to have a higher permeation coefficient, thought to be due a combination of the size and three hydrogen atoms which can interact more strongly with the PFA.

There have been few developments in fluoropolymers in recent years, as the requirements can be met with existing products. Teng (2012) observes that the focus is reduction of the cost of manufacturing the raw polymer, and provides some insights as to the evolution of the industry. An area of development has been published by Lahijani et al. (2011) regarding a new type of perfluoropolymer that can offer a continuous service temperature of 300°C

rather than 260°C. The authors attribute the superior properties on heat treatment of this new polymer to epitaxial co-crystallisation, however no attempt is made to explain what is meant by this term. It is argued the new polymer has a far better modulus retention than other perfluoropolymers, however data presented showing the modulus over 18 months of heat aging at 315°C for the new polymer only. Similarly the increase in permeation resistance of the new polymer after heat treating is shown to increase, however the statement that the new polymer shows 50% less permeation remains unsupported as no comparative data is presented. Unfortunately in this regard, the article is fairly typical of recent publications.

2.1.2 Applications

One of the main applications of perfluoroalkoxy is in the Chemical Processing Industry (CPI), where fluoropolymer lined pipe provides the inertness required for transporting corrosive substances at a significantly lower cost than metal alloys. ASTM F1545 (2009) provides standard requirements for plastic lined pipe, and specifies for PFA lined pipe the grade of material must be Type II as defined by ASTM D3307 (2010).

Stress crack resistance is crucial in the performance of a lined piping system, however particularly in later years permeation has received more attention. There are several articles published by DuPont regarding the use of fluoropolymers in the Chemical Processing Industry. Buxton, Goldsberry and Henthorn (1993) cover the failure modes of lined pipe through permeation and provide some information relating to permeation through thicker samples from 0.25mm up to 4.75mm in some cases. The authors note that the data collected varies considerably, however this is cited as “typical” with permeation tests. The permeation rate of methyl ethyl ketone through ECTFE, ETFE and PTFE is presented to support the rate of permeation increasing with temperature. The effect of polarity is also shown with permeation rates vs. temperature for benzene (non-polar) and water (polar) through ETFE and PTFE. The non-polar benzene permeates faster through PTFE than water does, as expected.

Another document by DuPont (1997) promotes the use of fluoropolymers in the chemical processing industry by giving examples of fluoropolymers being used in various components found in fluid handling systems. The article includes

basic material information on their PTFE, PFA, FEP and ETFE. The advice given for material selection is non-committal, stating the suitability for purpose should be tested prior to selection. The article reinforces the message that experience is invaluable when choosing the material, whilst testing is briefly described. There is no mention of the superiority of one fluoropolymer over another, interested parties are directed to their DuPont representative.

DuPont (2001) explain the factors affecting permeation in terms of the structure of the polymer, in a style similar to the article written by Imbalzano for DuPont on the basic chemistry and properties of fluoropolymers. Graphs showing the permeation of water vapour, oxygen, carbon dioxide and nitrogen support the claim that permeation decreases with an increase in film thickness. The article highlights the importance of understanding the limitations of permeation data to make sure the conclusions drawn are fully supported. The fact that there is a limited amount of useful data published regarding permeation is identified, and the suggestion is to generate data from testing components in process conditions. The main limitation of this article is that it does not consider permeation through a substantial thickness of fluoropolymer.

A couple of the manufacturers of fluoropolymer lined piping components have released articles specifically in regard to permeation, however they seem to have been produced for marketing purposes and so contain little in the way of technical information. Flowserve (1999) wrote an article seemingly as a response to claims that PFA has superior permeation performance to PTFE. It is designed to promote Flowserve products as having the highest permeation resistance, by highlighting their depth of knowledge, choice of material and manufacturing techniques. The authors lay out simple arguments regarding the importance of liner thickness, design and method of manufacture, permeation rates vary in different applications, and that no fluoropolymer has been proved to have superior permeation resistance over another. The article makes valid points, however very little evidence is available to support the conclusions made in the article. Most of the content has been taken directly from one of the three DuPont sources referenced, one of which being a private letter from DuPont to the Engineering Manager at Flowserve.

Yanik (2011) of Resistoflex published a white paper outlining advancements in the fluoropolymer lined pipe industry, however the focus of the paper is solely on PTFE lined pipe with no real mention of other materials such as PFA or FEP. The article promotes Resistoflex's "Next Generation" plastic lined pipe and fittings by comparing it to "all previous offerings in the industry". The claim is made that the crystalline matrix of the PTFE is damaged when it is heated and stretched to line a pipe with which the liner has an interference fit, and that a new method has been developed to avoid the pulling and stretching whilst the density of the PTFE is increased and strengthened. No details are given of this process, however this is not entirely unreasonable. Yanik recognises that anecdotal evidence has been used extensively to promote the finer technical variations of fluoropolymers used in lined piping systems, sometimes illogically, which has led to a devaluation in technical arguments used to support different products. However throughout the paper bold statements are made, contradicting historical information generally believed to be true, with no explanation provided within the main body of the text. On turning to the appendices for "further discussion" there is a startling lack of information from an author who wishes to support the claims made in his paper using experimental results. As one of the main players in the fluoropolymer lined pipe market, one can understand the reluctance to divulge sensitive data, however there is insufficient information provided to substantiate the claims made. In this respect the paper is similar to other "technical articles" – there is a significant lack of real data to allow the reader to come to their own conclusions. This lack of published information reinforces the requirement for experimental work conducted in this project, which provides a solid understanding from which to work. Yanik encourages the reader "to view claims that a given material is superior or inferior to "PTFE" with scepticism" and urges the consumer to consider the knowledge of the company when determining their supplier. This reiterates the importance of gaining a better scientific understanding of their materials and processes to apply to the existing practical knowledge.

Extrand (2003) discusses the suitability of various fluoropolymers for fluid handling applications, specifically in relation to the chemicals used in microelectronics manufacture. Specific insight is provided as to why the fully fluorinated polymers are more desirable for use in fluid handling applications,

whereas this is not usually recognised in other more general texts. The limitations of PVDF are due to its reduced chemical resistance to aqueous bases, organic bases and strong oxidising acids. ETFE and ECTFE are listed as higher performance than PVDF but being susceptible to attack by bases and harsh solvents, particularly at high temperature. The article mentions low fluorine grades of PFA specifically aimed at the semiconductor industry, as high levels of fluoride ions have the potential to damage silicon wafers.

Fleming et al. (2001) list the various merits of using fluoropolymers over stainless steel and glass in the pharmaceutical industry, referencing their inertness, resistance to corrosion, and non-wetting surface as key factors. The article is written by DuPont and the shortcomings of stainless steel and glass are emphasised prior to the section on the advantages of fluoropolymers. It is still well referenced and contains a reasonable amount of data to support the points made, however the style of language and level of explicit bias in the text varies from previous documents. The main conclusion, taken from a paper written by Hyde et al (1997), is that roughness of the surface is not a factor in biofilm adhesion to Teflon PFA HP, whereas for the other materials increasing the roughness of the surface increased the biofilm retention. This is supported by the data taken from the paper by Hyde et al (1997) showing injection moulded PFA to have the highest level of biofilm removal, despite it having a rougher surface finish than borosilicate glass and polypropylene. Machined PFA was shown to have the second highest level of biofilm removal, with that having the roughest surface finish of all sample materials. It is not strictly true however for the authors to state that roughness of the surface is not a factor in biofilm adhesion for Teflon PFA – machine PFA, with a rougher surface, had a lower rate of biofilm removal than injection moulded PFA. The biofilm release performance of PFA is attributed to the non-polar surface, which is not unreasonable given the high contact angle of water on PFA meaning it has low wettability. However water is a polar molecule, and it is important not to extrapolate the conclusions drawn from this work to non-polar process fluids.

2.2 Processing of Melt Processable Fluoropolymers

There are several different methods of forming melt processable fluoropolymers which are covered in this section. The process of polymer melt extrusion is described as it is key to most of the manufacturing methods used. Injection and

transfer moulding are discussed, and the main parameters of interest are explored.

Compression moulding is commonly used for thermosetting plastics, however semi-finished articles such as sheets, rods and films are also manufactured from melt processable fluoropolymers. Usually material, in pellet form or preformed, is preheated and put into an open heated cavity. The mould is closed and pressurised, forcing the plastic to fill the shape of the mould.

Blow moulding starts with the extrusion of molten polymer to form a tube called a parison. The bottom of the parison is sealed and the mould closed around it. Air is then blown into the plastic, which expands to take the shape of the mould. The part is ejected once the plastic has cooled. According to Aten, Libert, and Burch (2012) only relatively small items can be blow moulded using fluoropolymers. This is due to the limited melt strength of fluoropolymers with low enough viscosity to allow extrusion at a reasonable rate, as the item can tear or sag. Fluoropolymers of sufficient melt strength can only be extruded at slow speeds, leading to issues with the far end of the parison cooling which gives poor results.

In rotational moulding polymer is fed into a heated mould which rotates about two perpendicular axes simultaneously. The polymer flows and coats the inner surface of the mould before being cooled.

Melt processable fluoropolymers can be rotomoulded to manufacture lined vessels, however the high viscosity means high temperatures are required as rotolining is a relatively low shear process. Rotomoulding generally gives more uniform and greater wall thickness than blow moulding.

2.2.1 Extrusion

Extrusion refers to the process of forcing polymer through a die into a constant shape. The process can be either continuous, where the extrudate can theoretically be of infinite length, or semi-continuous where multiple components are manufactured. Typically tubing and wire coating are continuous processes, whereas injection and transfer moulding are discontinuous. Hudson (1995) lists the two types of extruders used in discontinuous processes as

reciprocating screw extruders, which are responsible for plastification of the melt, and ram extruders which are melt fed.

In a screw extruder the polymer granules are fed into a hopper and transferred to the feed zone of the screw and heated barrel arrangement. The rotation of the screw moves the polymer forwards through the melting zone of the screw where the channels become shallower. The polymer is melted by the friction and heat from the barrel. The melt is homogenised in the metering zone where the channel depth becomes constant again.

In ram extrusion the material is usually heated prior to loading into the extruder, where a ram pushes the polymer through the die. PTFE is not melt processable, however if it is in the format of fine powder and mixed with lubricant into a paste it can be extruded into tubes.

2.2.2 Injection Moulding

Injection moulding machines use a reciprocating screw to melt the polymer similar to the extrusion process. When there is sufficient molten polymer the screw is pushed forward to inject the melt through the nozzle and into the mould.

There are few documents available regarding injection moulding of fluoropolymers, however DuPont (1988) and Dyneon (2013) have published injection moulding guides for their fluoropolymers. There is also a small amount of information presented by Solvay (2014). The information provided in the books by Ebnesajjad (2000), (2002), (2013) and Ebnesajjad and Khaladkar (2004) has been discussed in the previous section. There is a reasonable level of agreement in these publications. There is the recommendation to process below the critical shear rate in order to prevent surface defects from melt fracture, however Solvay (2014) appear to be more concerned over warpage and dimensional stability. A substantial level of information is provided on the equipment and tooling, specifying it must be made out of corrosion resistant material. The tooling is held at a temperature significantly lower than the melt temperature of the polymer for injection moulding.

2.2.3 Transfer Moulding

Both screw and ram extruders are used in the process of transfer moulding which DuPont (1992) refer to as dynamic and static plastification. Dynamic plastification is similar to injection moulding in many respects as it employs a reciprocating screw that serves to melt the polymer. Due to the corrosive nature of molten fluoropolymers it is important the screw and barrel are made from corrosion resistant materials. Mark (2013) lists Hastelloy® C, Monel 400 or Xaloy 306 as suitable materials for the construction of the screw. Due to the high melt viscosity of fluoropolymers used in transfer moulding the rotation speeds are kept low to prevent excessive shearing forces damaging the screw and causing localised thermal degradation. Static plastification refers to injection of the polymer by ram extrusion. A charge of polymer is loaded into a pot and heated before being transferred into the mould.

One of the main differences between transfer and injection moulding is the tooling. To prevent premature cooling of the part in transfer moulding, the tooling is held at least at the melt temperature of the polymer, preferably above. The tooling for transfer moulding of lined piping components is slightly different again, as the liner is moulded directly into the metal pipework. A mandrel is located using end plates that are bolted to the flanges of the fitting to form the mould cavity for the fluoropolymer to fill to create the lining.

The polymers used for transfer moulding are highly viscous and as a result they have low critical shear rates. As discussed previously the critical shear rate of a polymer is defined as the onset of melt fracture. Melt fracture gives a frosty surface to the polymer, so to avoid this the shear rates the polymer is subjected to are much lower in transfer moulding than injection moulding.

There is very little published regarding transfer moulding of fluoropolymers. DuPont (1992) appear to be the only manufacturers to have released a transfer moulding guide, however Solvay (2014) have included a small amount of information on transfer moulding in their Hyflon PFA Design and Processing Guide. There is a similar level of information provided for transfer moulding as for injection moulding in the books by Ebnesajjad (2000), (2002), (2013) and Ebnesajjad and Khaladkar (2004). In the wider world of plastics processing transfer moulding appears to mainly refer to resin transfer moulding.

2.2.4 Key Process Parameters

There are several closely related parameters to consider when transfer moulding fluoropolymers using a pressure controlled injection. The injection pressure controls the rate of transfer, however this also depends on the viscosity of the polymer. The viscosity of the polymer is determined by the temperature, molecular weight, molecular weight distribution and any degradation of the polymer caused by the length of time it is exposed to high temperature. Viscosity also depends on the rate of injection itself, as most fluids are shear thinning i.e. there is less resistance to flow as the rate of flow increases. The rate of transfer partly determines the cooling of the metalwork and the polymer, which in turn affects the viscosity. Given the importance of viscosity, it is disappointing there is not more information published regarding the dependence on temperature and shear rate.

2.2.4.1 Change in Melt Flow Rate

One of the key themes in the processing guides is the degradation due to exposure to high temperatures for long periods of time. The maximum change in the Melt Flow Rate (MFR) of PFA is quoted as 20% by DuPont (1992) and Dyneon (2013), however no data is available to support this. Gangal (1989) acknowledges the degradation of PFA is determined by time and temperature, and states that “degradation is not significant if the change in melt flow rate of the resin during moulding is below 20%”. This statement is not supported with any figures or data. The indicators of degradation are listed as discolouration and the appearance of tiny bubbles. Interestingly, it is noted that slight discolouration can occur with high temperature, but that this may not negatively affect the material properties. Unfortunately this point is not expanded on. An extensive reference list is provided for the interested reader, however the text is lacking in citations, making it extremely difficult to cross reference certain pieces of information. Despite the lack of academic rigour this text is of importance as it is possibly where DuPont and Dyneon have taken their information from with regard to change in Melt Flow Rate with processing.

2.2.4.2 Critical Shear Rate

Gangal (1989) also quotes the critical shear rate for DuPont PFA 350 as $6s^{-1}$ at 372°C with a 5kg load, however there is no discussion of the experimental procedure or impact of this. This figure differs from that of $12s^{-1}$ quoted by

DuPont (1992) and (2013). Dyneon (2013) refer to the onset of melt fracture occurring at a critical velocity, however no data is provided as to what these values may be. Solvay (2014) stress that processing must occur below the critical shear rate of the polymer and list the range of M640 as 50-70s^{-1} and M620 as 10-15s^{-1}, however these values are not included in the technical data sheets of the individual polymer grades.

Rosenbaum, Hatzikiriakos and Stewart (1995) have published what appears to be one of the only documents available on the effect of shear rate during processing of melt processable fluoropolymers. Their work determined the onset of melt fracture of fluorinated ethylene propylene (FEP) to occur at shear stresses above 0.18MPa. The flow curves and photos show the stable region to exist up to 80s^{-1}, where the material is nearly Newtonian. Sharkskin is observed between 80s^{-1} and 100s^{-1}. At 100s^{-1} the pressure oscillations are more significant with the onset of stick slip behaviour, which continues to 700s^{-1}. What is highly relevant to this project is the fact that this paper identifies that the oscillations are not always obtained within the identified region. It is noted that for certain shear rates the flow becomes apparently stable, however the extrudate retains its stick slip appearance. A supershear region is identified between 700s^{-1} and 2000s^{-1}, where the pressure drop stabilises and the extrudate becomes smooth again. Above 2000s^{-1} gross melt fracture is found, and worsens with an increase in apparent shear rate. At lower temperatures (300°C) no superextrusion region was found, and at 325°C the region was found to shift significantly from 700s^{-1} to 2000s^{-1} to 470s^{-1} to 700s^{-1} (for 4100 FEP, for 3100 the region was wider - 250s^{-1} to 700s^{-1}).

2.2.4.3 Rate of Cooling

Another important consideration in processing is the rate of cooling, as PFA shrinks by between 3.5-6% depending on part thickness according to DuPont (1988). The rate of cooling also affects the crystallinity of the material, which in turn influences the properties of the final product, as explored previously. Gangal (1989) states that the crystallinity of virgin Teflon PFA is between 65-75%, and explains that decreasing the rate of cooling increases the level of crystallinity and value of specific gravity. Details of two samples are given: the crystallinity of an ice quenched sample is listed as 48%, with a specific gravity of 2.123; the crystallinity of a press cooled sample is listed as 58%, with a

specific gravity of 2.157. It is not clear from the text which grade of PFA was used in the experiment, however given the general lack of published information this data is the best indication of the effect of cooling rate on crystallinity (and therefore the final properties of the product).

2.3 Rheology

Transfer moulding, as with other methods of plastics processing, has developed more as a craft than an exact science. However in order to manufacture the increasingly complex products required by industry, the boundaries of the process are being pushed. A better understanding of the relationship between the process and the material is required as the behaviour of the material at each stage of the process affects the quality of the final component.

The study of the flow and deformation of matter is known as rheology. It relates the force applied to a material, the deformation as a result of the force and the time taken for the deformation to occur. Rheological investigations are often conducted by considering flow in regard to various models based on specific conditions. The relationships between shear stress, strain and shear rate were presented in Chapter 1. The material can respond elastically, demonstrate viscous flow, or rupture. Rupture occurs if the critical stress of the material is exceeded, however for PFA this is often referred to in terms of a critical shear rate. A purely elastic material deforms and stores the work done, and on releasing the stress the energy reverts the material back to its original shape. A metal spring exhibits this kind of behaviour, which can be defined by:

$$\text{Modulus, } G = \frac{\text{Stress, } \sigma}{\text{Recoverable Strain, } \varepsilon}$$

Conversely, in a viscous response, the energy from the shearing forces is dissipated as heat. Removing the shearing force causes the material to stop flowing, however it does not return to its original condition. Fluids that exhibit purely viscous behaviour are known as Newtonian fluids and have two types of viscosity given by:

$$\text{Shear Viscosity, } \eta = \frac{\text{Shear Stress, } \tau}{\text{Shear Strain Rate, } \dot{\gamma}}$$

$$\text{Extensional Viscosity, } \eta_E = \frac{\text{Tensile Stress, } \sigma}{\text{Extensional Strain Rate, } \dot{\varepsilon}}$$

Polymers tend to show viscoelastic behaviour, which is a combination of the viscous and elastic responses discussed. The Maxwell model can be used to demonstrate viscoelasticity, with a Hookean spring representing the elastic response connected to a dashpot which exhibits viscous deformation.

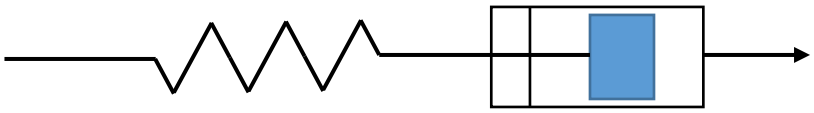

Figure 2.2: Diagram of the Maxwell model for viscoelasticity

Polymers usually display non-Newtonian behaviour, which means the viscosity varies non-linearly with shear strain rate. This can be described using a power law model in the region where shear stress is proportional to a power of shear rate:

$$\eta = K\dot{\gamma}^{n-1}$$

Where K is the power law viscosity constant and gives an indication of the viscosity at $1s^{-1}$, and n is the power law index. If n=1 the fluid is Newtonian, whereas lower values of n show the fluid demonstrates shear thinning behaviour (as discussed in Chapter 1). One of the limitations of the power law model is that it applies over a specific region, so may not fit the data well at shear rates above and below this. There are a range of other models that describe more fully the behaviour over the whole regime. The Carreau model can be used when a fluid exhibits a Newtonian behaviour at low shear rates, and is given by:

$$\eta = \frac{\eta_0}{[1-(\lambda\dot{\gamma})^a]^{\frac{1-n}{a}}}$$

Where η_0 is the viscosity in at zero shear rate in Pa.s, λ is the relaxation time in s, n is the power law index, and a signifies the width of the transition from $0s^{-1}$ and the start of the power-law region.

2.3.1 Rheometry

The flow behaviour of molten polymers can be characterised by rheometry through measuring the response to a well-controlled deformation. There are different types of rheometers depending on the information required; some can

provide data over a whole range of conditions, whilst others give a single piece of data which can be used to identify variations in batches of a polymer.

Rheometers can give information on the characteristics due to shear, extension and viscoelasticity, as well as flow phenomena such as slip and rupture. The relationship between shear stress and shear strain rate provides information on shear viscosity. The critical shear stress and shear rate can be observed by moving from steady flow conditions where the extrudate is smooth, to the onset of melt fracture where the appearance of the extrudate changes due to stick-slip behaviour.

The time dependence of the response of the polymer due to the viscoelastic nature must be accounted for and although it is not possible to create ideal steady shear conditions, flow in a capillary, between plates or concentric cylinders can be used. The flow behaviour of molten polymers is highly dependent on temperature so it must be accurately controlled. The main assumptions when investigating the rheology of materials are that the melt is incompressible, the density is constant through the flow and there is no preferred direction of the melt at rest.

2.3.1.1 Melt Flow Rate Testing

Melt Flow Rate (MFR) testing is an example of a rheometer which provides a single measurement to give an indication of the flow behaviour of a polymer under certain conditions. The test determines the amount of polymer that flows in a period of time, with units in g/10mins. The test conditions for various polymers are specified in international standards such as ASTM 1238 (2013) and ISO 1133 (2011), ensuring consistency and making MFR testing a widely used tool in industry.

The MFR indexer contains a heated barrel in which a capillary die is located. Polymer granules or pellets are heated in the barrel for a pre-determined time, and extruded by means of a piston loaded with a certain mass. The extrudate is collected during a given period of time and weighed to determine the MFR of the material. If the MFR indexer has the capability to measure the position of the piston and the melt density of the polymer at the test temperature is known, the MFR can be determined using the Melt Volume Rate (MVR).

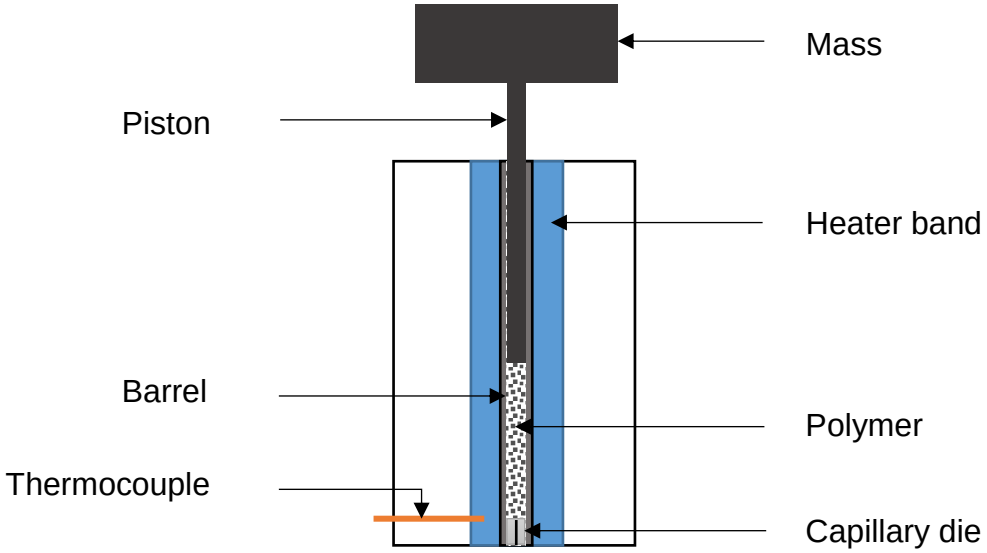

Figure 2.3: Diagram of a Melt Flow Rate indexer

MFR is not a rheological parameter and does not provide information on the viscosity of a polymer, as it represents a single point on a flow curve. It is possible for polymers to have the same MFR but behave entirely differently. MFR can be used as an indication of molecular weight, and is particularly useful for fluoropolymers as there is a lack of suitable methods for directly measuring the molecular weight of these materials.

2.3.1.2 Capillary Rheometry

The arrangement of a capillary rheometer is similar to a MFR indexer in that it contains a heated barrel in which a capillary die is located. Polymer granules or pellets are heated in the barrel for a pre-determined time and extruded through the die. Whereas the piston is loaded with a given mass in MFR testing, the piston is driven at a controlled rate in a capillary rheometer. The piston can be set to run at several different speeds during a test, allowing the flow to be investigated at a range of shear rates.

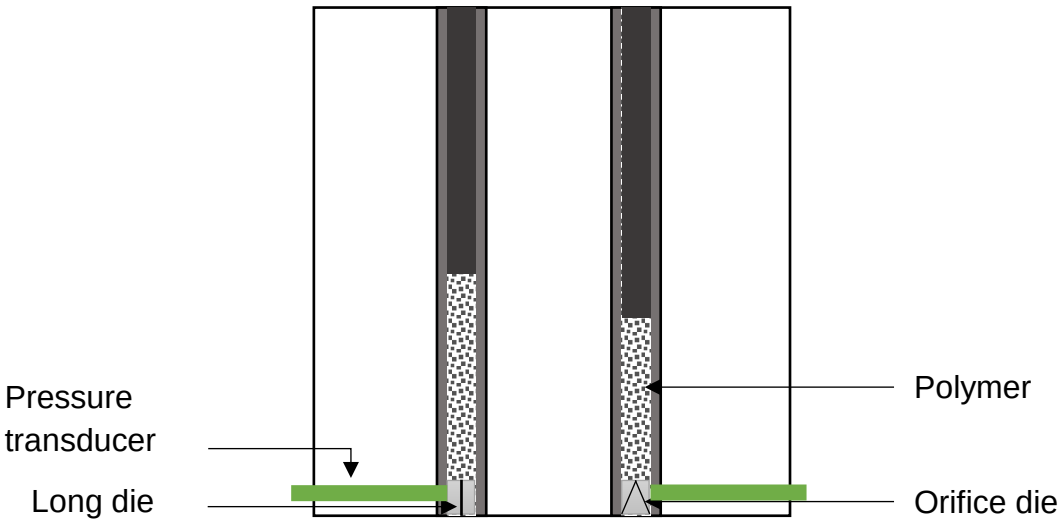

Figure 2.4: Diagram of a twin bore capillary rheometer

The melt pressure drop and the piston speed are used to determine the wall shear stress and wall shear rate using equations from Poiseuille law for capillary flow. The pressure of the melt is measured just above the die, which enables the shear stress to be calculated using:

$$\text{Wall Shear Stress, } \tau = \frac{R\Delta P}{2L}$$

Where R and L are the radius and length of the capillary, and ΔP is the pressure drop.

$$\text{Wall Shear Strain Rate, } \dot{\gamma} = \frac{4Q}{\pi R^3}$$

Where Q is the volumetric flow rate. The relationship between shear stress and shear strain rate for shear viscosity has already been given.

These equations provide apparent flow properties as there are various sources of error, listed by Cogswell (1981) as:

- Reservoir and friction losses
- Ends pressure drop
- Non-parabolic velocity profile
- Slip at the die wall
- Influence of pressure on viscosity

- Influence of pressure on volume
- Influence of heat generation
- Influence of decompression on temperature
- Modification of the material due to work in the die

Cogswell (1981) recommends corrections of the errors due to reservoir and friction losses and ends pressure drop, with the others thought to be mutually cancelling, especially those arising from generation of pressure and heat.

The barrel of the rheometer is essentially a larger capillary, so the system actually consists of two capillaries in series. During a test the piston moves down the barrel, shortening the length of the larger capillary and affecting the flow. To avoid this effect, the pressure is measured just above the die. This also removes any error arising from the friction between the piston and the barrel wall if the pressure was to be obtained from the force on the piston.

The ends pressure drop occurs as the melt enters and leaves the die. The entry pressure drop is more significant and is due to the energy required for the melt to move from the barrel into the capillary. This can be corrected using a twin bore arrangement, which allows pressure measurements to be taken simultaneously on both a long and short die. The pressure reading using only a long die gives the pressure change due to both shear and extensional viscosity. This can be corrected by using an orifice die, shown below in Figure 2.5.

Figure 2.5: Diagram showing capillary in a long die compared to a short die

This “infinitely” short die measures only the pressure due to extensional viscosity which is taken from the long die reading to give pressure due to shear flow only (ΔP). This pressure correction is known as the Bagley correction, and the resulting shear stress is given by:

$$\tau = \frac{R(\Delta P_L - \Delta P_O)}{2L}$$

Where ΔP_L is the long die pressure drop and ΔP_O is the orifice die pressure drop.

2.4 Summary

In conclusion, extensive research has shown there to be a general lack of information published concerning the effects of processing on melt processable fluoropolymers, particularly in regard to transfer moulding of perfluoroalkoxy. Much of the information available has been produced by the fluoropolymer manufacturers themselves, with varying levels of supporting data presented. This research therefore fills an obvious gap in understanding the effect of processing on perfluoroalkoxy.

Chapter 3

Experimental Equipment and Materials

Introduction

This chapter describes the equipment and materials used to conduct the experimental work in this study. The design and validation of a bespoke capillary rheometer is explained, along with the instrumentation and data acquisition system. Details are provided of the equipment used to carry out Melt Flow Rate (MFR) testing, tensile testing, Differential Scanning Calorimetry (DSC), and various forms of spectroscopy: Fourier Transform Infrared (FTIR), Near Infrared (NIR), and Raman. An overview of the materials used in the study is given, with details of the methods of preparation of the various samples required for the study also included.

3.1 Capillary Rheometer

Perfluoroalkoxy (PFA) is corrosive when molten so it is not possible to investigate rheological properties of the material without detrimentally affecting standard characterisation equipment. The apparatus used in this study was designed specifically for the project, with the barrel of the rheometer constructed from Hastelloy® C276 to prevent deterioration with prolonged exposure to PFA at high temperature. To ensure a high level of confidence in the results, tests were first conducted using Low Density Polyethylene (LDPE) and compared to data obtained from a Rosand RH10 twin bore capillary rheometer.

3.1.1 Mechanical Design

3.1.1.1 Overview

The rheometer design was based on a standard single bore capillary rheometer, as shown below in Figure 3.1.

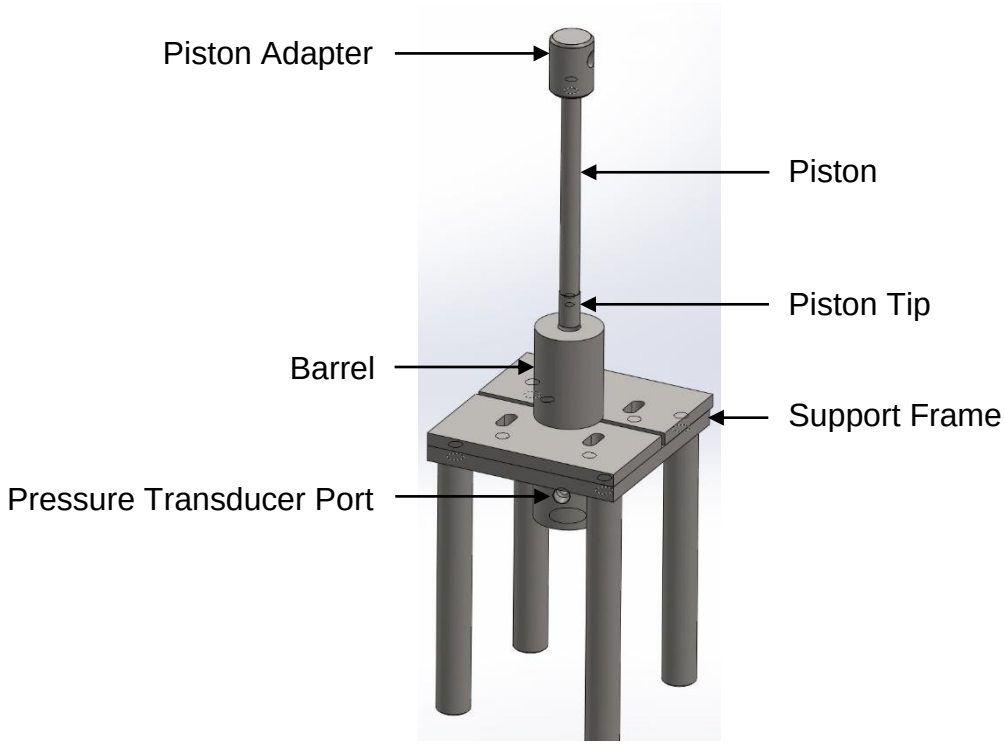

Figure 3.1: 3D model showing the rheometer assembly

The overall length of the Hastelloy® C276 barrel was 150mm with a bore of diameter 15mm, enabling standard capillary rheometer dies to be used. The internal surface was polished, ensuring a smooth finish to reduce pressure losses in the melt due to friction.

The external surface of the barrel had a 10mm deep groove cut circumferentially to accommodate the support frame at the centre of the body. The rheometer body was fixed to a support frame to allow collection of sample material. This was a simple arrangement of four legs attached to a base plate, with two clamping plates to hold the body. Heater bands were located around the two sections of the body to ensure the barrel was uniformly heated. The heater bands had an internal diameter of 50.8mm and were 60mm wide with the centre of the thermocouple hole 25mm from the edge.

The entrance to the barrel had a 10° taper to help guide the piston into the barrel. In order to prevent damage to either the piston or the internal surface of the barrel, the piston head was made from phosphor bronze.

To allow measurement of the pressure and temperature of the PFA, a ½”-20UNF port was required to locate a transducer, the details of which will be

provided in the section concerning instrumentation. A die nut holder was made to ensure the pressure transducer sat directly above the entrance to the die.

The equipment was originally designed to allow use of 1±0.005 mm standard tungsten carbide dies, however preliminary tests during commissioning showed the pressure took too long to equilibrate using these dies. To reduce the time taken for the pressure to equalise additional dies were manufactured from stainless steel with 2±0.005 mm and 3±0.005 mm diameter bores.

The condition of the piston head and the dies was checked periodically to ensure they were not compromised by corrosion.

3.1.1.2 Messphysik Tensometer

The arrangement was located on a Messphysik tensometer, with the crosshead providing a means of moving the piston within the rheometer body, see Figure 3.2 below.

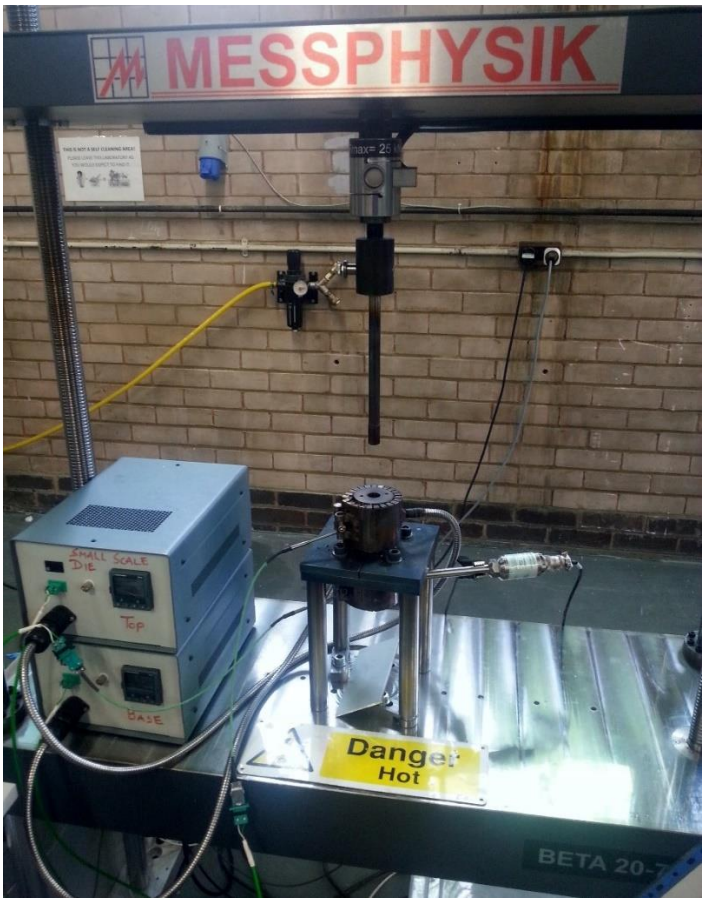

Figure 3.2: Photograph showing experimental arrangement of the capillary rheometer arrangement

The piston was connected to the tensometer crosshead with an adapter piece, labelled in Figure 3.1. PFA is highly viscous, so the whole assembly was attached to the lower platen of the tensometer to prevent it from lifting when the piston was retracted from the barrel on completion of a test. Fixing the assembly in place also ensured the bore of the barrel remained aligned with the piston to allow smooth travel. Detailed information on the tensometer is provided later in this chapter, as the same equipment was used for tensile testing of compression moulded samples of PFA material exposed to various process conditions.

3.1.1.3 Blockprogramming Control Software

The piston speed of the rheometer was controlled through the Messphysik tensometer Plastics Tensile Test software. Sequences were created using the blockprogramming function of the tensometer, allowing the Hastelloy® rheometer to run stepped shear tests similar to standard capillary rheometers. Examples of these tests are given in the section describing the experimental methods used. The blockprogramming function also enabled PFA samples to be produced that had been subjected to known shear rates; the relevant program is included in the discussion on the preparation of sample material.

3.1.2 Instrumentation

3.1.2.1 Melt Pressure and Temperature Measurement

Pressure drop measurements of the molten polymer were made using a Terwin 2000 series pressure transducer. The transducer was fitted with an integral J type thermocouple, allowing the temperature of the melt to also be recorded. This provided a way to ensure a) the PFA had reached the desired temperature and b) the temperature of the PFA was consistent through the length of the rheometer barrel.

Figure 3.3: Photograph showing experimental arrangement, in particular the location of the pressure transducer

Commonly, pressure transducers contain mercury or sodium-potassium, however the Terwin transducer is made solely from stainless steel at is has been designed to be suitable for food and pharmaceutical applications. The transducer consists of a rigid stem with strain gauge housing at one end, and a diaphragm at the other. The pressure applied to the diaphragm by the molten polymer is transmitted through the stem to a four-arm bonded foil Wheatstone bridge strain gauge. The housing of the strain gauge was directly connected to the end of the stem, however a flexible connection between the stem and housing is also common to reduce the temperature the strain gauge housing is exposed to. The maximum operating temperature of the diaphragm is 450°C, whilst the strain gauge is rated to 200°C. The repeatability is quoted as within ±0.1% of the full range output and the combined error within ±0.5% of the full range output. The working range of the transducer is 0-15,000 PSI, with the maximum pressure it is able to withstand being 25,000 PSI. The Terwin transducer, similar to many pressure transducers, contained a shunt resistor allowing indirect linear calibration from 0-80% of the full scale output with an associated error of ±0.1%.

3.1.2.2 Integrated Tensometer Load Cell

The tensometer is fitted with a 25kN load cell with a load resolution of 1:180,000. In this specific application the load cell provided a means to control the force the piston exerted on the PFA during the melting phase. Data from the load cell was recorded and the pressure the piston exerted on the PFA could be calculated. This enabled a comparison to be drawn with the data collected from the pressure transducer, which was particularly useful during the commissioning stage.

3.1.2.3 Extensometer

The Messphysik has a built in extensometer, which measures the change in length of the sample during tensile testing. In this specific application where the crosshead of the tensometer is responsible for the movement of the piston within the capillary rheometer arrangement, the extensometer provides data on the displacement of the piston. This information can then be manipulated to ensure the piston is moving at the required speeds.

3.1.3 Data Acquisition System

3.1.3.1 Hardware

The analogue pressure and temperature signals were fed into a Terwin µ400P series universal programmable process indicator via a 3m Teflon coated 8 core and screen cable assembly fitted with a D8 strain relief connector. The process indicator could be programmed to give outputs in the ranges of 0-5V, 0-10V, 0-20mA or 4-20mA, and was connected to a Pico Technology TC08 eight channel thermocouple data logging device. The TC08 unit transferred the pressure and temperature readings via USB to a PC running Windows XP. The process indicator displayed live pressure readings from the transducer and was useful in validating the data shown on the PC.

TC08s can be used in various applications as they have a wide operating temperature range from -270°C to +1820°C, and can also measure voltage. The maximum sampling rate of a TC08 is 10 samples per second, however a sampling rate of 1 sample per second gave sufficient resolution for this work. The conversion time is given as 100ms, with an additional 100ms for cold junction compensation. The accuracy of temperature readings is stated as the

sum of ±0.2 and ±0.5% °C, whilst the voltage accuracy is the sum of ±0.2 and ±10μV.

3.1.3.2 Software

PicoLog data acquisition software was used to record the PFA melt pressure and temperature data from the transducer. PicoLog is a Windows based package allowing real time collection, analysis and display of data. The data can be shown in numerical or graphical format, and exported to databases or saved in spreadsheet compatible comma separated variable (CSV) files. The software can collect up to a million samples, and has the ability to support multiple Pico data logging devices.

The Messphysik Plastics Tensile Test software not only provided control of the tests through the blockprogramming function, but also collected data from the load cell and extensometer of the tensometer. The rate of data sampling of the software was 500 samples per second.

3.1.4 Validation Study

A validation study was conducted using Low Density Polyethylene (LDPE) to ensure the data generated from the Hastelloy® capillary rheometer is reliable. This was necessary as there is very little data published on the rheology of PFA to compare the experimental results of this study to. Verification using standard capillary rheometer equipment was not possible due to the corrosive nature of molten PFA.

3.1.4.1 Experimental Detail

The viscosity of Dow LD150R LDPE material was investigated at eight shear rates in the range 50-5000s^{-1} using a Rosand RH10 twin bore capillary rheometer.

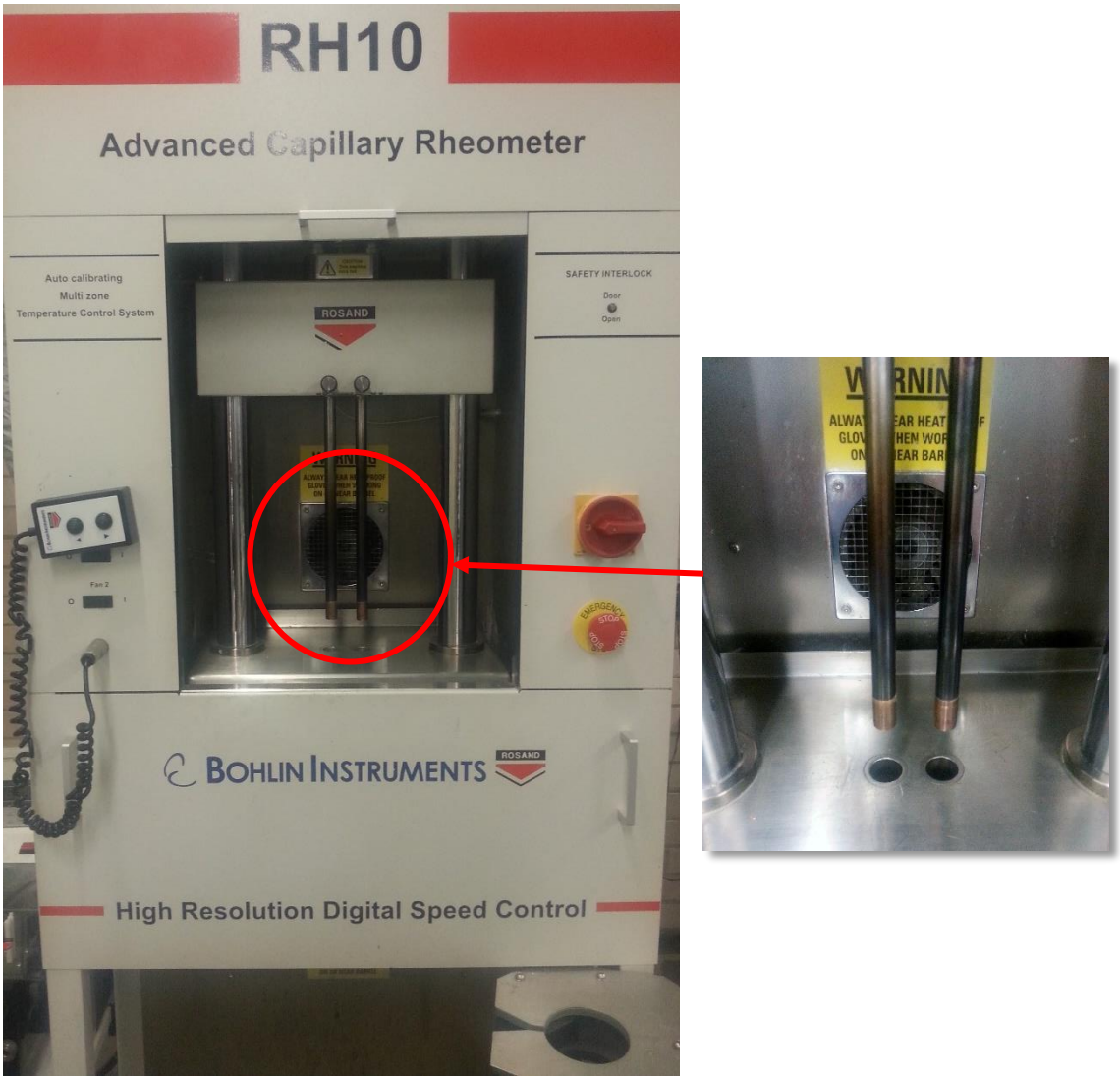

Figure 3.4: Photo of the Rosand RH10 capillary rheometer, inset shows a close up of the twin bore arrangement

The Hastelloy® rheometer was set to run at the same shear rates using the blockprogramming function within the Messphysik tensometer Plastics Tensile Test software. Preliminary tests were conducted with both the long and orifice dies to determine the times required at each shear rate for the pressure to equilibrate. In order to obtain a single pressure value at each shear rate the pressure was plotted against time, and an average value calculated over the period during which the pressure was stable.

3.1.4.2 Results

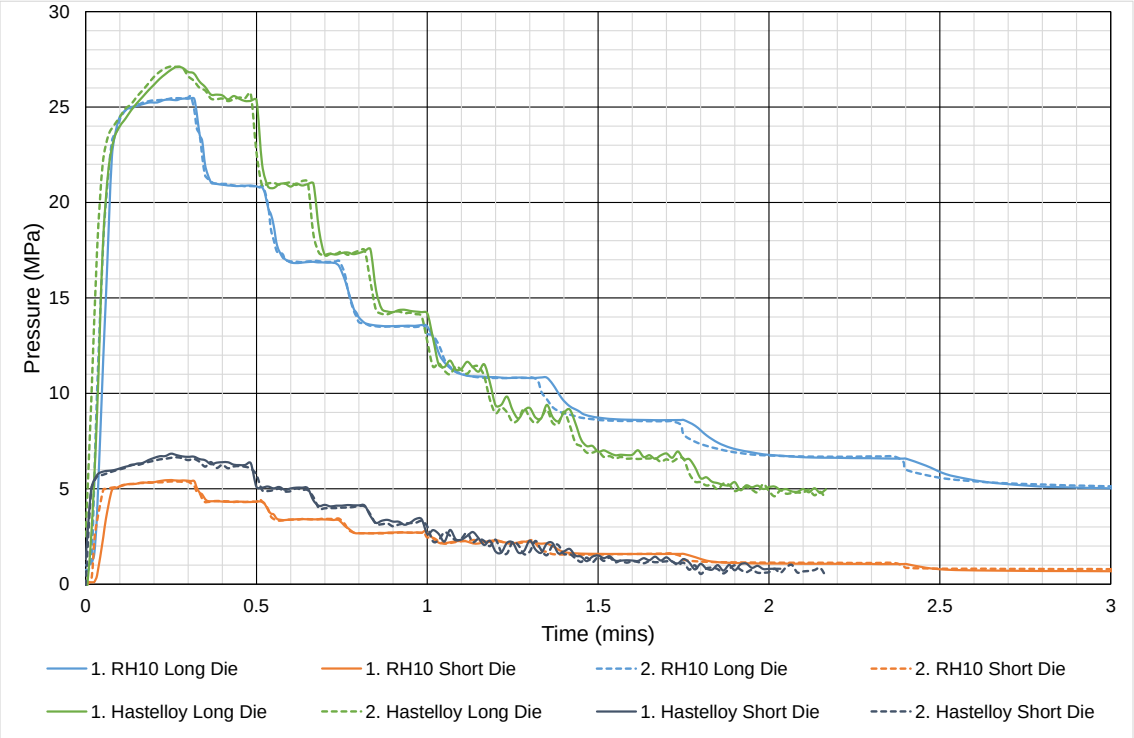

Figure 3.5: Graph showing pressures during two eight step decreasing shear tests conducted on the RH10 compared to four tests run on the Hastelloy® rheometer (two using each die)

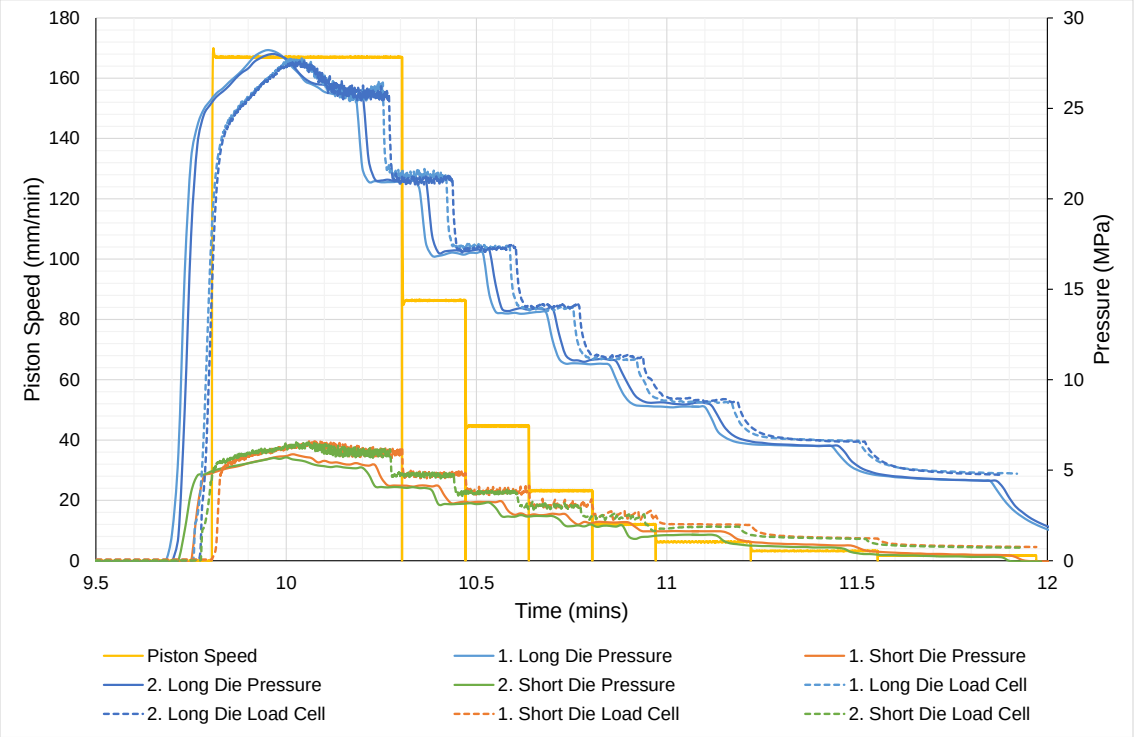

Figure 3.6: Comparison of pressure readings from the transducer located just above the die, and those calculated from the integrated load cell readings.

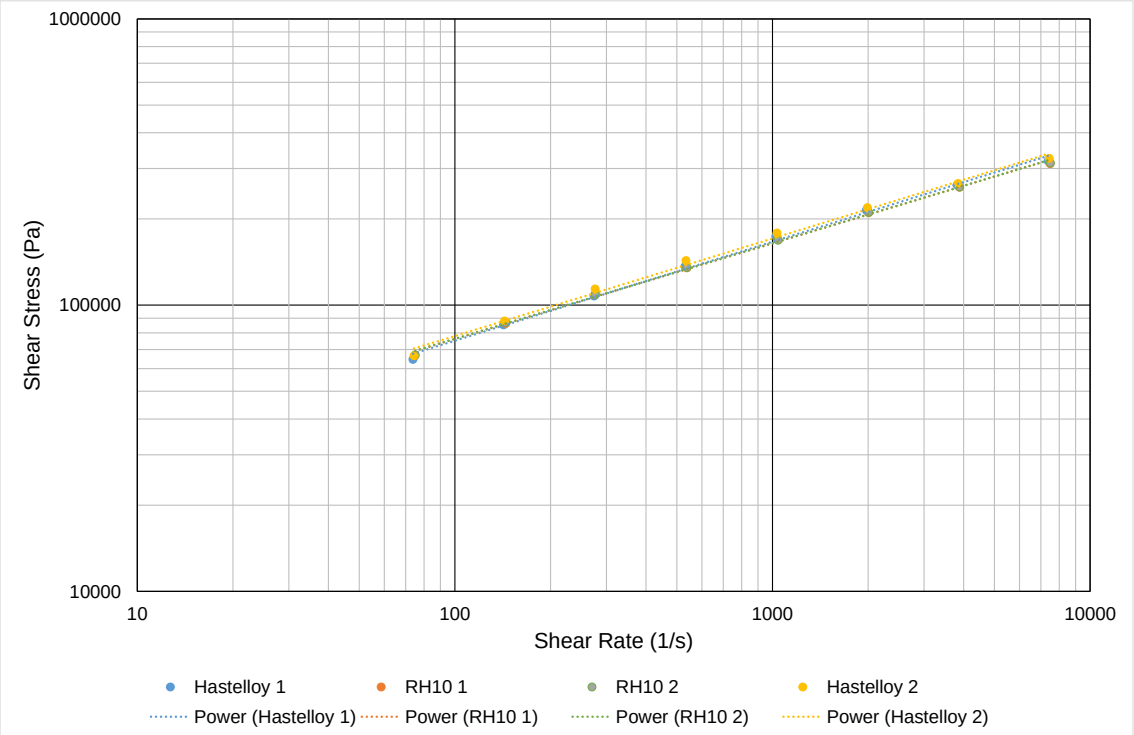

Figure 3.7: Bagley and Rabinowitsch corrected shear stress vs. shear rate data from RH10 and Hastelloy® rheometers

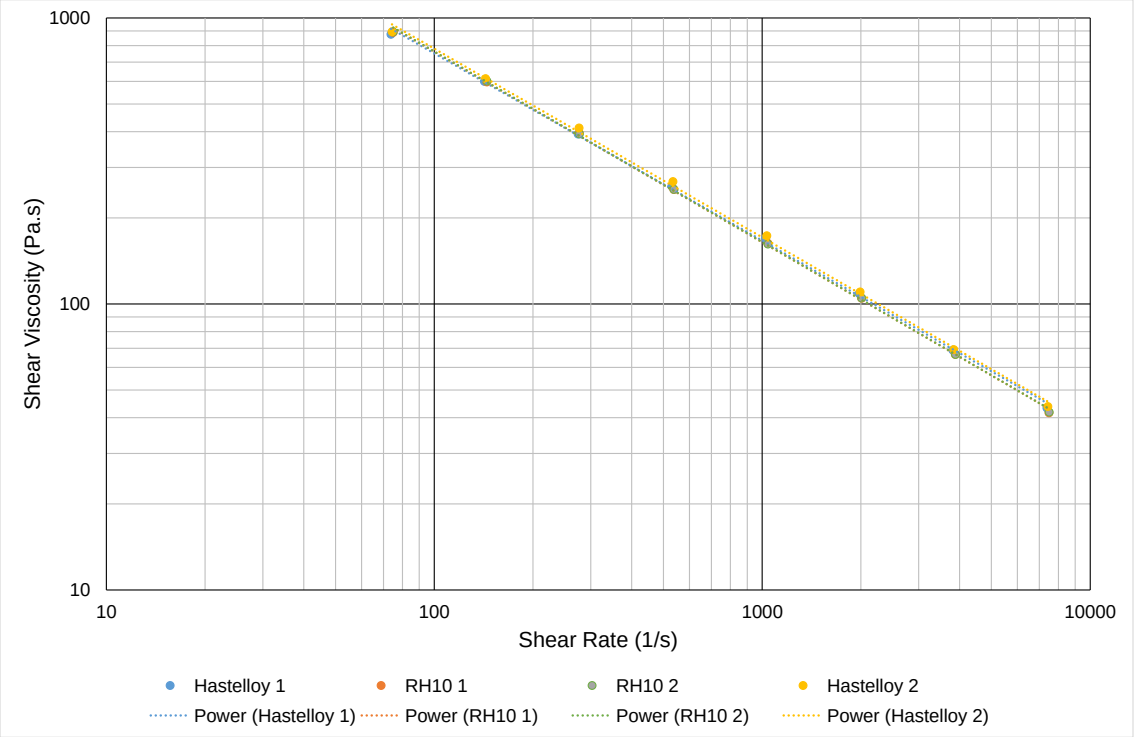

Figure 3.8: Bagley and Rabinowitsch corrected data showing viscosity with shear rate of LDPE with power law fit of data from RH10 and Hastelloy® rheometers

Figure 3.5 shows good agreement of the pressure data collected from the tests conducted using the RH10 and the Hastelloy® rheometer. The barrel of the Hastelloy® rheometer is much shorter than that of the RH10, so a relatively low compression force was applied during the melt phase to prevent excessive loss of LDPE material. This is likely to be the reason behind the pressure taking slightly longer to equalise at first using the Hastelloy® rheometer. The data from the repeats also shows the results are consistent, which provides a high level of confidence in the equipment.

The data presented in Figure 3.6 shows the pressure readings obtained from the transducer and those calculated from the integrated tensometer load cell to concur. The slight difference in time is due to using two monitoring systems, and does not cause any issues as we are only interested in average pressure readings once the system has stabilised.

The data collected using the RH10 and Hastelloy® rheometer agrees very well, as shown in Figures 3.7 and 3.8. Shear stress increases with an increase in shear rate, and viscosity decreases with increased shear rate as expected.

	K (Pa.s^n)	n
RH10	18800 ± 35	0.334 ± 0.001
Hastelloy®	18000 ± 552	0.343 ± 0.003

Table 3.1: Values of the power law and consistency indices (n and K) of LDPE obtained from the experimental data

3.1.4.3 Conclusion

The rheological data on LDPE obtained using the custom-built Hastelloy® rheometer concurs with that gained from a standard capillary rheometer. This work demonstrates the equipment works as intended, and provides confidence in the experimental data when investigating the rheological properties of PFA.

3.1.5 Experimental Methods

Studies conducted on the rheometer examined the effect of temperature, residence time, shear and typical processing history on the viscosity of the material.

As the Hastelloy® rheometer was single bore, each test sequence was conducted twice using two capillary dies: one long and one orifice die. These dies had 180° entrance and exit angles and dimensions 16 x 2±0.005 mm and 0.25 x 2±0.005 mm. This enabled the shear stress to be modified in order to take into account the pressure drop through the length of the die (Bagley correction).

The effect of temperature on the viscosity of unprocessed material was investigated at three relatively low shear rates, the test program for which is shown below in Sequence 3.1.

RAMP LOAD 50 1000N 0 1 0 0

STOP

CLOCK 6 min

RAMP LOAD 50 1000N 0 1 0 0

STOP

CLOCK 3 min

SPEED 6.67 mm/min

DOWN

CLOCK 60 sec

SPEED 13.34 mm/min

DOWN

CLOCK 30 sec

SPEED 26.67 mm/min

DOWN

CLOCK 20 sec

The initial melt phase of a standard capillary rheometer is achieved using the ramp and timer commands. This was used for each test to ensure the polymer had melted satisfactorily. The load was determined experimentally, with 1000N found to be suitable for the 16mm long die. Due to the relatively short length of the rheometer, this had to be reduced to 500N for the orifice die to prevent excessive loss of material prior to the experiment.

Sequence 3.1: Program used to determine effect of shear rate and temperature on viscosity.

On completion of a test, the piston was held in position and the temperature of the heaters was increased by 10°C. Once the controllers were showing the new set temperature had been reached, the program was repeated to obtain pressure data at the same shear rates. This procedure was carried out three times to obtain data at three different temperatures on the same charge of polymer.

All experiments to determine the dependence of viscosity on shear rate for the various samples of PFA material were conducted at 370°C between 5-400s^{-1}. Tests conducted on the PFA subjected to various residence times required manual compression to ensure there was sufficient material to obtain results at all shear rates.

RAMP LOAD 50 1000N 0 1 0 0

STOP

CLOCK 6 min

RAMP LOAD 50 1000N 0 1 0 0

STOP

CLOCK 3 min

SPEED 1.34 mm/min

DOWN

CLOCK 180 sec

SPEED 2.50 mm/min

DOWN

CLOCK 90 sec

SPEED 4.67 mm/min

DOWN

CLOCK 60 sec

SPEED 8.72 mm/min

DOWN

CLOCK 60 sec

SPEED 16.35 mm/min

DOWN

CLOCK 20 sec

SPEED 30.41 mm/min

DOWN

CLOCK 15 sec

SPEED 57.08 mm/min

DOWN

CLOCK 15 sec

SPEED 106.68 mm/min

DOWN

CLOCK 15 sec

A ramp rate of 50N/s was found to be sufficient to achieve the load within a relatively short period of time, without causing a significant overshoot.

A stop command was required to prevent the load being maintained during the melting time which would have resulted in an excessive loss of polymer.

Software from a Rosand RH10 capillary rheometer was used to determine the shear rates of each of the stages, from which the speed of the piston could be calculated.

The direction of piston travel needed to be specified.

The periods of time at each shear rate had to be determined experimentally. The stage needed to last long enough for the pressure to have equalised to provide an accurate reading, but must be minimised to ensure there is sufficient polymer remaining in the barrel for subsequent stages in the experiment. Again, this had to be adjusted for the orifice die which often lost more material during the melting phase, but this was compensated by the pressure equilibrating significantly faster.

ENDTEST

Sequence 3.2: Program for melting and determining viscosity of PFA at 8 shear rates in the region 5-400s^{-1}.

On completion of a test, the data was saved into spreadsheet compatible form. The pressure data from the melt transducer was analysed to gain an average value of the pressure after it had equalised at each shear rate. Tests were repeated three times to allow average values to be calculated.

3.2 Melt Flow Rate Testing

As discussed in the background, Melt Flow Rate (MFR) testing provides information on the amount of material that flows under a specified set of conditions in a certain period of time. The units of MFR are given in g/10mins, with lower values indicating a high viscosity and vice versa. A Ray-Ran 5 Series Advanced Melt Flow System Melt Flow Indexer (shown in Figure 3.9 below) was used to determine the MFR of samples of PFA exposed to a range of process conditions. The effect of temperature on the MFR of the unprocessed material was also investigated by altering the temperature at which the test was carried out.

Figure 3.9: Photo showing the Ray-Ran 5 Series Advanced Melt Flow System Melt Flow Indexer

The length of the barrel of the Ray-Ran 5 Series Advanced Melt Flow System Melt Flow Indexer was 162.61 ± 0.01mm. The bore of the barrel measured at the top, middle and bottom were 9.5542 ± 0.007mm, 9.5555 ± 0.007mm, and 9.5524 ± 0.007mm respectively. The temperature of the barrel could be set between 0-400°C, with the temperature profile of the cylinder at various distances from the test die given in Appendix D.

ASTM 1238 (2013) requires a 5.000kg load for testing the MFR of PFA, which was comprised of a 4.6669 ± 0.0233kg mass to account for the 0.3243 ± 0.0016kg piston arrangement. The diameter of the piston tip was 9.4678 ± 0.0070mm, with a length of 6.3754 ± 0.1000mm. Due to the low MFR of PFA, a standard die was used with dimensions: 2.0916 ± 0.0051mm (bore), 9.4780 ±

0.0076mm (diameter), and 8.018 ± 0.025mm (length). The die was made from Hastelloy® to prevent the surface or dimensions being affected by corrosion. The piston and cylinder liner were also made from Hastelloy® for the same reason.

The indexer has a multi-slicing feature, which provides 20 values of MFR over 5mm of travel in one test. The MFR is calculated using the density of the molten polymer at the test temperature and the volumetric flow rate. The piston travel is measured by an encoder with a resolution of 0.01mm, with the timer having an error of 0.07%. This meant tests to determine the effect of processing could be carried out simultaneously according to both Procedure A and Procedure B of ASTM 1238 (2013).

The die and piston were inserted into the bore of the cylinder during the initial heating of the machine to allow them to reach the set temperature of 372°C required by ASTM 1238 (2013). The equipment was allowed to stand for at least 15 minutes prior to commencement of testing to ensure the temperature had stabilised. The polymer charge was subjected to a pre-heat period of 7 minutes, with the piston and load in place. At the end of the pre-heat period only the higher mark on the piston was visible, indicating the piston to be in the correct position. The material extruded from the pre-heat period was discarded, whilst the extrudate over a 2.5min time period was collected. The extrudate was weighed to the nearest 0.01g using a quadruple beam scale with range 0-200g, and giving an error of ±0.04g/10mins in the MFR determined using Procedure A. The MFR results obtained using Procedure B were printed giving the average value and standard deviation. On completion of tests, the piston and die were removed, cleaned and relocated quickly in order to minimise cooling of the components. Tests were repeated five times to allow average values from both methods to be calculated.

The indexer was also used to obtain information on the change in MFR with temperature. The experimental procedure was identical to the standard one described above other than these tests were conducted between 330-380°C at 10°C intervals, rather than 372°C. Values of the melt density of PFA at different temperatures were not available so tests were conducted using only Procedure A.

3.3 Tensometer

The primary use of the Messphysik tensometer was discussed earlier in this chapter as the means of controlling the piston speed of the capillary rheometer via the moving crosshead. This section describes one of the more common uses of the equipment: testing the tensile properties of a material.

International standards such as ASTM 638 (2010) and ISO 527 (2012) specify the criteria for carrying out tensile testing of plastics, such as preparation of the test pieces, and conditions of testing. Test specimens are cut from sheet material or moulded to dimensions stated in the standard.

Figure 3.10: Example of a PTFE specimen prior to tensile testing

The test specimen is clamped in the jaws of the tensometer, and the extensometer is calibrated to ensure the accuracy of the strain measurements. The crosshead, driven by a motor, moves at a constant speed and the sample is stretched until it breaks.

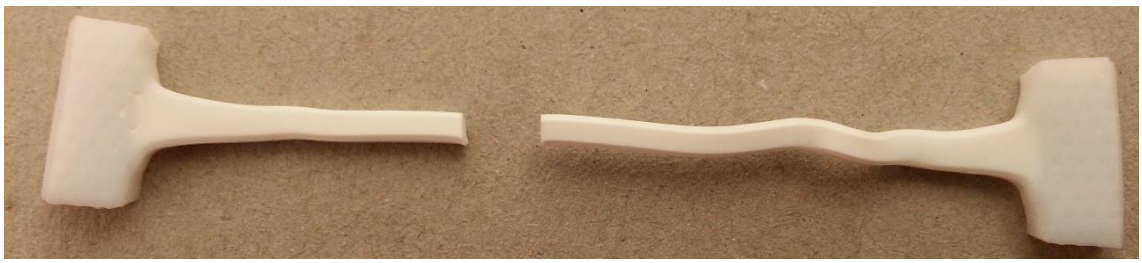

Figure 3.11: Same PTFE specimen as shown in Figure 3.10, after testing

The extent of the movement of the crosshead is determined by the use of limit switches. The change in length of the sample recorded by an extensometer, from which the strain the sample is subjected can be calculated. A load cell measures the force the sample is subjected to as a result of the constant speed deformation, and with manipulation gives the stress the piece is subjected to.

Various graphs can be plotted using the software, most commonly plotted is stress against strain. A range of values can also be calculated such as the elongation at break, the tensile strength and the yield point of the material.

The tensometer used in this work was a Messphysik Beta 20-7, 5/8 x 18 complete with 25kN load cell. The load capacity was rated at 20kN, with a testing speed range of between 0.001 – 750mm/min. The accuracy of the testing speed is quoted as better than 0.2%, with the resolution of standard speed/position control of 0.1µm.

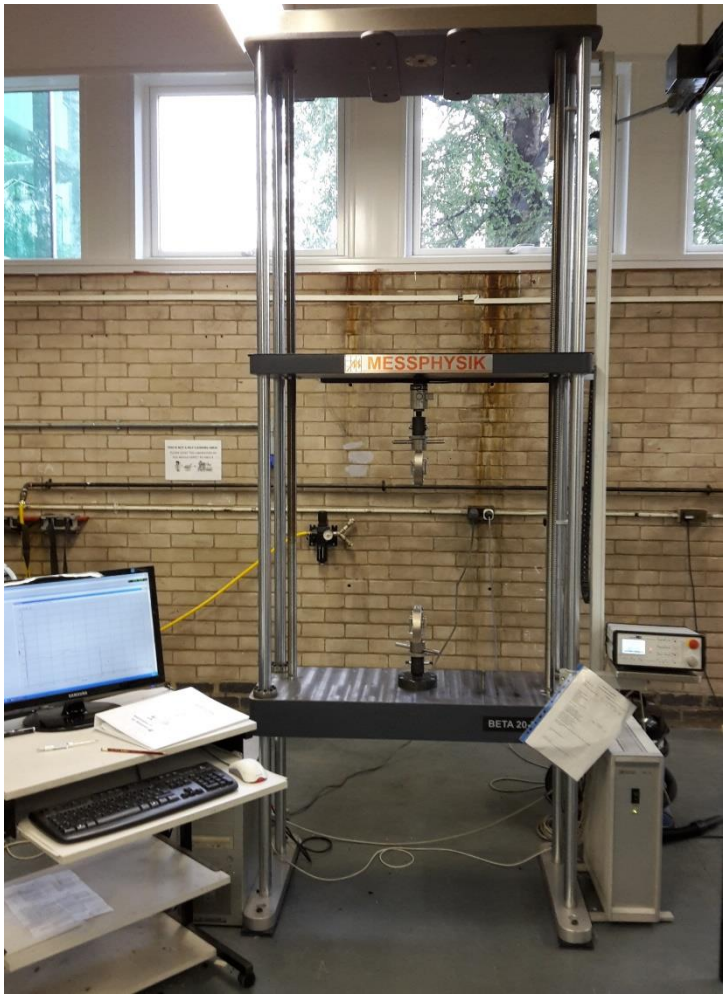

Figure 3.12: Messphysik Tensometer used in this work

Plaques of PFA were compression moulded using a heated press, details of which can be found in the section on the preparation of samples included at the end of the chapter. Test specimens were cut from these plaques using a Type 4 die cutter as detailed in ISO 37 (2011). The width and thickness of the narrow section of the sample was measured prior to testing using digital callipers with an accuracy of 0.01mm. The Plastics Tensile Testing software of the

Messphysik was used to test the samples at a speed of 50mm/min as defined by ASTM 3307 (2010). The extension of the sample was measured by the extensometer, whilst the force exerted on the material was detected using the load cell. The results were recorded using the Plastics Tensile Testing software and exported to a spreadsheet compatible file format for processing. The dimensions of the sample prior to testing were used to calculate the tensile stress from the force data measured by the load cell. Strain data was obtained using the data from the extensometer and the original separation of the jaws of the tensometer. Plotting the tensile stress against strain enabled values of the yield strength and elastic modulus of the different samples to be determined.

3.4 Differential Scanning Calorimetry

Differential Scanning Calorimetry (DSC) is used to determine transition temperatures of polymers by measuring heat flow. Two pans are heated at a constant rate, usually a few °C per minute. One of the pans is the reference, which remains empty, whilst the other contains a sample of a few milligrams. The pans are maintained at the same (changing) temperature, with each pan having energy supplied by independent heaters. The sample pan requires more energy in order to keep it at the same temperature as the reference pan. The difference in the rate of energy supplied between the pans is recorded with either time or temperature.

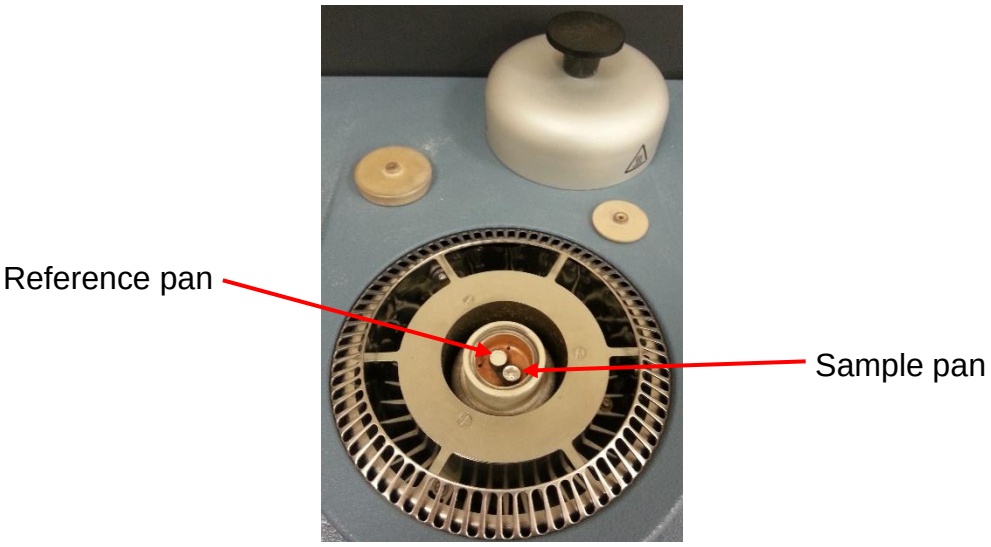

Figure 3.13: Photo showing the sample and reference pans located in the furnace

In order to keep the rate of temperature change constant when the polymer reaches a temperature where a transition, such as melting, occurs the amount of energy supplied must vary. Melting is an endothermic process, meaning energy is absorbed from the surroundings. During the transition the temperature of the sample does not change as the energy is being used to change the structure of the polymer from crystalline to amorphous. More energy is supplied to the sample pan in order to maintain it at the same temperature as the reference pan. This difference in energy supplied appears as a curve on the graph of heat flow rate as a function of time or temperature, an example of which is shown below in Figure 3.14.

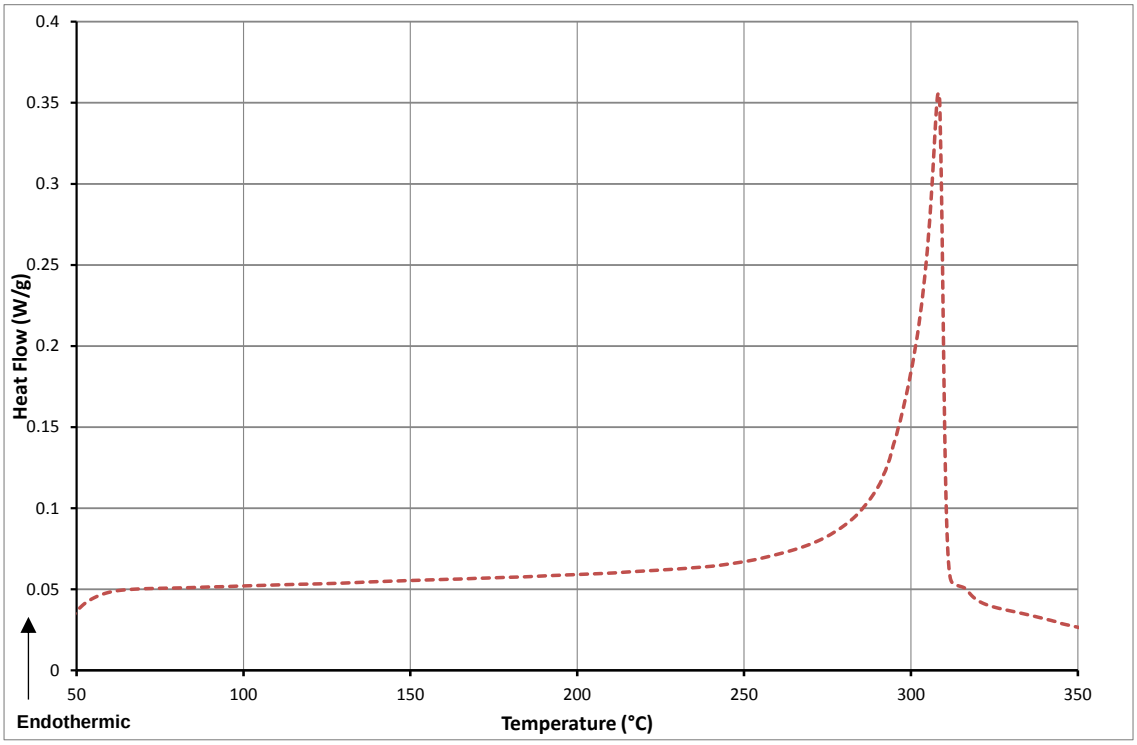

Figure 3.14: DSC trace of heat flow with temperature showing melting transition

Transitions such as crystallisation are exothermic processes which release energy to their environment, giving a subsequent drop in the heat flow to the sample pan.

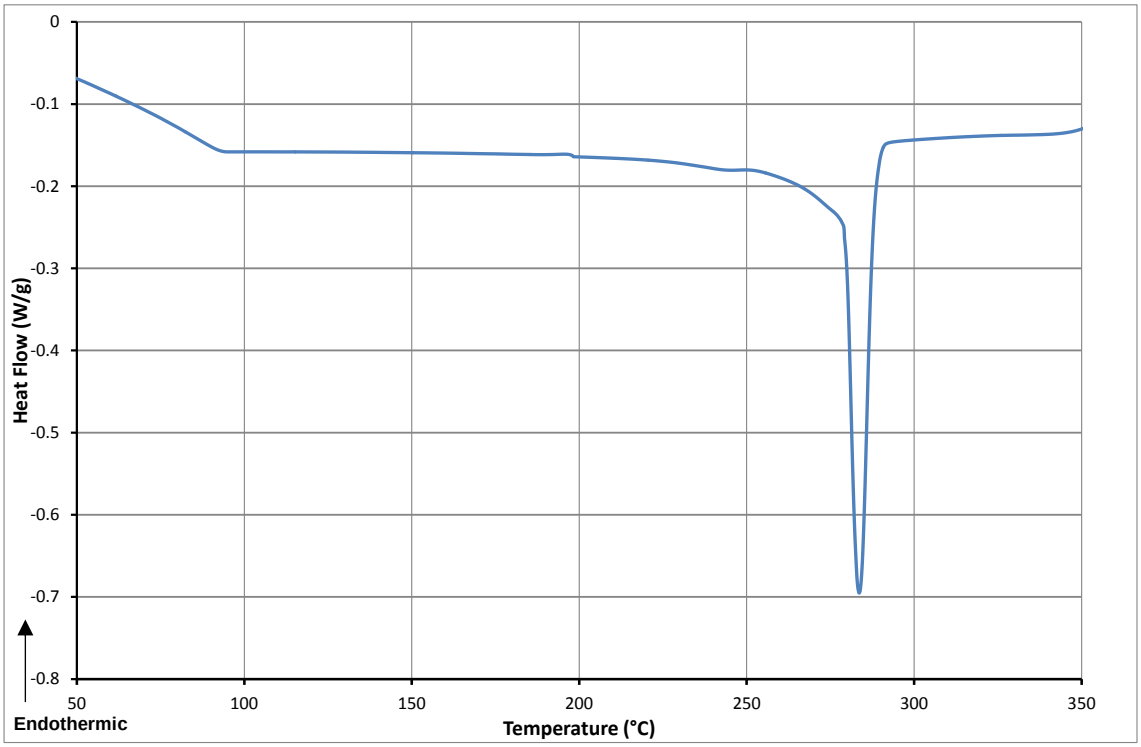

Figure 3.15: DSC trace of heat flow with temperature showing transition at which crystallisation takes place

DSC can determine the changes in a material due to processing by using a heat/cool/heat cycle. The first heat removes the unknown history, whilst the controlled cooling cycle provides known conditions for the second heat. The second heat cycle allows comparisons to be made between materials that have been exposed to different process conditions.

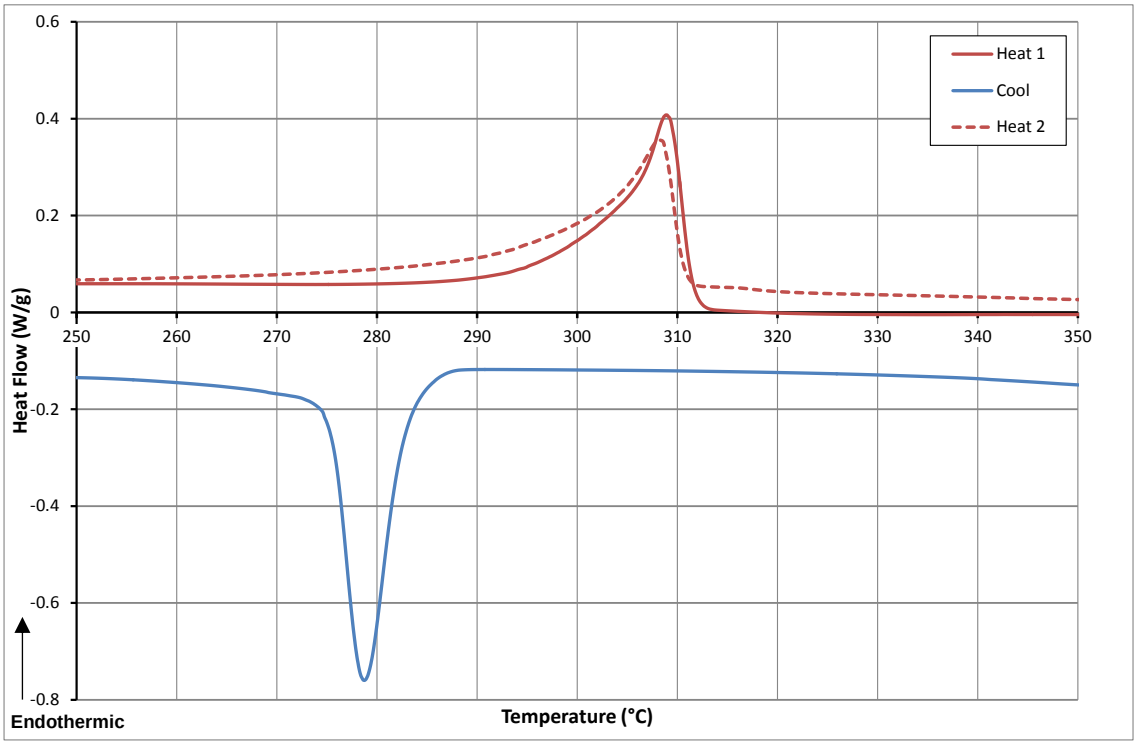

Figure 3.16: Graph showing a heat/cool/heat cycle of a processed material

Figure 3.17: Photo showing the DSC Q20 used in this research

A DSC Q20 was used in this work. It has a temperature range from ambient to 725°C, with a quoted accuracy of ±0.1°C and a precision of ±0.05°C.

Heat/cool/heat test regimes were used with heating and cooling rates of 10°C/min from 40-360°C. This type of test enabled the second heating curves of

polymers exposed to various conditions to be compared to those of unprocessed polymer to shown any changes in the material. The results were exported to a spreadsheet compatible file format for processing. The peak of the endotherm was taken as the melting point, and the enthalpy was calculated as the area under the curve.

3.5 Spectroscopy

Spectroscopy is the study of the interaction of electromagnetic radiation with matter. Infrared spectroscopy can be used to determine the structure of materials through the vibrations of molecules. There are two different ways vibrating molecules can interact with electromagnetic radiation of the appropriate frequency. The radiation can be absorbed if it is of the same frequency of the normal mode of vibration of the molecule. The energy will then be transferred to other molecules or re-radiated. The other way the electromagnetic radiation can interact with the molecule is by scattering. Raman scattering occurs if there is a change in frequency of the radiation due to the scattering. This change in frequency is equal to the one of the normal modes of vibration of the molecule.

An infrared spectrum is collected by passing infrared radiation though a sample and determining the amount of radiation absorbed at each frequency. The frequency of the peaks in the absorption spectrum are the same as the normal modes of vibrations of molecules in the material.

In general, spectrometers emit radiation with a continuous spectrum over a range of infrared wavelengths. They contain a dispersive element to separate the radiation into its fundamental wavelengths. The radiation passes through the sample or is reflected from the surface, and the intensity of the radiation is measured resulting in a spectrum. The spectrum shows the frequencies of the vibrations of the bonds of the atoms in the material, enabling the sample to be identified.

Not all modes of vibration of a particular molecule can be observed by infrared spectroscopy, and similarly with Raman spectroscopy. In order for a mode to be ‘infrared active’ it must have an oscillating dipole moment, whereas for a mode to be ‘Raman active’ it must have oscillating electrical polarisability. This highlights the requirement for both types of spectroscopy.

3.5.1 Fourier Transform Infrared

Fourier Transform Infrared spectroscopy (FTIR) can be used to investigate the mid-infrared range, typically in the range of 400-4000cm^{-1}. It can allow the identification of unknown materials and can be used to detect the composition of a material.

Early infrared spectrometers used a prism to separate the wavelengths, but the scan range was limited and the repeatability was poor. Prism monochromators were replaced by gratings, however the scan speed was low and the wavelength accuracy was poor. Monochromators were replaced by interferometers which have drastically reduced scan times.

Fourier Transform (FT) spectrometers consist of a light source containing the full spectrum of wavelengths to be investigated. The light passes through a collimator to make the light rays parallel, which improves the clarity of the signal. FT spectrometers usually contain a Michelson interferometer, which is a configuration of mirrors. A beam splitter separates the IR source into two, sending one beam to a fixed mirror and the other to a mirror that is moved by a motor. The beams reflect and recombine at the beam splitter, providing a signal referred to as an ‘interferogram’. The interferogram contains data on all the frequencies of the infrared source, so the detector receives the total transmitted intensity as a function of the displacement of the mirror. A Fourier transform is performed on the intensity versus displacement data to separate the wavelengths and obtain the spectrum giving the intensity at each frequency. One of the main benefits of FTIR arises from the simultaneous collection of information from all wavelengths, giving a better signal to noise ratio for a given time, or a shorter scan for a given resolution.

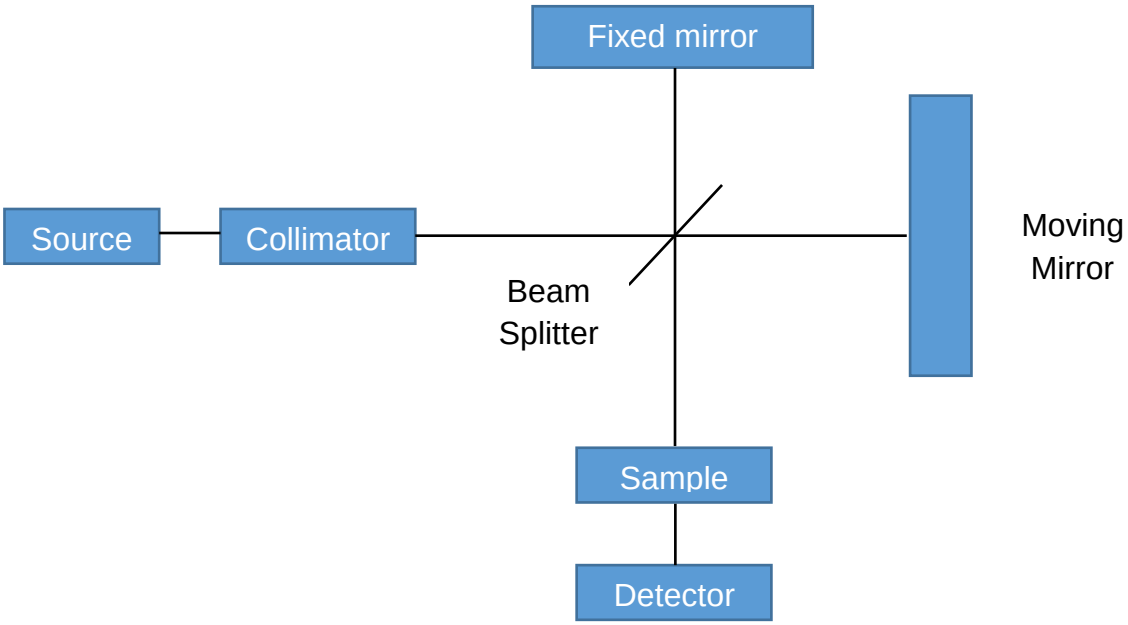

Figure 3.18: Simplified diagram of an FTIR spectrometer

The FT spectrometer used in this study was a Nicolet iS50 FT-IR, as shown below in Figure 3.19. The instrument was equipped with a Tungsten-Halogen white light source with a spectral range of 7800-350cm^{-1}. The optical resolution in the Mid-IR range is quoted as less than 0.09cm^{-1} with a wavenumber precision of better than 0.01cm^{-1}. The signal to noise ratio of a 1 minute scan peak to peak is 4cm^{-1} (55000:1) and with a 5 second scan is 4cm^{-1} (13000:1). The analogue to digital converter of the spectrometer is 24 bit, and runs on a Windows 7 operating system.

The Nicolet iS50 FT-IR has an Attenuated Total Reflection (ATR) module with a round Type IIa diamond crystal of diameter 2.8mm. The sampling zone is 2mm, with a refractive index of 2.4 at 1000cm^{-1}. The module has a 45° angle of incidence (single bounce) and a depth of penetration of 2.0µm at 1000cm^{-1} for a sample material with a refractive index of 1.5. The maximum sample thickness is 12.7mm and the detector is a dedicated broad band DTGS (deuterated triglycine sulphate).

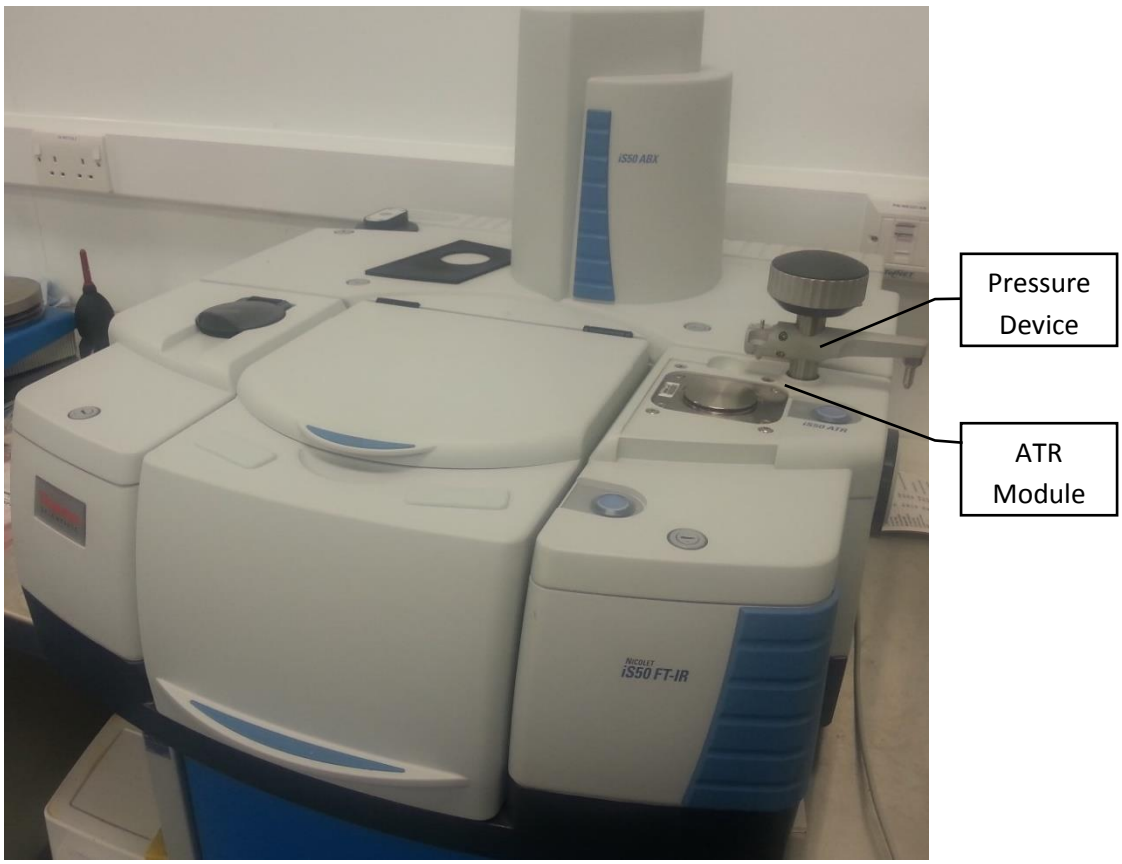

Figure 3.19: Photo showing the Nicolet iS50 FT-IR spectrometer used in this study

ATR uses evanescent waves generated by total internal reflectance. The infrared light passes though the ATR crystal such that it is reflected more than once from the internal surface in contact with the sample. The reflection produces an evanescent wave which penetrates between 0.5-2μm into the sample. The sample absorbs certain frequencies (as previously discussed), and changes in the evanescent wave are picked up by the detector. For the sample to absorb the energy of the evanescent wave the refractive index of the sample must be lower than that of the ATR crystal. To prevent distortion of results the sample must be in good contact with the ATR crystal, this is commonly achieved by used of a pressure device (labelled on Figure 3.19 above). The depth of penetration is determined by several factors: the wavelength of the light, the angle of incidence, the sample being tested, and the indices of refraction of the ATR crystal. The number of reflections can be altered by varying the angle of incidence.

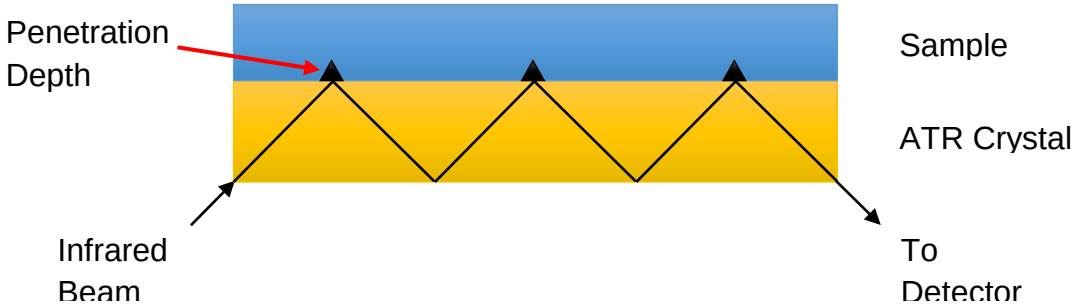

Figure 3.20: Diagram showing how ATR works. Total internal reflectance of the infrared beam in the ATR crystal produces evanescent waves which penetrate the sample. Certain frequencies are absorbed depending on the sample, and the altered beam is picked up by the detector.

Investigation of the materials in this study was conducted using the ATR module to ensure good reproducibility of results and to minimise the preparation of the sample material. A background scan was conducted prior to collection of the sample spectrum to ensure all features seen were as a result of the material itself and not the equipment. The spectra were analysed using Thermo Scientific OMNIC™ software, enabling the wavenumbers of the peaks to be identified. These could then be assigned to the normal modes of vibrations of the molecules to identify the bonds within the material. Scans of material subjected to various conditions allowed investigation of the differences in the material due to prolonged exposure to high temperature or shear rates, the results of which will be presented later.

3.5.2 Near Infrared

Near Infrared (NI) typically refers to the range 4000-14000cm^{-1}, and can penetrate much further than mid-range FTIR. The equipment used for NI spectroscopy is very similar to that used for FTIR spectroscopy, the principles of which are explained in the previous section.

Whereas the mid infrared region gives clean absorption bands enabling the attribution of bonds, NIR produces a more complex spectrum of broad bands making it difficult to identify the structure of the material. Chemometric tools such as Multiple Linear Regression (MLR), Principal Component Regression (PCR) and Partial Least Square Regression (PLS) are commonly used to gain useful information from the data collected. These work by assuming a linear relationship between the data and a property value, such as concentration.

The NIR spectrometer used in this study was an Antaris II NIR, as shown below in Figure 3.21. The equipment has a long life high intensity halogen NIR source, a Michelson interferometer and a high sensitivity high stability matched Indium Gallium Arsenide photodiode detector. The spectrometer has a spectral range of 12000-3800cm^{-1} (833-2630nm) with a resolution of 4cm^{-1} (0.6nm at 1250nm). The wavenumber reproducibility is quoted as better than 0.05cm^{-1} (0.008nm at 1250nm), the wavenumber repeatability gives a standard deviation of less than 0.006cm^{-1} with 10 measurements, and the accuracy of the wavenumber is given as ±0.03cm^{-1} (0.005nm at 1250nm).

Figure 3.21: Photo showing the Antaris II NIR spectrometer used in this work

The spectra of various samples of PFA were taken using the integrating sphere vial. As stated, the main drawback of NIR spectroscopy is the difficulty in assigning specific features to chemical components. Statistical techniques such as Partial Least Squares (PLS) and Principal Component Analysis (PCA) were used in the Thermo Scientific TQ Analyst™ software to investigate the correlation between samples exposed to various residence times.

3.5.3 Raman

Raman spectroscopy differs from infrared spectroscopy in that the spectrum is comprised of the change in frequency of monochromatic radiation due to scattering rather than absorption. The energy of the scattered radiation is in the

region of 10^{-8} – 10^{-6} of the incident radiation, so a high intensity laser is often used in conjunction with a very sensitive detector. The monochromatic light scatters off the sample, is collected by a lens and sent through a monochromator. The elastic scattered radiation is filtered out, with the remaining light dispersed using a notch or band pass filter and picked up by the detector. The light is separated into its constituent wavelengths and the intensity as a function of wavelength or wavenumber is recorded.

The apparatus used in this work was a DXR™ SmartRaman Spectrometer, shown in in Figure 3.22 below. The spectral range is 3500-50cm^{-1}, with a resolution of 5.0cm^{-1}. The measurement area is quoted as 10μm-5mm and the laser wavelength is 532nm.

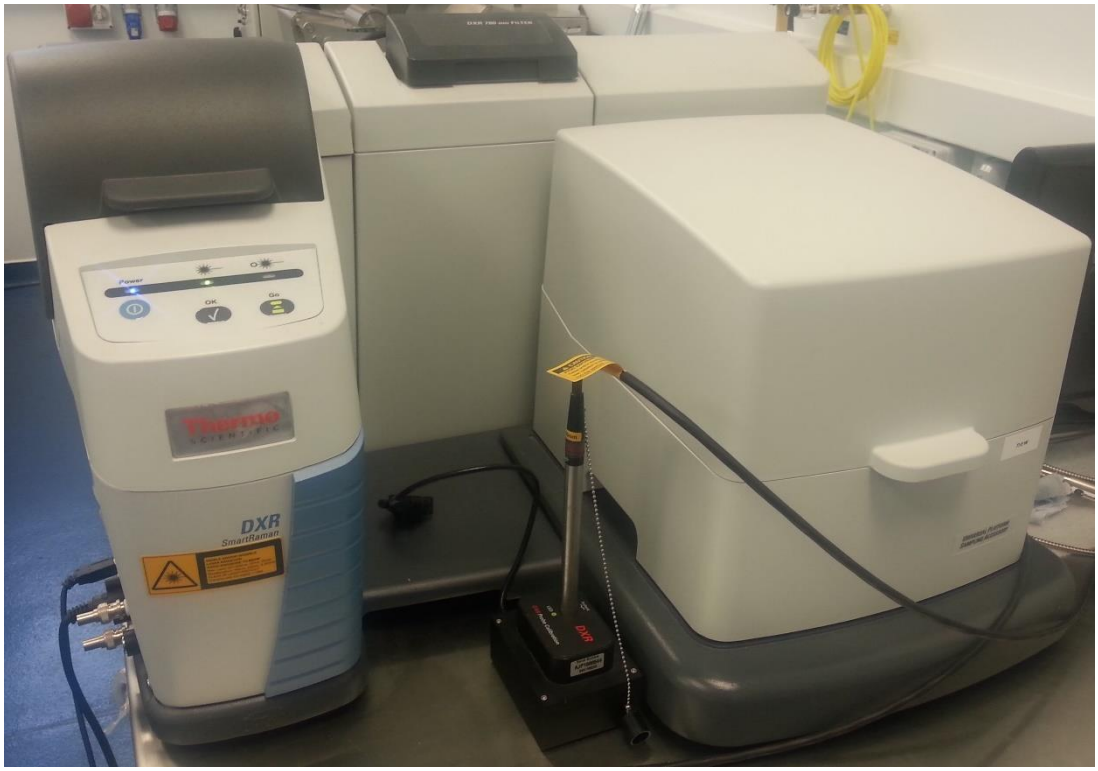

Figure 3.22: Photo showing the DXR™ SmartRaman Spectrometer used

Raman can be used to determine the chemical and physical structure of a material. Raman spectroscopy is often used for characterising morphology as variations in individual bands such as broadening/narrowing can show changes in the crystallinity of materials. Plaques of PFA subjected to different rates of cooling were investigated and analysed using the DXR™ SmartRaman Spectrometer and OMNIC™ software.

3.6 Materials

The three types of PFA investigated in this study are all commercial grades used by CRP for lining piping components predominantly for use in the chemical processing industries. These polymers are used in transfer moulding due to their high melt viscosities. A summary of typical values of various material properties is shown below in Table 3.2. Full details are included in the product information provided by the supplier in Appendix A.

Manufacturer	Chemours	Dyneon	Chemours
Grade	350 TJ	6502TZ	C980
MFR (g/10mins)	2	2	3
Density (kg/m^3)	2150	2150	2150
Melt Point (°C)	305	308	284
Tensile Strength at Break (MPa)	28	34	36
Elongation at Break (%)	300	360	300
Flexural Modulus (MPa)	625	550	700
Folding Endurance (cycles)	500000	3100000	80000

Table 3.2: Typical properties of the grades of PFA used in this study

C980 contains 3-5% carbon black to impart static dissipating properties to the material. The analysis of C980 is presented alongside the unfilled ‘virgin’ polymers in the following section. It should be noted that this level of additive has a significant impact upon the characteristics, making it difficult to directly compare the antistatic and virgin materials.

3.6.1 Preparation of Samples

3.6.1.1 Constant Shear

As discussed in the background, manufacturers advise processing PFA below its critical shear rate to avoid damaging the polymer. Samples were generated

at rates significantly above the critical shear rate to investigate whether there was any effect on the material properties. The capillary rheometer arrangement was used to generate these samples, with the blockprogramming sequence given in the relevant section concerning the capillary rheometer discussed earlier. The material was subjected to the standard heating conditions to ensure a homogenous melt, prior to being extruded at a constant rate.

RAMP LOAD 50 1000N 0 1 0 0

STOP

CLOCK 6 min

RAMP LOAD 50 1000N 0 1 0 0

STOP

CLOCK 3 min

SPEED 267 mm/min

DOWN

POSITION <= 1 mm

ENDTEST

The initial melt phase of a standard capillary rheometer is achieved using the ramp and timer commands. This was used for each test to ensure the polymer had melted satisfactorily. The load was determined experimentally, with 1000N found to be suitable for the 16mm long die. Due to the relatively short length of the rheometer, this had to be reduced to 500N for the orifice die to prevent excessive loss of material.

The position of the tensometer was calibrated, enabling the use of a command to stop the movement of the piston at the end of a sequence. This prevented any damage to the equipment from the piston travelling too far and contacting the die. A mechanical stop was also set as a failsafe, which acted to terminate the program if triggered.

Sequence 3.3: Program for melting and generation of PFA material subjected to a constant shear rate, in this case $1000s^{-1}$.

The material purged from the rheometer during the melting phase was removed to ensure the sample material was not contaminated with material subjected to different shear rates. The extrudate was collected and cut up into small pieces using shears, to allow rheological testing and plaques to be compression moulded for tensile testing.

3.6.1.2 Residence Time

An area of perhaps greater interest is that of the effect of residence time of PFA material at elevated temperature. To investigate this, samples of each of the grades were made by wrapping the pellets in industrial duty aluminium foil. They were then heated for four and eight hours in a large oven set to 380°C for production use. The samples were left to cool to room temperature on removal from the oven, before being granulated. The dimensions of the samples meant the material needed to be cut into thin slices using a bandsaw prior to pelletisation using the machine shown in Figure 3.23 below.

Figure 3.23: Photo showing the equipment used to pelletise the sample material

The pellets were made as small as possible using this equipment, however they were still too large to be used for test material in the capillary rheometer. The pellets were fed through a benchtop granulator, shown below in Figure 3.24.

Figure 3.24: Photo showing equipment used to granulate the samples

Figure 3.25: Photo showing the sample material after the granulation process

The equipment used for pelletising and granulating the samples was vacuumed after each material has been processed to reduce the risk of contamination as much as possible.

3.6.1.3 Processed Material

Tests were also conducted on PFA material that had been subjected to the processing conditions during transfer moulding of lined piping components at CRP. An amount of waste material is produced from transfer moulding of PFA. This waste is collected and processed for reuse. There are two sources of waste material produced from the two methods of transfer moulding. Small amounts of molten PFA are purged from the nozzle of machines where the PFA is melted by travelling along a screw through a heated barrel.

Figure 3.26: Photo showing material purged from the nozzle of a transfer moulding machine

Static melting, where the PFA granules are held in a pot and melted, generates small pods of material as it is not possible or desirable for all the material in the pot to be injected into the fitting.

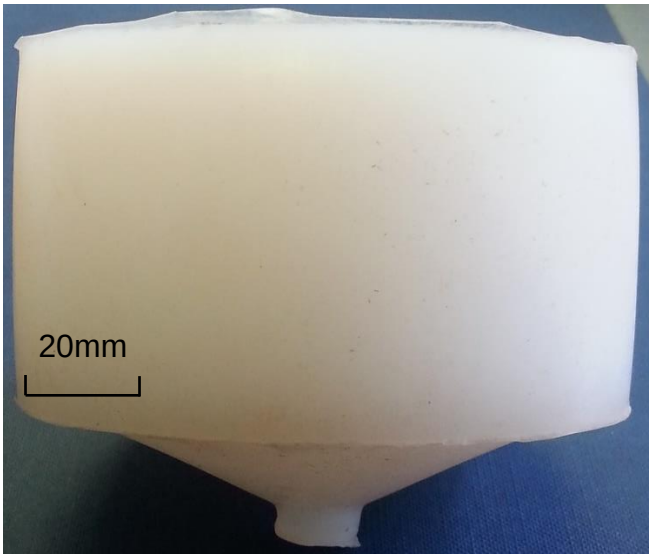

Figure 3.27: Photo showing pod of PFA generated from static melting of PFA

Samples of each of these types of material were pelletised using the granulator shown below in Figure 3.28.

Figure 3.28: Photo showing equipment used to granulate samples of processed PFA

3.6.1.4 Tensile Testing

Plaques were compression moulded using a hot press set to 340°C at The University of Leeds, similar to the one shown in Figure 3.29 below.

Figure 3.29: Photo showing the press at The University of Bradford

Brass plates were lined with industrial duty foil coated with Frekote 44NC mould release agent to improve the ease of removal of the PFA sample. The agent was applied with a lint free cloth and left for 5 minutes to allow the solvent to evaporate. A picture frame mould of thickness 1.2mm containing approximately 37g of polymer was sandwiched between the plates and held under minimal pressure in the press.

The samples were held for a pre-heat time of 4mins to ensure the granules had melted sufficiently to flow and form a good quality sample. The plates were then pressurised in increments of 0.5 tonnes and held for 15s from 0.5-2 tonnes. The temperature controllers were then set to 0°C and the water cooling switched on full. When the plates reached 200°C the water cooling ceased and the heaters were set back to 340°C. The pressure was released, the plates removed and placed between two larger plates at room temperature. The samples were

allowed to cool for 10 minutes to prevent the material from curling on removal. The cooling plates were quenched in a water bath to return them to ambient temperature prior to being used again.

3.6.1.5 Cooling Rates

Samples of 350TJ exposed to various cooling rates were manufactured by Chemours. The fast cooled sample (A) was quenched in a water bath directly after moulding, whereas the normally cooled sample (B) remained in the press with the plates cooled by passing 40°C water through. The slow cooled sample (C) remained in the press, with the heaters switched off without water cooling. The effect on the crystallinity of the sample can be seen in Figure 3.30 below, with the slow cooled sample having an opaque appearance due to light scattering off the crystalline regions.

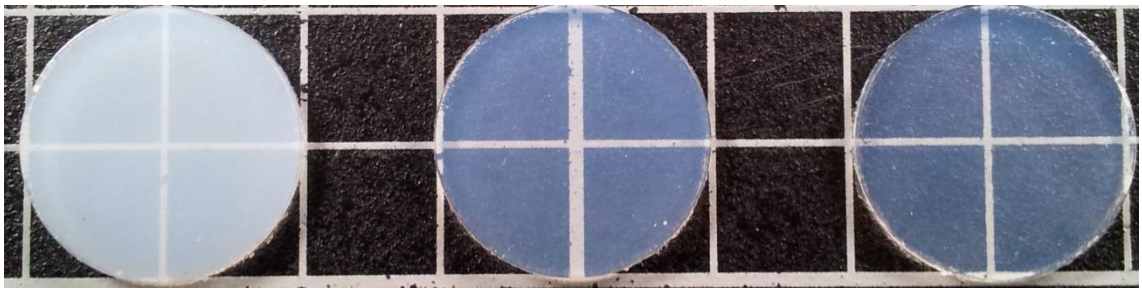

Figure 3.30: Photo showing the samples of 350TJ cooled at different rates. From left to right: sample C, sample B and sample A

Chapter 4

Results

Introduction

This chapter presents the results of the analytical techniques used to determine the effect of processing on the material properties of PFA. The chapter is arranged such that the results are grouped by the experiments conducted on each sample to show the effect of each condition on the material.

4.1 Base Comparison of Grades

There is a limited amount of data available on PFA, so the aim of these experiments was to generate basic material information such as viscosity curves and infrared spectra. This information and data from tensile testing and Differential Scanning Calorimetry (DSC) provide a baseline to enable comparison of the results obtained from testing samples of PFA exposed to various conditions.

4.1.1 Determination of Viscosity

Viscosity curves of the three grades of PFA at 370°C generated using the Hastelloy® capillary rheometer are shown below in Figure 4.1. Figures 4.2 and 4.3 show the instabilities in the apparent wall shear stress during various tests where the shear rate was increased in increments.

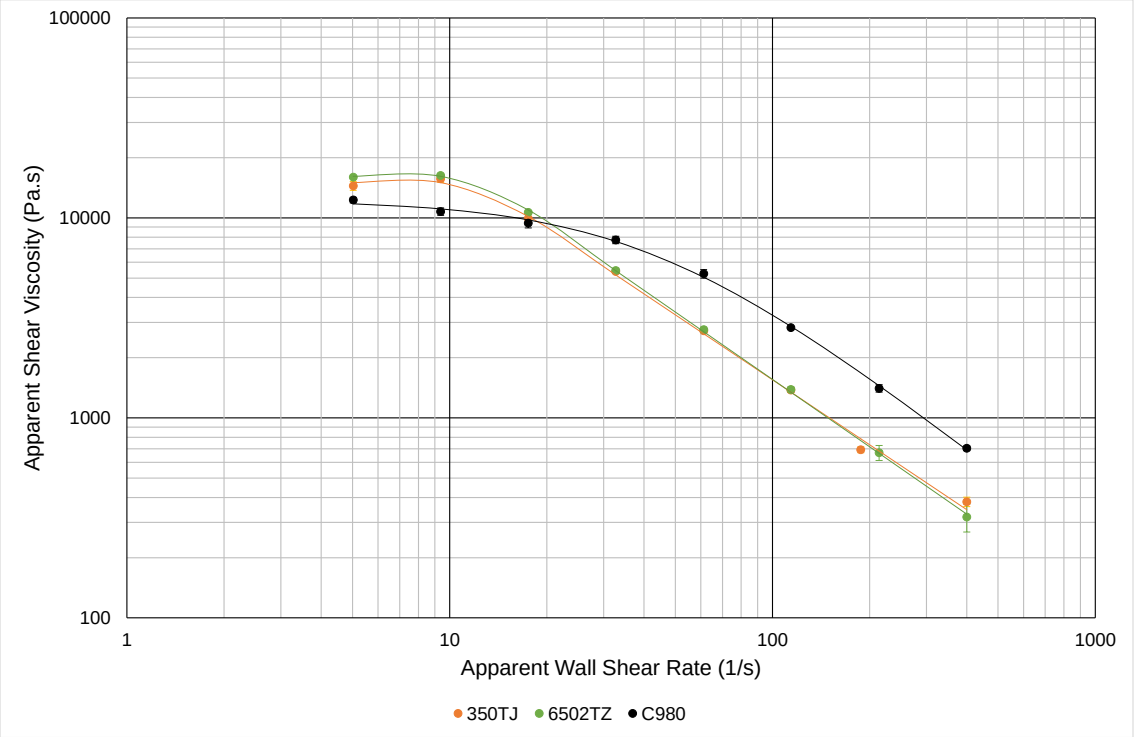

Figure 4.1: Comparison of the viscosity of the three grades of PFA with a Carreau fit applied

Polymer	n	a	η_0 (Pa.s)	λ (s)
350TJ	0	83.69	15012	0.096
6502TZ	0	167.00	15963	0.102
C980	0	2.39	11454	0.037

Table 4.1: Parameters obtained from Yasuda Carreau fits to experimental data

Figure 4.1 shows all three grades exhibit shear thinning behaviour, however the n values generated using the Solver function in Microsoft Excel could not be made to reflect this. This is possibly due to slip at the higher shear rates, resulting in a lower apparent shear viscosity. As the zero values of n are clearly incorrect they have been omitted from further tables showing the parameters obtained for the model. It is expected that the use of specialist software such as the curve fitting function in Origin would generate n values of between 0 and 1 to reflect the shear thinning behaviour observed experimentally. There is generally good agreement between the virgin materials, however 6502TZ is slightly more viscous at low shear rates than 350TJ. This is reflected in the value of the viscosity at zero shear rate (η_0) generated by the Yasuda Carreau model. Below $20s^{-1}$ C980 is less viscous than the virgin grades, at higher shear

rates it becomes more viscous. This behaviour could be due to the presence of the carbon black additive in C980. The viscosity data in the processing range contrasts the values of melt flow rate values quoted on the material certificates for the materials shown below:

1.92g/10mins for 350TJ

2.2g/10mins for 6502TZ

2.80g/10mins for C980

This demonstrates melt flow rate is a limited indicator of the shear behaviour over the range of rates at which PFA can be processed. The shear rates the material is exposed to during MFR testing are very low - typically below $5s^{-1}$, which explains the better agreement below $20s^{-1}$.

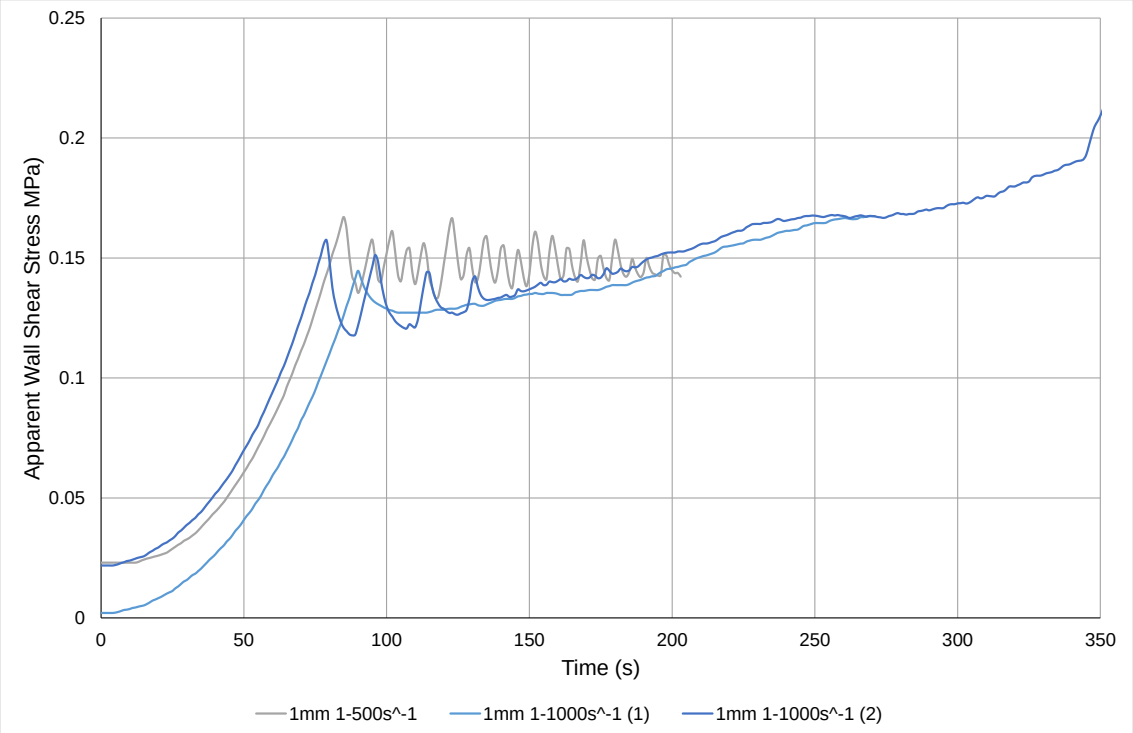

Figure 4.2: Apparent wall shear stress with time of three tests during which the shear rate was increased in equal increments using a 1mm die on unprocessed 350TJ at 370°C

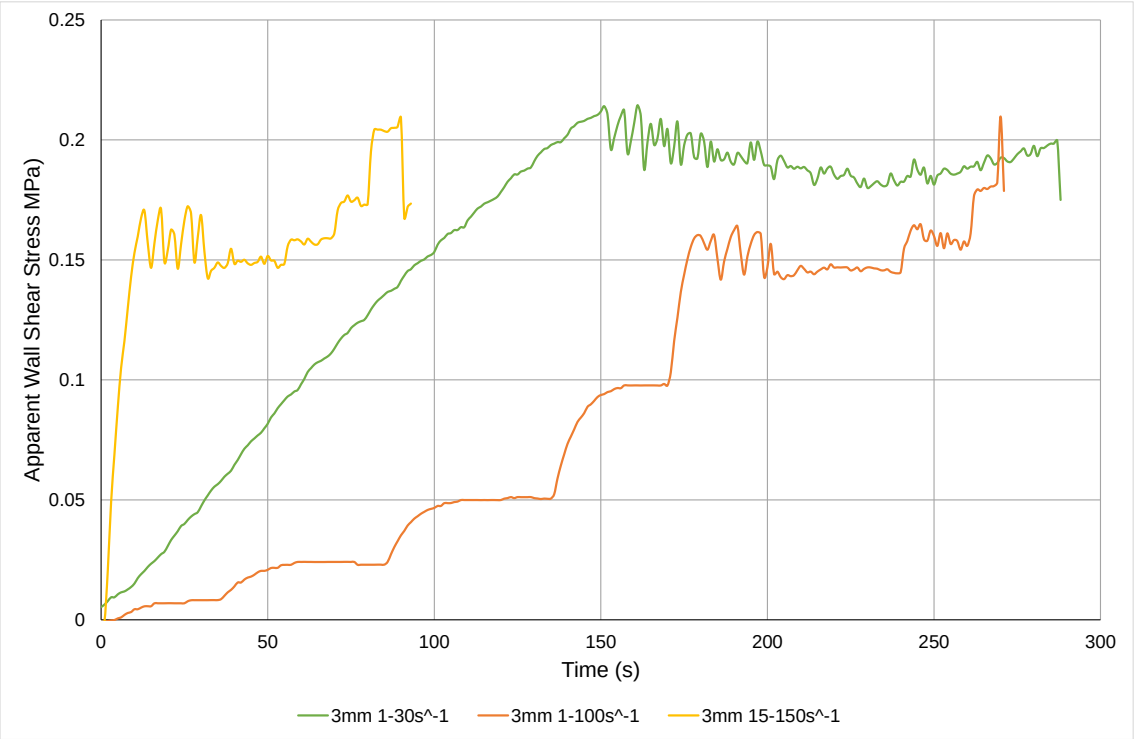

Figure 4.3: Apparent wall shear stress with time of three tests spanning different shear rate ranges using a 3mm die on unprocessed 350TJ at 370°C

Theoretically the two tests shown in Figure 4.2 running between 1-1000s^{-1} were identical, however the results from one show fluctuations in the apparent wall shear stress whilst the other did not. Similar inconsistent unstable flow has been reported by Rosenbaum, Hatzikiriakos and Stewart (1995) in their paper on flow implications in the processing of tetrafluoroethylene/hexafluoroethylene copolymers. Using a 1mm die the onset of the instability occurs at approximately 150s^{-1} in the test running from 1-500s^{-1}. With a 3mm die the instability appears to occur around 15s^{-1}. The test has an effect on the magnitude of the apparent wall shear stress: a testing shear rate range of 1-30s^{-1} shows an instability at 0.2MPa, significantly higher than 0.15MPa from testing between 15-150s^{-1}. This could be a time dependent effect due to the viscoelastic nature of the polymer.

4.1.2 Tensile Testing

Stress vs. strain curves of the three grades of PFA generated using the Messphysik tensometer are shown below in Figure 4.4.

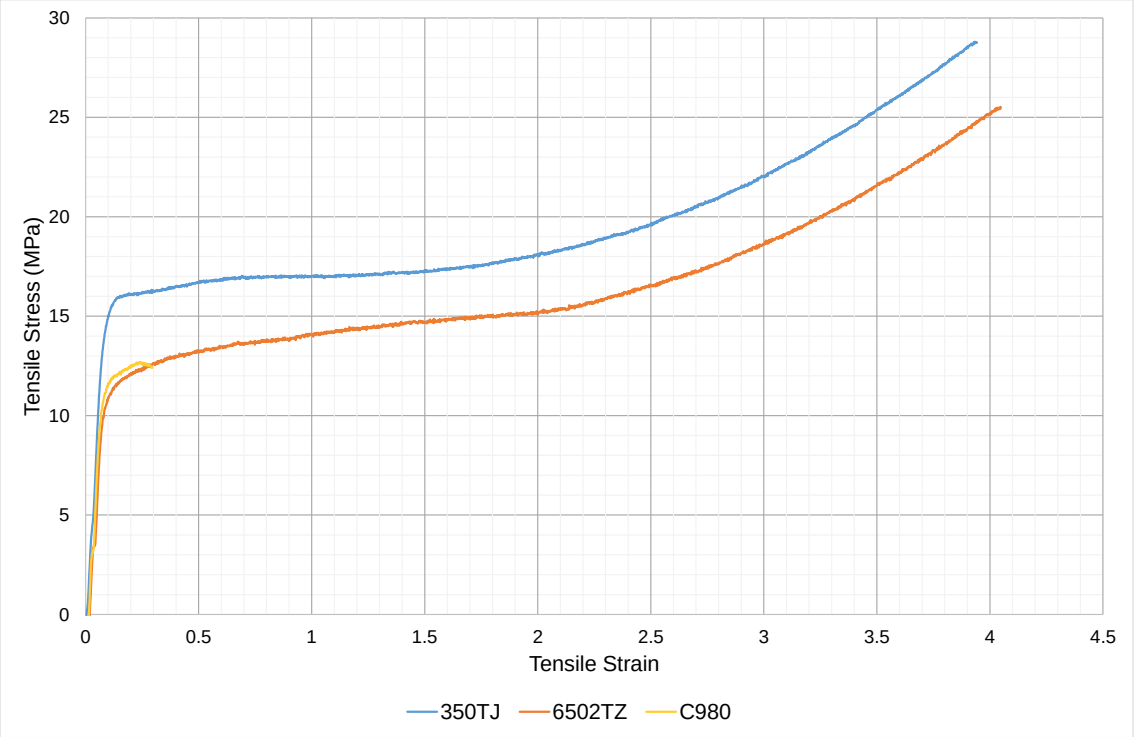

Figure 4.4: Each curve is the average of 5 tests, displayed to the lowest elongation of the data set

Sample	Yield Strength (MPa)	Elongation at Break (%)	Modulus (MPa)
350TJ	8.53 ± 0.61	410.8 ± 10.5	298.7 ± 17.6
6502TZ	6.87 ± 0.62	469.3 ± 35.4	271.3 ± 14.0
C980	6.56 ± 0.41	51.5 ± 22.1	304.7 ± 18.3

Table 4.2: Average and standard deviation of 5 tests

The stress strain diagram in Figure 4.4 shows PFA behaves as a soft elastic plastic. 6502TZ in particular does not appear to have a well-defined yield point, so the yield strength has been taken as the stress at which the material begins to deviate from Hookean behaviour. The virgin polymers followed very similar curves, however the 350TJ material exhibited a higher yield strength and modulus. A greater yield strength means the material can withstand a higher stress before deforming plastically and gives an idea of the upper limit of the load than can be applied. An increased elastic modulus corresponds to a stiffer material, so 350TJ can withstand a higher load prior to elastic deformation. The values of elongation at break of the virgin materials were well above the typical

values stated in the material literature. They show virgin PFA is a ductile material that demonstrates significant plastic deformation before failure.

The samples of C980 suffered premature breakage, almost certainly due to the quality of the plaque. It was particularly difficult to produce satisfactory plaques using the static dissipating polymer, with shrinkage voids being a particular problem. Various conditions were tried to no avail, and with the time restraints of the project the best plaque representing each sample was used. The tensile strength given in the product information for the material is listed as 36MPa, with the elongation at break quoted as 300%.

4.1.3 DSC

The second heating curves showing the melting point of the PFA materials used in this study are shown below in Figure 4.5.

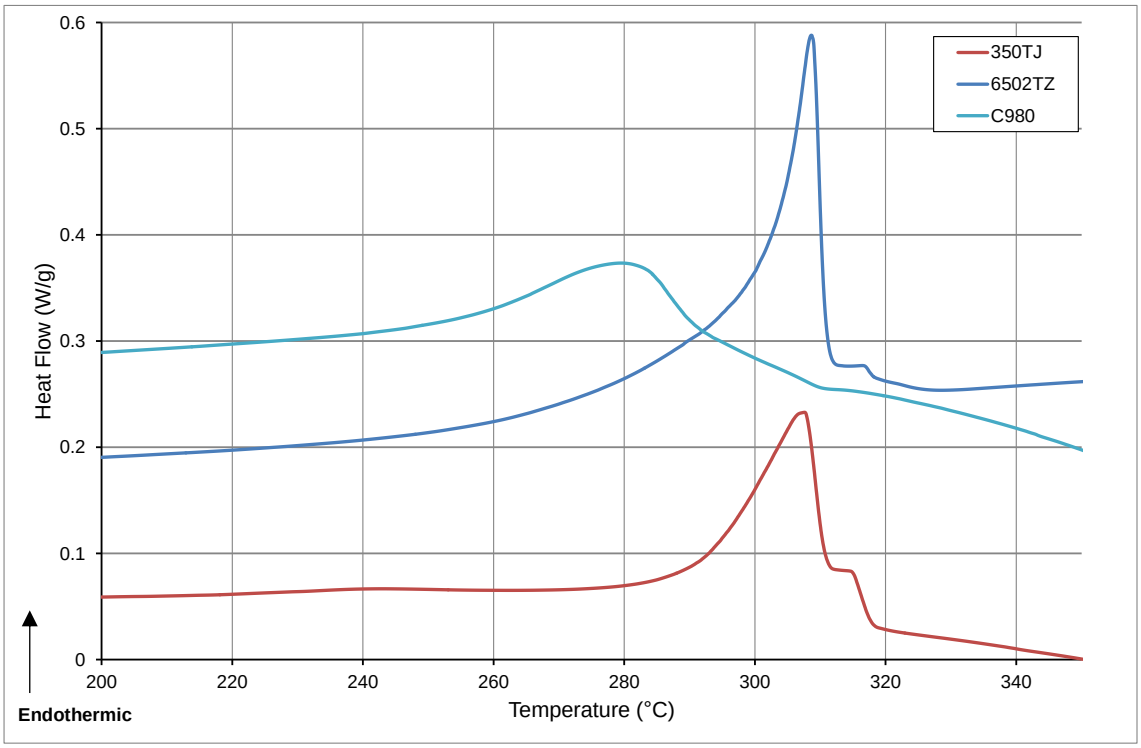

Figure 4.5: DSC traces obtained from the second heating cycles of the unprocessed PFA materials used in this study

		Heat 1	Heat 2
350TJ	**Melt (°C)**	307.2 ± 0.2	308.9 ± 0.2
	Enthalpy (J/g)	12.6 ± 0.5	8.5 ± 0.5
	Crystallinity (%)	18.9 ± 0.7	12.7 ± 2.8
6502TZ	**Melt (°C)**	307.0 ± 0.5	308.6 ± 0.4
	Enthalpy (J/g)	12.5 ± 1.1	12.5 ± 2.4
	Crystallinity (%)	18.7 ± 1.7	18.7 ± 3.6
C980	**Melt (°C)**	284.4 ± 0.3	279.2 ± 0.4
	Enthalpy (J/g)	14.1 ± 2.4	17.7 ± 2.1
	Crystallinity (%)	21.0 ± 3.5	26.5 ± 3.1

Table 4.3: Values of the melting peak endotherm and enthalpies of the first and second heating cycles

Monson, Moon and Extrand (2008, p.142) use a value of the melting enthalpy of PFA in a 100% crystalline state, H_f, given by Runt (1986) as 67J/g to calculate the crystalline mass fraction, x_c. This value has been used to determine the mass fraction crystallinity of the samples from the melt enthalpies, ΔH, using the following equation:

$$x_c = \frac{\Delta H}{H_f}$$

The melt temperatures obtained from the second heating of the virgin PFA materials are higher than the values of 304°C and 305°C quoted on the material certificates for 350TJ and 6502TZ respectively. The melt temperature of C980 is not given on the material certificate, however at 279°C the value of the second melt is lower than 284°C given as a typical value on the technical data sheet, and is nearly 30°C lower than the virgin PFA materials. The peak is much wider than those of the virgin materials, indicating it has a broader distribution of crystal sizes. The peaks of the virgin materials are very similar, with both having a shoulder at the high temperature side of the main transition. This shoulder or second peak could be a polymorph, indicating virgin PFA has more than one crystal structure. 350TJ has a slightly broader peak than 6502TZ, demonstrating it has a slightly wider crystal size distribution.

4.1.4 Spectroscopy

The spectra obtained from Fourier Transform Infrared Spectroscopy are shown below in Figures 4.6 to 4.11.

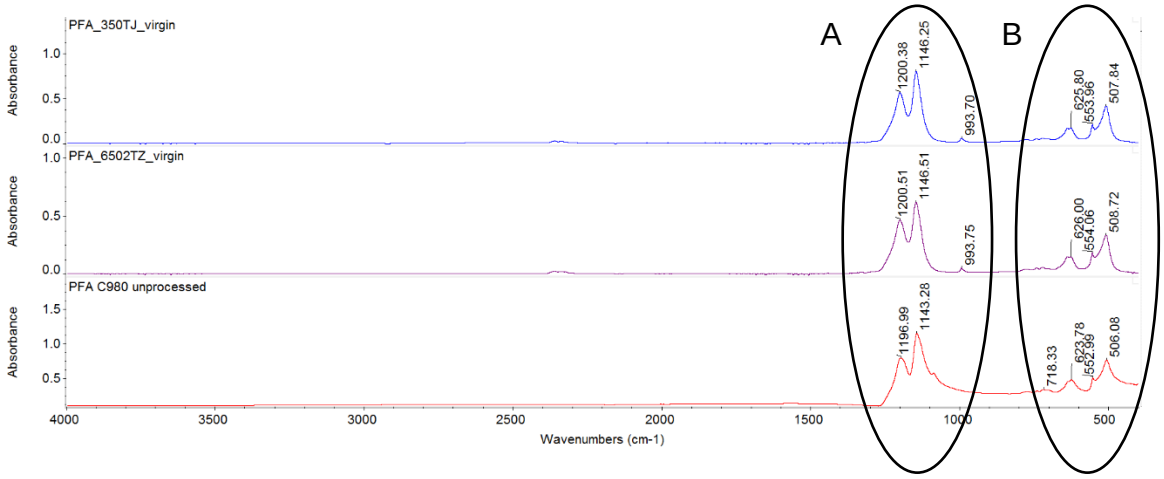

Figure 4.6: Spectra of each of the three grades of PFA

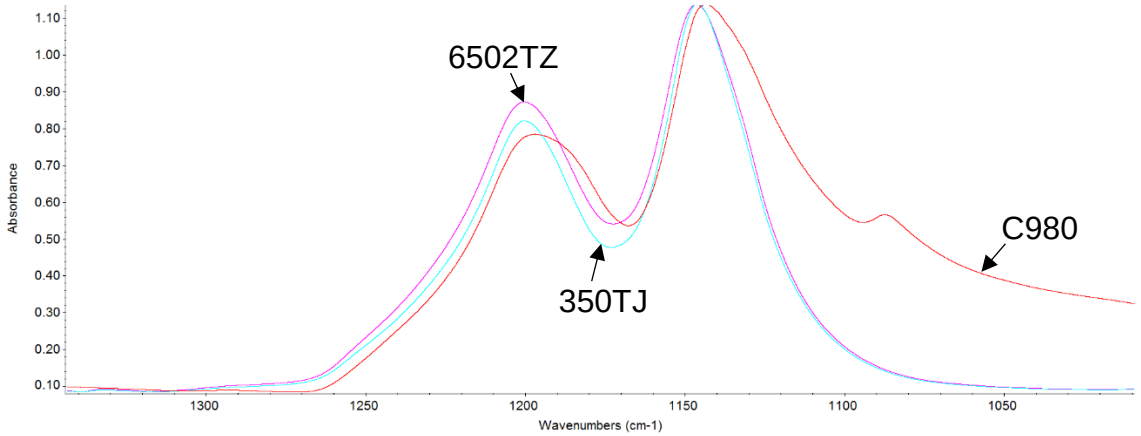

Figure 4.7: Superimposed spectra from section A in Figure 4.6

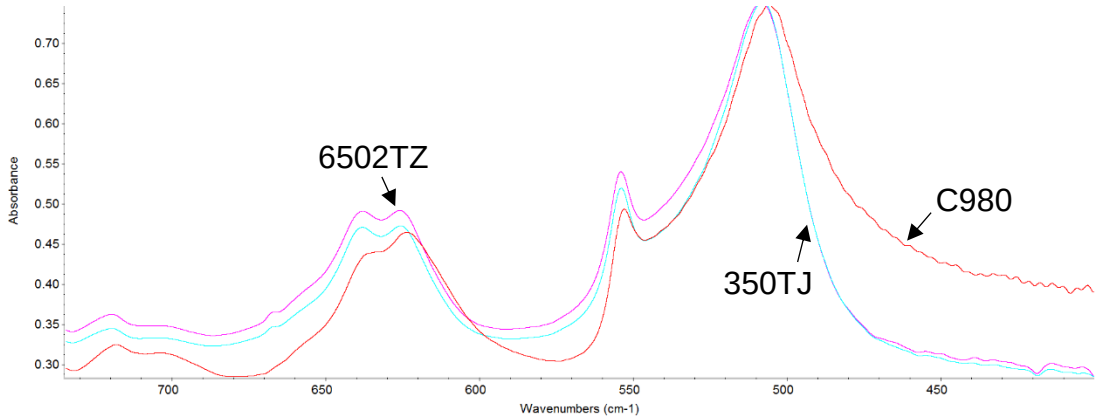

Figure 4.8: Superimposed spectra from section B in Figure 4.6

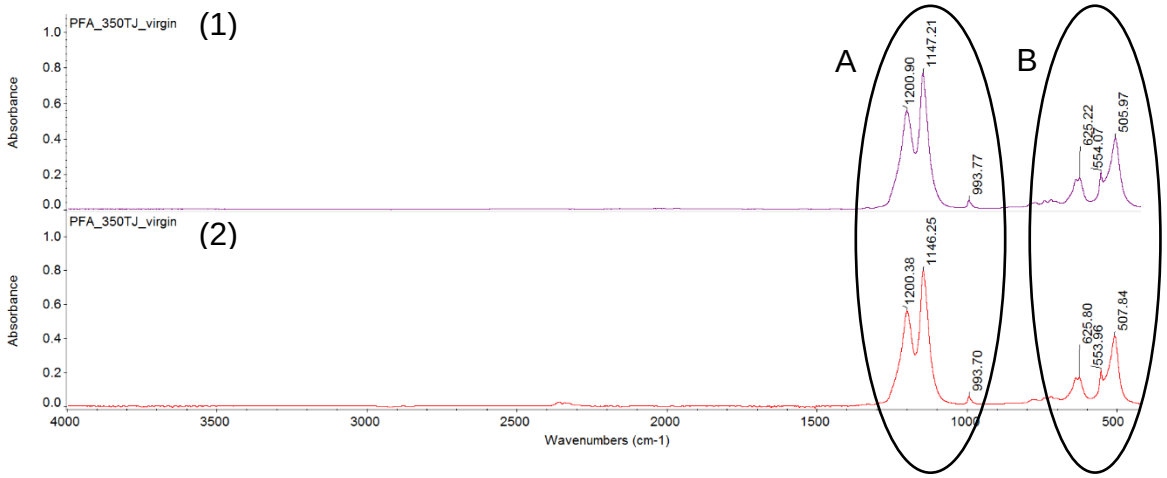

Figure 4.9: Comparison of spectra obtained from samples of 350TJ from two different batches

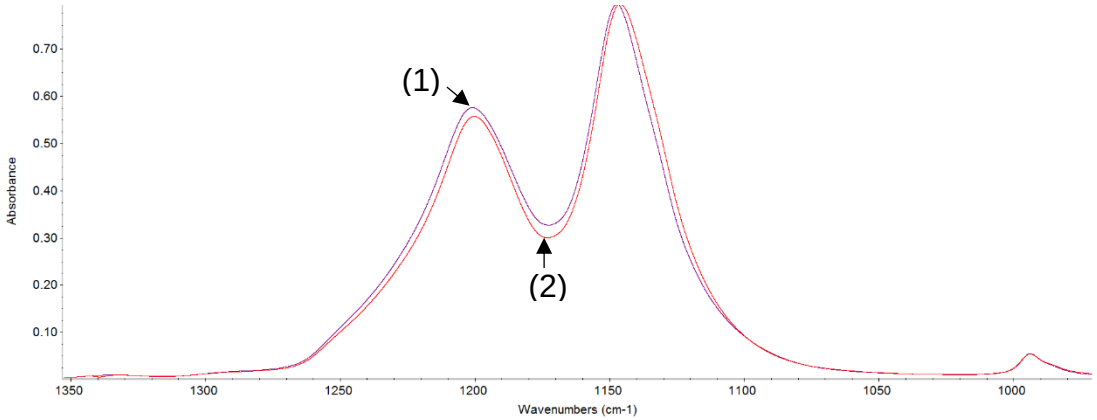

Figure 4.10: Superimposed spectra from section A in Figure 4.9

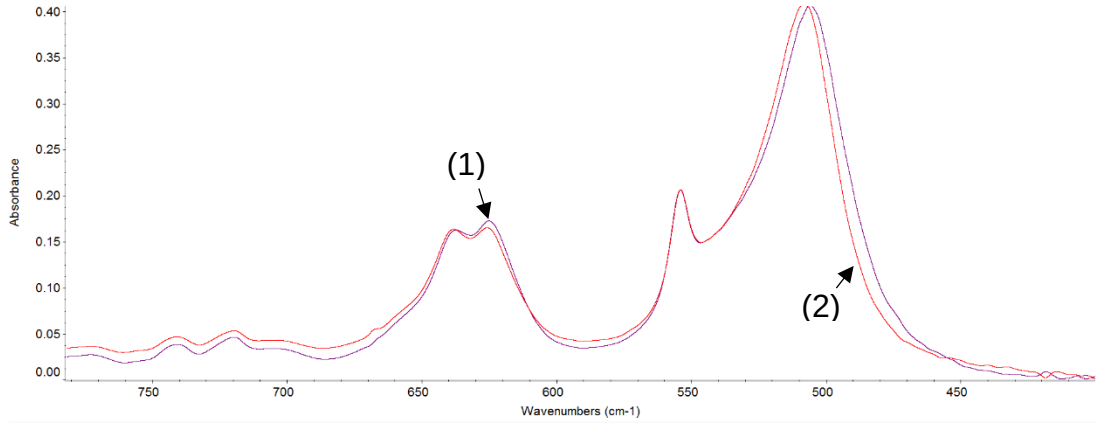

Figure 4.11: Superimposed spectra from section B in Figure 4.9

350TJ (1)	350TJ (2)	6520TZ	C980
1200.90	1200.38	1200.51	1196.99
1146.25	1146.25	1146.51	1143.28
993.77	993.70	993.75	-
638.82	639.30	639.30	-
625.22	625.80	626.00	623.78
554.07	553.96	554.06	552.99
505.97	507.84	508.72	506.08

Table 4.4: Wavenumbers of the peaks in the spectra of the unprocessed PFA samples

The spectra obtained from FTIR shows there is some variation in the wavenumbers of the peaks of the different materials. The wavenumbers are similar to those listed by Dargaville (2002), who identifies the dominant bands as belonging to the various modes of CF_2 from information published by Hummel and Scholl (1988), Legeay et al. (1998) and Wu et al. (2000) as: 1199cm^{-1}, 1146cm^{-1}, 715–774cm^{-1}, 553cm^{-1} and 507cm^{-1}. Legeay et al. (1998) attributes the peaks at 638cm^{-1} and 625cm^{-1} as being from groups in crystalline area for PTFE due to CF stretching and bending, and the peak at 508cm^{-1} as being indicative of a large crystalline region. As there is little variation in the peak heights and wavenumbers of the samples of PFA investigated, the FTIR spectra will not be discussed further in the main body of the text, however they have been included in an appendix for completeness.

4.2 Effect of Temperature

Temperature is a key factor affecting the viscosity of a material and again there is little published information in this area. The aim of these experiments was to obtain data on the change in viscosity with temperature. This information can then be used to optimise processing conditions.

4.2.1 Melt Flow Rate Testing

The change in Melt Flow Rate (MFR) with temperature of the three grades of PFA is show below in Figure 4.12.

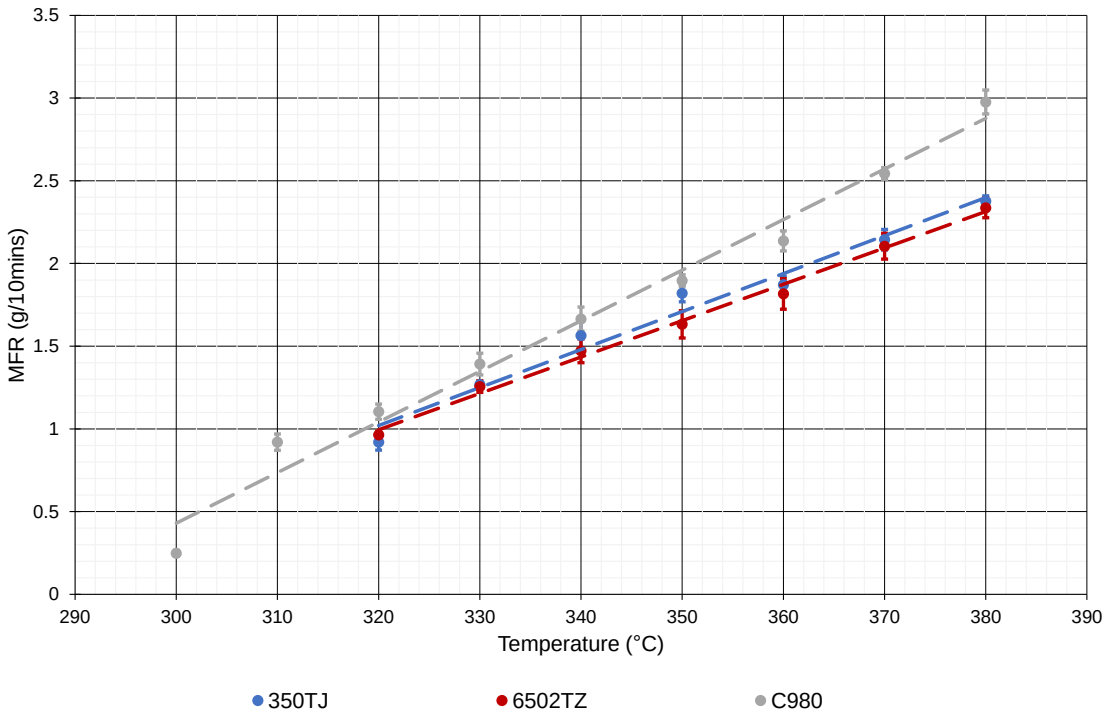

Figure 4.12: MFRs of the unprocessed PFA materials used in this study at various temperatures

The MFRs of the materials at the standard test temperature of 372°C defined by ASTM 1238 (2013) are comparable to the values given on the material certificates. The virgin grades have similar values of MFR, which are much lower than that of C980. The virgin PFA grades behave similarly with the change in temperature, however the MFR of C980 decreases at a greater rate. All grades show a linear reduction in MFR with increasing temperature over the range studied. From these results the implication is that all the grades of PFA investigated flow more easily at higher temperatures, however MFR gives an indication of viscosity only at low shear rates. The results obtained from the capillary rheometer allow a better understanding of the effect of temperature on the viscosity of PFA.

4.2.2 Viscosity

The data generated on the capillary rheometer showing the dependence of viscosity on the temperature of PFA is presented below in Figures 4.13 to 4.18.

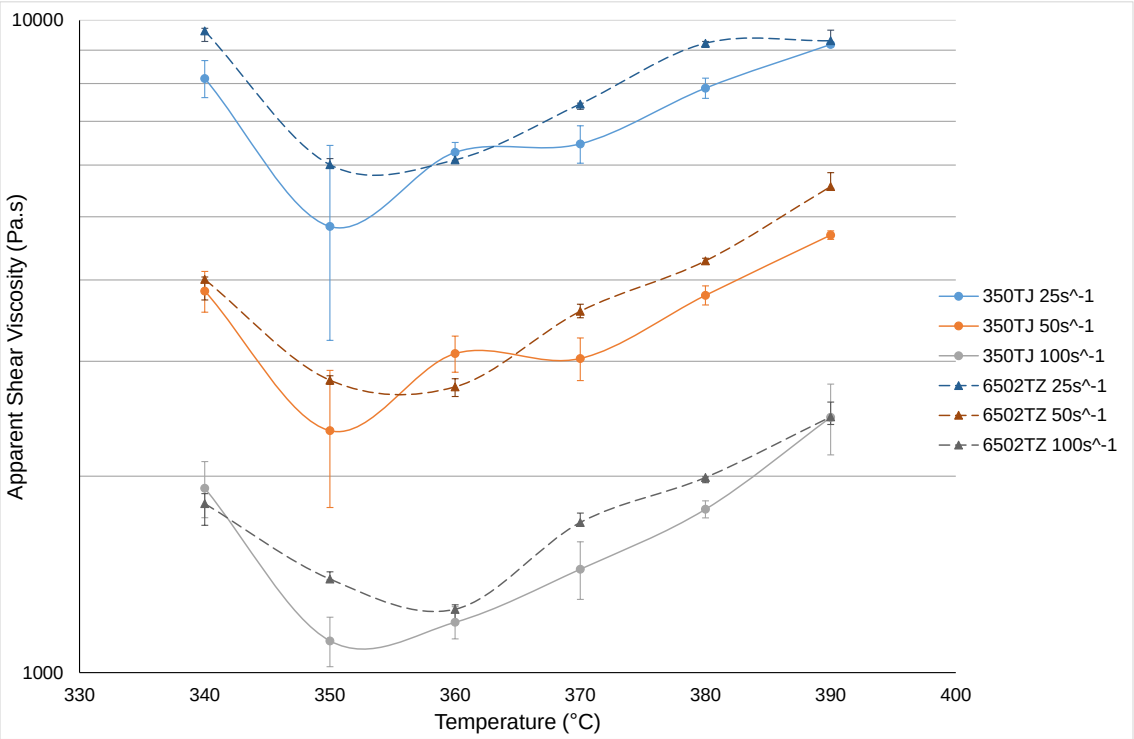

Figure 4.13: Effect of temperature on viscosity (Bagley corrected) at 25, 50 and 100s^{-1} of the virgin grades of PFA

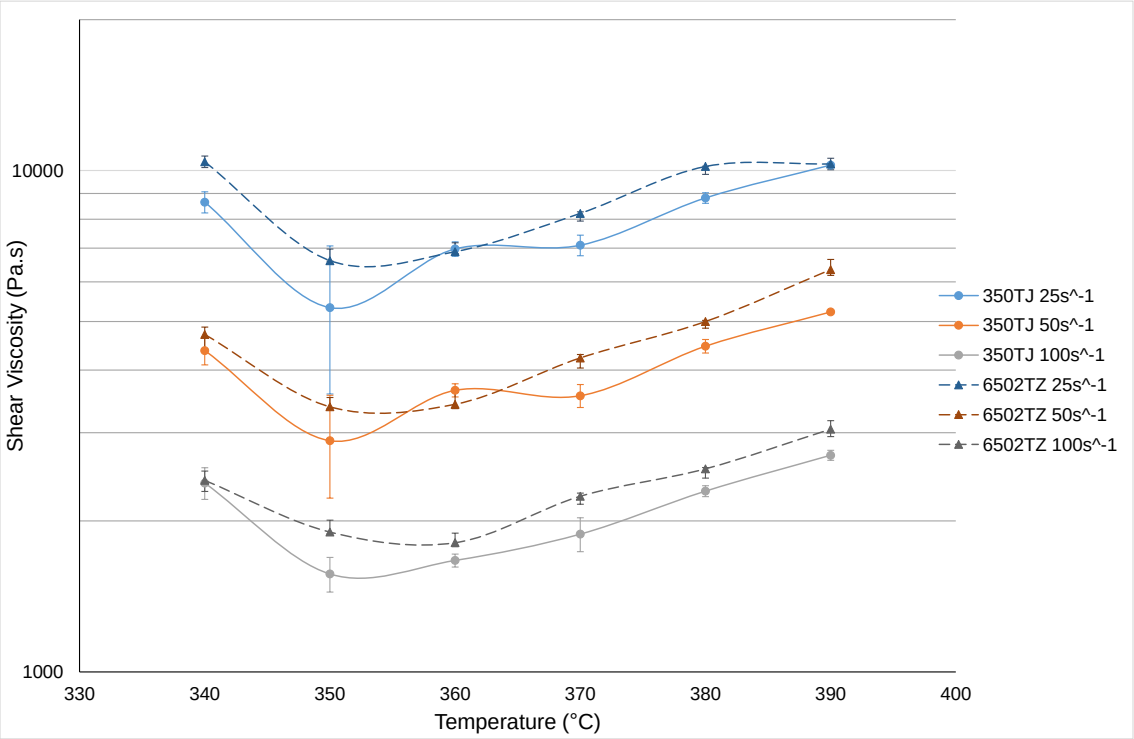

Figure 4.14: Effect of temperature on shear viscosity (without Bagley correction) at 25, 50 and 100s^{-1} of the virgin grades of PFA

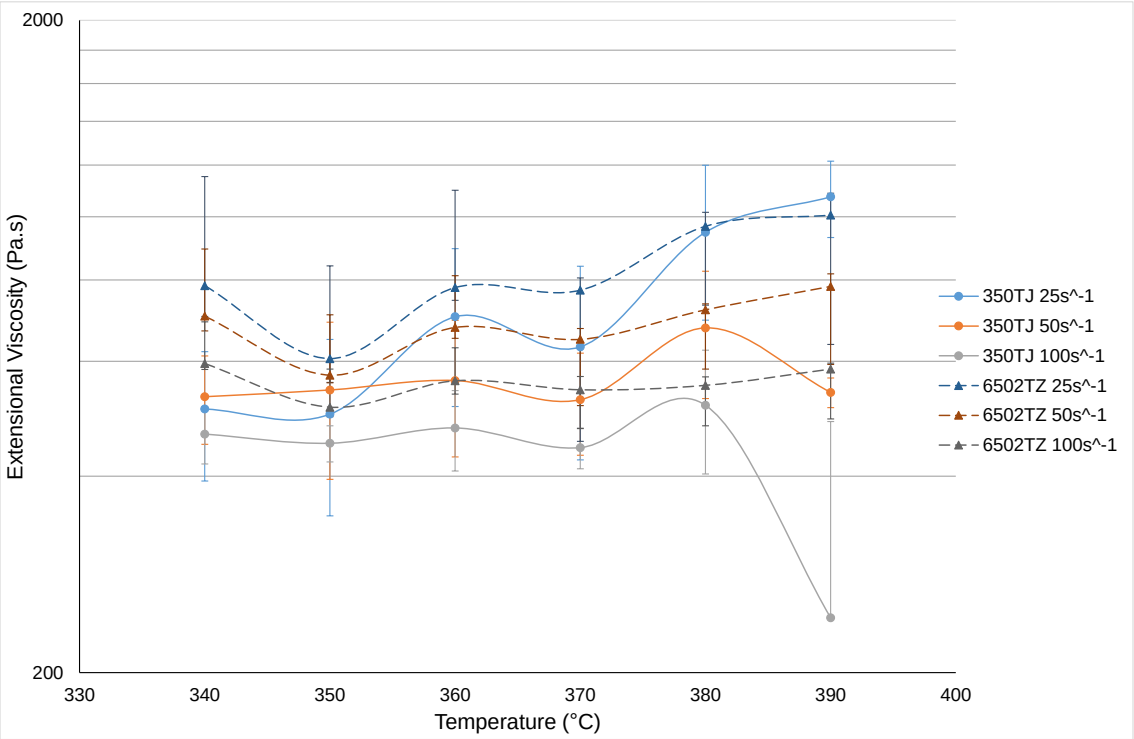

Figure 4.15: Effect of temperature on extensional viscosity at 25, 50 and 100s^{-1} of the virgin grades of PFA

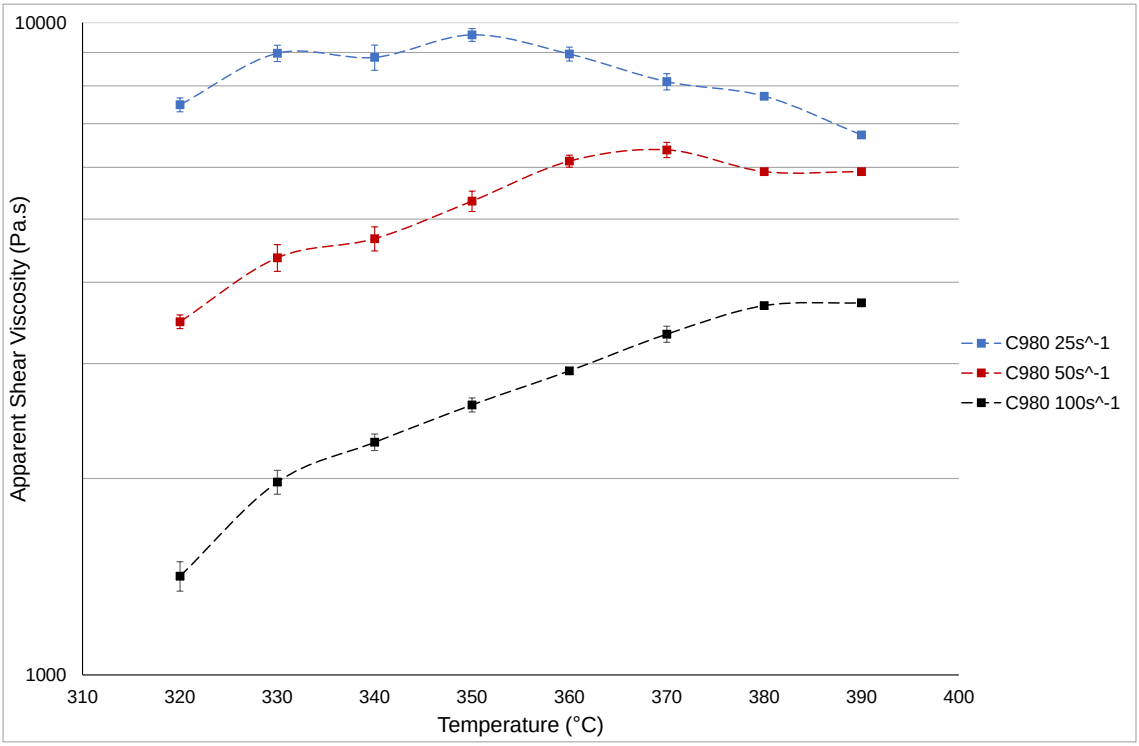

Figure 4.16: Effect of temperature on viscosity (Bagley corrected) at 25, 50 and 100s^{-1} of C980 PFA

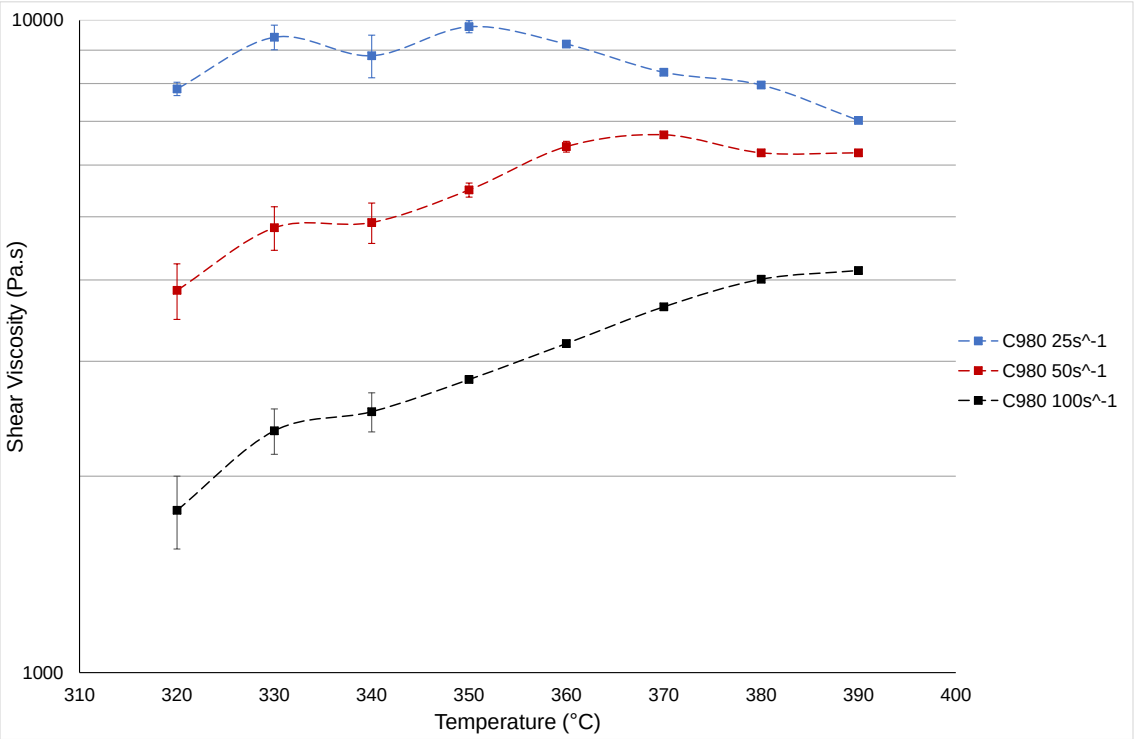

Figure 4.17: Effect of temperature on shear viscosity (without Bagley correction) at 25, 50 and 100s^{-1} of C980 PFA

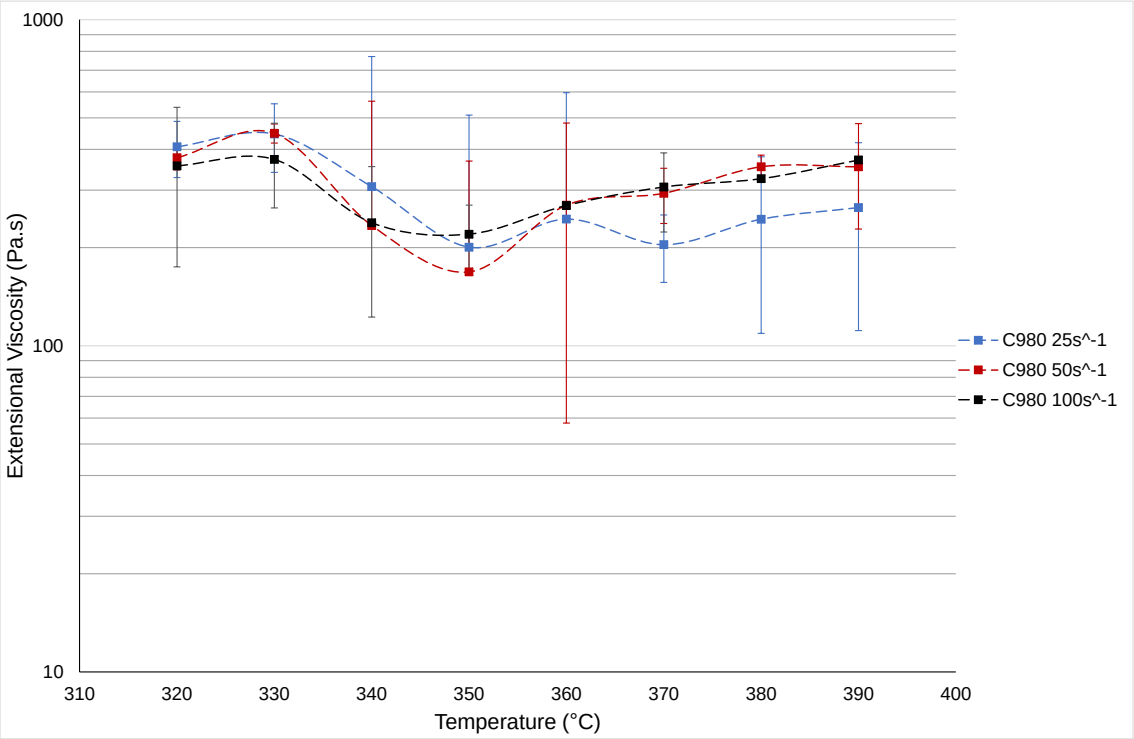

Figure 4.18: Effect of temperature on extensional viscosity at 25, 50 and 100s^{-1} of C980 PFA

The flow data for all grades of PFA is more complex than expected, especially when considering the linear drop in MFR with decreased temperature. The

virgin grades both show a similar dependence on temperature with a noticeable drop in viscosity from 340-350°C, which follows the anticipated trend, however the viscosity roughly plateaus at 350-360°C then rises with temperature. This behaviour is demonstrated at each of the shear rates investigated so it is concluded to be a real effect. The increase in viscosity could be explained by an increase in molecular weight at the higher temperatures, possibly caused by crosslinking. Currently there are no suitable methods for directly measuring the molecular weight of PFA, however this could be investigated if an appropriate method is identified in the future. There could be an element of wall slip occurring at the lower temperatures investigated, which may be responsible for viscosity data that is lower than expected. This could be examined by conducting a specific study as a follow up exercise to the work described in this project.

The viscosity of C980 is quite different from that of the virgin polymers, demonstrating a general increase in viscosity with temperature. The peaks of the curves appear to shift with shear rate, with the maximum viscosity at $25s^{-1}$ at approximately 350°C, $50s^{-1}$ at approximately 370°C, and $100s^{-1}$ plateauing at 380-390°C. The minimum viscosity for all shear rates looks to be 320°C, which is difficult to explain without further data. C980 has a melt point of 284°C, but at temperatures lower than 320°C the pressure exceeded the safe working limit of the melt transducer and the load cell of the tensometer.

Considering the components of the viscosity data by separating the pressure measurements enables calculation of the shear viscosity (derived from the pressure measurements using only the long die) and the extensional viscosity (orifice die pressure measurements only). The extensional viscosity data shows a similar trend to the shear viscosity albeit not quite as clearly. This could suggest there is increased adhesion of the polymer to the die wall at higher temperatures, which would be more significant for the long die due to the increased surface area.

4.3 Effect of Residence Time

There are concerns over the length of time PFA can be held at processing temperatures before the material is compromised due to degradation. The aim of these experiments was to obtain data on the change in material properties

with exposure to processing temperature using the samples detailed in Chapter 3.

4.3.1 Melt Flow Rate Testing

The change in Melt Flow Rate (MFR) with length of time exposed to processing temperature of the virgin grades of PFA is show below in Figure 4.19.

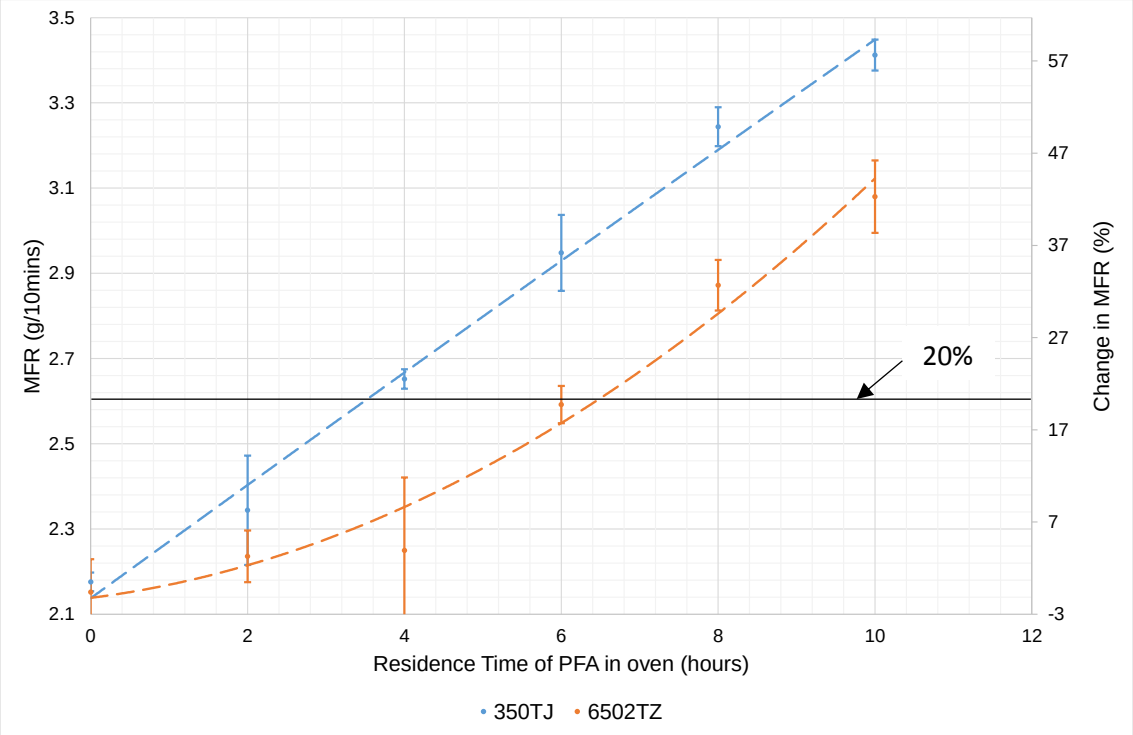

Figure 4.19: Change in MFR with residence time of the virgin PFA materials used in this study, error bars represent standard deviation of 5 tests conducted on each sample

The change in Melt Flow Rate (MFR) is used as an indication of the level of degradation of PFA. The maximum acceptable increase of 20% is quoted in a number of articles as being the limit at which the mechanical properties of the PFA begin to be compromised. This value is reached after an exposure time of 3½ hrs for 350TJ, but not until over 6hrs for 6502TZ. The error bars in the data are significant, so the conclusion that 6502TZ is less affected by residence time at temperature than 350TJ is tentative.

4.3.2 Viscosity

The data generated on the Hastelloy® capillary rheometer showing the change in viscosity due to residence time at processing temperature of the three grades of PFA is presented below in Figures 4.20 to 4.22.

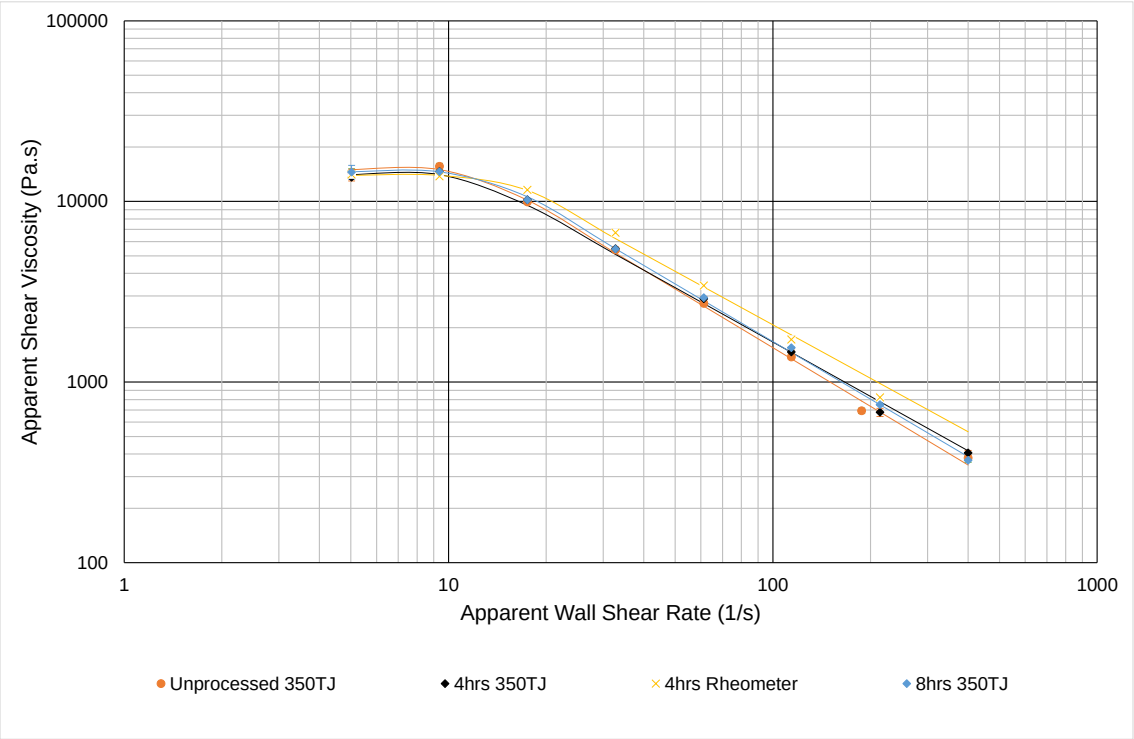

Figure 4.20: Carreau fit of 350TJ subjected to various residence times

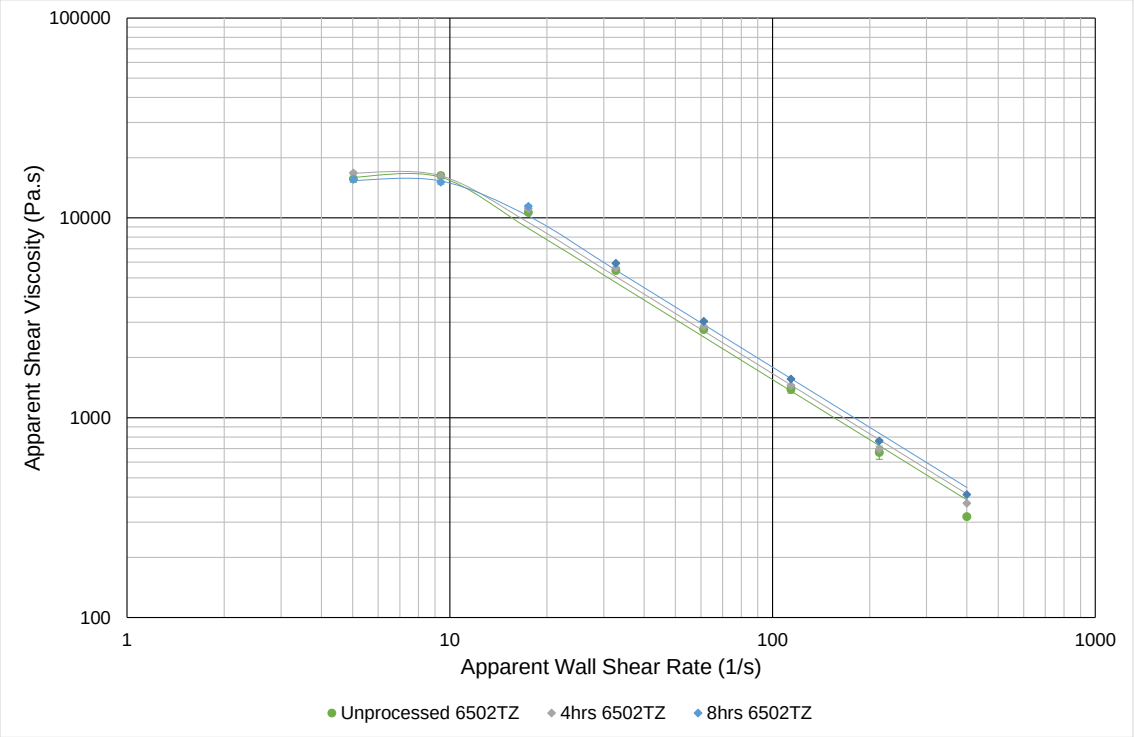

Figure 4.21: Carreau fit of 6502TZ subjected to various residence times

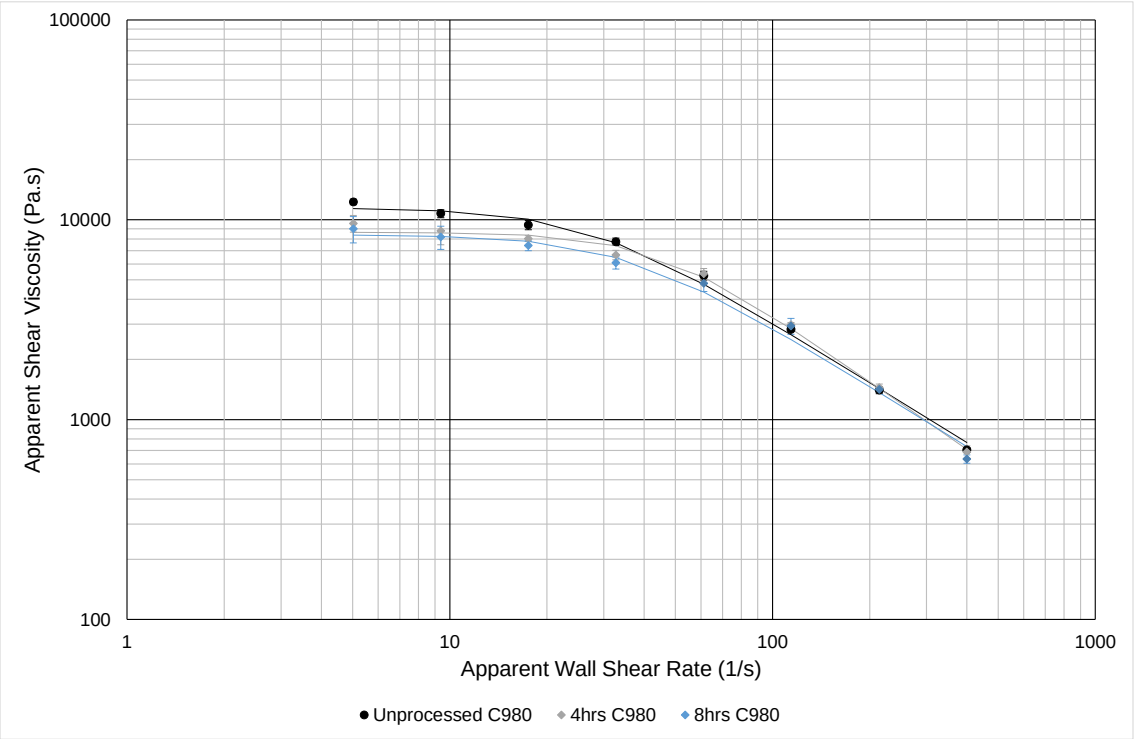

Figure 4.22: Carreau fit of C980 subjected to various residence times

		a	η_0 (Pa.s)	λ (s)
350TJ	**Unprocessed**	83.69	15012	0.096
	4hrs	65.53	14085	0.085
	4hrs (Rheometer)	75.45	13939	0.069
	8hrs	89.07	14590	0.077
6502TZ	**Unprocessed**	167.00	15963	0.103
	4hrs	12.80	16753	0.101
	8hrs	12.39	15380	0.086
C980	**Unprocessed**	2.39	11454	0.037
	4hrs	2.71	8656	0.023
	8hrs	2.38	8406	0.029

Table 4.5: Parameters obtained from fitting of Yasuda Carreau model to experimental data

Figures 4.20 to 4.22 show the Carreau model fits the data well for all shear rates investigated. The values of viscosity at zero shear rate should decrease with a longer exposure to temperature to correspond to the MFR results discussed previously, however only C980 reflects this behaviour. It is possible this is due to the MFR testing being conducted at shear rates lower than those investigated using the rheometer.

4.3.3 Tensile Testing

Stress vs. strain curves of the samples of virgin PFA exposed to various residence times at temperature as described in Chapter 3 are presented below in Figure 4.23. The data for C980 is displayed on a separate graph in Figure 4.24.

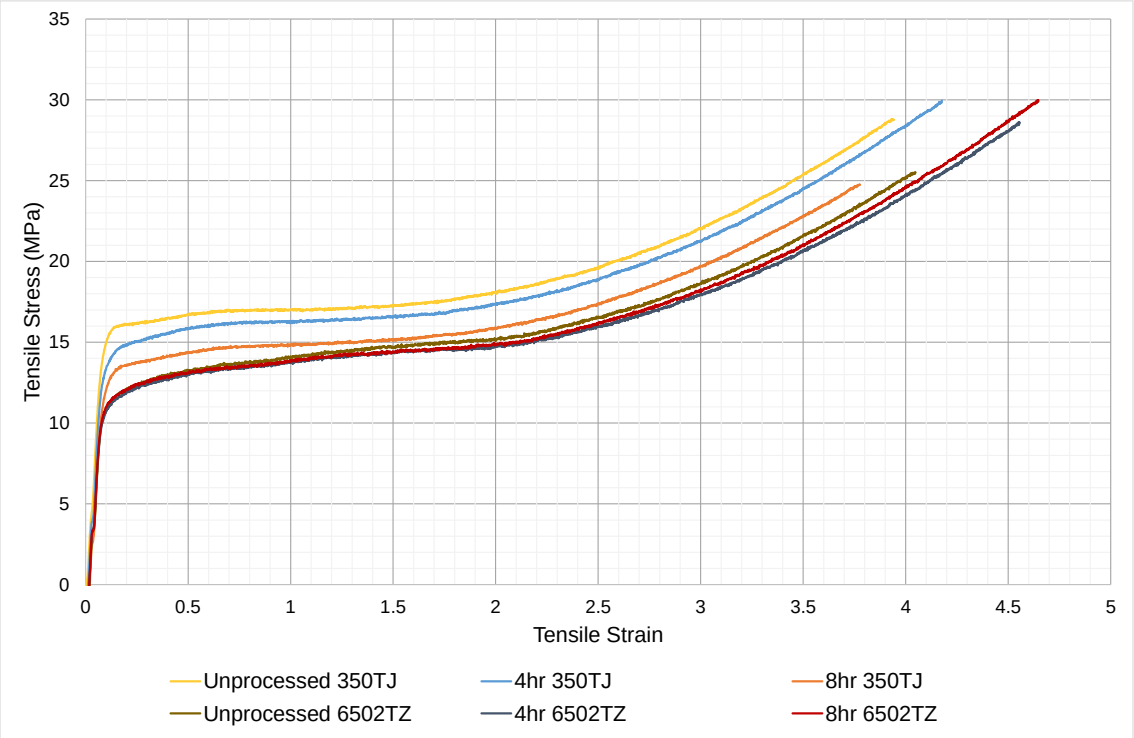

Figure 4.23: Stress vs. strain data for the virgin PFA grades exposed to various residence times. Each curve is the average of 5 tests, displayed to the lowest elongation of the data set.

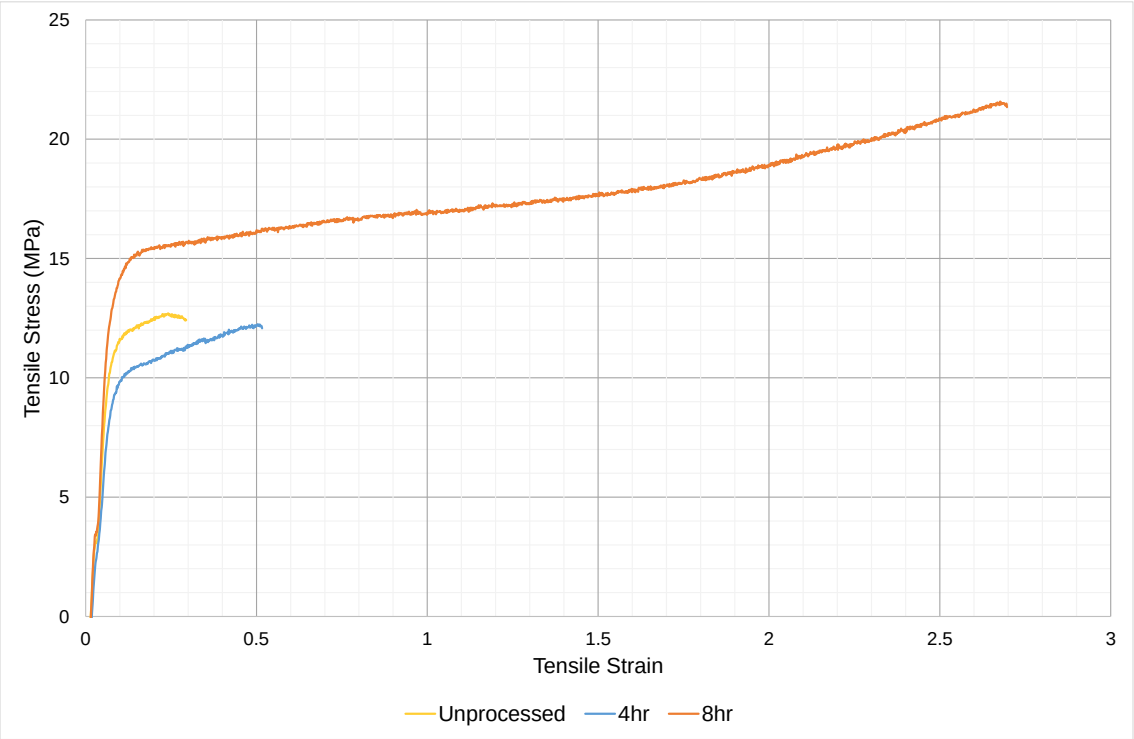

Figure 4.24: Stress vs. strain data for C980 exposed to various residence times. Each curve is the average of 5 tests, displayed to the lowest elongation of the data set.

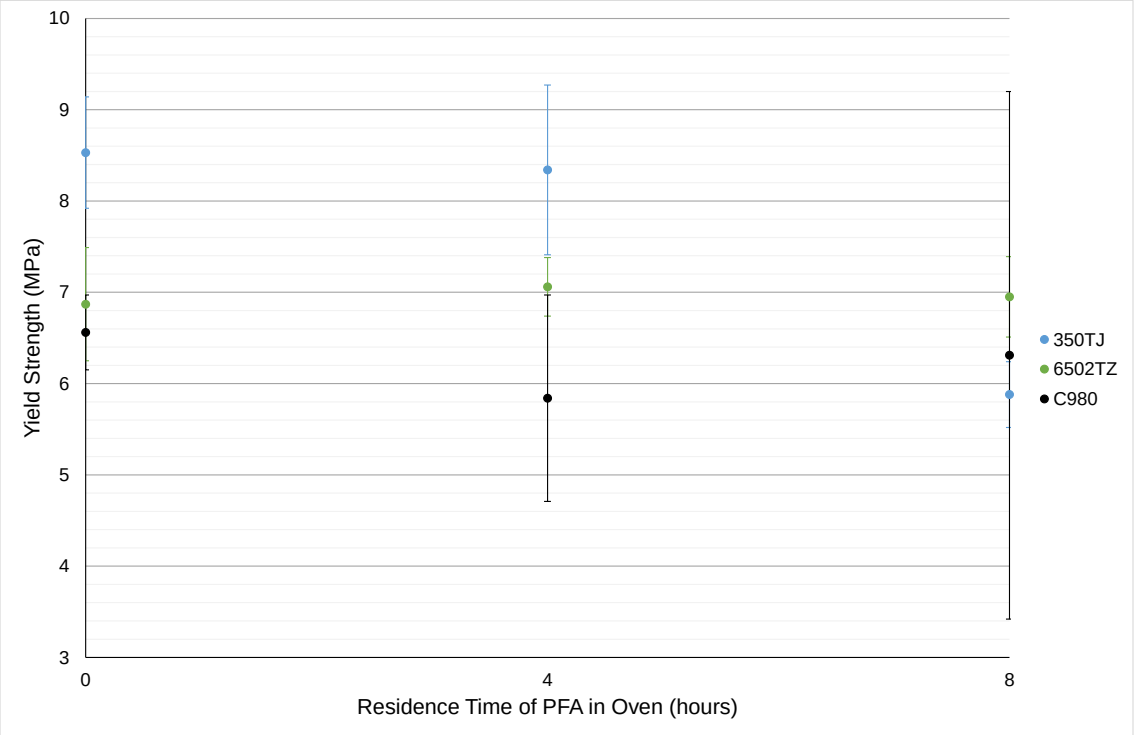

Figure 4.25: Values of the yield strength of the samples from the average and standard deviation of 5 tests

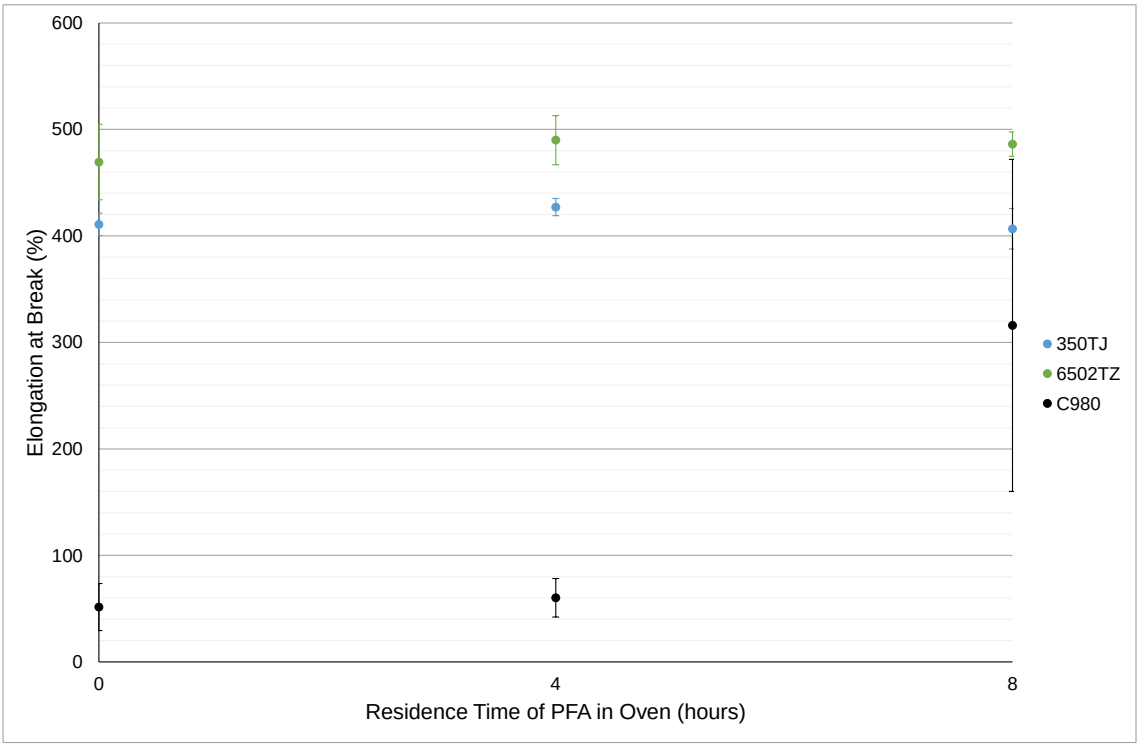

Figure 4.26: Values of the elongation at break of the samples from the average and standard deviation of 5 tests

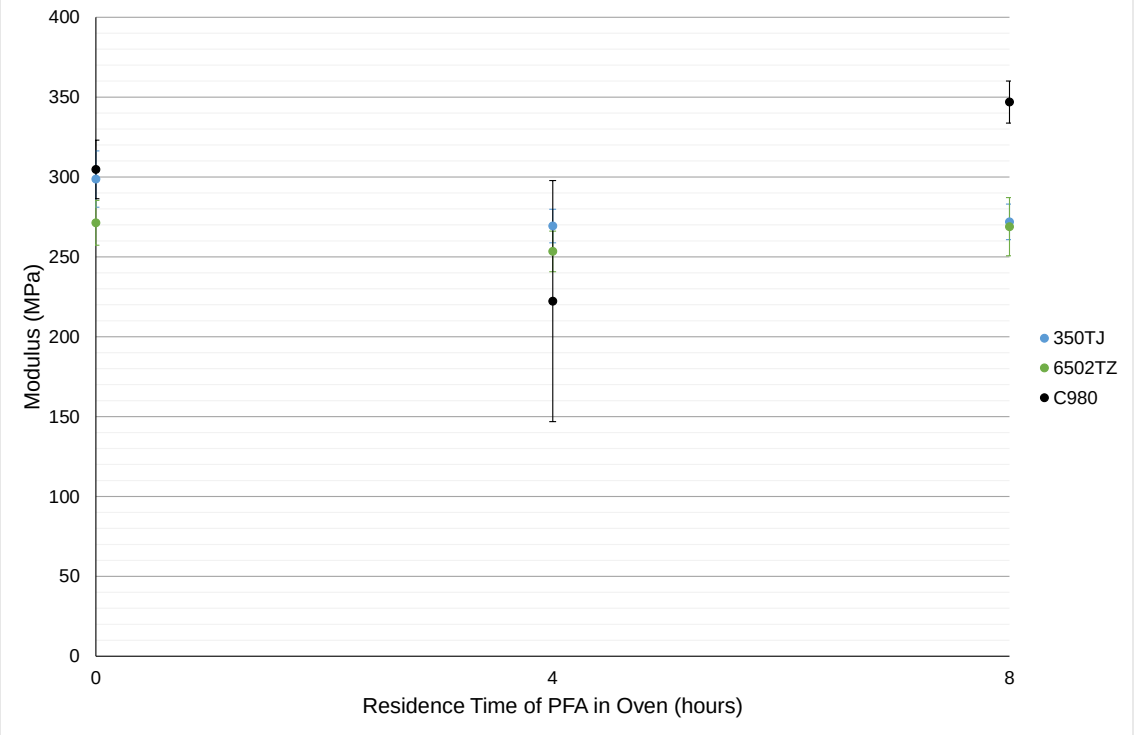

Figure 4.27: Values of the modulus of the samples from the average and standard deviation of 5 tests

The virgin PFA gave more consistent results, with the curves of each of the samples of 6502TZ exposed to 4 and 8hrs being almost identical. This contrasts

with the data from the samples of 350TJ, which shows the properties to decrease with increasing residence time. This leads to the conclusion that 6502TZ is more process stable than 350TJ, however the stress strain curves indicate that 350TJ aged for 8hrs has superior properties to 6502TZ. The properties of 350TJ may decrease with increased residence time due to a reduction in the molecular weight. Whilst the viscosity of the samples held for various periods does not appear to decrease (see Figures 4.20 to 4.22), MFR testing could be used to substantiate this conclusion. The elongation at break of all samples is still above the minimum required value in ASTM D3307 (2013) of 300%, and above the values given on the material certificates.

As with the unprocessed samples of C980, the material aged for 4hrs suffered premature breakage, almost certainly due to the quality of the plaque. It is assumed there is a change that occurs in the polymer between 4-8hrs that allows it to flow and create a better quality plaque, as the moulding conditions remained unchanged for each of the samples. The stress-strain curve of the material aged for 8hrs is similar to the data from testing of the virgin PFA grades, and the elongation at break is above the minimum value of 300%.

4.3.4 DSC

The second heating curves showing the melting peak endotherms of the PFA materials used in this study are shown below in Figures 4.28, 4.29 and 4.30.

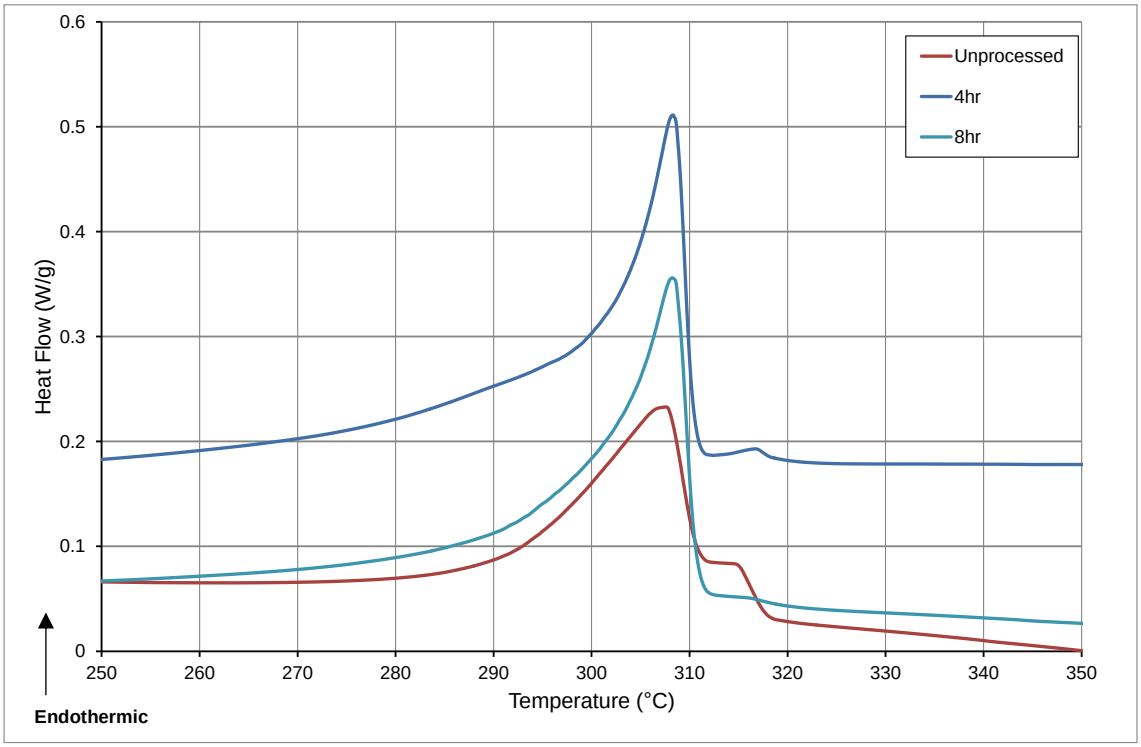

Figure 4.28: DSC traces showing the second heating of samples of Chemours 350TJ exposed to various residence times

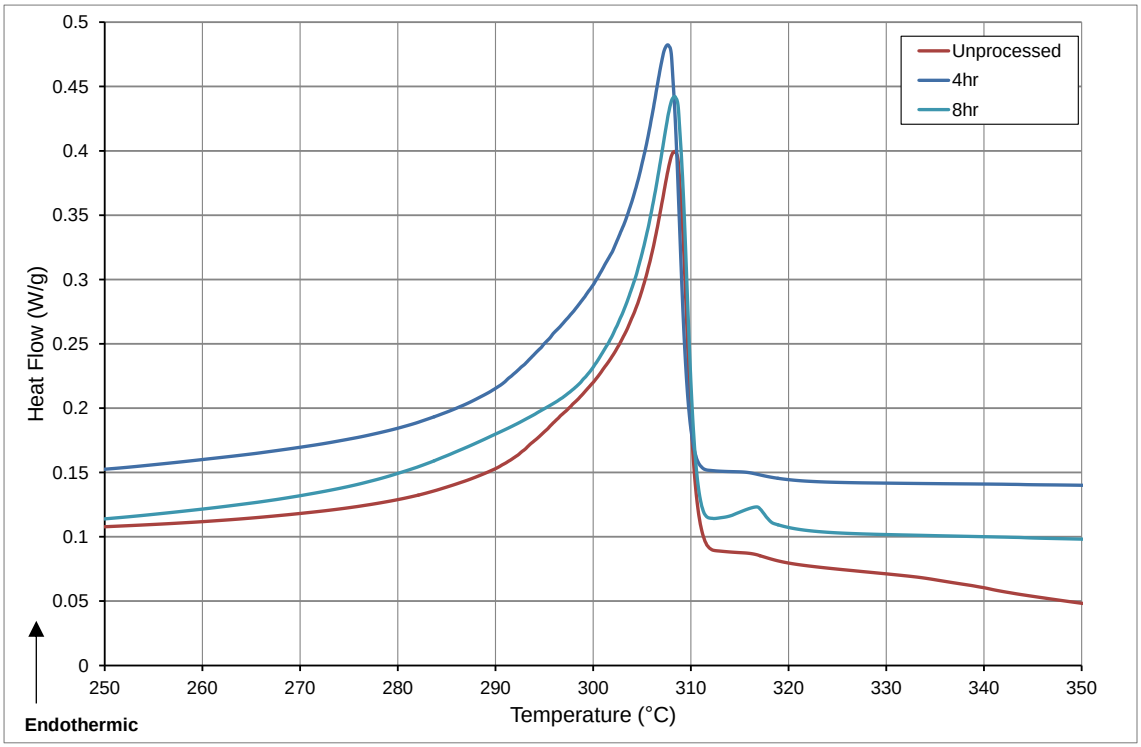

Figure 4.29: DSC traces showing the second heating of samples of Dyneon 6502TZ exposed to various residence times

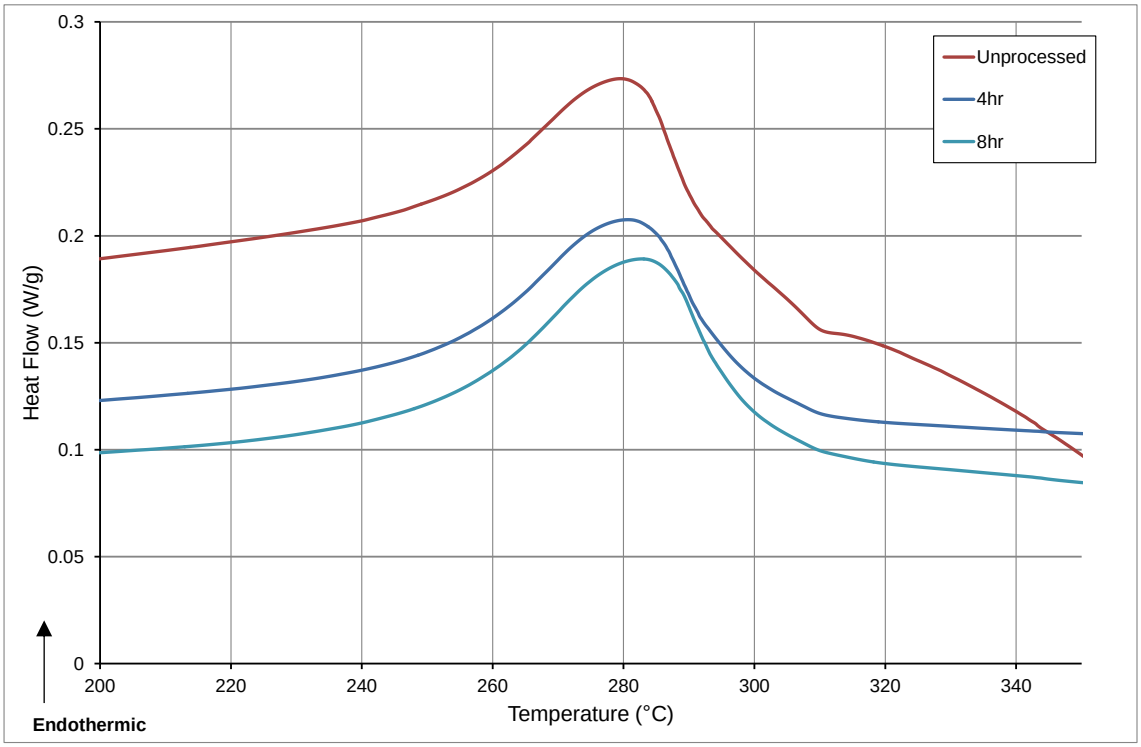

Figure 4.30: DSC traces showing the second heating of samples of Chemours C980 exposed to various residence times

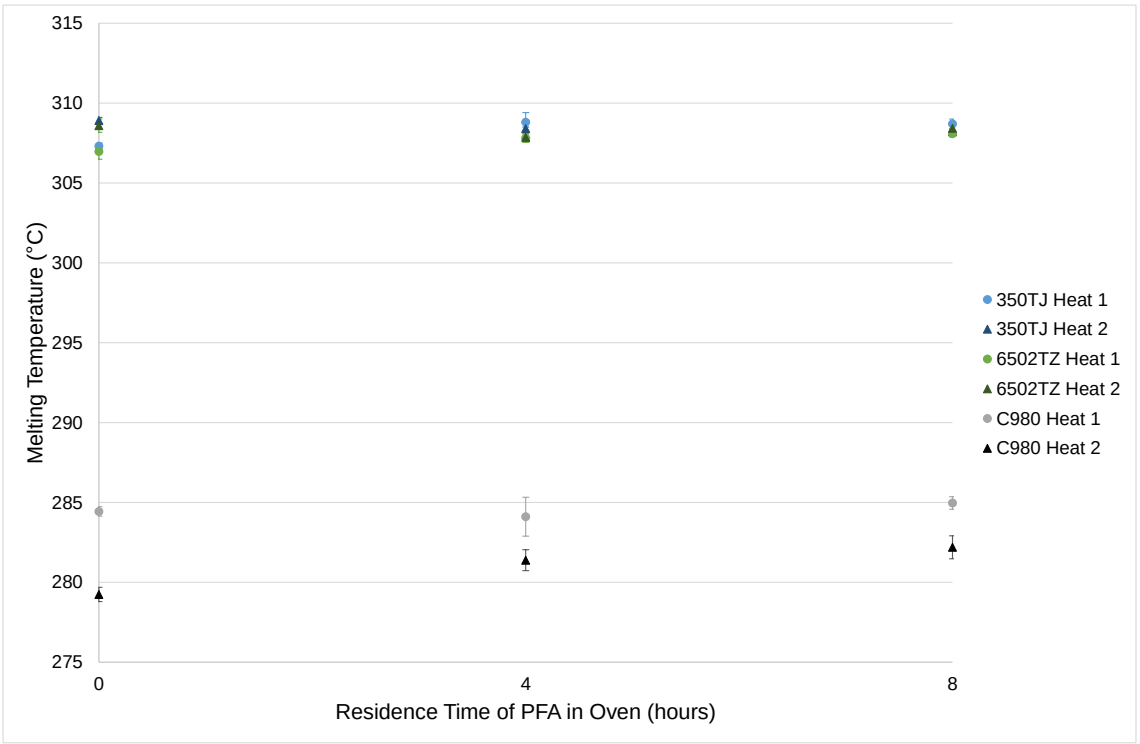

Figure 4.31: Values of the melting peak endotherm of the first and second heating cycles

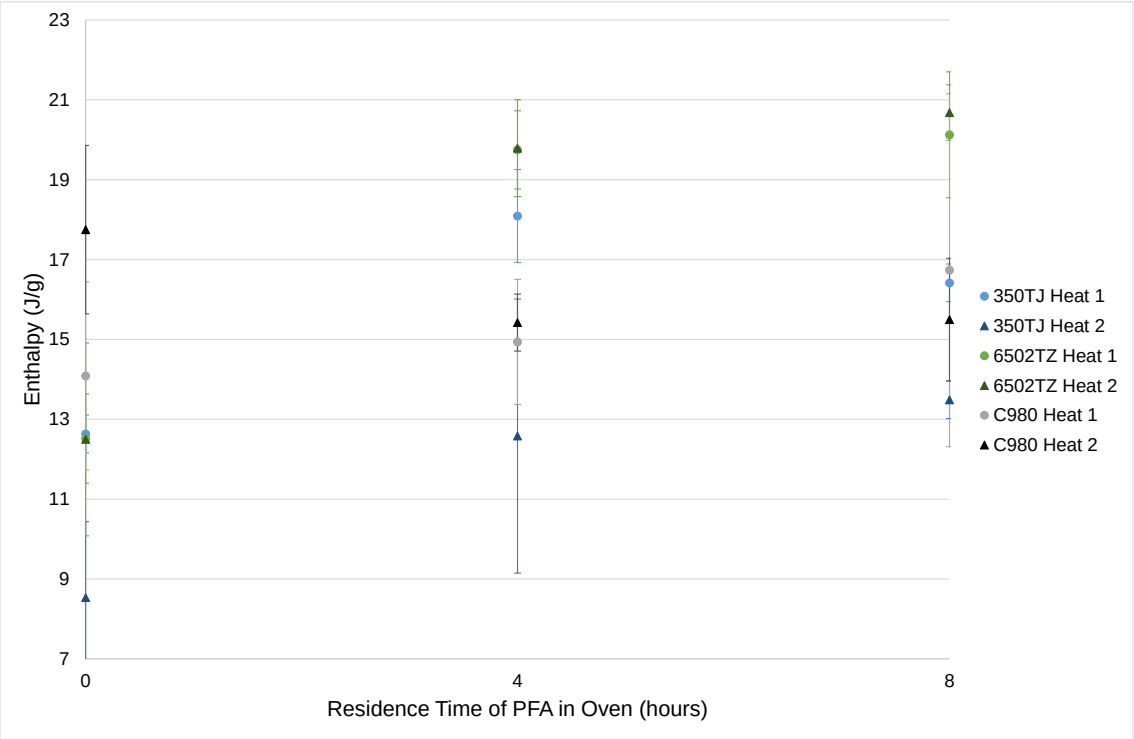

Figure 4.32: Values of the enthalpies of the first and second heating cycles

Figure 4.33: Level of crystallinity of the material of the first and second heating cycles

The data shows a slight drop in melt temperature with residence time for virgin PFA, however the 4hr aged 6502TZ has a lower melt temperature than the same material aged for 8hrs. There is a reasonably regular increase in enthalpy

with residence time for the virgin grades, however this trend is reversed for the carbon filled PFA. For all grades the error bars are significant for the unprocessed material, making it difficult to draw conclusions with a high level of certainty. The melt temperature of C980 shows a slight increase with residence time, however this effect can be absorbed easily by the uncertainties. Figure 4.30 shows a reduction in the shoulder of 350TJ with residence time, however this trend is not shown with the other virgin PFA as the shoulder only appears after 8 hrs heat aging. The presence of more than one crystalline structure could be further investigated using x ray techniques.

4.3.5 Near Infrared Spectroscopy

The spectroscopic techniques used on the samples of PFA exposed to various residence times at temperature as described in Chapter 3 are presented in this section. As previously discussed in 4.1.4, spectra obtained by FTIR are included in an appendix due to the limited differences observed. The analysis using Partial Least Squares (PLS) and Principal Component Scores (PCS) on the spectra obtained from Near Infrared Spectroscopy are presented below.

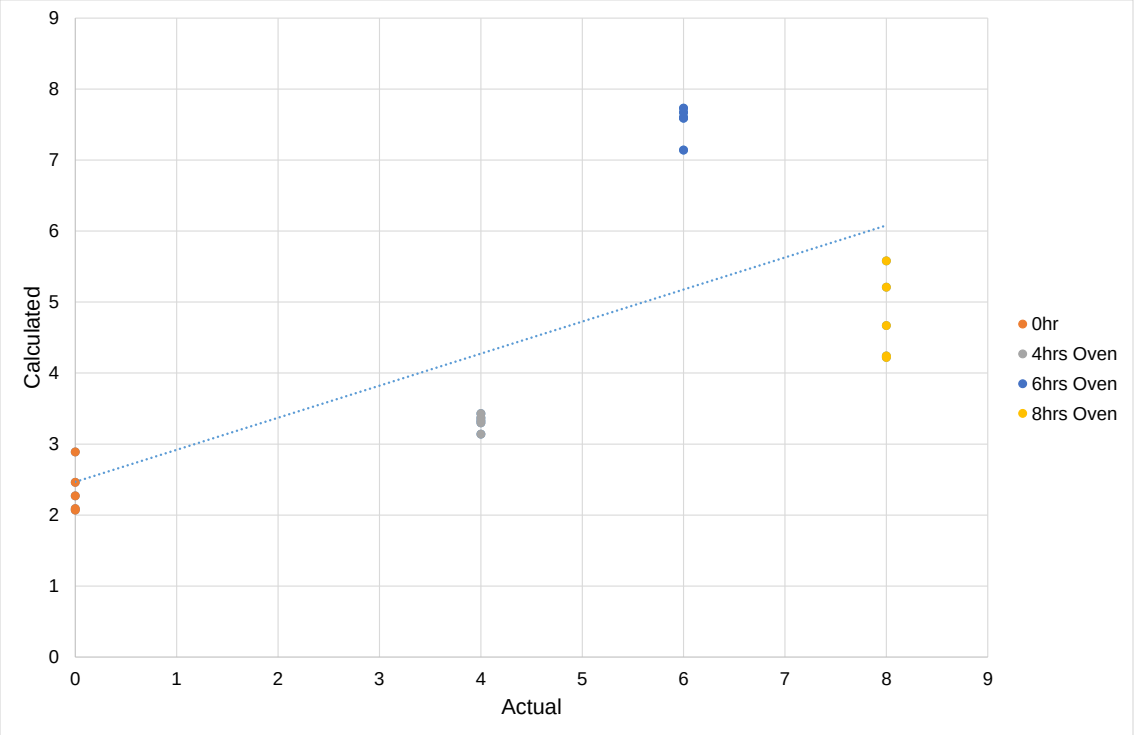

Figure 4.34: Partial Least Squares regression of the samples of 350TJ with a correlation coefficient of 0.6722

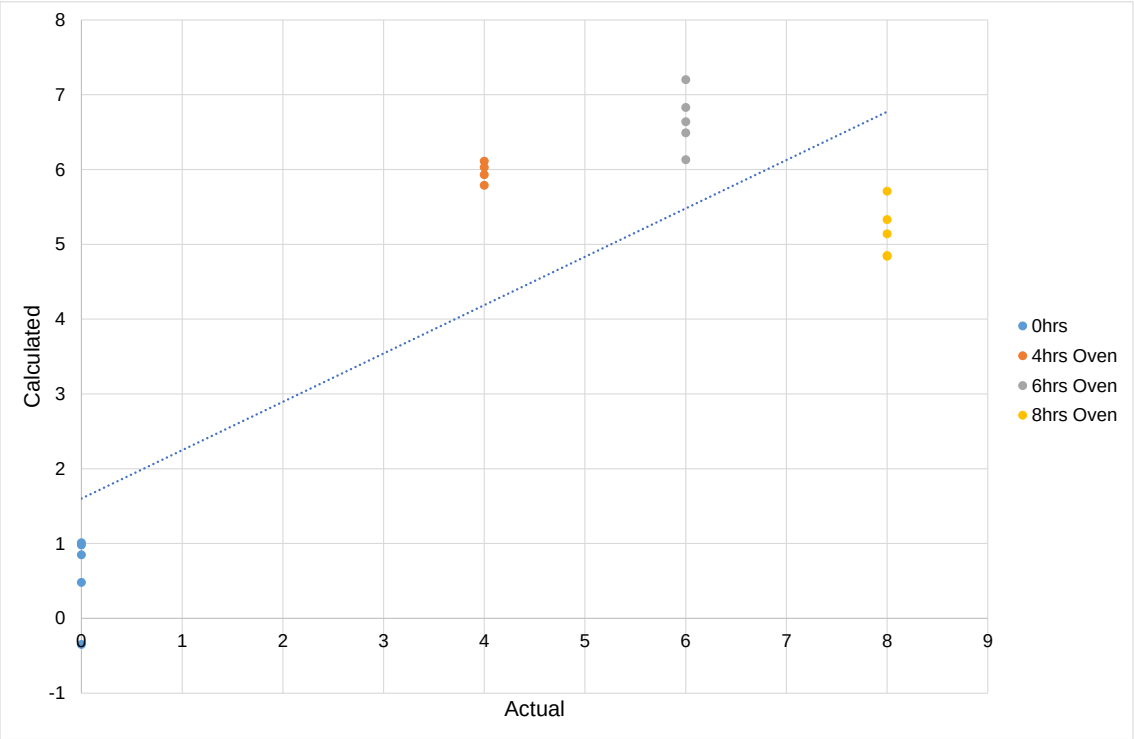

Figure 4.35: Partial Least Squares regression of the samples of 6502TZ with a correlation coefficient of 0.8039

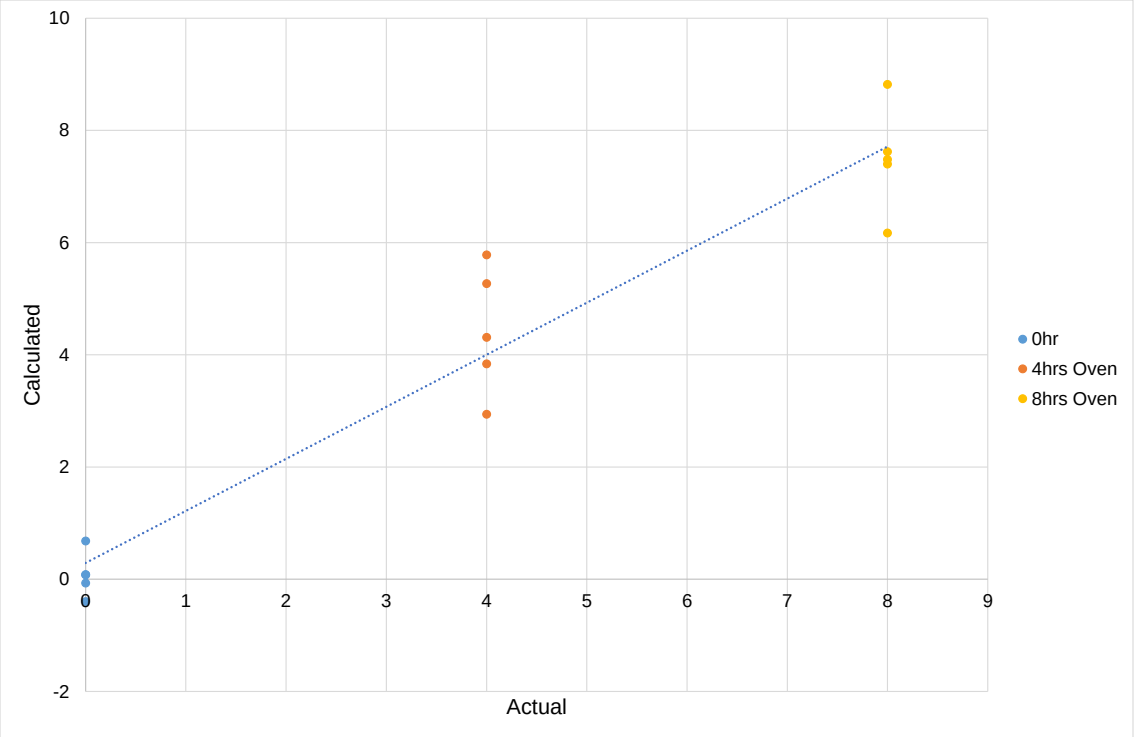

Figure 4.36: Partial Least Squares regression of the samples of C980 with a correlation coefficient of 0.9635

Partial Least Squares shows a reasonable level of correlation between the samples, however the spread of the data points makes it difficult to estimate the heat history of a sample to a good degree of accuracy.

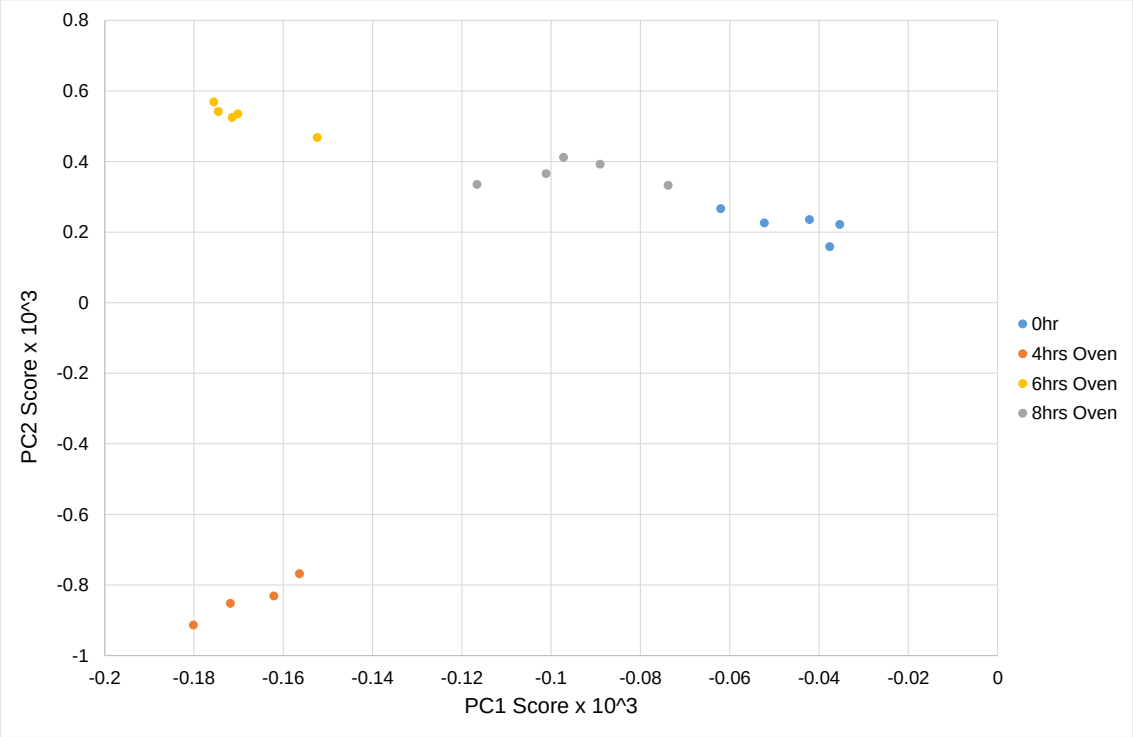

Figure 4.37: Principal Component Scores of the samples of 350TJ

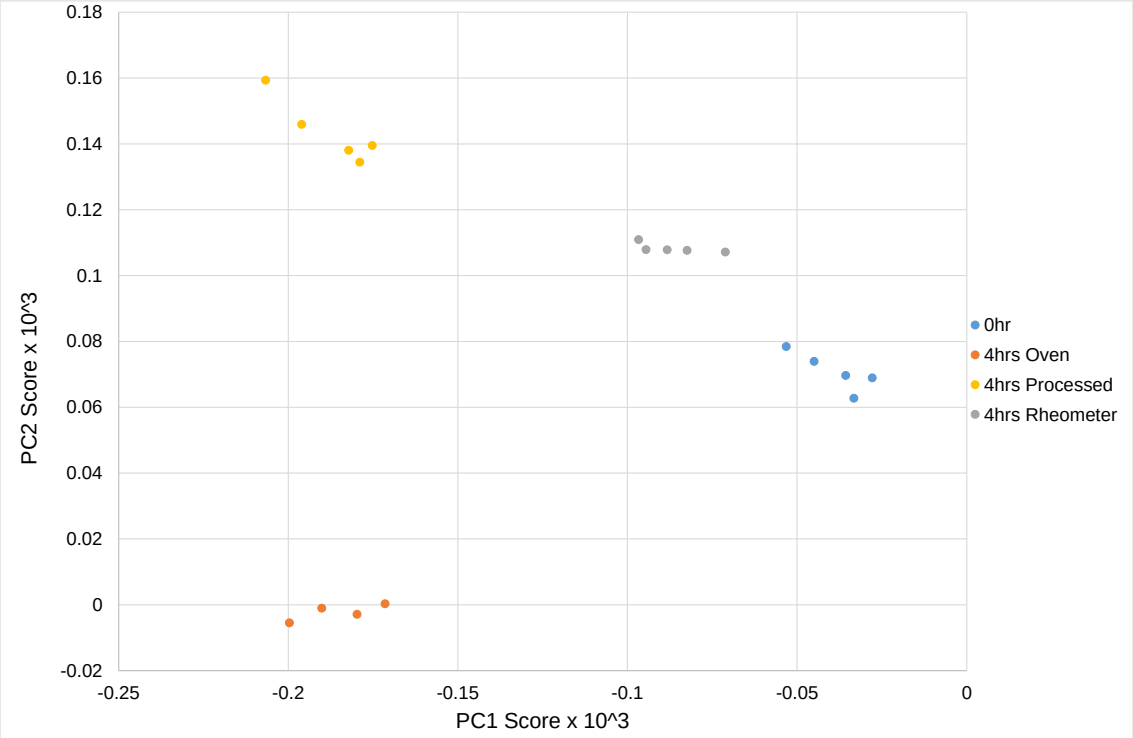

Figure 4.38: Principal Component Scores of the samples of 350TJ aged using various methods

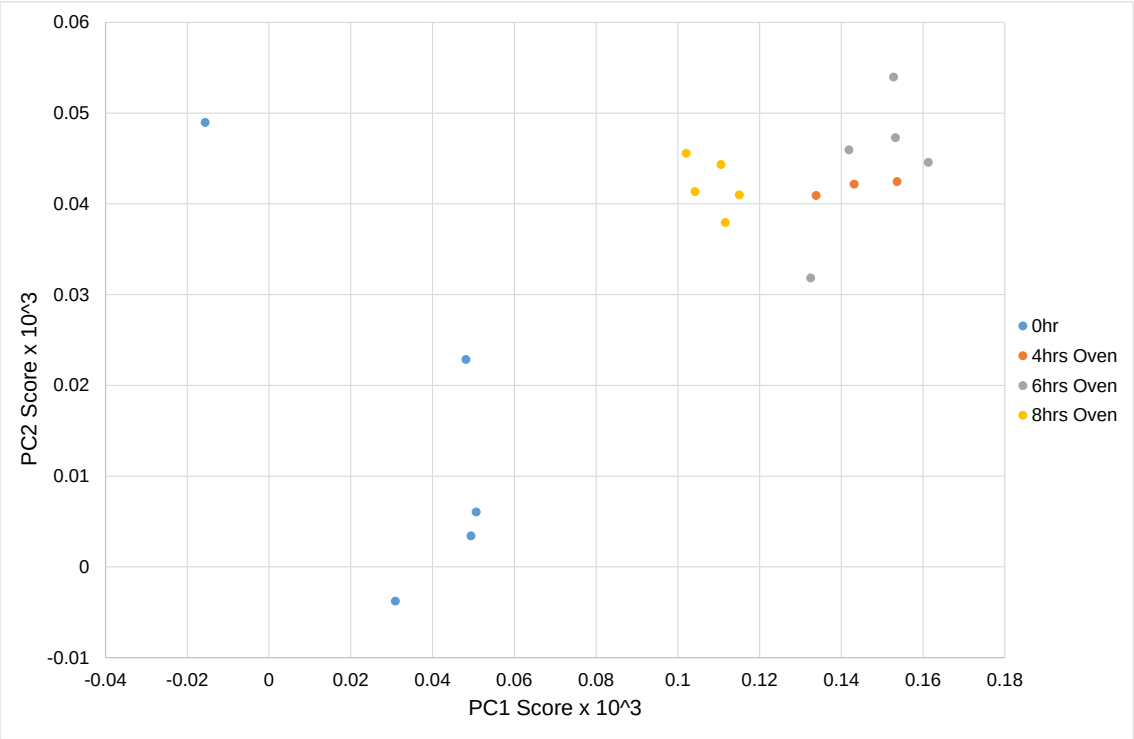

Figure 4.39: Principal Component Scores of the samples of 6502TZ

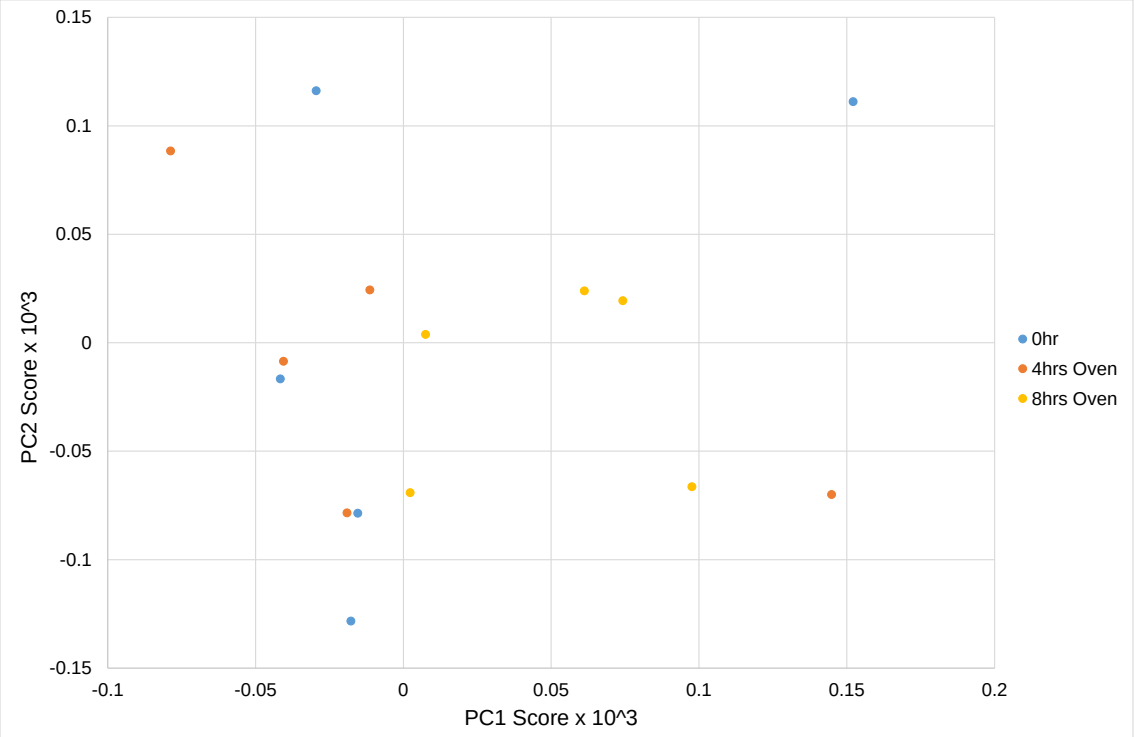

Figure 4.40: Principal Component Scores of the samples of C980

Principal Component Analysis shows an element of grouping of the aged samples of virgin PFA. Figure 4.40 demonstrates the method is unsuitable for investigating C980. The results are thought to be due to laser heating of the material due to the carbon black content.

4.4 Effect of Shear

Fluoropolymer suppliers advise processing below the critical shear rate of PFA to avoid compromising the material properties, however no data has been published to support this. It is unclear whether the advice stems from the use of PFA in wire coating applications, where unstable flow conditions would be a cause for rejection. The aim of these experiments was to quantify the change in material properties due to exposure to high shear rates using the samples detailed in Chapter 3.

4.4.1 Viscosity

The data generated on the Hastelloy® capillary rheometer showing the change in viscosity due to exposure to high shear of the three grades of PFA is presented below in Figures 4.41 to 4.43.

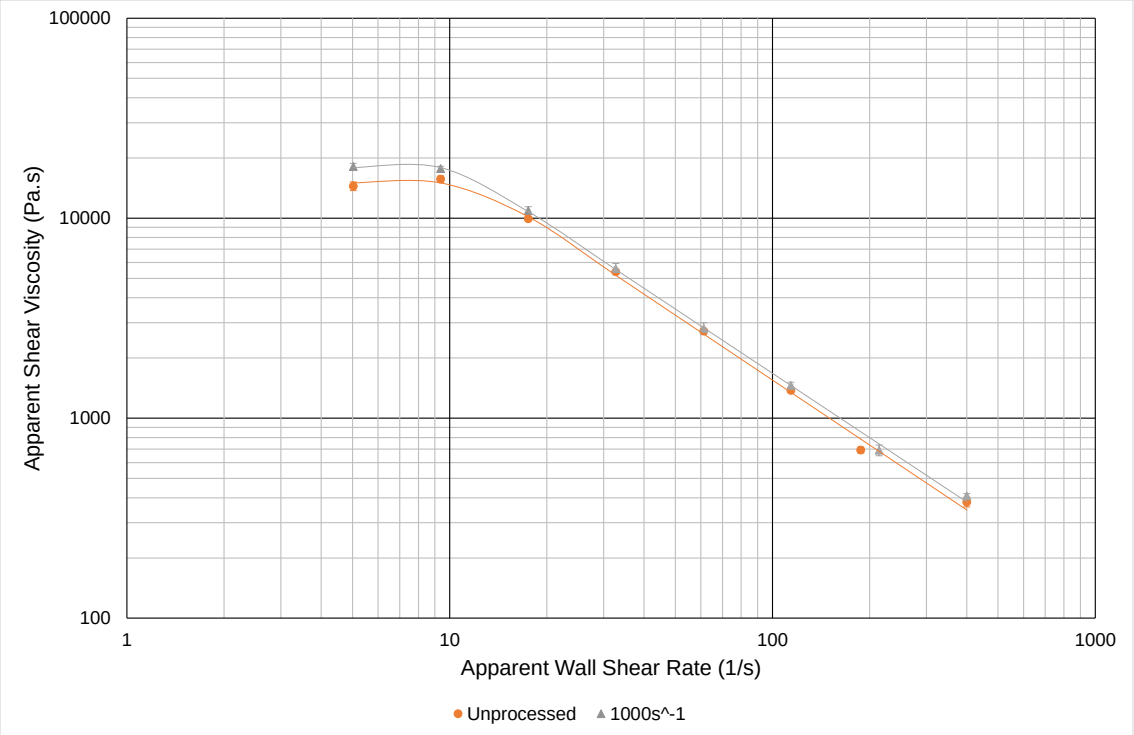

Figure 4.41: Carreau fit of 350TJ showing the effect of being subjected to a shear rate of $1000s^{-1}$

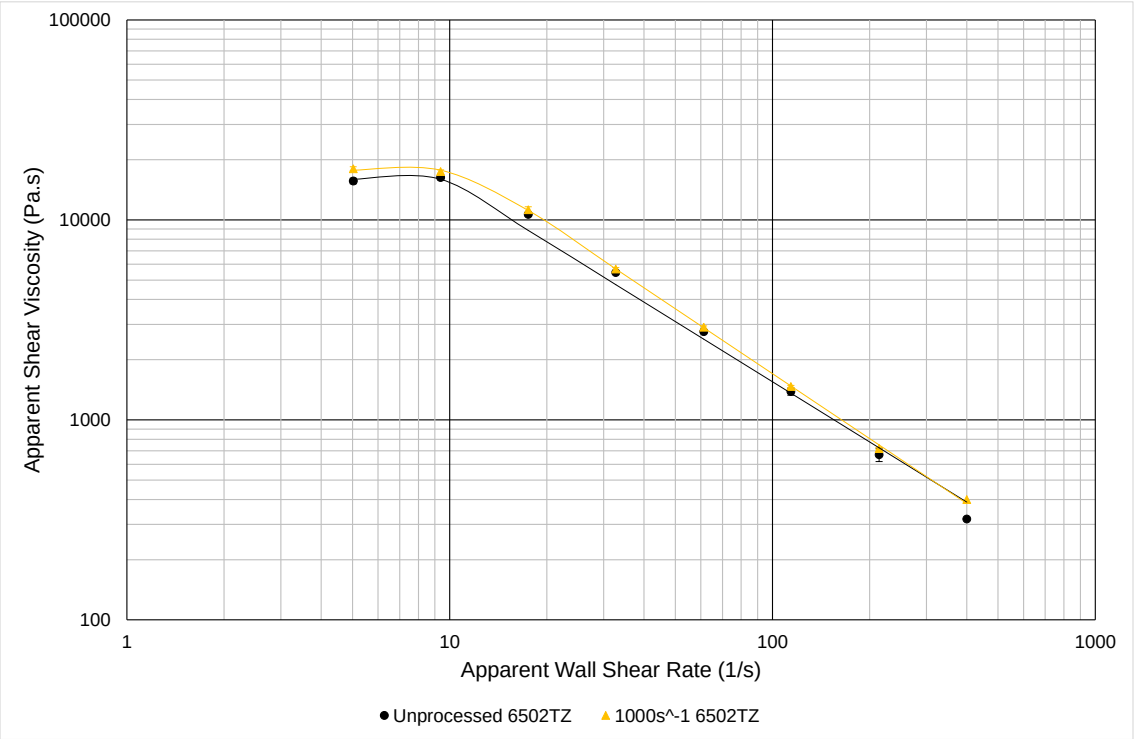

Figure 4.42: Carreau fit of 6502TZ showing the effect of being subjected to a shear rate of $1000s^{-1}$

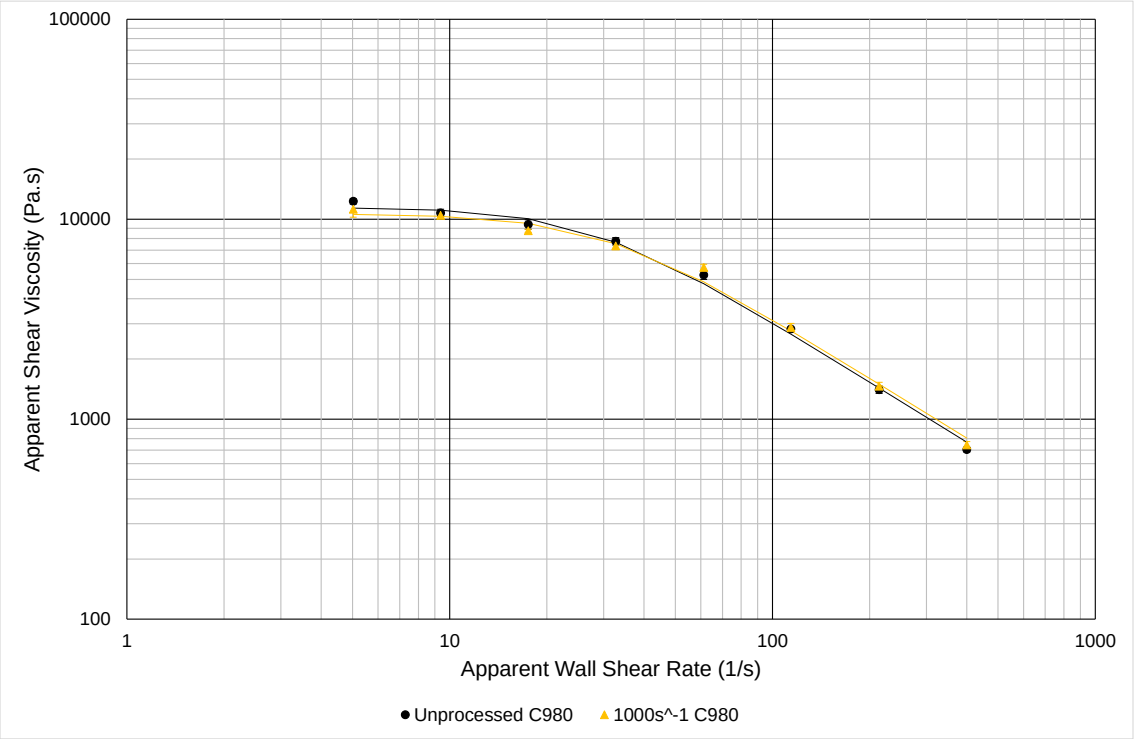

Figure 4.43: Carreau fit of C980 showing the effect of being subjected to a shear rate of $1000s^{-1}$

		a	η_0 (Pa.s)	λ (s)
350TJ	**Unprocessed**	83.69	15012	0.096
	1000s^-1	36.19	18116	0.108
6502TZ	**Unprocessed**	167.00	15963	0.103
	1000s^-1	18.41	18010	0.105
C980	**Unprocessed**	2.39	11454	0.037
	1000s^-1	2.29	10635	0.033

Table 4.6: Parameters obtained from Yasuda Carreau fits to experimental data

The viscosity of the samples of PFA exposed to high shear rates increased slightly, indicating that they have not been damaged. The values of the parameters for the Carreau fit were obtained by minimising the sum of errors in Excel using the Solver add in. The Carreau model fits the data well in general, the values of n have been discussed previously in section 4.3.2.

4.4.2 Tensile Testing

Stress vs. strain curves of the samples of virgin PFA exposed to high shear rates as described in Chapter 3 are presented below in Figure 4.44. The data for C980 is displayed on a separate graph in Figure 4.45.

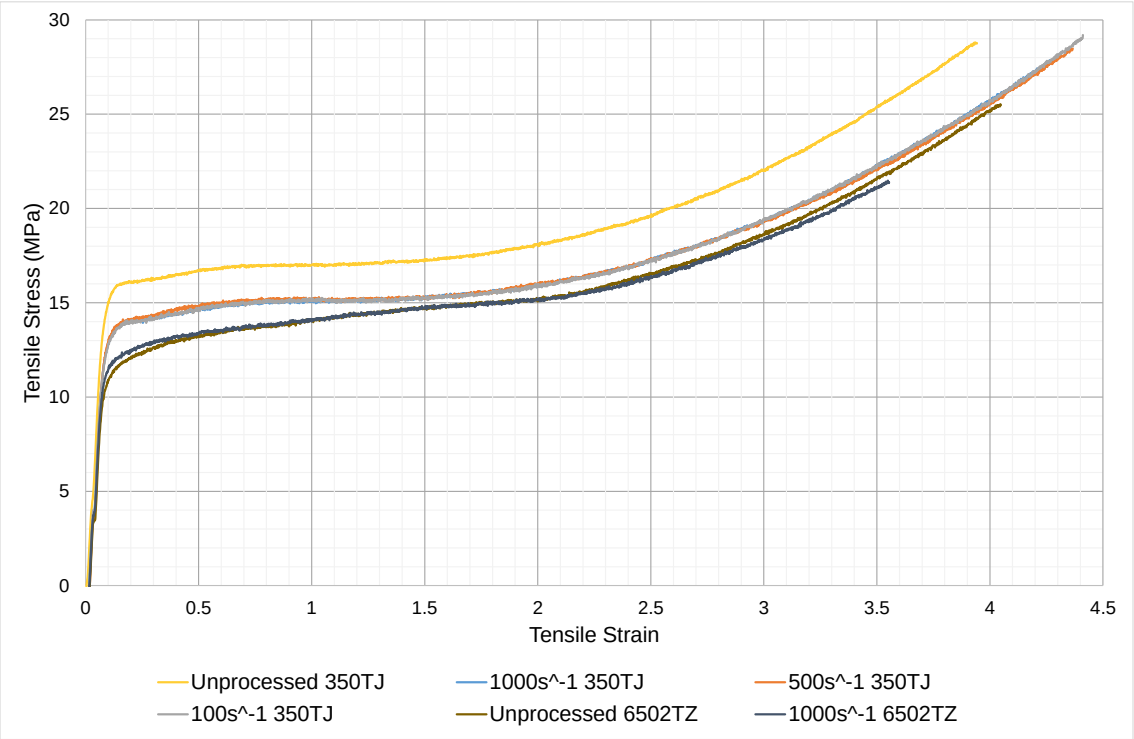

Figure 4.44: Stress vs. strain data for the virgin PFA grades exposed to various shear rates. Each curve is the average of 5 tests, displayed to the lowest elongation of the data set.

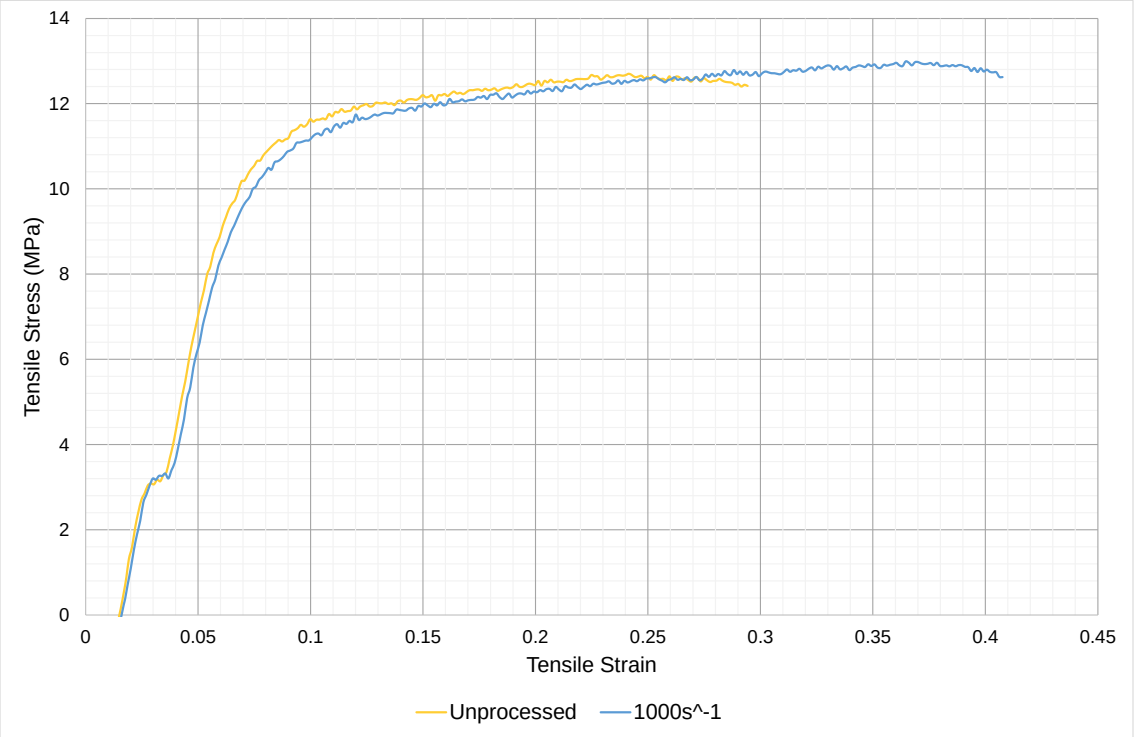

Figure 4.45: Stress vs. strain data for C980 exposed to $1000s^{-1}$. Each curve is the average of 5 tests, displayed to the lowest elongation of the data set.

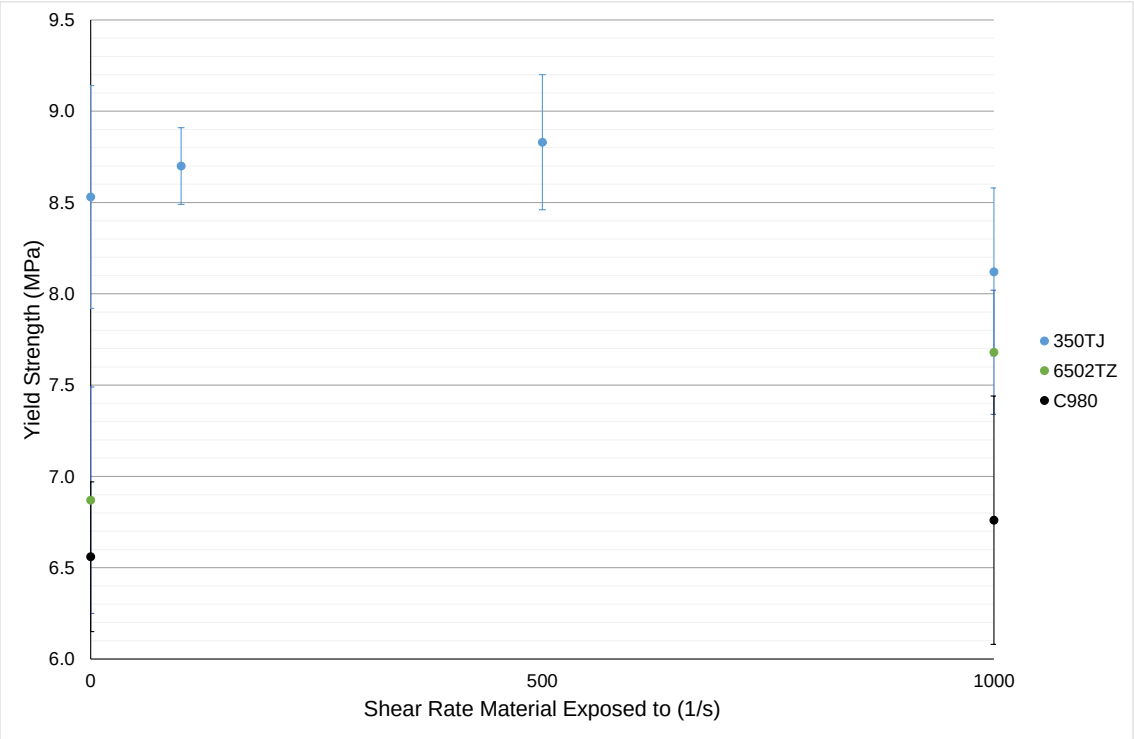

Figure 4.46: Values of the yield strength of the samples from the average and standard deviation of 5 tests

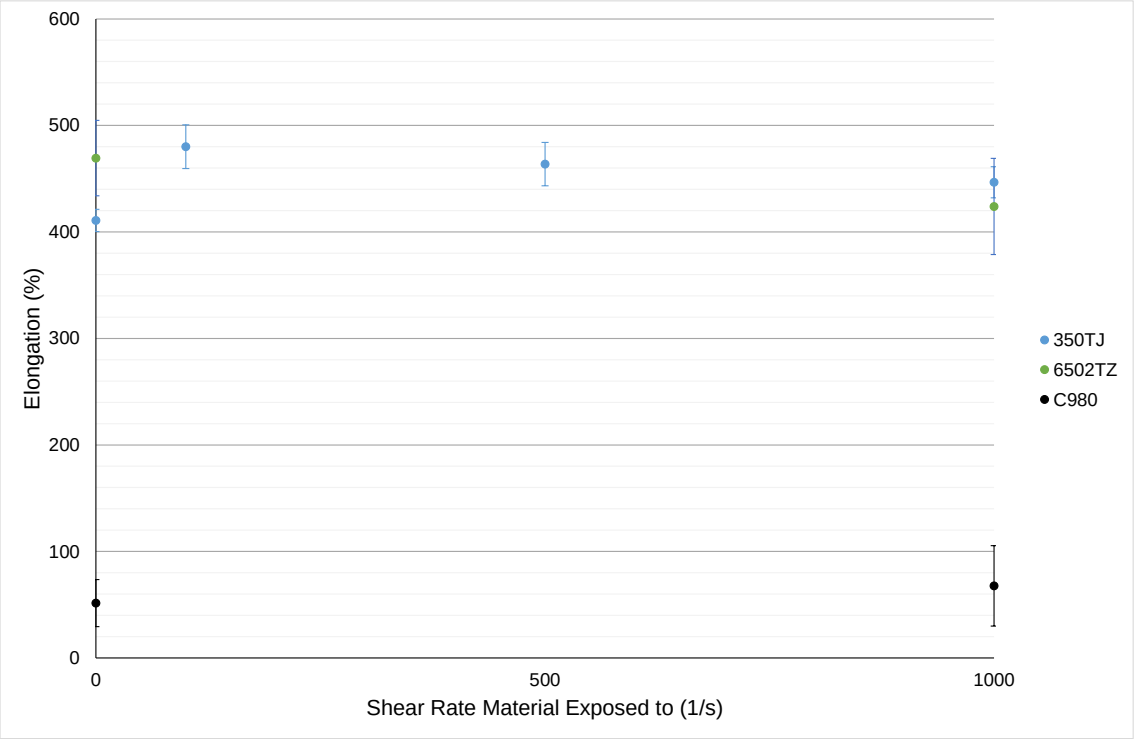

Figure 4.47: Values of the elongation at break of the samples from the average and standard deviation of 5 tests

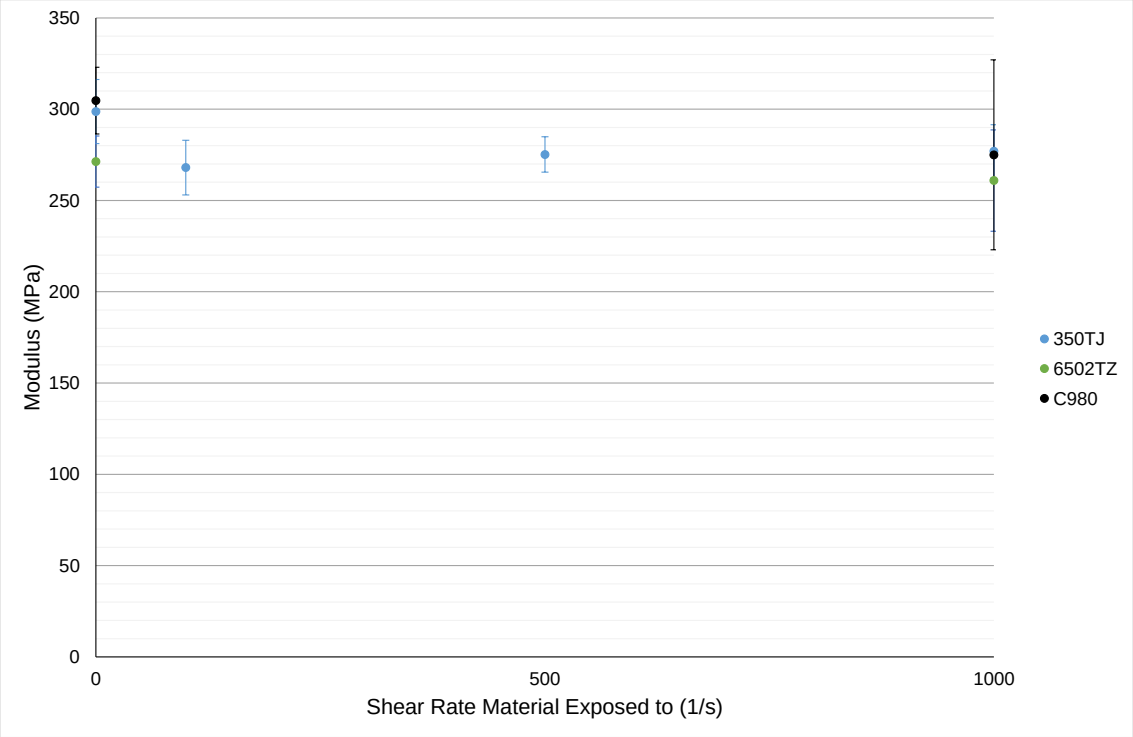

Figure 4.48: Values of the modulus of the samples from the average and standard deviation of 5 tests

Figure 4.44 shows the stress strain curve for the sample of 6502TZ exposed to 1000s^{-1} follows the same path as the unprocessed material, however the sheared material does result in a lower modulus and elongation at break. The samples of 350TJ exposed to shear have a significantly different curve to that of the unprocessed sample, however the data of all the sheared samples is very similar. The modulus of the sheared material is reduced by up to 10%, accompanied by a 5% reduction in yield strength, however the elongation at break increases by up to 17%. This shows subjecting 350TJ to high shear does affect the mechanical properties, however the level of shearing does not seem to affect the magnitude of the change seen in the material. The values of elongation are still above the minimum required by ASTM D3307 (2013). The samples of C980 once again showed premature breakage, demonstrating the requirement for an improved compression moulding procedure for the preparation of the plaques.

4.4.3 DSC

The second heating curves of the PFA exposed to various shear rates are shown below in Figures 4.49, 4.50 and 4.51.

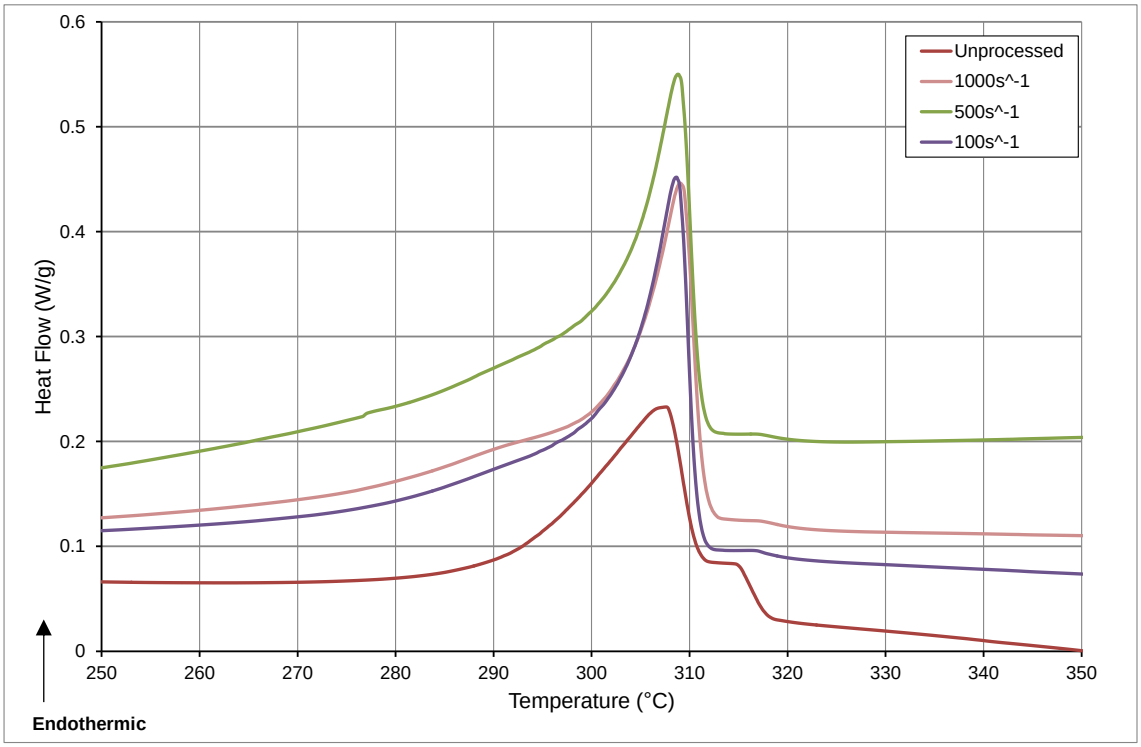

Figure 4.49: DSC traces showing the second heating of samples of Chemours 350TJ exposed to different shear rates

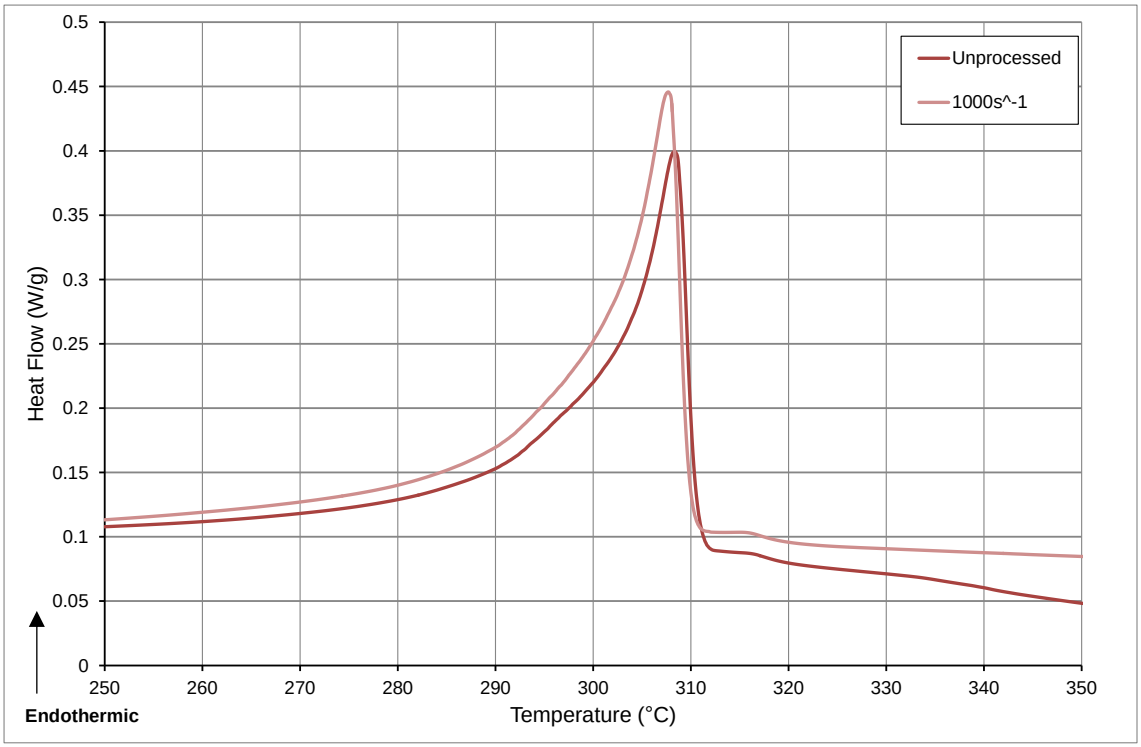

Figure 4.50: Comparison showing the second heating of unprocessed Dyneon 6502TZ to material exposed to a shear rate of $1000s^{-1}$

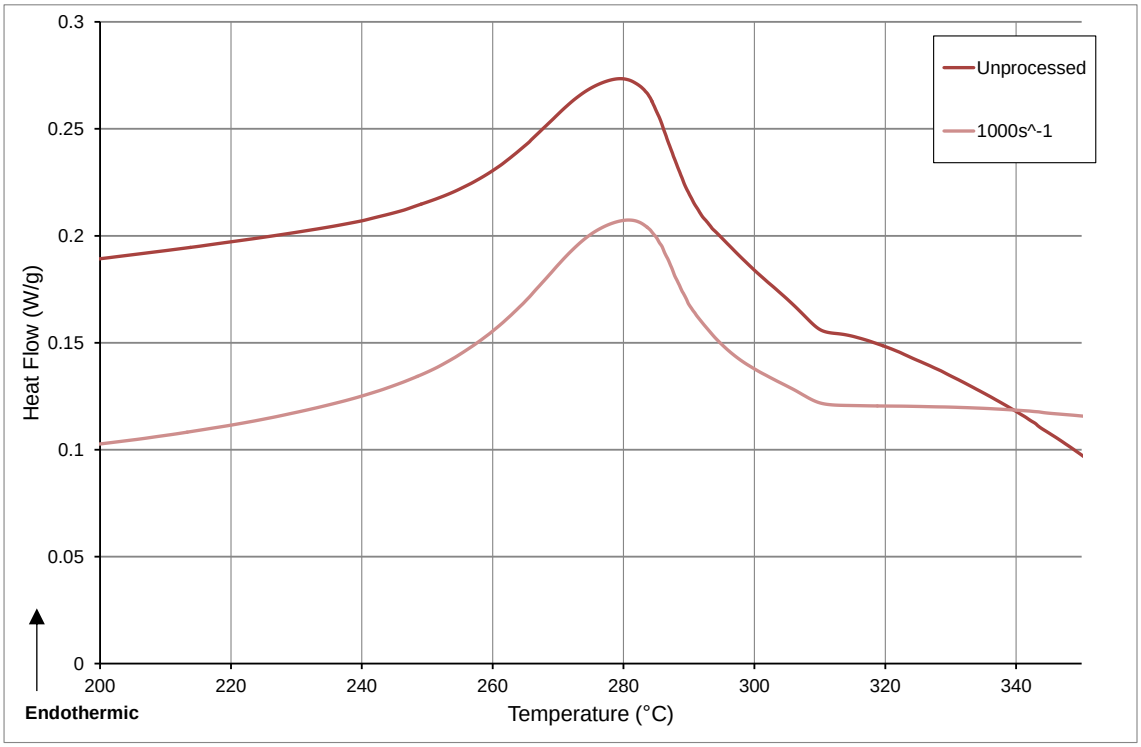

Figure 4.51: Comparison showing the second heating of unprocessed Chemours C980 to material exposed to a shear rate of $1000s^{-1}$

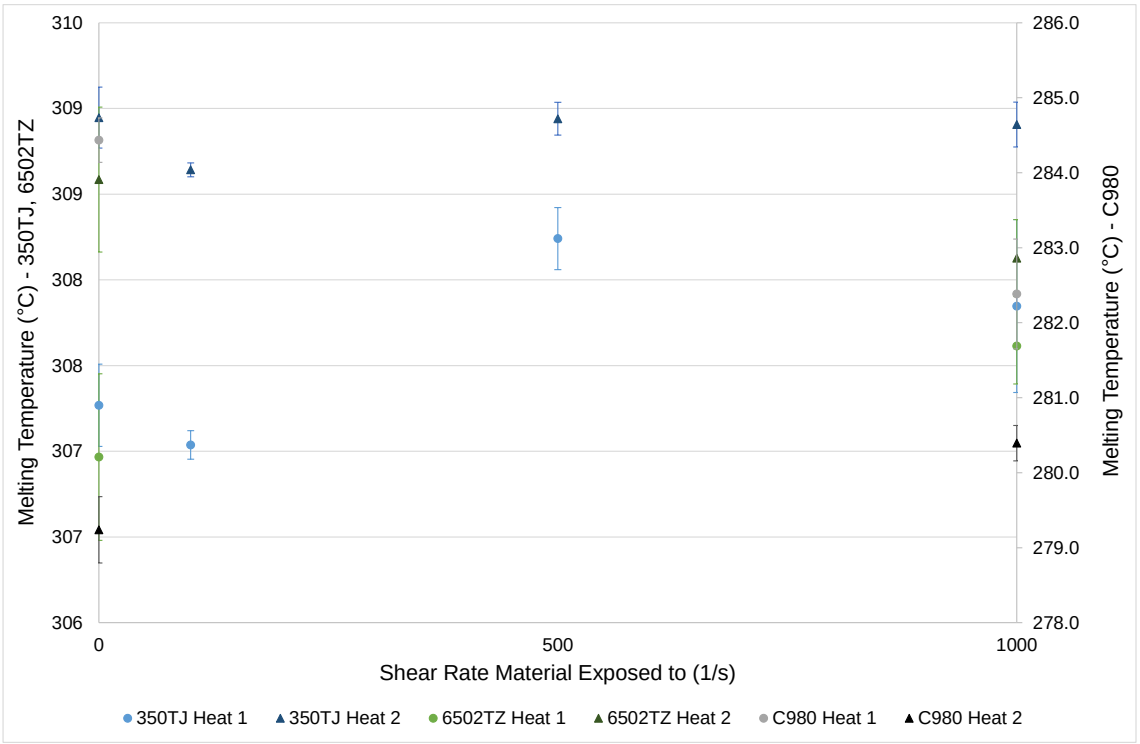

Figure 4.52: Values of the melting peak endotherm of the first and second heating cycles

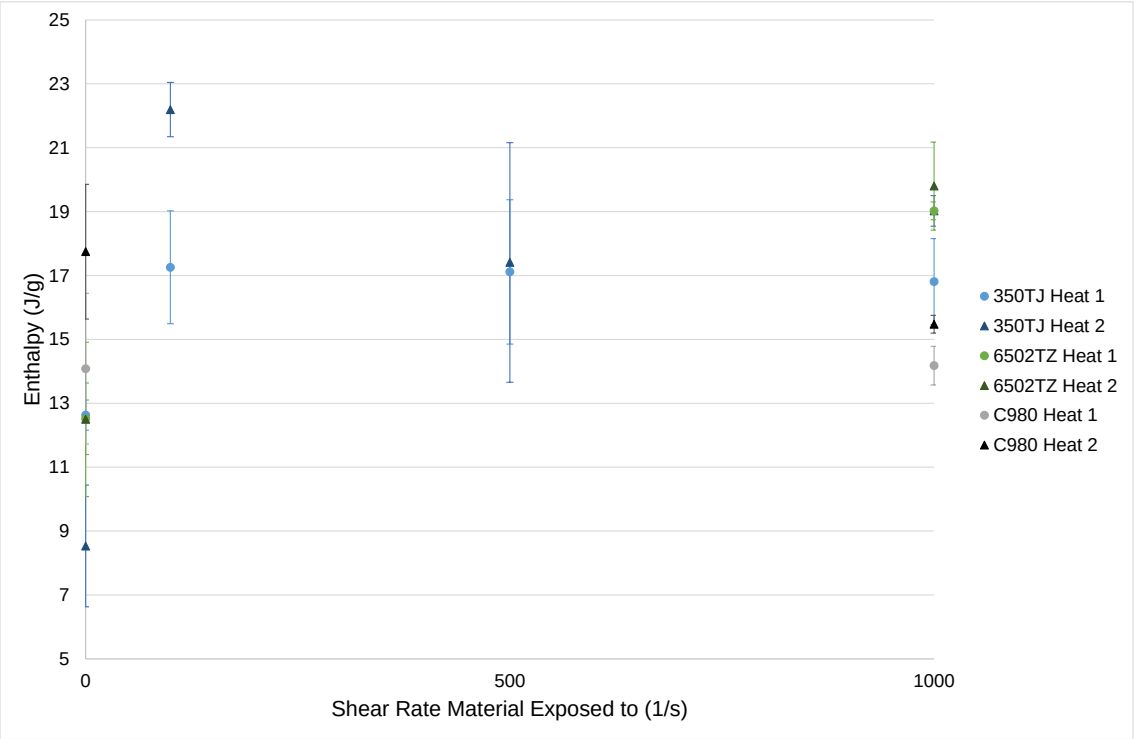

Figure 4.53: Values of the enthalpies of the first and second heating cycles

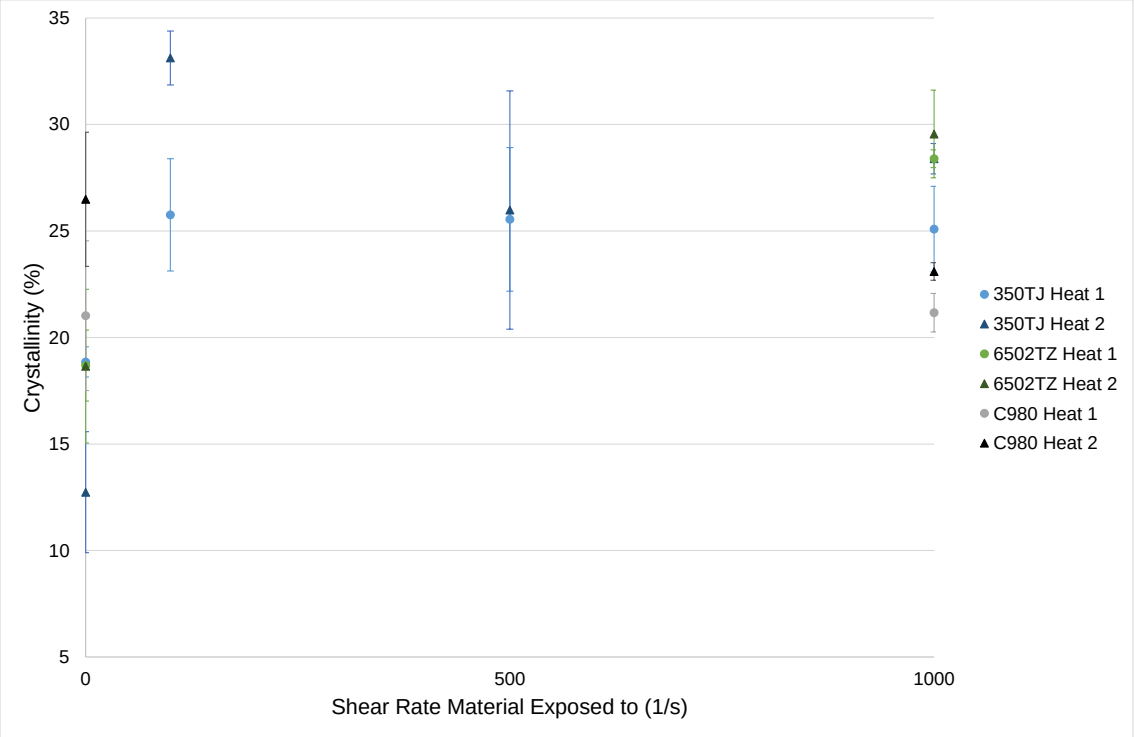

Figure 4.54: Level of crystallinity of the material of the first and second heating cycles

There is very little change in the melting temperature of all virgin grades processed at various shear rates. The enthalpy of the sheared 350TJ increases, however there is no clear relation to the level of shear the sample was

subjected to. The enthalpy of 6502TZ looks to increase with shearing, whereas the melting temperature is not significantly affected. Sheared static dissipating PFA also shows a more pronounced increase in melt temperature. The enthalpy of C980 decreases, however the error associated with the enthalpy of both samples is significant.

4.5 Effect of Processing

The results of various techniques to analyse the differences in material properties due to exposure to specific conditions have been presented. The aim of the experiments presented in this section was to obtain results from material that has been subjected to a combination of these conditions, which is more representative of a typical manufacturing environment.

4.5.1 Viscosity

The data generated on the Hastelloy® capillary rheometer showing the change in viscosity due to exposure of the 350TJ grade of PFA to typical transfer moulding conditions is presented below in Figure 4.55.

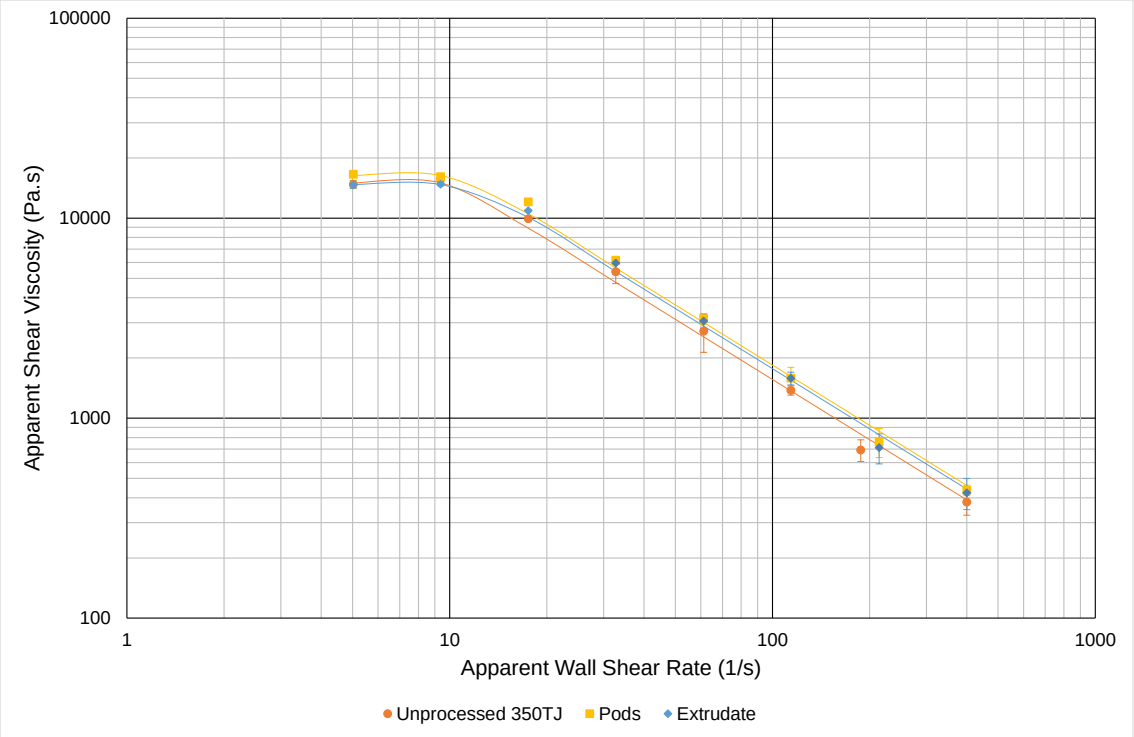

Figure 4.55: Carreau fit of 350TJ after processing

	a	η_0 (Pa.s)	λ (s)
Unprocessed	83.69	15012	0.096
Extrudate	51.31	14719	0.083
Pods	83.68	16334	0.089

Table 4.7: Parameters obtained from fitting of Carreau model to experimental data

The viscosity of the extrudate and the pods are very similar and are both higher than the unprocessed material. When comparing these results to the experiments on single effects this increase in viscosity is likely to be due to the residence time at temperature rather than the shear rate the polymer has been exposed to.

4.5.2 Melt Flow Rate Testing

The change in Melt Flow Rate (MFR) of the virgin grades of PFA exposed to various residence times in a transfer moulding pot is show below in Figure 4.56.

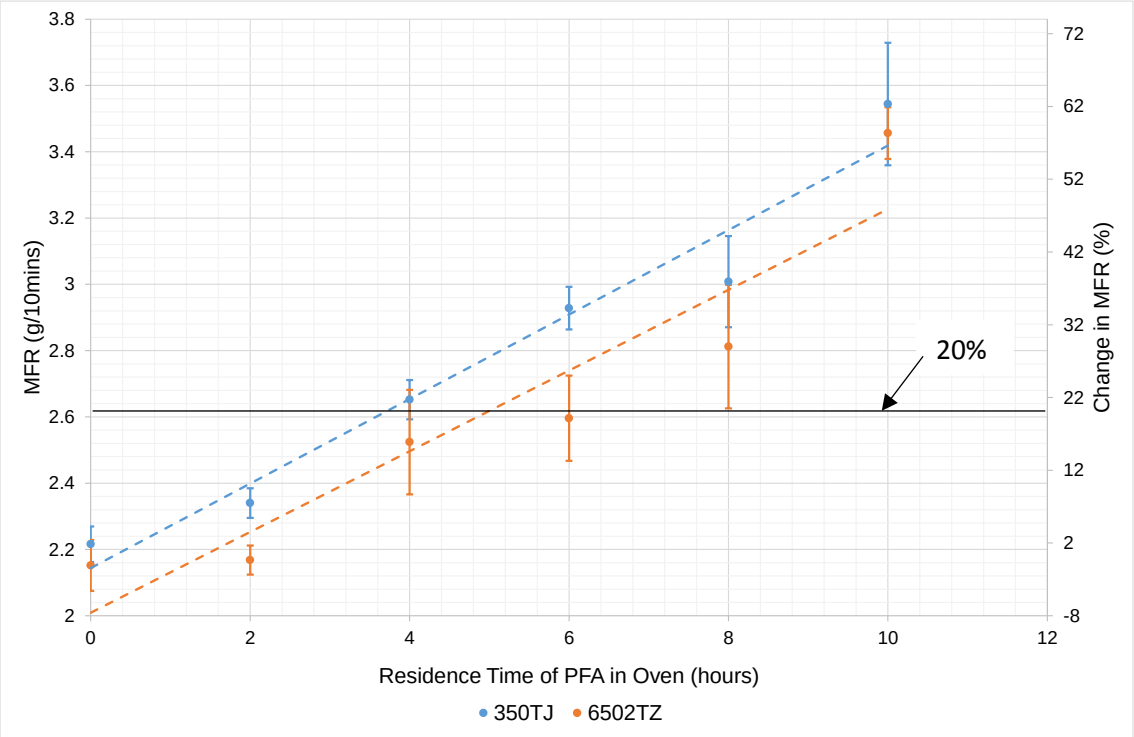

Figure 4.56: Change in MFR with residence time in a transfer moulding pot of the virgin PFA materials used in this study

The MFR of the samples held in a transfer moulding pot increase with residence time as expected from the results obtained from the thermally aged samples

discussed in 4.3.1. The graph suggests 350TJ can be held for 4½hrs before the 20% anecdotal maximum increase in MFR is reached, whereas 6502TZ can be held for nearly 6hrs. The time 6502TZ can be held before a 20% in MFR is seen is very similar to the samples exposed to purely thermal effects (prepared by wrapping the pellets in aluminium foil prior to heating in an oven). Preparing the material by melting it in a pot and holding under pressure rather than by simply wrapping the pellets in foil appears to have increased the time at which 350TJ can be held from approximately 3½hrs to 4½hrs. This could possibly be explained by the temperature gradient across the pot during heating, as the material wrapped in foil would have heated more uniformly and quickly due to a larger surface area to volume ratio, leading to a harsher heat history.

4.5.3 DSC

The second heating curves of the PFA exposed to transfer moulding conditions are shown below in Figures 4.57 and 4.58, while curves of the samples exposed to 10hrs residence time in a transfer moulding pot are shown in Figures 4.62 and 4.63. Data from an investigation of damaged PFA with a crumbly texture is included in Figure 4.67 to show the extent of change required to produce a significant difference in the DSC trace.

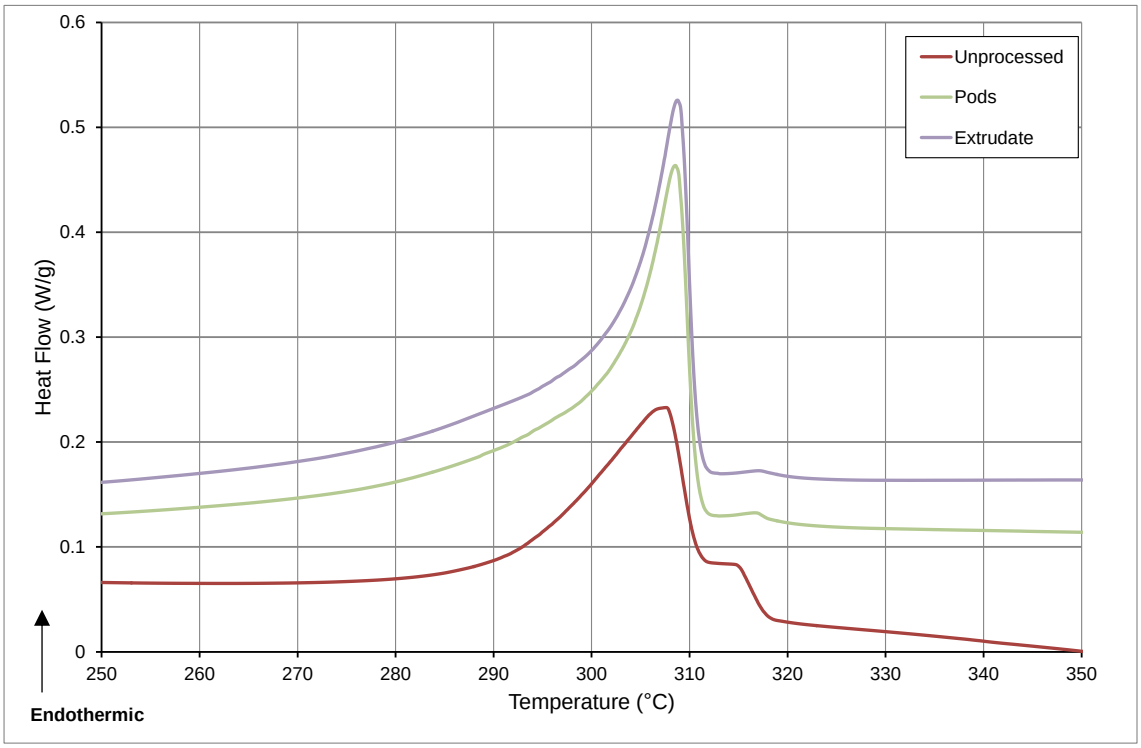

Figure 4.57: DSC traces showing the second heating of processed samples of Chemours 350TJ

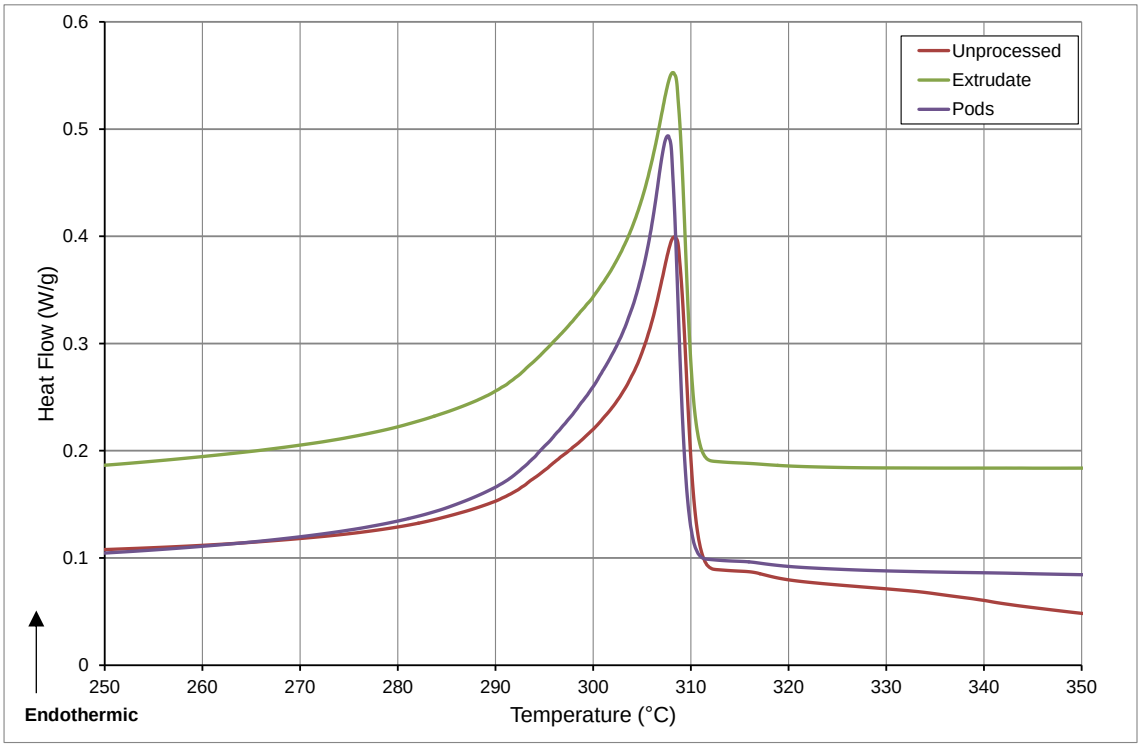

Figure 4.58: DSC traces showing the second heating of processed samples of Dyneon 6502TZ

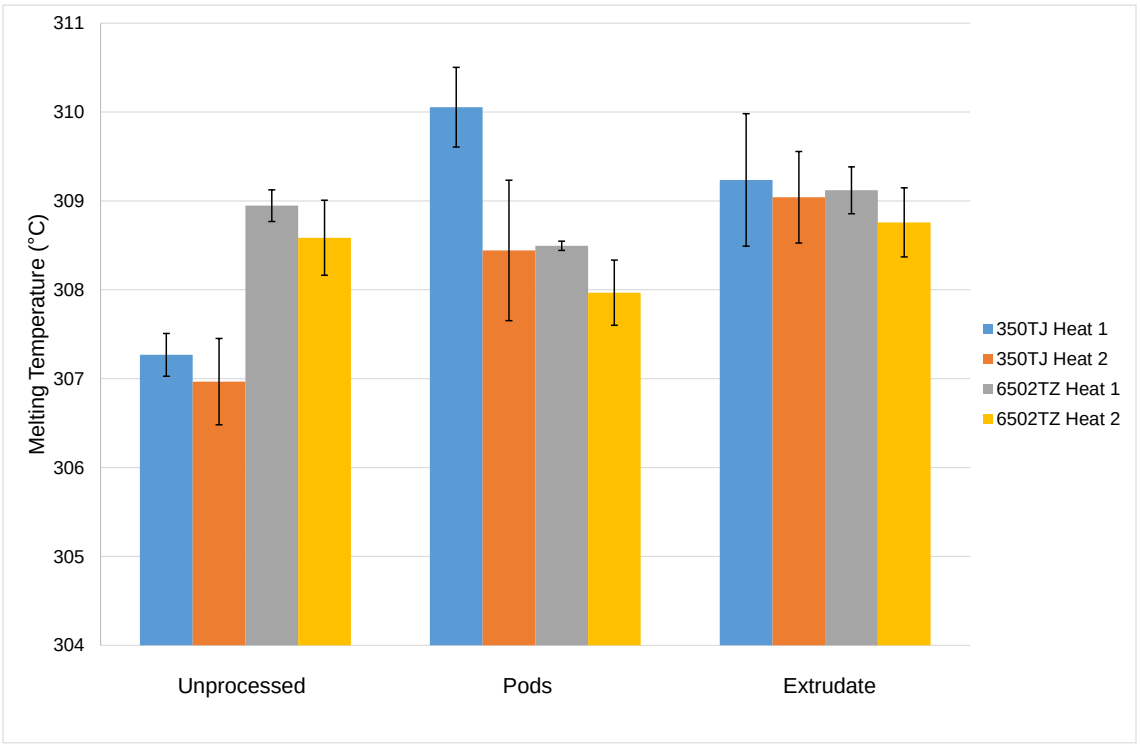

Figure 4.59: Values of the melting peak endotherm of the first and second heating cycles

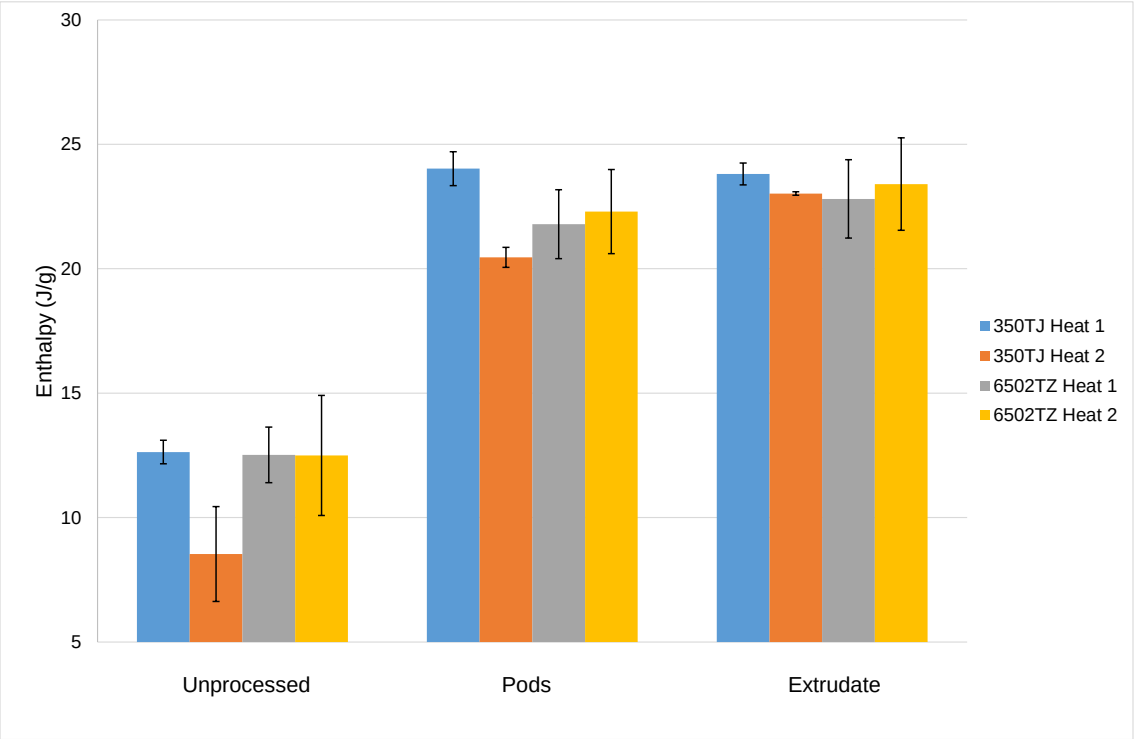

Figure 4.60: Values of the enthalpies of the first and second heating cycles

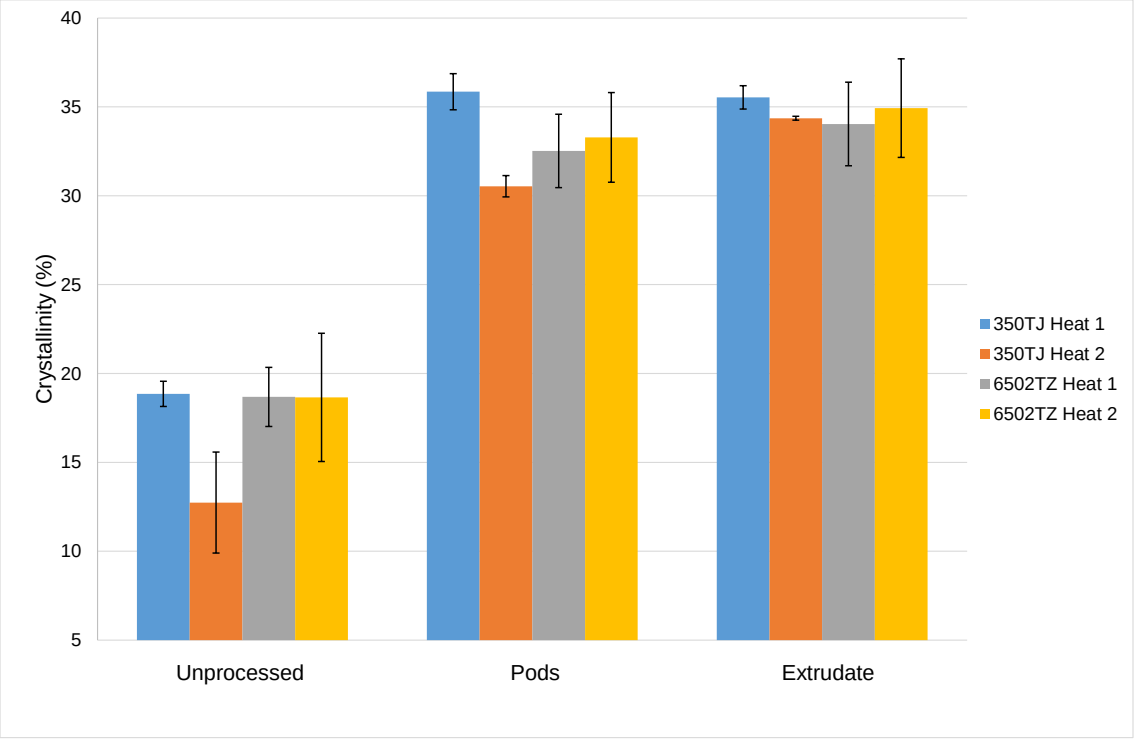

Figure 4.61: Level of crystallinity of the material of the first and second heating cycles

The data shows a reduction in the melt temperature of the pod material, and an increase for the extrudate. The enthalpy of the material from both the pods and extrudate increases.

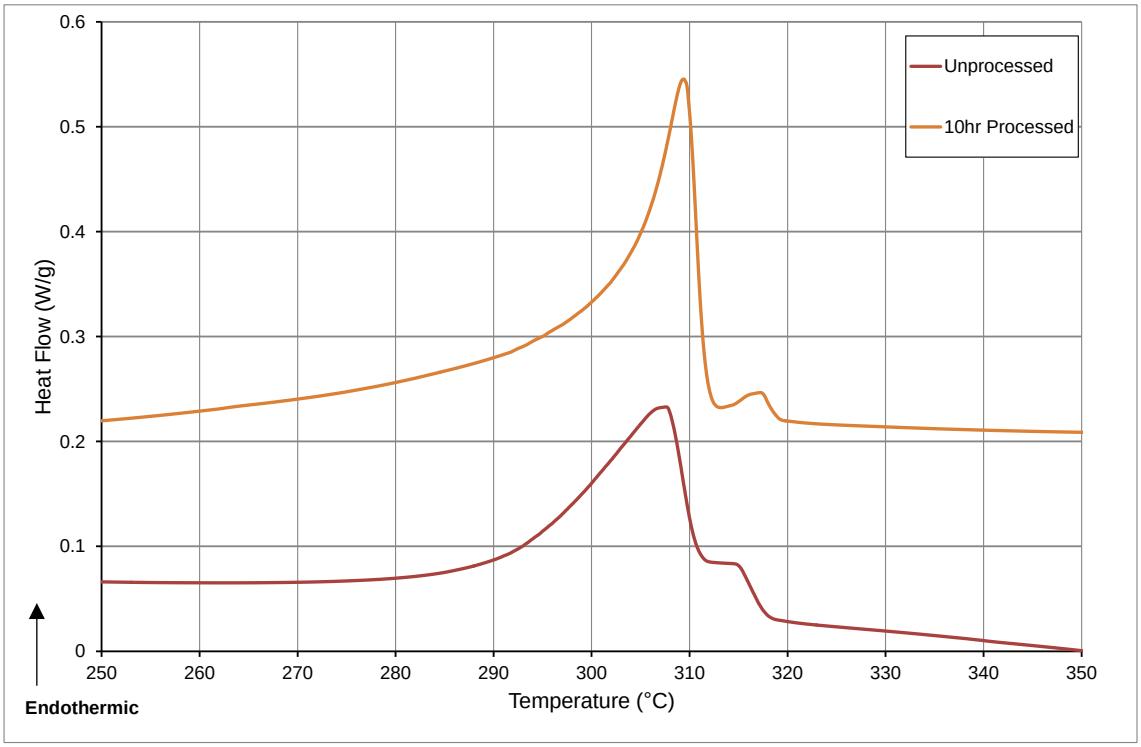

Figure 4.62: Comparison of DSC traces showing the second heating of unprocessed Chemours 350TJ and the same polymer held for 10hrs residence time in a transfer moulding pot

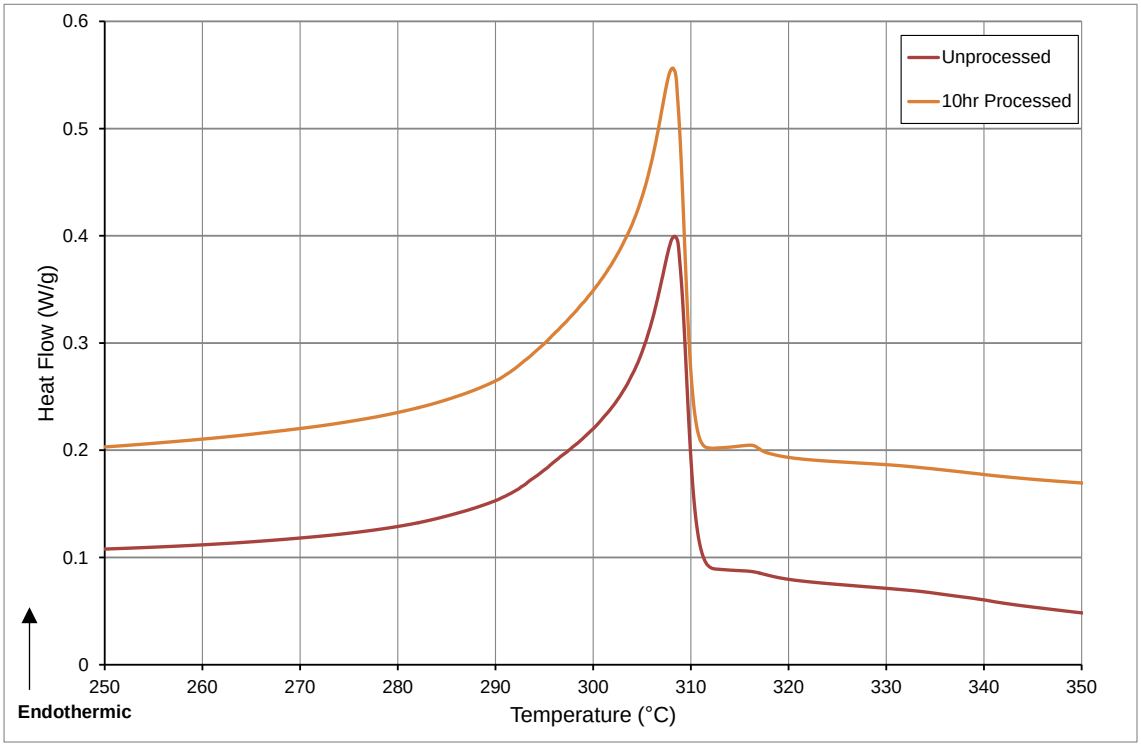

Figure 4.63: Comparison of DSC traces showing the second heating of unprocessed Dyneon 6502TZ and the same polymer held for 10hrs residence time in a transfer moulding pot

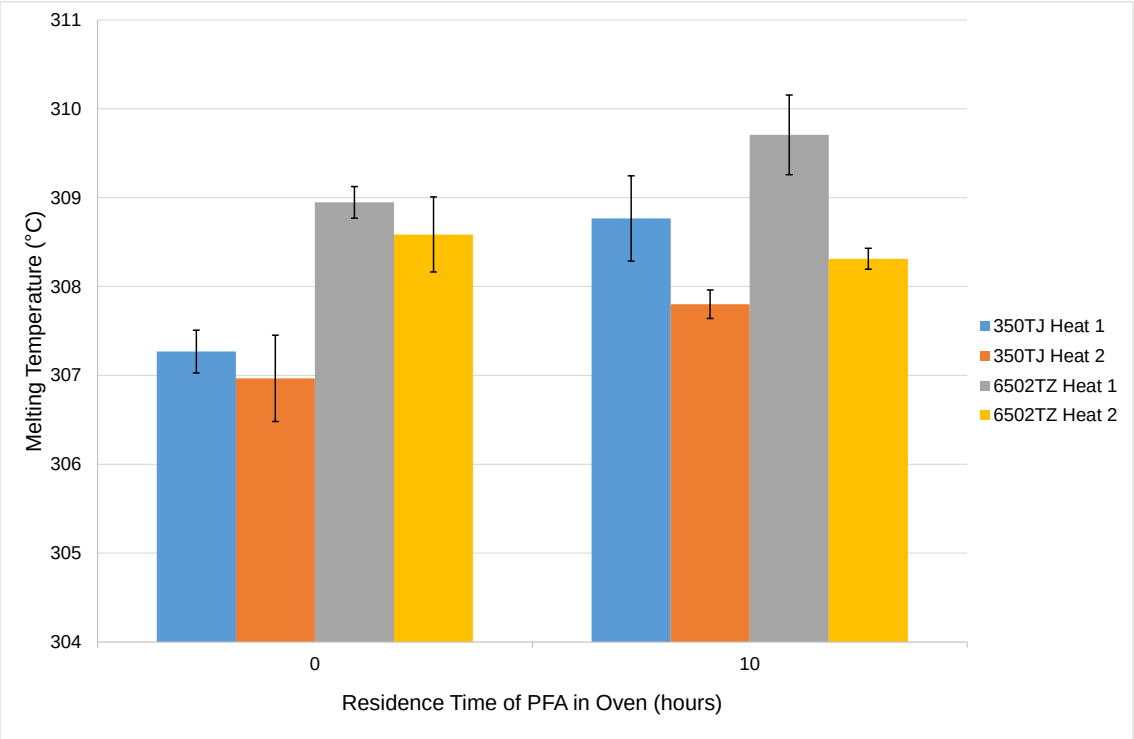

Figure 4.64: Values of the melting peak endotherm of the first and second heating cycles

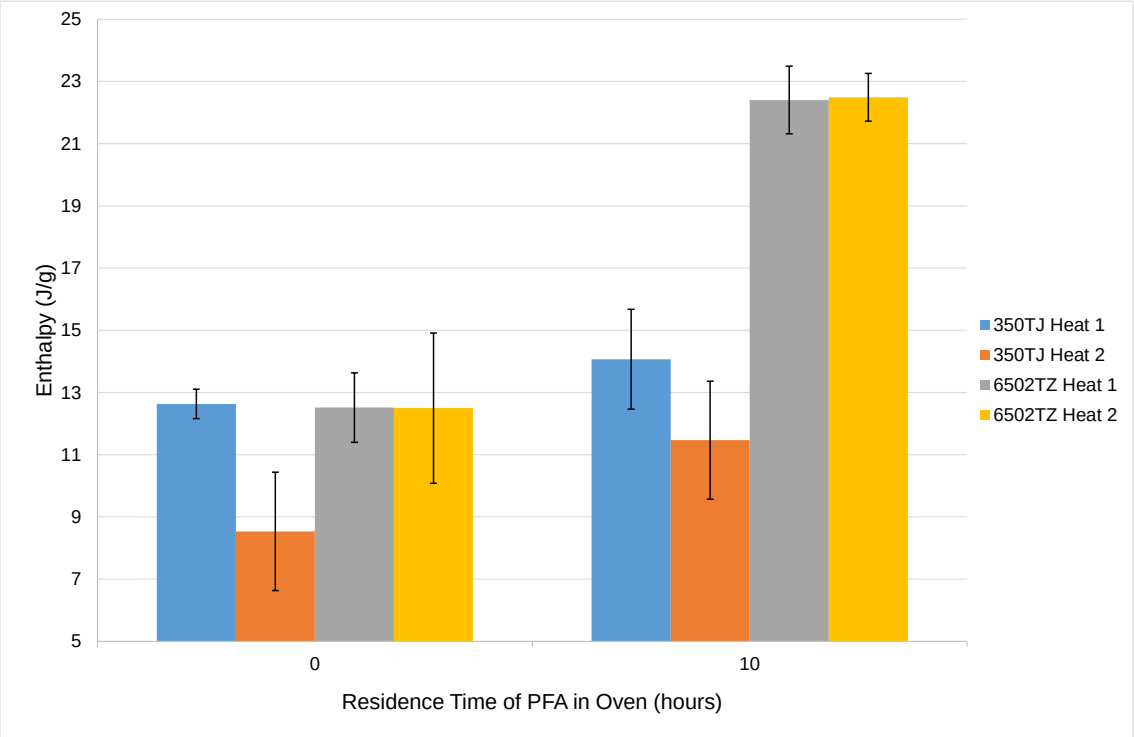

Figure 4.65: Values of the enthalpies of the first and second heating cycles

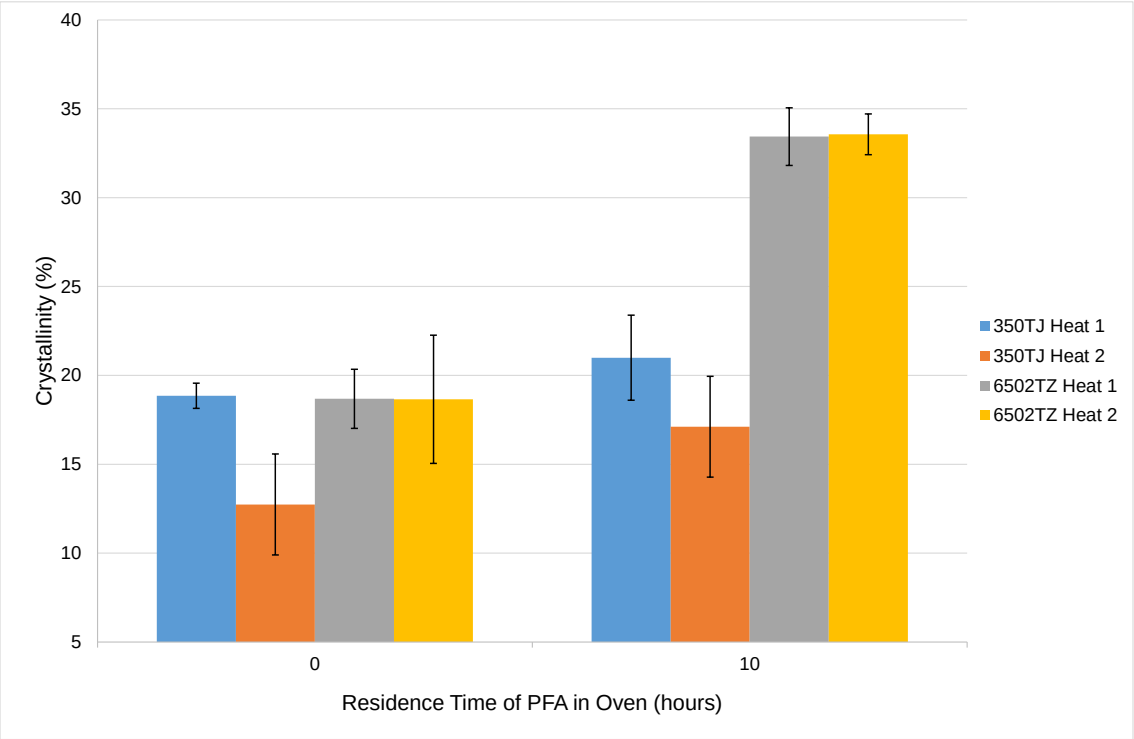

Figure 4.66: Level of crystallinity of the material of the first and second heating cycles

350TJ shows an increase in melt temperature and enthalpy after 10hrs residence time in a transfer moulding pot. The enthalpy of the Dyneon PFA increase more dramatically, however the melt temperature falls slightly.

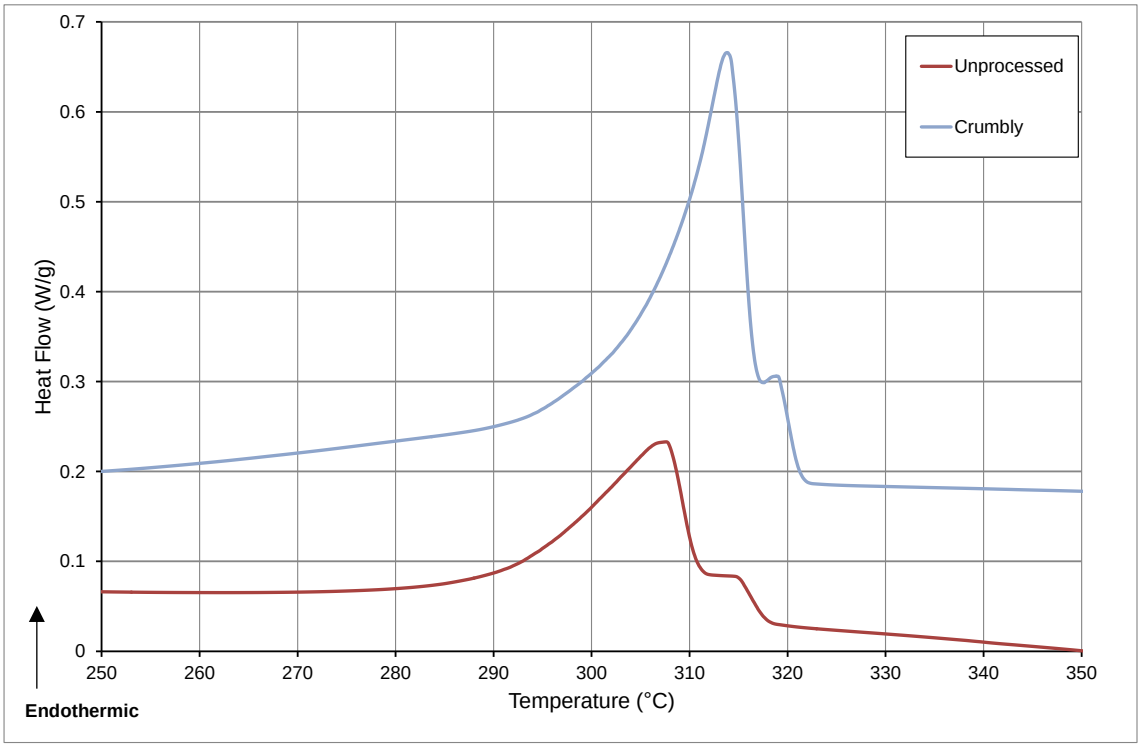

Figure 4.67: Comparison of DSC traces showing the second heating of unprocessed Chemours 350TJ and severely damaged material

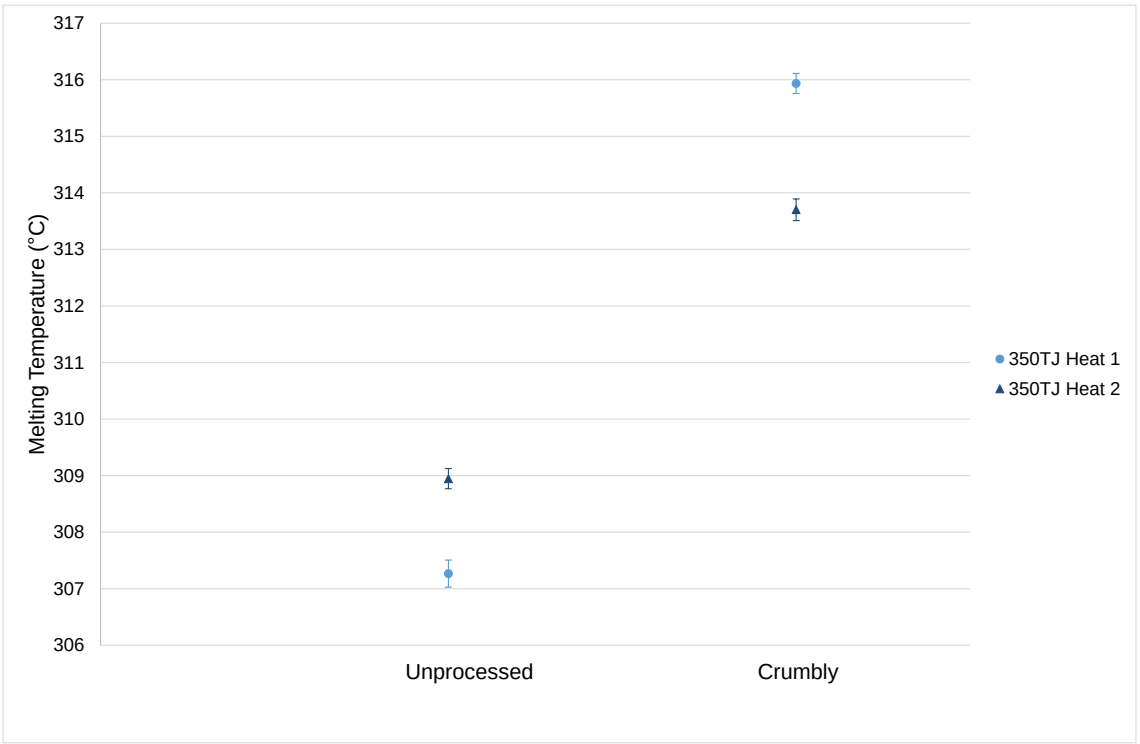

Figure 4.68: Values of the melting peak endotherm of the first and second heating cycles

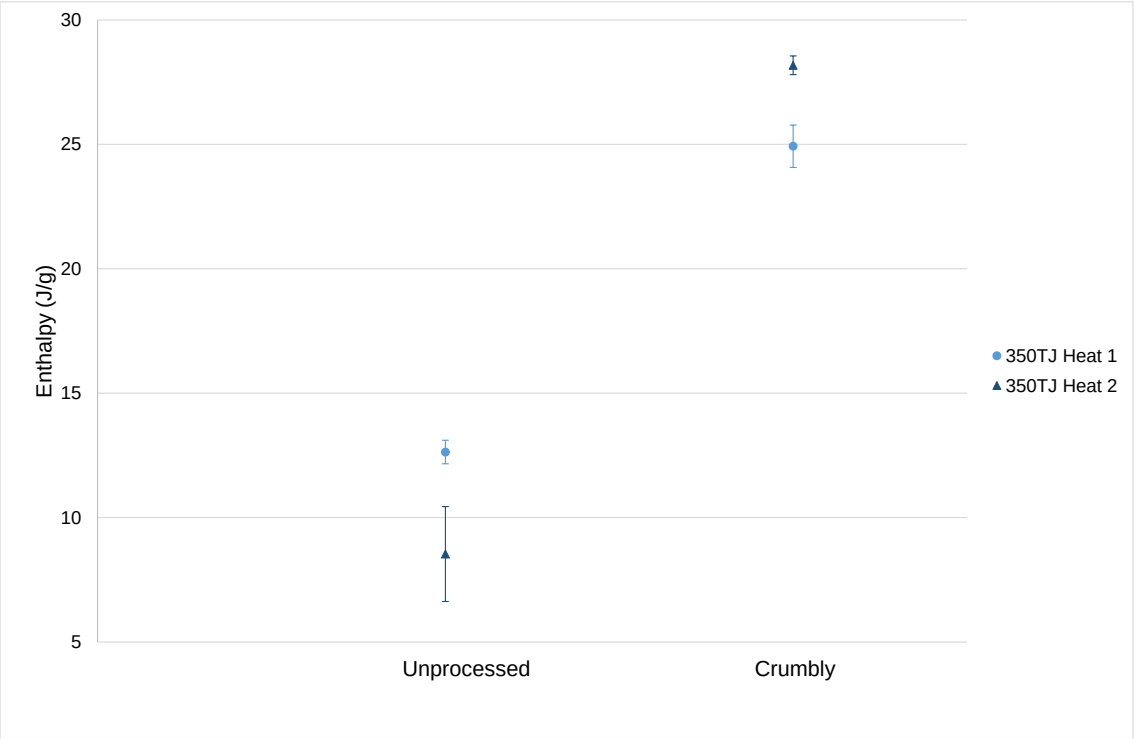

Figure 4.69: Values of the enthalpies of the first and second heating cycles

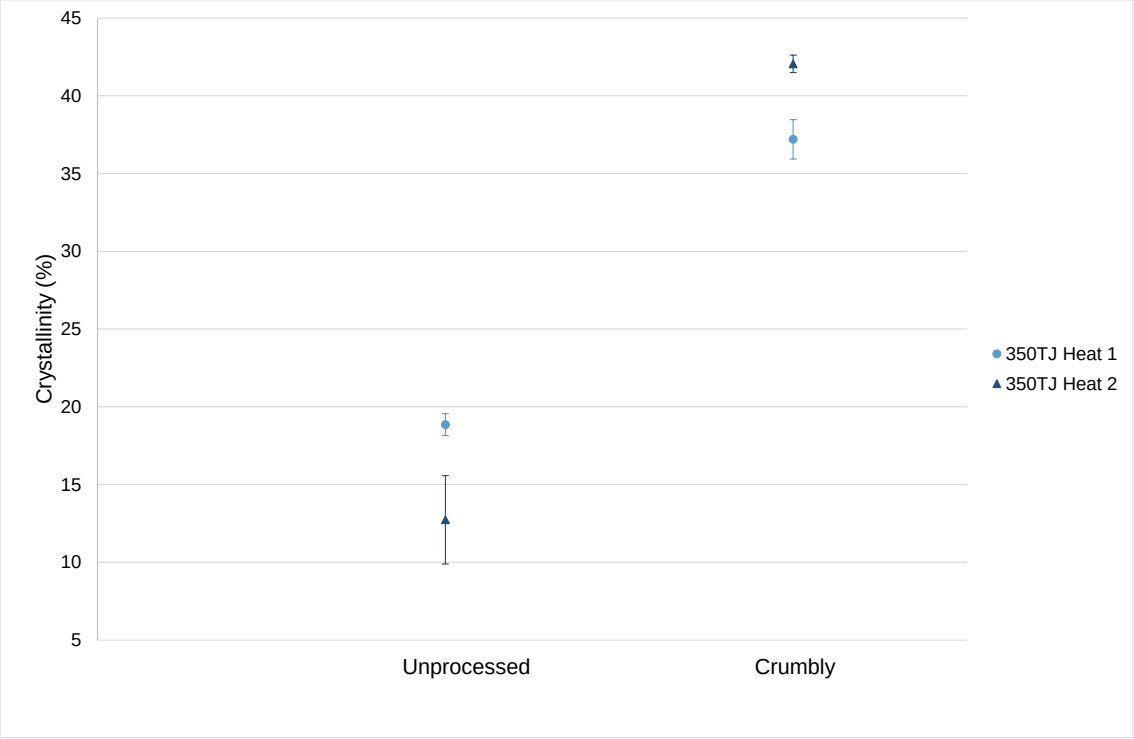

Figure 4.70: Level of crystallinity of the material of the first and second heating cycles

The crumbly PFA had a distinctly different appearance, however the exact processing conditions are unknown. The melt temperature has increased significantly, as has the enthalpy. There is evidence of a second polymorph

emerging again in Figure 4.67, which may lead to significant changes in the material properties depending on the structure of crystal A and crystal B. It is worth noting in this case however, that from a quality perspective testing would not be required on such a sample as the damage could be easily seen visually.

4.5.4 Near Infrared Spectroscopy

The spectroscopic techniques used on samples of PFA exposed to various residence time is a transfer moulding pot are presented in this section. As previously discussed in 4.1.4, spectra obtained by FTIR are included in an appendix due to the limited differences observed. The analysis using Partial Least Squares (PLS) and Principal Component Scores (PCS) on the spectra obtained from Near Infrared Spectroscopy are shown below in Figures 4.71 to 4.74.

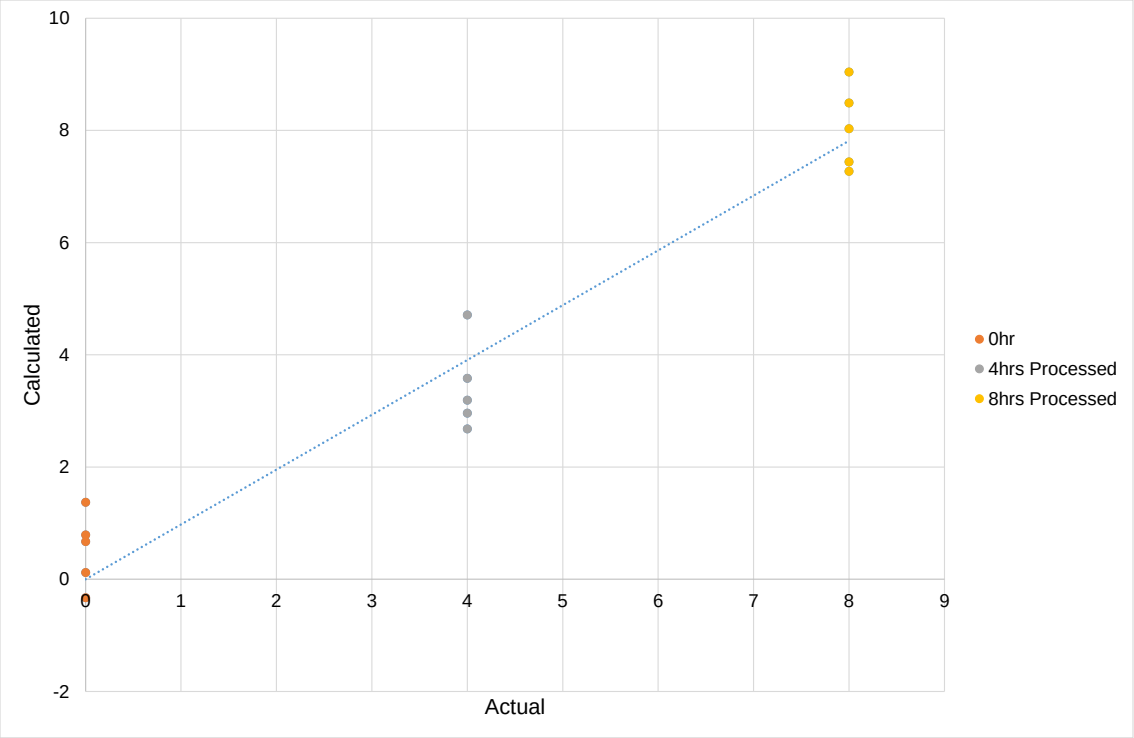

Figure 4.71: Partial Least Squares regression of NIR spectra of unprocessed 350TJ and samples held for various residence times in a transfer moulding pot, with a correlation coefficient of 0.9701

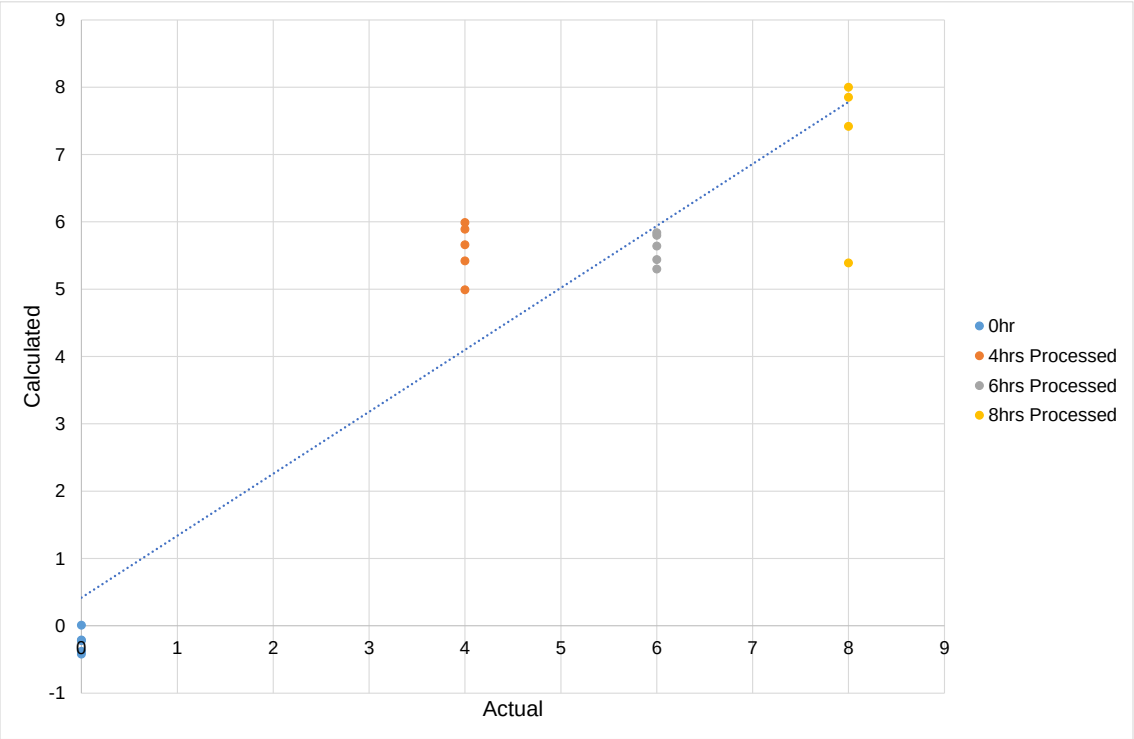

Figure 4.72: Partial Least Squares regression of NIR spectra of unprocessed 6502TZ and samples held for various residence times in a transfer moulding pot, with a correlation coefficient of 0.9321

Partial Least Squares regression showed a better correlation for 350TJ than for the other samples subjcted to various residence times. However the spread of data points of the 6502TZ samples makes it difficult to quantify the heat history of the material.

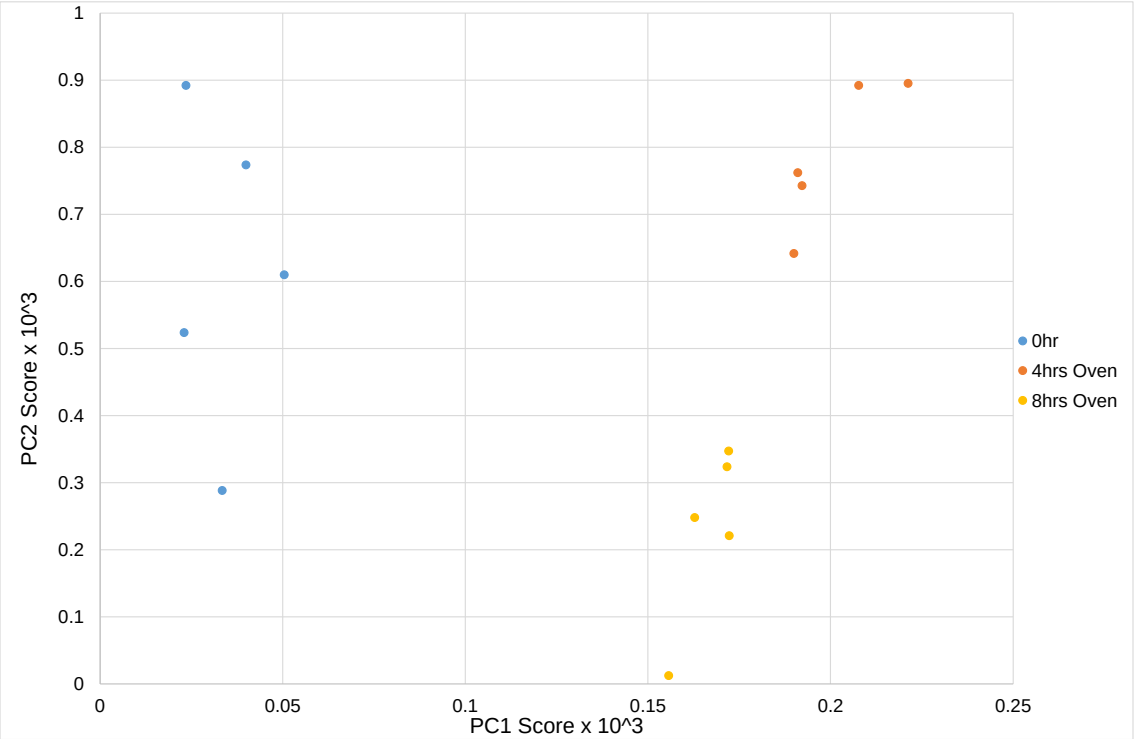

Figure 4.73: Principal Component Scores of NIR spectra of unprocessed 350TJ and samples held for various residence times in a transfer moulding pot

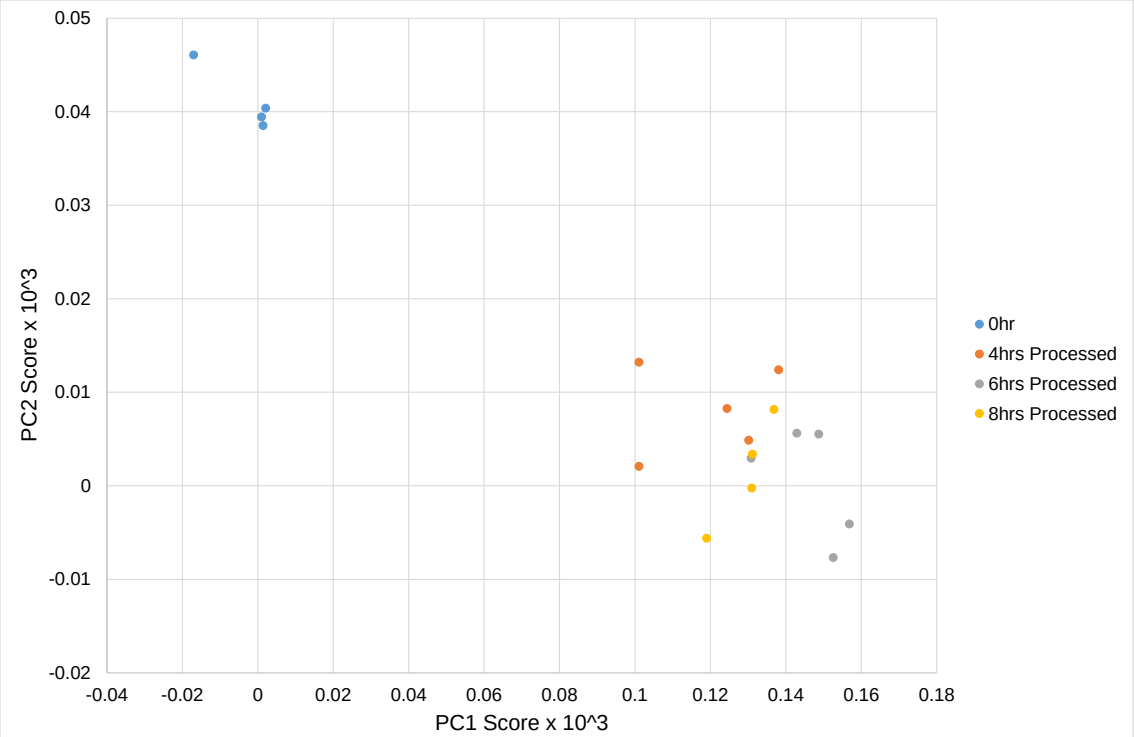

Figure 4.74: Principal Component Scores of NIR spectra of unprocessed 6502TZ and samples held for various residence times in a transfer moulding pot

Principal Component Analysis of the samples showed more successful grouping of 350TJ material than 6502TZ.

4.6 Effect of Cooling Rate

The rate of cooling of polymers tends to have a significant impact on the level of crystallinity, and therefore the properties of the material. The aim of these experiments was to obtain data from material that has been subjected to various rates of cooling to assess the impact on material properties.

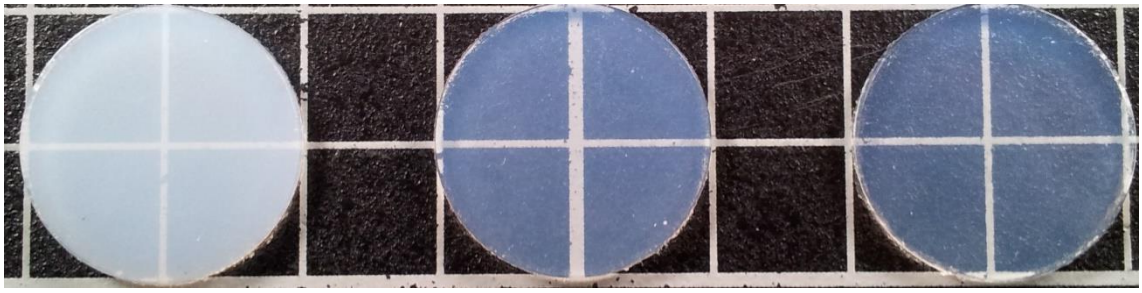

Figure 4.75: Photo showing the samples of 350TJ cooled at different rates. From left to right: Sample cooled in the press with the heaters switched off without water cooling, sample cooled in the press with the plates cooled by passing 40°C water through, and sample quenched in a water bath directly after moulding

4.6.1 Tensile Testing

Stress vs. strain curves of the samples of 350TJ exposed to various cooling rates are presented below in Figure 4.76.

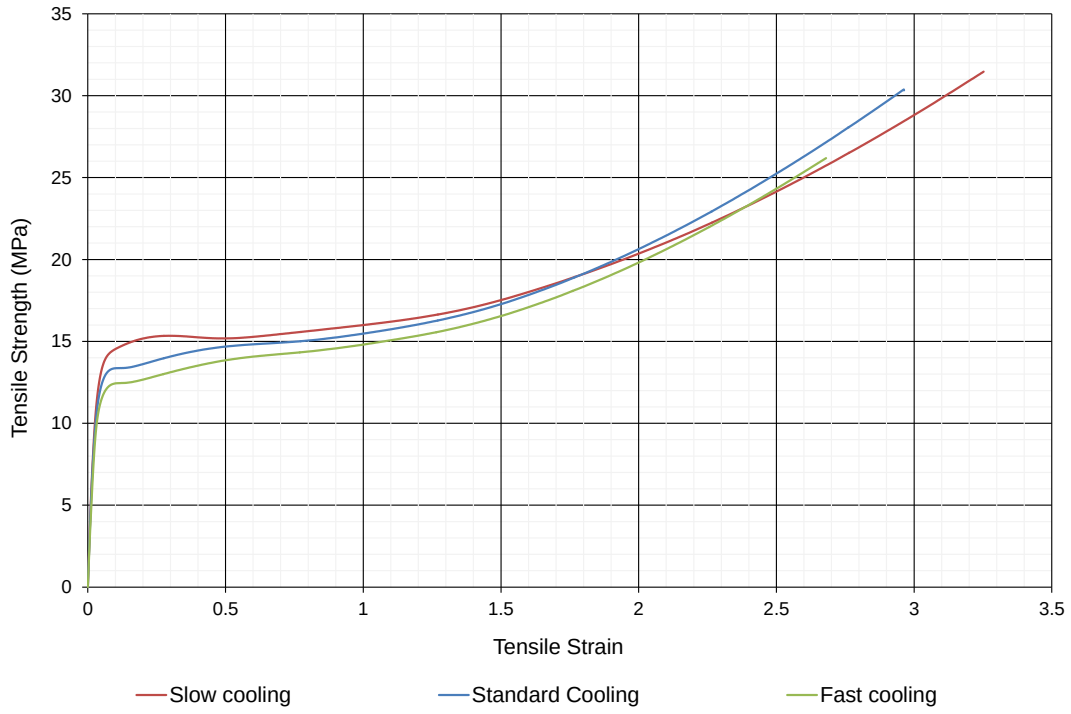

Figure 4.76: Stress vs. strain data for the samples of 350TJ exposed to various cooling rates. Each curve is the average of 5 tests, displayed to the lowest elongation of the data set.

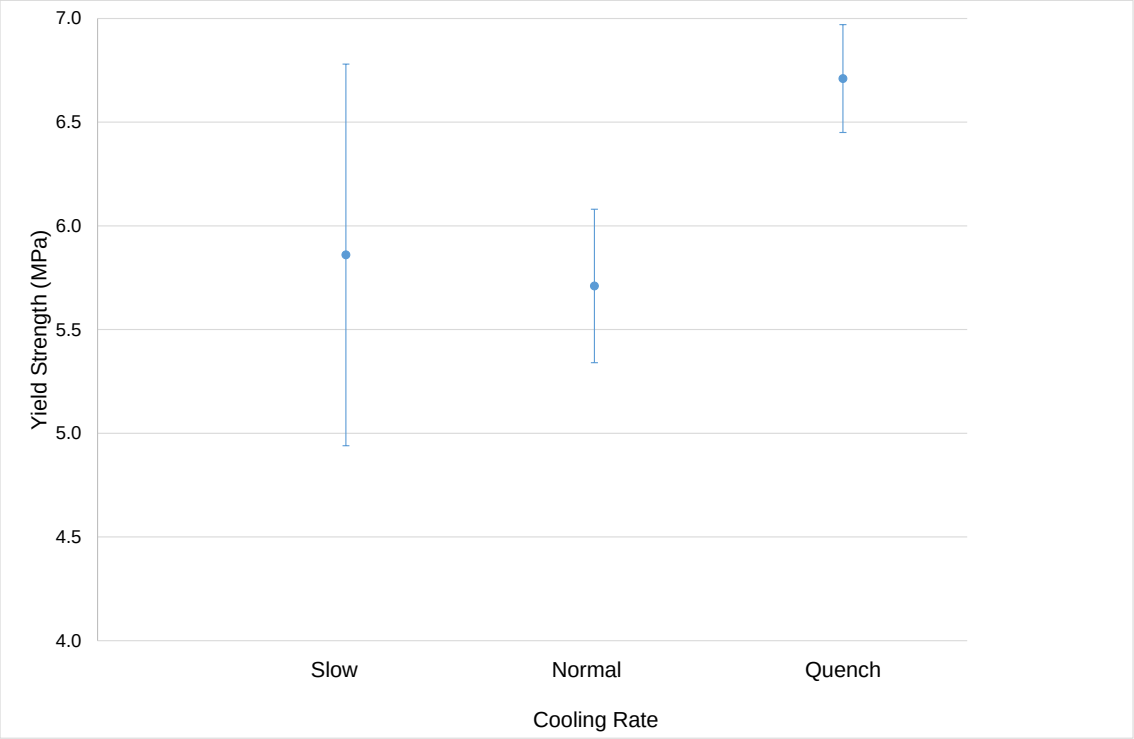

Figure 4.77: Values of the yield strength of the samples from the average and standard deviation of 5 tests

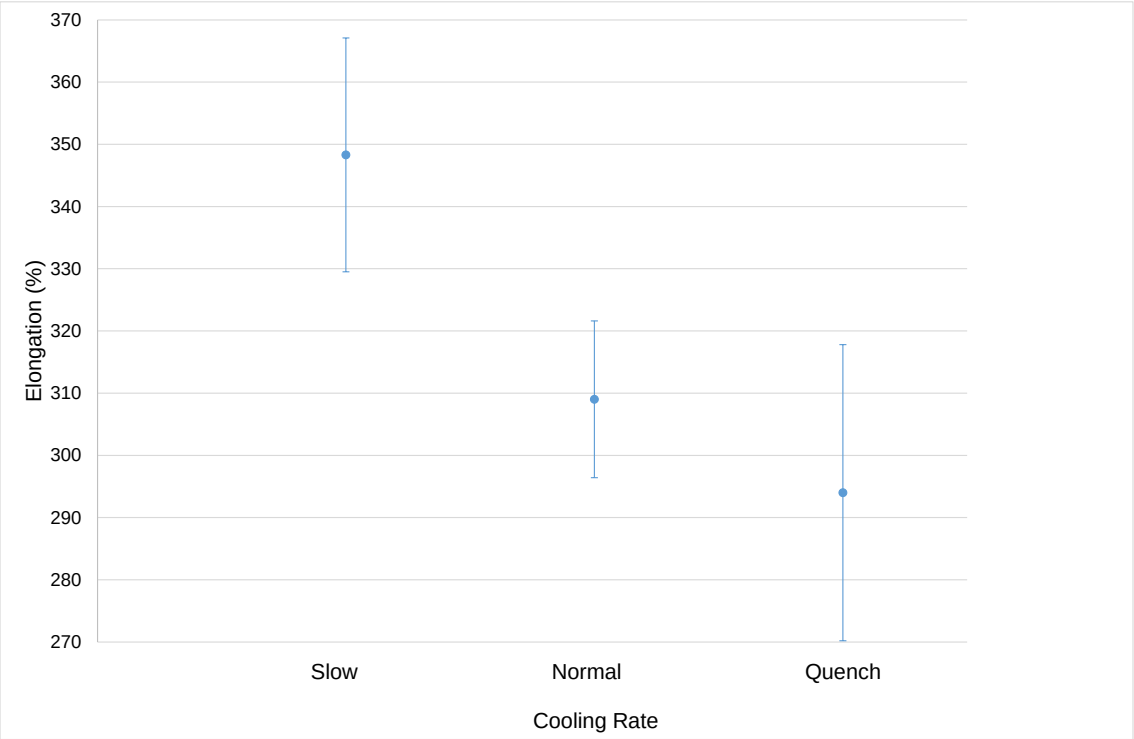

Figure 4.78: Values of the elongation at break of the samples from the average and standard deviation of 5 tests

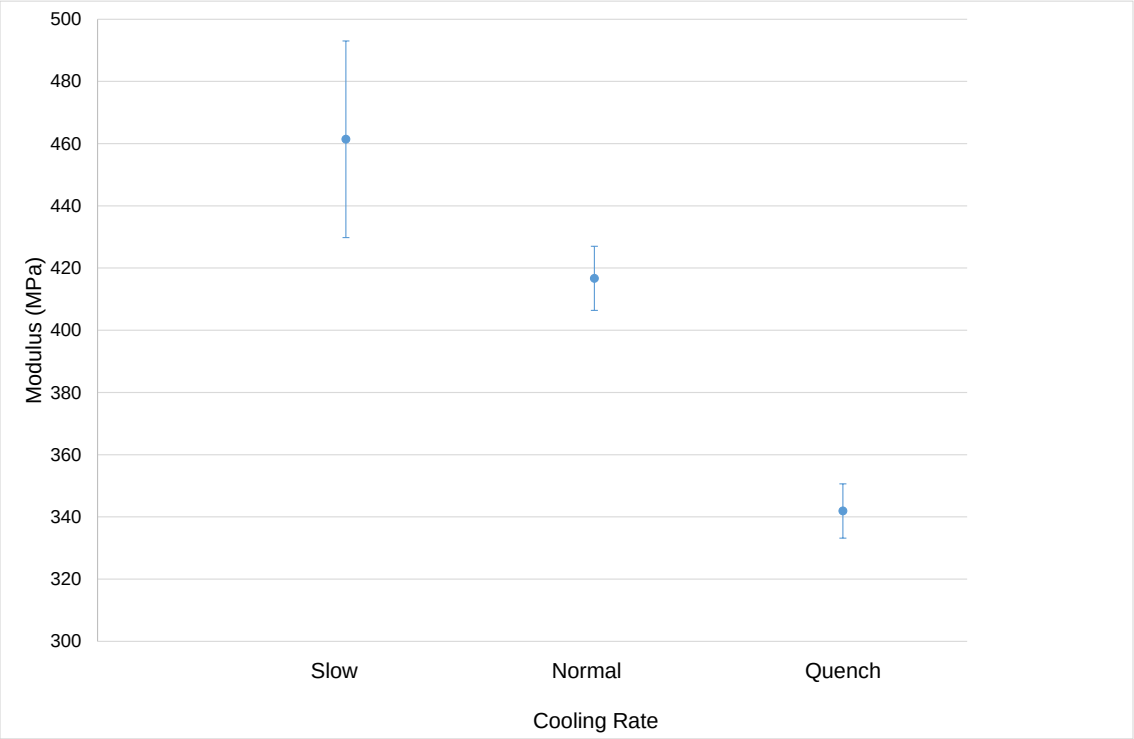

Figure 4.79: Values of the modulus of the samples from the average and standard deviation of 5 tests

The graph shows the yield strength generally increases as the rate of cooling decreases, as the level of crystallinity of the material also increases. This also

serves to increase the strain the samples can withstand prior to failure and leads to a greater elastic modulus.

4.6.2 DSC

The second heating curves of the PFA exposed various cooling rates are shown below in Figure 4.80.

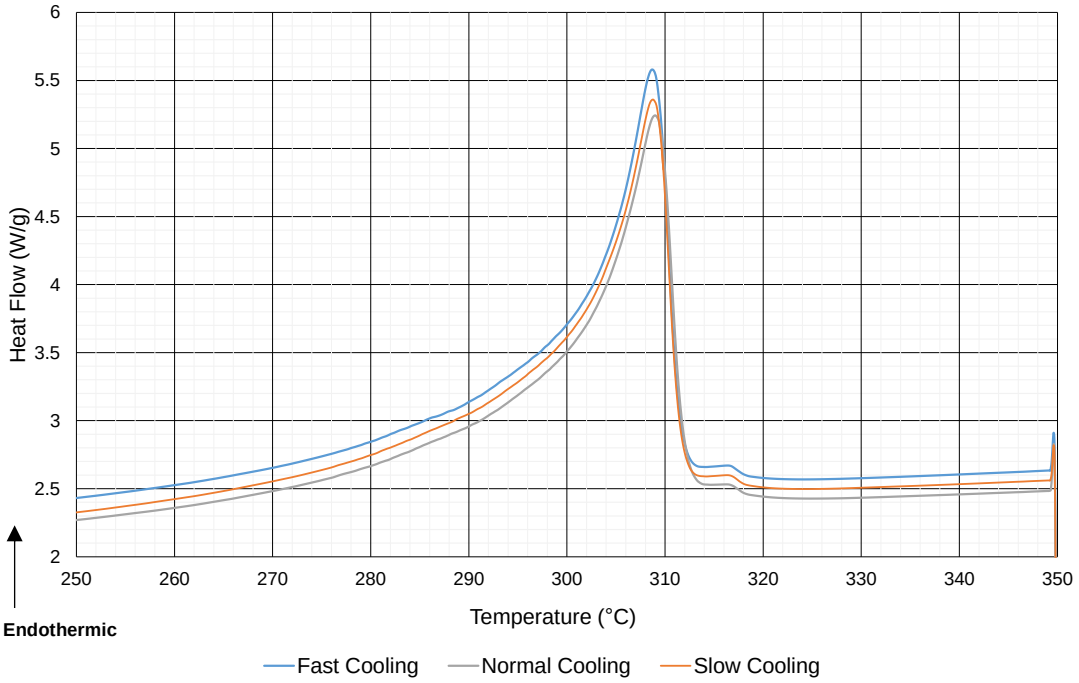

Figure 4.80: Comparison of second heating curves obtained from the samples of 350TJ subjected to various cooling rates

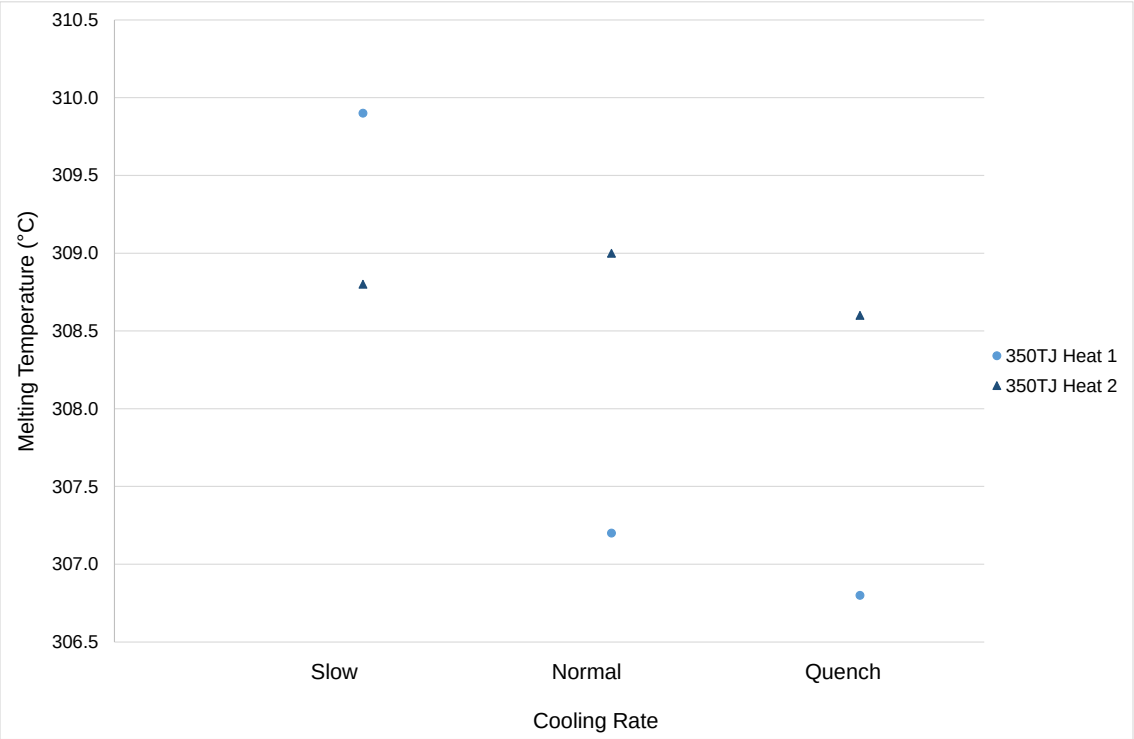

Figure 4.81: Values of the melting peak endotherm of the first and second heating cycles

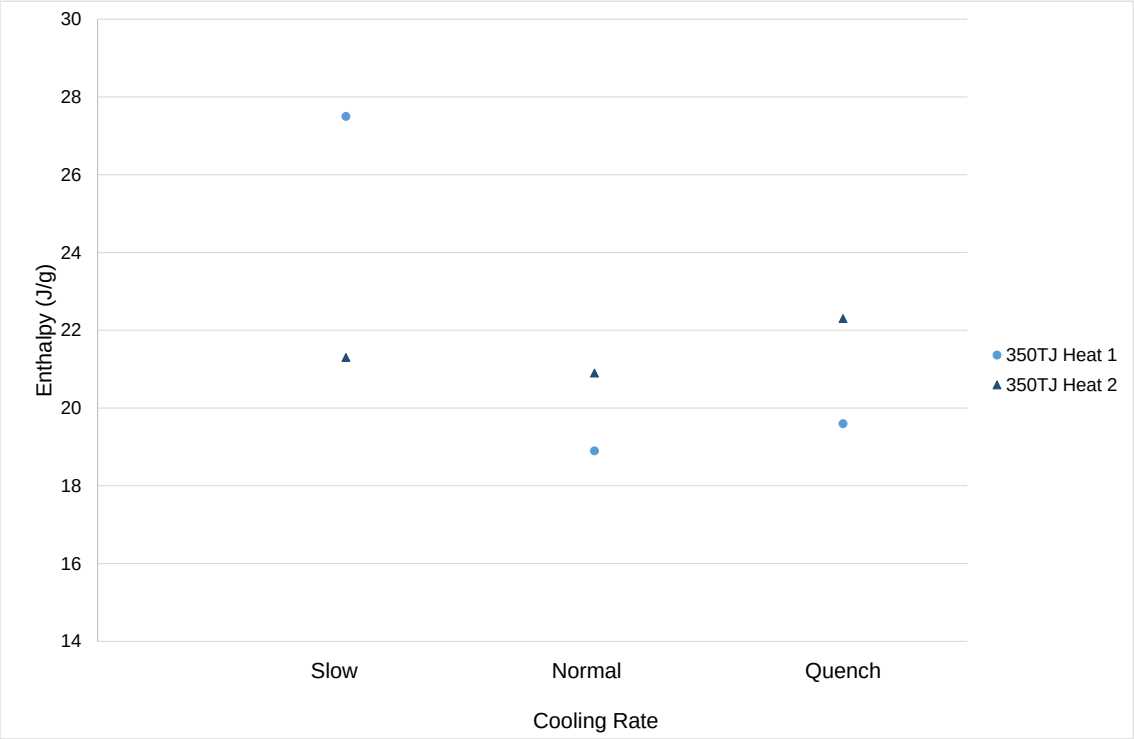

Figure 4.82: Values of the enthalpies of the first and second heating cycles

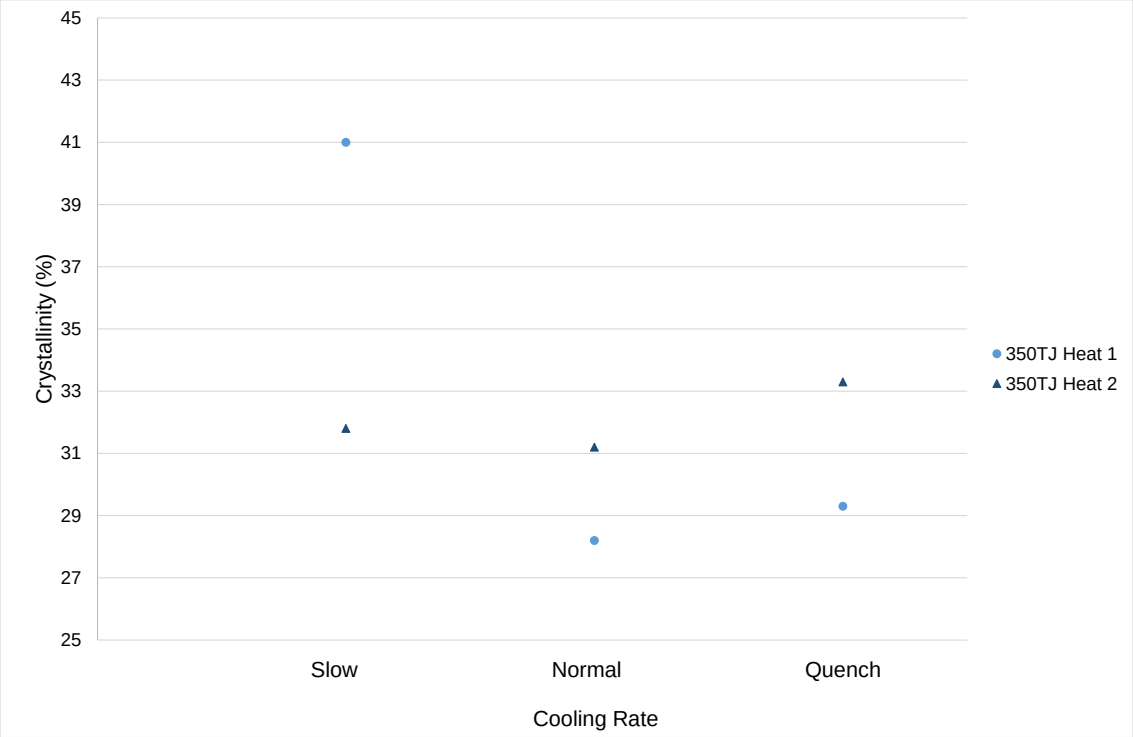

Figure 4.83: Level of crystallinity of the material of the first and second heating cycles

The first melt temperature of the samples dropped with an increase in the cooling rate, as the level of crystallinity of the material is reduced the faster the sample is cooled. The enthalpies of the first heating cycle showed the increase in crystallinity of the slow cooled sample, however quenching the material did not appear to significantly reduce the crystallinity when compared to a sample subjected to standard cooling conditions. There were no significant changes in the melt temperatures and enthalpies of the second heating cycle, showing the material had not been altered as a result of the cooling rates. This shows the rate of cooling can be altered to improve the process and/or the final product properties without compromising the integrity of the polymer.

4.6.3 Raman Spectroscopy

The spectroscopic techniques used on samples of PFA exposed to various cooling rates are presented in this section. As previously discussed in 4.1.4, spectra obtained by FTIR are included in an appendix due to the limited differences observed. The spectra obtained from Raman Spectroscopy on the samples of 350TJ exposed to various cooling rates is presented below in Figures 4.84 to 4.87.

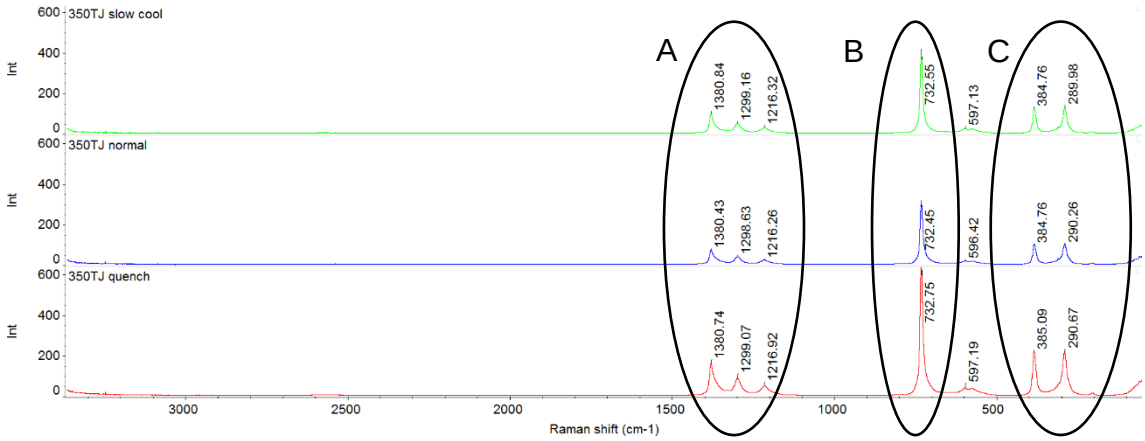

Figure 4.84: Comparison of spectra obtained from the samples of 350TJ subjected to various cooling rates

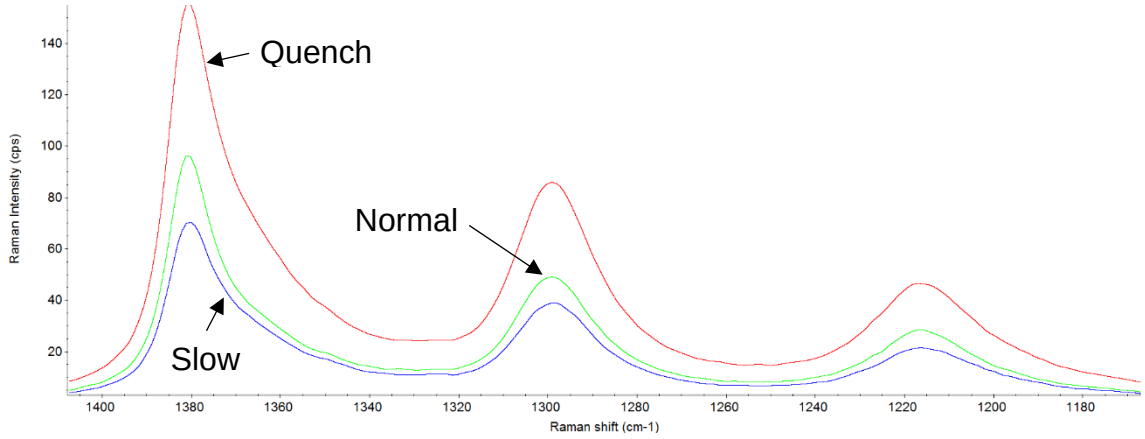

Figure 4.85: Superimposed spectra from section A in Figure 4.84

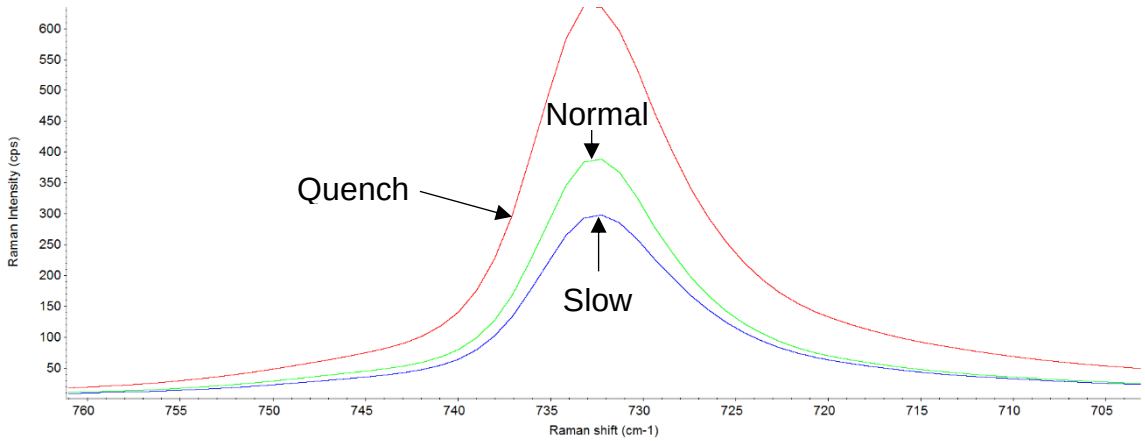

Figure 4.86: Superimposed spectra from section B in Figure 4.84

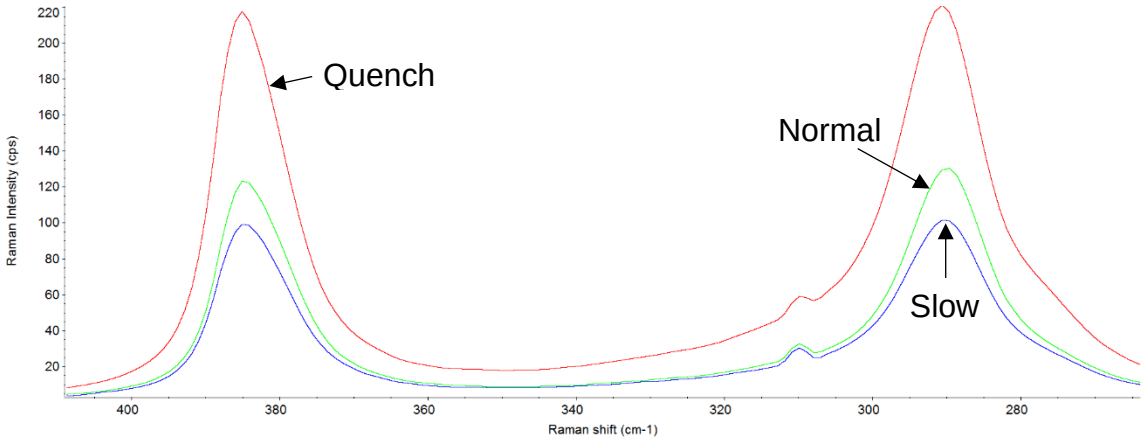

Figure 4.87: Superimposed spectra from section C in Figure 4.84

Slow	Normal	Quench
1380.84	1380.43	1380.74
1299.16	1298.63	1299.07
1216.32	1216.26	1216.92
732.55	732.45	732.75
597.13	596.42	597.19
384.76	384.76	385.09
289.98	290.26	290.67

Table 4.8: Wavenumbers of the peaks in the spectra of the PFA samples

There are no significant changes in the wavenumbers of the peaks of the Raman spectra for the samples subjected to various cooling rates. There are several publications which include Raman spectra of PTFE and/or PFA, detailed as follows.

Using 488 nm radiation at 250 mW power Legeay et al. (1998) found that the Raman spectrum of PFA is very similar to that of PTFE and attributes the bands as follows:

1380cm^{-1}	Splitting of two F_2 symmetry lines
1299cm^{-1}	
1218cm^{-1}	
792cm^{-1}	CF_4 A_1 symmetry stretching
597cm^{-1}	Splitting of two F_2 symmetry lines
579cm^{-1}	
560cm^{-1}	
384cm^{-1}	Splitting of E symmetry mode
291cm^{-1}	

Dargaville (2002) also states that the Raman spectrum of PFA is the same as for PTFE:

1382cm^{-1}	Symmetrical CF_2 stretching
1301cm^{-1}	
1217cm^{-1}	Asymmetrical CF_2 stretching
734cm^{-1}	C-C stretching
600cm^{-1}	CF_2 rocking and wagging
575cm^{-1}	
386cm^{-1}	CF_2 bending
292cm^{-1}	CF_2 stretching

Mihaly et al. (2006)

1379cm^{-1}	CF stretching
1296cm^{-1}	CF_2 asymmetric stretching
1213cm^{-1}	C-C stretching
735cm^{-1}	CF_2 symmetric deformation (A_1 mode)
594cm^{-1}	CF_3 symmetric deformation
571cm^{-1}	
386cm^{-1}	CF_2 twisting
291cm^{-1}	CF_2 wagging

Chapter 5

Discussion

5.1 Introduction

This chapter summarises the experimental results presented in Chapter 4 in relation to the objectives of the project. The methods used are reviewed in terms of their suitability and the outcomes from the analysis of the effect of each of the processing conditions investigated are discussed.

The aim of this work was to increase the level of scientific understanding of the effects of processing on the properties of perfluoroalkoxy (PFA). Specific project objectives were to:

1. Explore the suitability of different analytical methods for identifying the condition of PFA due to various process variables
2. Characterise the rheology of PFA under typical processing conditions
3. Determine the influence on PFA viscosity of:
    a. temperature
    b. shear
    c. residence time at temperature
4. Ascertain whether exposing PFA to high shear rates damages the polymer
5. Quantify the change in material properties as a result of the residence time at processing temperature
6. Examine the consequence of the rate of cooling on the structure and the mechanical properties of PFA
7. Investigate the correlation between the results generated from Melt Flow Rate testing and the viscosity data obtained from the capillary rheometer for samples of PFA exposed to the same conditions

A summary of the key results is given in the following sections, with further detail and the significance to CRP highlighted in each of the areas discussed.

5.2 Suitability of Analytical Techniques

The flow behaviour of PFA wasn’t previously known, so capillary rheometry provided invaluable data on the impact of shear rate and temperature on the viscosity of the unprocessed PFA materials. These are key parameters in the processing of PFA, however nothing has been published in this area,

highlighting the importance of this work. Capillary rheometry is more suitable than Melt Flow Rate testing for characterising flow behaviour, as MFR provides a single value under restricted conditions. Results from the capillary rheometer did not show substantial variations in the data for samples exposed to different processing conditions, whereas the effect of residence time on the material appeared to be quite significant using MFR testing. Capillary rheometry is more appropriate when exploring unfamiliar PFA materials, as it provides comprehensive data that can be applied to determine suitable process parameters. MFR testing appears to be more sensitive to change in the material as it is conducted at very low shear rates (less than $5s^{-1}$), and can therefore be used in more of a quality role to quantify the level of change in a material due to processing. Due to the uncertainty around the anecdotal value of the maximum acceptable change in MFR of 20%, the value of MFR itself is insufficient. Further work is required to correlate the change in MFR with a change in another material property to create a solid framework from which to base product quality decisions on.

Of the analytical techniques utilised in this research, tensile testing yielded valuable data on the impact of residence time and exposure to shear. Again, there is no data to substantiate the claims regarding degradation with exposure to high temperature or the damaging effects of high shear rates given in the literature, so this type of quantitative information is extremely valuable to processors. In this regard it is the best candidate to combine with MFR to quantify the change in the polymer due to processing, as mentioned in the previous section. Tensile testing also proved to be suitable for comparison of the unprocessed virgin PFA materials, and could therefore be used in conjunction with the capillary rheometer in investigation of new PFA materials. The results of tensile testing on C980 were compromised due to the unexpected difficulty in determining compression moulding conditions required to produce an adequate plaque from which to cut the samples. This could be resolved by adjusting the moulding conditions to form a better quality plaque, free from shrinkage voids.

Other than providing information on the melting temperature of the various samples, the data obtained from Differential Scanning Calorimetry (DSC) did not show consistent trends with regard to the condition of the material. There

are no distinct patterns in the values of enthalpy and melt temperature with the sample thickness reported by Extrand and Monson (2006) in their work investigating the permeation resistance of DuPont LP film. Their values of enthalpy are between 16-20J/g, which they claim to be within the range reported by Kerbow and Sperati (1999). Monson, Moon and Extrand (2008) show that the melt temperature and enthalpy increase as the rate of cooling decreases for DuPont 440HP, 450HP, 451HP, 950HP+ and 951HP+. Of these polymers, 450HP and 451HP are comparable with 350TJ and 6502TZ as they are unfilled Type II PFAs as defined by ASTM D3307 (2010). The values of enthalpy for the samples are similar in magnitude (3.2J/g to 27.5J/g). The results obtained for the samples subjected to standard cooling (press cooled by water at 40°C) and quench cooled from this current study reflect the trends shown by Monson, Moon and Extrand (2008). Overall however, the data obtained from DSC in this work has not been found to display coherent trends, with the exception of determining the effect on crystallinity of samples subjected to different cooling rates. Therefore it is not proposed as a particularly suitable method for determining the effect of processing conditions on PFA.

Generally spectroscopy is unsuitable for investigation of C980 due to the carbon black content. Scheirs (2000) attributes the difficulty of obtaining an infrared transmission spectrum to the similar size of the carbon black particle to the incident wavelength, promoting scattering dependent on the wavelength shown by the baseline increase at higher wavenumbers. Problems are also identified with Raman spectroscopy, Loadman (2012) notes the laser beam is generally absorbed by very dark samples which causes sample heating. Photoacoustic FTIR spectroscopy is recommended to overcome these difficulties. Fourier Transform Infrared spectroscopy was however useful for obtaining information on the unprocessed material, and would probably be more so for identifying the differences between a wider range of various grades of PFA from other manufacturers. There was little variation in the spectra obtained for the samples exposed to different conditions, which is not altogether unreasonable as 6502TZ and 350TJ are both thermally stabilised unfilled grades of PFA. Near Infrared (NIR) spectroscopy showed more potential as a method for determining the process history of PFA material as there is a varying degree of correlation for the samples exposed to various times at processing temperature. Therefore

a more expansive study of NIR is required to build robust models. The Raman spectra showed differences in the peak heights of the samples subjected to different cooling rates however the trend was not fully coherent, possibly due to the polymorphic behaviour.

5.3 Determination of Basic Properties

The viscosity of the two virgin PFA materials was found to be very similar over the range of shear rates investigated, whereas C980 was found to be more viscous in the region where processing is expected to occur. This is an important finding as the Melt Flow Rate (MFR) of C980 is significantly higher than virgin PFA. MFR indicates the average molecular weight of a polymer, with a lower value of MFR corresponding to a higher average molecular weight polymer. Generally viscosity increases with molecular weight, so the higher value of MFR for C980 is often taken to mean that it should flow more easily. It should be recalled that MFR values are obtained at low shear rates and only represent a single point on the viscosity curve. This highlights the inability to fully describe the flow behaviour which is a key consideration in transfer moulding. This is especially the case for pressure driven injection, where the speed of transfer is highly dependent on the viscosity of the material.

Virgin PFA acts as a Newtonian fluid below approximately $10s^{-1}$, and displays shear thinning behaviour following a Power law fit above this. C980 is shear thinning over the whole region investigated, however this becomes more pronounced at shear rates higher than $20\text{-}60s^{-1}$. Applying the Carreau model using the Solver function in Excel accurately fitted the behaviour over the whole region for both the filled and unfilled grades. Chhabra and Richardson (2011) state that the value of n must lie between 0 and 1 for shear thinning fluids. The zero values of the power index, n, are unexpected from the Carreau model and the dearth of information prevents any comparisons to the work of others being made. A possible conclusion is that PFA is extremely shear thinning, however it is possible the results have been affected by slip at higher shear rates. This would lead to lower pressure readings and therefore a reduction in the apparent shear viscosity. Additional work could be conducted using dies of different length to diameter ratios to investigate slip conditions. Regardless of the parameters, the model fits the experimental data well and the data shows the

difference in flow behaviour of the materials, providing useful information for processors of PFA.

The tensile deformation behaviour of the virgin polymers demonstrated that two materials behave in approximately the same way. Tensile results showed 350TJ has a higher yield strength than 6502TZ meaning it can withstand a higher stress prior to plastic deformation. Unfortunately the samples of C980 experienced premature failure so no comparison could be drawn between the tensile behaviour of filled and unfilled PFA. These results alone are not directly relevant to the processing of PFA, as the samples had experienced a very short heat history. They did however provide a useful baseline from which to compare the samples exposed to various conditions. This will be discussed further in the relevant sections.

Differential Scanning Calorimetry (DSC) confirmed the melt temperatures of the virgin PFAs to be very similar, with the width of the melting peak endotherms suggesting a narrow crystal size distribution. The broader peak of C980 indicates it has a wider range of crystal sizes. This may be necessary to increase the processability of the material, as it is more viscous that the virgin polymers despite the melt temperature being nearly 30°C lower.

The FTIR spectra of the virgin materials are very similar, with the only significant difference in the last peak of the spectra obtained from FTIR at 507cm^{-1}. However there was a significant difference seen in this peak for two samples of unprocessed 350TJ from different batches, highlighting the method may not be suitable for this work. Spectroscopy picks up changes to the chemical structure of the polymer, if these are only very slight, it is not unreasonable that they are not detected. There are a couple of peak shifts in the spectrum of C980, however further testing of the filled PFA gave poor results indicating spectroscopy is not a suitable for this material.

5.4 Effect of Temperature

The viscosity of the two virgin grades showed similar dependence on temperature, whereas the behaviour of C980 was significantly different. The trends of the materials are not as expected, and they are not particularly well understood. Generally the viscosity of polymers decreases as temperature increases, however after the drop in viscosity of the virgin polymers from 340-

350°C, the viscosity roughly plateaus at 350-360°C then rises with temperature. C980 demonstrates a general increase in viscosity with temperature, however there is some dependence on shear rate as the peaks of the curves shift. The apparent minimum viscosity of C980 at 320°C is difficult to explain without further data. This could not be investigated further as below 320°C the pressure exceeded the safe working limit of the melt transducer and the load cell of the tensometer.

The lack of available information prevents comparison to published results and limits the opportunities to provide further insight. The tests were conducted on the same charge of polymer in the ranges 340-360°C and 370-390°C so whilst it is possible the experimental method contributed to the trend seen in the results it is unlikely. It is possible crosslinking occurred due to the increased residence time, particularly at the higher temperature, which would have led to increased viscosity. However, there appears to be very little effect on viscosity due to residence times of 4 and 8hrs, so it is concluded the 30mins difference from the lowest and highest temperatures the charge was subjected to is insignificant. There may have been increased adhesion of the polymer to the die wall at the higher temperatures which would also give artificially high viscosities. Another possibility is the occurrence of an element of wall slip at the lower temperatures investigated, which may be responsible for viscosity data that is lower than expected. If the results were affected by the amount of polymer in the barrel of the rheometer it would be reasonable to expect to see a repeated trend from 340-360°C and 370-390°C however this is not the case. The tests were conducted three times to give average values with relatively low standard deviations, and the behaviour is demonstrated at each of the shear rates investigated, so there is a high level of confidence in the results.

The results obtained from the capillary rheometer highlight the limitations of using melt flow rate (MFR) testing as a means to understand the effect of temperature on the flow characteristics of PFA. The results from MFR testing on the virgin polymers showed a linear reduction in MFR with decreasing temperature, which indicates the viscosity increases with decreased temperature as less polymer flows in a given time. These results are reasonable as they were obtained at low shear rates in the Newtonian region of the graph, however it emphasises the importance of conducting testing under conditions

similar to those expected during processing of the polymer. The results generated agree with the graph by DuPont (1992) showing the apparent viscosity with temperature of PFA 350. Apparent viscosity is another parameter obtained at one shear rate only, and is of limited use when the shear rate at which the measurement was taken is not reported (as in the case with the graph presented by DuPont). The tests conducted by DuPont are likely to have been below the critical shear rate of PFA 350, which is approximately $12s^{-1}$, significantly lower than $25s^{-1}$ the capillary rheometer was set to run at to determine the effect of temperature on viscosity. It is therefore not unreasonable the two methods do not show the same results.

5.5 Effect of Residence Time

There is a substantial increase in the Melt Flow Rate (MFR) of samples exposed to various times at processing temperature. MFR testing appears to be the most sensitive method for determining change in the polymer as the shear rates the polymer is exposed to are quite low. Gangal (1989) appears to be the first to list the 20% maximum change in MFR as an acceptable indicator for degradation of PFA, however there is no data presented to support his view. DuPont (1992) provide a graph showing the change in melt flow number with time at different temperatures for PFA 350, however it is not particularly useful as a comparison. The residence time is only up to an hour, the lowest temperature curve is 395°C whereas the polymer in this study has been aged at approximately 370°C, and 350TJ has been thermally stabilised so it is expected to perform better than 350. The MFR results from this study offer updated information, however alone they are not tremendously useful given the lack of confidence in the maximum allowable increase.

A slight increase was seen in viscosity of all the samples exposed to various times at temperature, which was unexpected given the results of MFR testing. Thermal degradation of fluoropolymers is not well understood, however Concannon and Rummel (1984) propose for perfluorinated polymers one of the primary mechanisms is chain scission, whereby the main chains are split into shorter segments. This reduces the molecular weight of the polymer, which would cause a reduction in the viscosity of the polymer. They do however note that the end groups of the polymer complicate studying the means of

degradation. The material held for 4hrs in the barrel of the rheometer demonstrates the most dramatic change in viscosity. The reason behind this is not particularly well understood, however it is not unreasonable to propose there may have been some interaction between the polymer and the wall of the barrel which may have led to the development of higher pressure measurements. It is reasonable to conclude the material had not degraded as there was no decrease in the viscosity of the polymers, and no discernible colour change, which is observed to be a sign of degradation by many including Reinhardt (1969) and Hiraga et al. (2003).

The tensile deformation behaviour did not change for the samples of 6502TZ exposed to different residence times, however the mechanical properties of 350TJ reduce corresponding to the length of time at temperature. Both virgin polymers still exceed the minimum required value of 300% for the elongation at break defined by ASTM 3307 (2010). The mechanical properties of 350TJ are superior to those of 6502TZ, even after 8hrs at processing temperature, however 6502TZ shows a higher stability at temperature. This type of information allows fluoropolymer processors to choose the polymer they use based on their requirements both for processing and in terms of final product performance. There is little to be gained from the tensile data on C980 due to the premature breakage of samples, however it is tentatively proposed the polymer has not suffered significant degradation as the viscosity remains largely unchanged.

The data obtained from Differential Scanning Calorimetry does not follow common trends and the discrepancies between the two virgin materials prevent a conclusion being drawn with any certainty.

Variations in the samples of material subjected to different residence times at processing temperature were identifiable by Fourier Transform Infrared (FTIR) and Near Infrared (NIR) spectroscopy. Overall the changes seen in the spectra obtained from FTIR do not form a coherent trend from which to base a conclusion, however NIR provided useful information. Applying statistical methods such as Partial Least Squares (PLS) regression showed correlation between the aged samples, however the data spreads were such that it would be difficult to determine the residence time of an unknown sample without more in depth calibration studies. Similarly, Principal Component Analysis shows an

element of grouping of the aged samples of virgin PFA. It is probably worth investigating whether more closely controlled samples provide a reduced spread of data for each residence time.

5.6 Effect of Shear

A small increase in viscosity was seen for the samples exposed to high shear rates, similar to the differences seen for the samples held at various residence times. The generally accepted indicator that degradation has occurred is a decrease in the viscosity so it is concluded that no significant degradation has taken place.

Similar to the samples exposed to various residence times, the stress strain curves do not change for the samples of 6502TZ exposed to a high level of shear, whereas those of 350TJ reduce corresponding to the level of shear. Both virgin polymers still exceed the minimum required value of 300% for the elongation at break defined by ASTM 3307 (2010). The mechanical properties of 350TJ do not change with the level of shear as one would perhaps expect, implying that once the material has been sheared above a certain amount the effect is negligible. This information could prove useful to processors who are interested in increasing their rate of injection. The mechanical properties of 350TJ even when sheared are superior to those of 6502TZ, however 6502TZ is more process stable.

Again, data from DSC of the virgin samples is insufficient to draw general conclusions, particularly when considering the lack of agreement shown by the Chemours samples.

Differences in the spectra of the samples exposed to high shear rates were seen, however they did not form an intelligible pattern.

5.7 Effect of Processing

The MFR of the samples held in a transfer moulding pot increase with residence time as expected. The results from these samples are compared to those of PFA wrapped in foil and held at temperature for various lengths of time (see below).

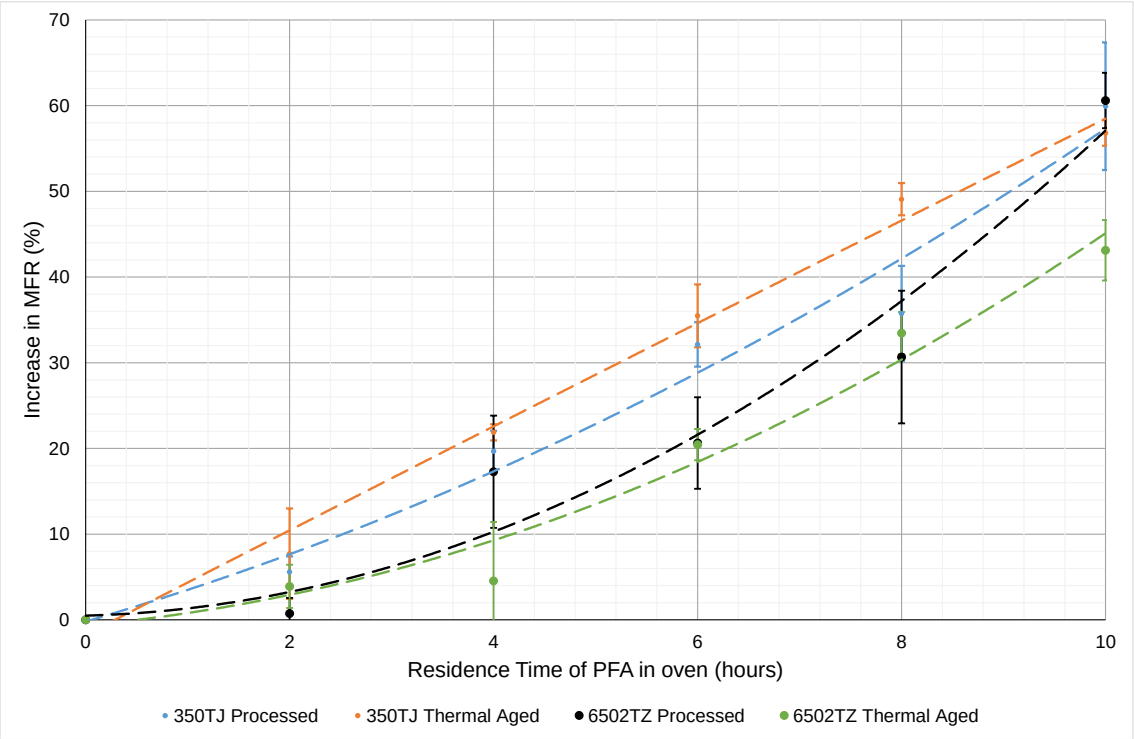

Figure 5.1: Difference in MFR of 350TJ and 6502TZ subjected to two different methods of thermal aging

Figure 5.1 suggests that 350TJ held in a transfer moulding pot and pressurised after the melt period can be held for 4½hrs before the 20% anecdotal maximum increase in MFR is reached. This seems to have increased the time at which 350TJ can be held from approximately 3½hrs from the data obtained from the samples wrapped in foil and heated. The times before a 20% in MFR is seen for both types of samples of 6502TZ are similar, around 6hrs, however the act of processing looks to have decreased the residence time. This contrasting data makes it difficult to draw a conclusion regarding the effect of the method of manufacture of the sample. Sepe (2013) notes that a value of 20% is relatively low, and can sometimes be quoted by the supplier to delegate responsibility to the processor. The author goes on to explain that much of the work conducted to establish the maximum acceptable increases in MFR was determined using viscosity. In some cases the maximum acceptable increase in viscosity was found to be 30%, however this was translated as a 30% increase in MFR (it is actually approximately 43%). This is also likely to have contributed to the conservative estimates of allowable increases in MFR. The lack of supporting data for the historical value of a 20% tolerable increase in MFR highlights the need to define the maximum acceptable increase using data. The key

information the data tells us is that MFR is a suitable method for quantifying the effect of exposure to processing temperature, and that MFR does increase with time at temperature, as expected.

The viscosity of the extrudate and the pods are very similar and are both slightly higher than the unprocessed material. This follows the same trend as the results of the material exposed to shear and residence time.

DSC shows significant increases in the melting temperature and the enthalpy for samples of PFA that had a distinctly different appearance, unfortunately the exact processing conditions are unknown. It is worth noting in this case however, that from a quality perspective testing would not be required on such a sample as the material would have been rejected from an aesthetic point of view.

Partial Least Squares regression of the data obtained from NIR spectroscopy showed a better correlation for 350TJ than for the other samples subjcted to various residence times. However the spread of data points of the 6502TZ samples makes it difficult to quantify the heat history of the material without further work. Principal Component Analysis of the samples showed more successful grouping of 350TJ material than 6502TZ. This could potentially be improved by better control over the manufacture of the sample material. As with the samples held at processing temperature for various lengths of time, these samples were located in an oven also being used for manufacturing purposes. This meant the air temperature of the oven was not constant, as the door would have been opened several times during the residence time of the sample in order to remove components for moulding. The reasonable success of the differentiation of samples exposed to various residence times means the method could be used as an investigative technique to determine the heat histories of unknown samples.

There were variations seen in the spectra obtained by FTIR spectroscopy for the pods and extrudate for both the virgin materials. The main difference was in the wavenumber of the peak at 507cm^{-1}, however this was also shown in the samples of 350TJ from different batches. This makes it difficult to infer anything from the data. Small changes are seen in other peaks, however there are no strong trends shown. As the results of the samples exposed to various times at

temperature and high shear do not show coherent patterns, it suggests there are no detectable chemical changes in the material.

5.8 Effect of Cooling Rate

In general a slower rate of cooling leads to a higher level of crystallinity in a material, and potentially larger crystals. This is reflected in the melting temperatures of the first heating cycle of DSC, as a higher melting temperature indicates a higher level of crystallinity. After the controlled cooling cycle the melting temperatures of the second heating are very similar, showing the rate of cooling has no lasting effect on the structure of the material as expected. A higher melting enthalpy indicates a higher level of crystallinity which is seen in the initial heating of the slow cooled sample of 350TJ, but the reverse was not true for the quench cooled sample. The lowest value of the melting enthalpy is gained from the material subjected to standard cooling (press cooled by water at 40°C), which is unexpected and difficult to explain, especially when compared to the data obtained by Raman spectroscopy.

The peaks in the Raman spectra of the samples of 350TJ subjected to different cooling rates demonstrate good agreement with the values published in the literature. There are no significant changes in the wavenumbers of the peaks which is as expected, as the rate of cooling would not induce a chemical change in the polymer. The quench cooled sample has broader peaks demonstrating a lower level of crystallinity, as anticipated. The normal and slow cooled samples have sharper peaks, but it cannot be explained why the sample subjected to normal cooling appears to have a higher level of crystallinity than the slowly cooled sample.

The spectra obtained by FTIR did not show any differences in the wavenumbers of the peaks, as expected as there should be no chemical change associated with the rate of cooling and therefore crystallinity of the material. However, the peaks did show a trend whereby those of the slow cooled material were higher, followed by the normally cooled sample, with the lowest peaks belonging to the quench cooled sample. This reflects the expected pattern for crystallinity, as the more intense peaks are associated with higher levels of crystallinity.

The results demonstrated the expected trend whereby the slower the rate of cooling, the greater the yield strength and elastic modulus, and redcues the

strain the material can withstand prior to failure. This is due to the increased level of crystallinity making the material stiffer. However the strength of the material is less of a concern from a lined pipe manufacturer's perspective in the traditional sense, as the metalwork of the fitting is providing much of the mechanical strength. The critical factor for lined pipe application is the resistance to Environmental Stress Cracking (ESC), which is reduced when the level of crystallinity in the material is increased. Therefore in order to provide enhanced resistance to ESC, PFA lined components should be cooled quickly. This does have an effect of the permeation resistance, as the reduced crystallinity from rapid cooling will reduce the permeation resistance of the liner.

5.9 Summary

The project generated valuable novel information and was deemed successful by interested parties. The rheometer designed for the project worked exceptionally well, enabling the characterisation of flow behaviour over a wide range of shear rates the polymer is likely to see during the transfer moulding process. Exposing PFA to high temperature for extended periods of time has been shown to have a limited effect on the mechanical properties of the polymer. Previously there had been no data available to support or disprove this anecdotal evidence. Similarly, the effect of processing the polymer above the critical shear rate on the mechanical properties has been shown to be negligible. This enables the process window to be expanded in terms of injection rates, potentially extending the flow paths of the polymer to mould more complex and larger fittings.

Overall, the results from tensile testing and FTIR spectroscopy showed good agreement with each other and the literature, whereas the trends shown in the data acquired from DSC and Raman spectroscopy were not entirely coherent. The work has generally shown the rate of cooling does have a bearing on the properties of PFA, with the mechanical properties most affected.

Chapter 6

Conclusions and Further Work

The aim of this work was to increase the level of scientific understanding of the effects of processing on the properties of perfluoroalkoxy. The aims were to determine the effects of temperature and shear rate on the viscosity of the material, and quantify the level of change in the material due to exposure to high shear rate and various residence times at processing temperature. On the basis of the experimental work conducted, the following is concluded:

6.1 Conclusions

1. The bespoke rheometer was successfully designed, built and validated and enabled investigation of the flow behaviour of three transfer moulding grades of perfluoroalkoxy over a range of 5-400s^{-1} and showed the unfilled grades from different manufacturers (Chemours 350TJ and Dyneon 6502TZ) behaved similarly. The PFA containing carbon black at a level of 3-5% (Chemours C980) was found to have significantly higher viscosity at shear rates likely to be experienced during processing.

2. The dependence of the viscosity of PFA on temperature is complex as it does not decrease as temperature increases. The behaviour is similar for both virgin PFA materials, but varies significantly for the carbon black filled PFA.

3. Tensile testing was effective in demonstrating the differences in mechanical properties of the virgin materials as a result of exposure to processing temperature and high shear rates.

4. 6502TZ is superior in terms of process stability to 350TJ as it displays no change in tensile properties due to shear or residence time.

5. The mechanical properties of 350TJ are compromised by exposure to high shear rates. The level of the shear rate does not seem to alter the effect as the shift in the stress strain curves is the same for samples exposed to 100s^{-1}, 500s^{-1} and 1000s^{-1}.

6. The residence time at processing temperature was also found to reduce the mechanical properties of 350TJ. The shifts in the stress strain curve were proportional to the length of time the material had been exposed to processing temperature.

7. Melt Flow Rate was found to reflect changes in the material as a consequence of exposure to processing temperature, however the results did vary depending on the method of preparation of the sample material.

8. The changes in flow curves due to residence time at processing temperature or exposure to high shear are minimal.

9. Correlation of the virgin samples exposed to various residence times at processing temperature was possible by conducting analysis on the spectra obtained from Near Infrared spectroscopy using Partial Least Square regression and Principal Component Scores.

10. Differential Scanning Calorimetry showed 350TJ and 6502TZ to have a narrow crystal size distribution and a similar melting temperature, whereas the crystal size distribution of C980 is much broader and the melt temperature is nearly 30°C lower.

11. Fourier Transform Infrared spectroscopy was found to have limited use in determining the differences between virgin grades of PFA, suggesting a negligible change in the chemical structure.

12. Tensile testing of the unprocessed virgin material showed 350TJ to have higher mechanical properties than 6502TZ.

13. There were no clear trends seen in the data obtained from Differential Scanning Calorimetry, showing it is not useful for distinguishing between process histories for the grades of PFA examined in this study.

14. Infrared and Raman spectroscopic methods were found to largely be unsuitable for examination of PFA with carbon black additive due to laser heating of the material.

15. The process conditions required to compression mould a plaque of virgin PFA were found to be significantly different for PFA with carbon black additive. As a result, tensile testing did not yield useful data for C980.

16. Overall capillary rheometry was found to provide information regarding the change in viscosity due to shear and temperature that was not previously available. Tensile testing and melt flow rate testing have been found to be suitable techniques to determine the change in PFA due to processing.

6.2 Future Work

The following suggestions are made for further work:

1. The range of polymers investigated could be extended to include high purity grades to obtain information on their basic properties and determine whether they provide increased resistance to thermal degradation.

2. One limitation of the Blockprogramming software was the inability to program a test where the shear rate increased continuously, preventing a thermal degradation test at low shear rate. This kind of test could provide information on the rate of change of viscosity with exposure to processing temperature.

3. Tensile testing was found to be a suitable method for determining the effect of processing on the mechanical properties of PFA. Development of the compression moulding capability for PFA with carbon black additive should give samples that do not fail prematurely.

4. The samples subjected to various residence times at processing temperature were prepared in the ovens that were being used for manufacturing purposes. This meant the air temperature was not constant due to fittings being removed from the oven for moulding. Producing samples under a more controlled environment may give better correlation, particularly for Principal Component Analysis and Partial Least Squares regression of Near Infrared spectra.

5. The values of the parameters for the Carreau model generated by use of Solver function in Microsoft Excel were unexpected. Further analysis of the rheological data using a dedicated software fitting program is recommended.

6. A study of slip using dies of different lengths with the same length to diameter ratio would provide further information on the possible reasons behind the effect of temperature on viscosity

7. Rotational rheometry removes the possibility of wall slip as it is a low shear method and should also provide more information on the effect of temperature on viscosity.

8. A more in depth study of the effects of cooling rate on the level of crystallinity would help to quantify the DSC results seen in this work.

References

ASTM Standards (2009) *F1545-97, Standard Specification for Plastic Lined Ferrous Metal Pipe, Fittings and Flanges*. West Conshohocken, PA: ASTM International.

ASTM Standards (2010) *D3307-10, Standard Specification for Perfluoroalkoxy (PFA)-Fluorocarbon Resin Molding and Extrusion Materials*. West Conshohocken, PA: ASTM International.

ASTM Standards (2013) *D1238-13, Standard Test Method for Melt Flow Rates of Thermoplastics by Extrusion Plastometer*. West Conshohocken, PA: ASTM International.

ASTM Standards (2010) *D638-10, Standard Test Method for Tensile Properties of Plastics*. West Conshohocken, PA: ASTM International.

Aten, R. M., Libert, S. A. and Burch, H. E. (2012) *Core/shell polymer and fluoropolymer blending blow molding and blown film process*. United States Patent and Trademark Office Patent no. US 8192677 B2 [Online]. Available at: http://www.google.co.uk/patents/US8192677 (Accessed: 23 August 2015).

Banks, R. E., Smart, B. E. and Tatlow J. C. (1994) *Organofluorine Chemistry: Principles and Commercial Applications*. New York: Plenham Press

Buxton, L. W., Goldsberry, D. R., and Henthorn, G. V. (1993) Fluoropolymer-Lined Chemical Systems and Permeation, Technical Information, DuPont

Chhabra, R. P. and Richardson, J. F. (2011) *Non-Newtonian Flow and Applied Rheology: Engineering Applications*. Oxford: Butterworth-Heinemann

Cogswell, F. N. (1981) *Polymer Melt Rheology A Guide for Industrial Practice*. Great Britain: George Godwin Limited.

Concannon, T. P and Rummel, M. K. (1984) *Polytetrafluoroethylene resin with degradation retarder*. United States Patent and Trademark Office Patent no. US 4425448 A [Online]. Available at: https://www.google.co.uk/patents/US4425448 (Accessed: 16 August 2015).

Dargaville, T. R. (2002) Studies of the Radiation Chemistry and Grafting of a Fluoropolymer. PhD thesis, University of Queensland.

Drobny, J. G. (2001) *Technology of Fluoropolymers*. Florida: CRC Press LLC

DuPont (1988) Injection Moulding Guide for Melt Processable Fluoropolymers, Technical Information

DuPont (1992) Teflon/Tefzel Transfer Moulding Guide, Technical Information

DuPont (1997) Teflon®/Tefzel® fluoropolymer resin: For Performance and Value in CPI Equipment, Technical Information

DuPont (2001) Teflon® Finishes in the Chemical Processing Industry: Permeation – Its Effects on Teflon® Fluoropolymer Coatings, Technical Information, DuPont

DuPont (2011) DuPont Fluoropolymers, Technical Information

DuPont (2013) DuPont™ Teflon® PFA 350 Molding and Extrusion Resin, Product Information

Dyneon (2013) Injection Moulding Guide for Dyneon PFA, Technical Information

Ebnesajjad, S. (2000) *Fluoroplastics, Volume 1: Non-Melt Processable Fluoroplastics*. New York: William Andrew Inc.

Ebnesajjad, S. (2015) *Fluoroplastics, Volume 2: Melt Processible Fluoroplastics*. 2nd edn. New York: William Andrew Inc.

Ebnesajjad, S. (2013) *Introduction to Fluoropolymers: Materials, Technology and Applications*. New York: William Andrew Publishing.

Ebnesajjad, S. and Khaladkar, P. R. (2004) *Fluoropolymer Applications in the Chemical Processing Industries*. New York: William Andrew Inc.

Elsevier (2015) '*Sina Ebnesajjad.*' Available at: http://store.elsevier.com/Sina-Ebnesajjad (Accessed 23 August 2015).

Extrand, C. W. (2003) 'The use of fluoropolymers to protect semiconductor materials.' *Journal of Fluorine Chemistry*, 122, pp. 121-124.

Extrand, C. W. and Monson, L. (2006) 'Gas Permeation Resistance of a Perfluoroalkoxy-Tetrafluoroethylene Copolymer.' *Journal of Applied Polymer Science*, 100, pp. 2122-2125.

Fleming, J. R., Kemkes, D., Chatten, R. G., Crenshaw, L. E. and Imbalzano, J. F. (2001) Material of Construction for Pharmaceutical and Biotechnology Processing: Moving into the 21st Century, Technical Information, DuPont

(1999) PFA vs. PTFE: Debunking the Myth, Technical Information, Flowserve

FluoroConsultants Group (2015) '*About us*'. Available at: http://www.fluoroconsultants.com (Accessed 23 August 2015).

Gangal, S. V. (1989) 'Tetrafluoroethylene Polymers,' in Kroschwitz, J. I., ed., *Encyclopedia of Polymer Science and Engineering,* 2nd edn., *Volume 16*. New York: Wiley-Interscience, pp. 577-642

Hiraga, Y., Noda, T., Imanishi, H. and Komatsu S. (2003) *Method for stabilizing fluorine-containing polymer*. United States Patent and Trademark Office Patent no. US 6664337 B2 [Online]. Available at: https://www.google.co.uk/patents/US6664337 (Accessed: 16 August 2015).

Hudson, R. (1995) *Developments in the European Extrusion Industry*. UK: iSmithers Rapra Publishing

Hyde, F. W., Alberg, M. and Smith, K. (1997) 'Comparison of Fluorinated Polymers Against Stainless Steel, Glass and Polypropylene in Microbial Biofilm Adherence and Removal.' *Journal of Industrial Microbiology and Biotechnology*. 19, pp. 142-149.

Imbalzano, J. F., Washburn, D. N., and Mehta, P.M. (1991) 'Basics of Permeation and ESC in Relation to Fluoropolymers.' *Chemical Engineering*. 98, 1, pp. 105-108.

Imbalzano, J. F. (1995) Teflon®/Tefzel® fluorocarbon resin/fluoropolymer resin: Basic Chemistry and Properties, Technical Information, DuPont

ISO Standards (2011) 1133, *Plastics - Determination of the melt mass-flow rate (MFR) and melt volume-flow rate (MVR) of thermoplastics*. London, UK: BSI Standards Limited

ISO Standards (2011) *37, Rubber, vulcanized or thermoplastic — Determination of tensile stress-strain*. London, UK: BSI Standards Limited

ISO Standards (2012) *527, Plastics — Determination of tensile properties*. London, UK: BSI Standards Limited

Kerbow, D. L. and Sperati, C. A. (1999) 'Physical Constants of Fluoropolymers,' in Brandrup, J., Immergut, E. H., Grulke, E. A. (eds.) *Polymer Handbook, 4th edition*. New York: Wiley, pp. V/31–V/48

Kontopoulou, M. (2012) *Applied Polymer Rheology: Polymeric Fluids with Industrial Applications*. New Jersey: John Wiley & Sons

Lahijani, J., Samija, M. P., Pruce, G. M., and Netta, J. L. (2011) 'A New Class of Perfluoropolymers: High-Temperature Epitaxial Co-Crystalline (ECC) Perfluoropolymer Resins' Technical Information, DuPont

Legeay, G., Coudreuse, A., Legeais, J.-M., Werner, L., Bulou, A., Buzarea, J.-Y., Emery, J. L., Silly, G. (1998) 'AF fluoropolymer for optical use: spectroscopy and surface energy studies comparison with other fluoropolymers.' *European Polymer Journal*, 10, pp. 1457-1465.

Loadman, M. J. (2012) *Analysis of Rubber and Rubber-like Polymers*. London: Springer Science & Business Media.

Mark, H. F. (2013) *Encyclopedia of Polymer Science and Technology, Concise*. New Jersey: John Wiley & Sons.

McKeen, L. W. (2009) *Fatigue and Tribological Properties of Plastics and Elastomers*. 2nd edn. Oxford: Elsevier.

Mihaly, J., Sterkel, S., Ortner, H. M., Kocsis, L., Hajba, L., Furdyga, E., and Mink, J. (2006) 'FTIR and FT-Raman spectroscopic study on polymer based high pressure digestion vessels.' *Croatica Chemica Acta*, 79 (3), pp. 457-501.

Monson, L., Moon, S. I., and Extrand, C. W. (2009) 'Gas Permeation Resistance of a Perfluoroalkoxy-Tetrafluoroethylene Copolymer.' *Journal of Applied Polymer Science*, 111, pp. 141-147.

Moon, S. I., and Extrand, C. W. (2011) 'Hydrogen Chloride and Ammonia Permeation Resistance of Tetrafluoroethylene-Perfluoroalkoxy Copolymers.' *Industrial and Engineering Chemistry Research*, 50, pp. 2905-2909.

O'Hagan, D. (2008). 'Understanding organofluorine chemistry. An introduction to the C–F bond'. *Chemical Society Review* 37, pp. 308–19

Parker, S. F., Williams, K. P. J., Meehan, P., Adams, M., A, and Tomkinson, J. (1994) 'Analysis of carbon black-filled polymers by vibrational spectroscopy.' *Applied Spectroscopy*, 48, pp. 669-673.

Reinhardt, H. F. (1969) *Salicylate stabilized fluoro-polymers*. United States Patent and Trademark Office Patent no. US 3438934 A [Online]. Available at: https://www.google.co.uk/patents/US343934 (Accessed: 16 August 2015).

Rosenbaum, E. E., Hatzikiriakos, S. G. and Stewart, C. W. (1995). 'Flow implications in the processing of tetrafluoroethylene/hexafluoropropylene copolymers.' *International Polymer Processing*, 3, pp. 204-212

Runt, J. P. (1986) 'Crystallinity Determination,' in Mark, H. F. and Kroschwitz, J. I. (eds.) Encyclopedia of Polymer Science and Engineering, 2nd ed. New York: Wiley, 4, pp. 482-519

Scheirs, J. (2000) *Compositional and Failure Analysis of Polymers: A Practical Approach*. England: John Wiley & Sons

Sepe, M. P. (2013) *Melt Flow Rate Testing—Part 5*.' Available at: http://www.ptonline.com/columns/melt-flow-rate-testingpart-5 (Accessed: 21/08/2015)

Solvay (2014) Hyflon® PFA Design and Processing Guide, Technical Information

Teng, H. (2012) 'Overview and the Development of the Fluoropolymer Industry.' Appl. Sci., 2, pp. 496-512

Utracki, L. A. (1998) '2.2.3 Speciality Polymers,' in Utracki, L. A. *Commercial Polymer Blends*. New York: Chapman and Hall, pp. 44-52 (45)

Whelan, T. (1994) *Polymer Technology Dictionary*. UK: Chapman & Hall

Wu, M., Ray. M., Fung K. H., Ruchman M. W., Harder, D and Sedlack, A. J. (2000) 'Stand-off detection of chemicals by UV Raman Spectroscopy.' *Applied Spectroscopy*, 54 (2000) pp. 800–806.

Yanik, D. (2011) ‘Generational Advancements in Fluoropolymer Lined Piping Systems’, Technical Information, Resistoflex

Appendix A

Material Data Sheets

A.1 350TJ

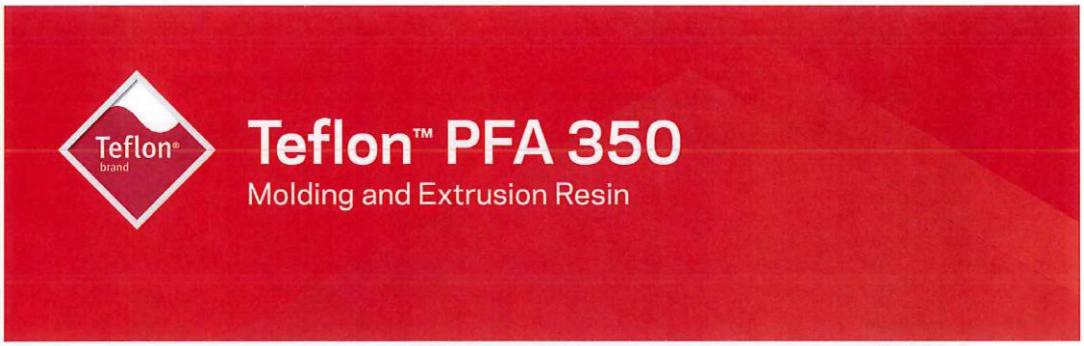

Product Information

For inventory control purposes, product name may be followed by an X.

Products labeled PFA 350 and PFA 350 X are equivalent, and all information in this document is applicable to both.

Typical Applications

Applications for Teflon™ PFA 350 include extruded tubing for use in handling aggressive fluids at high pressures; chemical linings for pipes used in the chemical processing industry; film for high flex service; and traditional extruded, injection-molded, or blow-molded articles requiring the unique performance of Teflon™.

Description

Teflon™ PFA 350 is a general-purpose fluoroplastic resin available in pellet form. Compared with other grades of Teflon™ PFA, its most unique features are a relatively low flow rate, greatly increased flex life, and enhanced resistance to environmental stress-cracking over both Teflon™ PFA 340 and 345 (Teflon™ PFA 350 has a typical MIT folding endurance of 500,000*, compared to that of 15,000 and 50,000 for Teflon™ PFA 340 and 345, respectively). Teflon™ PFA 350 is preferred when extended service is required in hostile environments involving chemical, thermal, and mechanical stress. Table 1 shows the typical property data for Teflon™ PFA 350.

Teflon™ PFA 350 is used when traditional extrusion and molding processes are required for producing products with the superior properties of a fluoroplastic resin. Compared to other thermoplastics, the high melt strength and thermal stability of Teflon™ PFA 350 can be used to improve processing rates. Compared with other fluoroplastics, creep resistance at high service temperatures provides a superior balance and level of end-use properties. Teflon™ PFA 350 combines the processing ease of conventional thermoplastics with many properties similar to those of polytetrafluoroethylene.

Properly processed products made from neat Teflon™ PFA 350 resin provide the superior properties characteristic of fluoroplastic resins: chemical inertness, exceptional dielectric properties, heat resistance, toughness and flexibility, low coefficient of friction, non-stick characteristics, negligible moisture absorption, low flammability, performance at temperature extremes, and excellent weather resistance.

In a flame situation, products of Teflon™ PFA 350 resist ignition and do not promote flame spread. When ignited by flame from other sources, their contribution of heat is very small and added at a slow rate with very little smoke.

Chemours™

Processing

Teflon™ PFA 350 can be processed by conventional melt extrusion, and by injection, compression, transfer, and blow molding processes. High melt strength and heat stability permit the use of relatively large die openings and high temperature draw-down techniques that increase production rates. Reciprocating screw injection molding machines are preferred. Corrosion-resistant metals should be used in contact with molten fluoroplastic resin. Extruder barrel should be long, relative to diameter, to provide residence time for heating the resin to approximately 390 °C (730 °F). For more detailed processing information, including recommended draw-down ratios, consult your Chemours sales representative.

Safety Precautions

WARNING! VAPORS CAN BE LIBERATED THAT MAY BE HAZARDOUS IF INHALED.

Before using Teflon™ PFA 350 resin, refer to the Safety Data Sheet and the latest edition of "The Guide to the Safe Handling of Fluoropolymer Resins," published by The Society of the Plastics Industry, Inc. (www.fluoropolymers.org) or by PlasticsEurope (www.plasticseurope.org). Open and use containers only in well-ventilated areas using local exhaust ventilation (LEV). Vapors and fumes liberated during hot processing of Teflon™ PFA 350 should be exhausted completely from the work area. Contamination of tobacco with these polymers must be avoided. Vapors and fumes liberated during hot processing and which are not properly exhausted, or from smoking tobacco or cigarettes contaminated with Teflon™ PFA 350 may cause flu-like symptoms such as chills, fever, and sore throat. This may not occur until several hours after exposure and will typically pass within about 24 hours. Mixtures with some finely divided metals, such as magnesium or aluminum, can be flammable or explosive under some conditions.

Storage and Handling

The properties of Teflon™ PFA 350 resin are not affected by storage time. Ambient storage conditions should be designed to avoid airborne contamination and water condensation on the resin when it is removed from containers.

Freight Classifications

Teflon™ PFA 350 resin is classified as "Plastics, Materials, Pellets."

Packaging

Teflon™ PFA 350 is supplied as pellets and is available in 25-kg multilayer bags with an integral polyethylene liner.

Table 1: Typical Property Data for Teflon™ PFA 350 Molding and Extrusion Resin

Property	Test Method		Unit	Typical Value
GENERAL				
Melt Flow Rate	ISO 12086	ASTM D3307	g/10 min	2
Melting Point	—	ASTM D4591	°C (°F)	305 (581)
Specific Gravity	—	ASTM D792	—	2.15
Critical Shear Rate, 372 °C (702 °F)	—	—	1/s	12
MECHANICAL				
Tensile Strength	ISO 12086	ASTM D3307	MPa (psi)	
23 °C (73 °F)				28 (4,000)
250 °C (482 °F)				14 (2,000)
Ultimate Elongation	ISO 12086	ASTM D3307	%	
23 °C (73 °F)				300
250 °C (482 °F)				500
Flexural Modulus	ISO 178	ASTM D790	MPa (psi)	
23 °C (73 °F)				625 (90,000)
250 °C (482 °F)				69 (10,000)
MIT Folding Endurance (0.20 mm, 8 mil film)	—	ASTM D2176†	Cycles	500,000*
Hardness Durometer	ISO 868	ASTM D2240	—	D55
ELECTRICAL				
Dielectric Strength, Short Time, 0.25 mm (0.010 in)	IEC 243	ASTM D149	kV/mm (V/mil)	80 (2,000)
Dielectric Constant, 1 MHz (10^6 Hz)	IEC 250	ASTM D150	—	2.03
Dissipation Factor, 1 MHz (10^6 Hz)	IEC 250	ASTM D150	—	<0.0002
Volume Resistivity	ISO 1325	ASTM D257	ohm·cm	10^{18}
OTHER				
Water Absorption, 24 hr	—	ASTM D570	%	<0.03
Weather and Chemical Resistance	—	—	—	Outstanding
Limiting Oxygen Index	ISO 4589	ASTM D2863	%	>95
Continuous Service Temperature‡	—	—	°C (°F)	260 (500)
Flammability Classification†	—	UL 94	—	V-0

* Depending on fabrication conditions
† Historical standard
‡ Definition of continuous service temperature: The continuous service temperature is based on accelerated heat-aging tests, and represents the temperature at which tensile strength and ultimate elongation retain 50% of the original values after 20,000 hr thermal aging. Continuous service temperature above 260 °C (500 °F) may be feasible, depending on such factors as chemical exposure, support from the substrate, etc. When considering uses of Teflon™ PFA 350 above 260 °C (500 °F), preliminary testing should be done to verify suitability.
† These results are based on laboratory tests under controlled conditions and do not reflect performance under actual fire conditions; current rating is a typical theoretical value.
Note: Teflon™ PFA 350 meets the requirements of ASTM D3307, Type II
Typical properties are not suitable for specification purposes.
Statements or data regarding behavior in a flame situation are not intended to reflect hazards presented by this or any other material when under actual fire conditions.

HOW TO USE THE TEFLON™ BRAND NAME WITH YOUR PRODUCT

Teflon™ is a registered trademark of Chemours for its brand of fluoroplastic resins, coatings, films, and dispersions. The Teflon™ brand name is licensed by Chemours in association with approved applications. Without a trademark license, customers may not identify their product with the Teflon™ brand name, as Chemours does not sell such offerings with the Teflon™ trademark. Unlicensed customers may refer to the Chemours product offering with only the Chemours name and product code number descriptor as Chemours sells its product offerings. There are no fair use rights or exhaustion of rights to use the Teflon™ trademark from buying from Chemours, a Chemours customer, or a distributor without a trademark license from Chemours.

If you are interested in applying for a trademark licensing agreement for the Teflon™ brand, please visit www.teflon.com/license

CAUTION: Do not use Chemours materials in medical applications involving permanent implantation in the human body or contact with bodily fluids or tissues, unless the material has been provided from Chemours under a written contract that is consistent with Chemours policy regarding medical applications and expressly acknowledges the contemplated use. For further information, please contact your Chemours representative. You may also visit www.teflon.com/industrial to download a copy of the "Chemours POLICY Regarding Medical Applications" and "Chemours CAUTION Regarding Medical Applications." For medical emergencies, spills, or other critical situations, call (866) 595-1473 within the United States. For those outside of the United States, call (302) 773-2000.

The information set forth herein is furnished free of charge and based on technical data that Chemours believes to be reliable. It is intended for use by persons having technical skill, at their own discretion and risk. The handling precaution information contained herein is given with the understanding that those using it will satisfy themselves that their particular conditions of use present no health or safety hazards. Because conditions of product use are outside our control, Chemours makes no warranties, express or implied, and assumes no liability in connection with any use of this information. As with any material, evaluation of any compound under end-use conditions prior to specification is essential. Nothing herein is to be taken as a license to operate under or a recommendation to infringe any patents.

For more information, visit teflon.com/industrial
For sales and technical support contacts, visit teflon.com/industrialglobalsupport

Replaces: K-26137
C-10105 (7/15)

A.2 6502TZ

Product Data Sheet

3M™ Dyneon™
Fluoroplastic PFA 6502TZ

Product Description

3M™ Dyneon™ Fluoroplastic PFA 6502TZ, a fully fluorinated copolymer made from tetrafluoroethylene and perfluorvinylether, is characterized by its excellent temperature resistance, optimal chemical and weathering resistance and very good dielectric capabilities.

Special Features

- Wide service temperature range
- Extremely high weathering resistance and UV stability
- High limiting oxygen index: Does not support combustion
- Good non-stick characteristics
- Broad processing window
- Improved mould release property
- High transparency
- Excellent, almost universal resistance to solvents and chemicals
- Excellent electrical insulation properties, e.g.: dielectric breakdown strength, dielectric constant
- Smooth surfaces
- Good low-friction properties
- Improved stress crack resistance

Properties	Test method	Unit	Value*
Specific Gravity	DIN EN ISO 12086	g/cm³	2.15
Melting Point	DIN EN ISO 12086	°C	308
Melt Flow Index (372 °C/5 kg)	DIN EN ISO 1133	g/10 min	2
Limiting Oxygen Index (LOI)	ASTM D2863	%	> 95
Hardness Shore D	ASTM D2240/ISO 868	-	60
Tensile Strength at Break (23 °C)	ASTM D638	MPa	34
Elongation at Break (23 °C)	DIN EN ISO 527-1	%	360
Flexural Modulus	DIN EN ISO 527-1	MPa	550
MIT Folding Endurance (200 µm film)	ASTM D 2176	double folds	3.1 Mio.

* typical values

3M

Product Data Sheet

3M™ Dyneon™
Fluoroplastic PFA 6502TZ

Typical Properties

In comparison to the N grades the 3M Dyneon Fluoroplastic PFA T grades are chemically modified to show additional benefits: The 3M Dyneon Fluoroplastic PFA T grades show a high thermal processing stability resulting in a broad processing window. In addition, they are easily released from moulds, show an improved stress crack resistance and a smooth surface.

Typical Applications

Generally, 3M Dyneon Fluoroplastic PFA T grades are used for corrosion protection in valves, pumps, tanks, tubes and pipes, or heating cables. 3M Dyneon Fluoroplastic PFA 6502TZ, with a Melt-Flow-Index (372 °C/5 kg) of 2 g/10 min, is a material with a high viscosity and is used in low shear processes like thick walled extrusion, linings, transfer moulding or tube extrusion, especially when a broad processing window and an easy release from the mould is required.

Processing Recommendations

3M Dyneon Fluoroplastic PFA 6502TZ can be processed according to the known processing methods for thermoplastic polymers. All machine parts coming into contact with the melt or fumes of 3M Dyneon Fluoroplastic PFA 6502TZ should be made from highly corrosion resistant materials – usually high-nickel alloys such as Inconel® 625, Haynes® 242, Hastelloy® C, and Reiloy®. Off-gases and decomposition products during processing shall be managed via an appropriate exhaust fume management system, especially at the extruder die. For safe processing of Dyneon PFA please also check safety instructions below.

Typical processing temperatures for Dyneon PFA lie between 360 °C and 390 °C. The high melt viscosity makes 3M Dyneon Fluoroplastic PFA 6502TZ a standard material for tube extrusion and transfer moulding, especially when a broad processing window and an easy release from the mould is required.

Tube extrusion:

For the tube extrusion a 25-45 mm D extruder with a cylinder L/D ratio of 25-30:1 is required. The cylinder should have 3-4 heating zones that are independent from each other. Typical draw down ratios go up to max 25:1. The ideal draw down balance is 1.00.

Hastelloy®, Haynes® 242, and Reiloy® are registered trademarks of Haynes International.
Inconel® is a registered trademark of Special Metals Corporation.

Storage and Handling

3M™ Dyneon™ Fluoroplastic PFA 6502TZ can be stored for a relatively long period of time provided it is stored in a clean, dry place. 3M™ Dyneon™ Fluoroplastic PFA 6502TZ is hydrophobic and generally does not require drying before processing unless high humidity conditions create surface moisture adsorption. (Opened containers should be tightly resealed to prevent dust contamination from static charge accumulation and moisture ingress).

Safety Instructions

Follow the normal precautions observed with all fluorothermoplastic materials.

Please consult the Material Safety Data Sheet and Product Label for information regarding the safe handling of the material. By following all precautions and safety measures, processing these products poses no known health risks. General handling/processing precautions include: 1) Process only in well-ventilated areas. 2) Do not smoke in areas contaminated with powder/residue from these products. 3) Avoid eye contact. 4) If skin comes into contact with these products during handling, wash with soap and water afterwards. 5) Avoid contact with hot fluoropolymer.

Potential hazards, including release of toxic vapours, can arise if processing occurs under excessively high temperature conditions. Vapour extractor units should be installed above processing equipment. When cleaning processing equipment, do not burn off any of this product with a naked flame or in a furnace.

Delivery Form

3M™ Dyneon™ Fluoroplastic PFA 6502TZ is delivered in Pellet form.

Packaging sizes are:

- 50 kg cardboard box, containing two PE-bags with 25 kg content each

Product Data Sheet

3M™ Dyneon™
Fluoroplastic PFA 6502TZ

Important Notice

All information set forth herein is based on our present state of knowledge and is intended to provide general notes regarding products and their uses. It should not therefore be construed as a guarantee of specific properties of the products described or their suitability for a particular application. Because conditions of product use are outside Dyneon's control and vary widely, user must evaluate and determine whether a Dyneon product will be suitable for user's intended application before using it.

The quality of our products is warranted under our General Terms and Conditions of Sale as now are or hereafter may be in force.
Technical information, test data, and advice provided by Dyneon personnel are based on information and tests we believe are reliable and are intended for persons with knowledge and technical skills sufficient to analyze test types and conditions, and to handle and use raw polymers and related compounding ingredients.

No license under any Dyneon or third party intellectual rights is granted or implied by virtue of this information.
General recommendations on health and safety in processing, on work hygiene and on measures to be taken in the event of accident are detailed in our material safety data sheets.

You will find further notes on the safe handling of fluoropolymers in the brochure "Guide for the safe handling of Fluoropolymers Resins" (download link) by PlasticsEurope, Box 3, B-1160 Brussels, Tel. +32 (2) 676 17 32.

You can also download it with your smartphone using the QR code below.

Customer Service

Europe
Phone: 00 800 396 366 27
Fax: 00 800 396 366 39
Italy
Phone: 800 7 910 18
Fax: 800 7 810 19
USA
Phone : +1 800 810 8499
Fax : +1 800 635 8061

Technical Service Fluoroplastics

Dyneon GmbH
3M Advanced Materials Division
Industrieparkstraße 1
84508 Burgkirchen
Germany
Phone: +49 8679 7 4709
Fax : +49 8679 7 5037

Technical Service Fluoroelastomers & Polymer Processing Additives

3M Belgium N.V.
3M Advanced Materials Division
Canadastraat 11,
Haven 1005
2070 Zwijndrecht
Belgium
Phone: +32 3 250 7868
Fax: +32 3 250 7905

Technical Service PTFE Compounds

Dyneon B.V.
3M Advanced Materials Division
Tunnelweg 95
6468 EJ Kerkrade
The Netherlands
Phone: +31 45 567 9600
Fax: +31 45 567 9619

We will gladly supply further contact details for our full network of global sales offices. Alternatively, find them here.

Web Site: www.dyneon.eu

Printed in Germany

Status: Jul. 2013

A.3 C980

Teflon™ PFA C-980

Fluoroplastic Resin

Product Information

Typical Applications

Anti-static linings of components used in the chemical processing industries; industrial film; articles requiring superior electrical, chemical, and thermal properties.

Description

Teflon™ PFA C-980 (perfluoroalkoxy) fluoroplastic resins combine the chemical and high temperature resistance of Teflon™ PFA with anti-static levels of electrical conductivity.

Properly processed products made from Teflon™ PFA C-980 resins provide the superior properties typical of fluoroplastics: retention of properties after service estimated at 250 °C (482 °F), useful properties at -196 °C (-321 °F), and chemical inertness to nearly all industrial chemicals and solvents. Molded products have moderate stiffness, excellent toughness, low coefficient of friction, non-stick characteristics, resistance to creep at high service temperatures, and excellent weather resistance.

These resins can be processed by traditional transfer molding processes. They have high melt strength and thermal stability at high processing temperatures.

Processing

Teflon™ PFA C-980 fluoroplastic resins can be processed by conventional thermoplastic techniques: by melt extrusion, and by compression, transfer, and blow molding processes. Drying at 100 °C (212 °F) for 4 hours is suggested to remove any absorbed moisture. Corrosion-resistant metals should be used in contact with molten resin. Extruder barrel should be long, L/D ratio 20:1 to 25:1, to provide residence time for heating the resin to approximately 390 °C (194 °F). Due to its low viscosity, Teflon™ PFA C-980 can be melt extruded.

Safety Precautions

Before using Teflon™ PFA C-980 resin, refer to the Safety Data Sheet and the latest edition of "The Guide to the Safe Handling of Fluoropolymer Resins," published by The Society of the Plastics Industry, Inc. (www.fluoropolymers.org) or by PlasticsEurope (www.plasticseurope.org). Open and use containers only in well-ventilated areas using local exhaust ventilation (LEV). Vapors and fumes liberated during hot processing of Teflon™ PFA C-980 should be exhausted completely from the work area. Contamination of tobacco with these polymers must be avoided. Vapors and fumes liberated during hot processing that are not properly exhausted, or from smoking tobacco or cigarettes contaminated with Teflon™ PFA C-980, may cause flu-like symptoms, such as chills, fever, and sore throat. This may not occur until several hours after exposure and will typically pass within about 24 hours. Mixtures with some finely divided metals, such as magnesium or aluminum, can be flammable or explosive under some conditions.

Storage and Handling

The properties of Teflon™ PFA C-980 resins are not affected by storage time. Ambient storage conditions should be designed to avoid airborne contamination and water condensation on the resin when it is removed from containers. Drying at 100 °C (212 °F) for 4 hours is suggested to remove any absorbed moisture.

Packaging

Teflon™ PFA C-980 is supplied as pellets and is packaged in 45.4-kg drums with a polyethylene inner lining.

Chemours™

Table 1: Typical Property Data for Teflon™ PFA C-980 Fluoroplastic Resin

Property	Test Method[1]		Unit	Typical Value
General				
Melt Flow Rate at 372 °C (702 °F)/5.0 kg weight	ISO 12086	D 3307	g/10 min	3.0
Melting Point	—	D 4591	°C	284
Specific Gravity	—	D 792	—	2.15
Critical Shear Rate, 372 °C (702 °F)	—	—	1/s	12
Mechanical				
Tensile Strength	ISO 12086	D 3307	MPa (psi)	36 (5,200)
Elongation	ISO 12086	D 3307	%	300
Flexural Modulus, 23 °C (73 °F)	ISO 178	D 790	MPa (psi)	700 (101,500)
MIT Folding Endurance	—	D 2176	Cycles	80,000
Electrical				
Volume Resistivity[2]	ISO 3915	—	Ohm-m	0.10
Other				
Water Absorption, 24 hr	—	D 570	%	<0.03
Weather and Chemical Resistance	—	—	—	Excellent

Typical properties are not suitable for specification purposes.
[1] ASTM unless otherwise specified.
[2] Volume Resistivity as measured on compression molded plaques. Resistivity is very sensitive to processing technique and conditions. Injection molded plaques are typically higher.

HOW TO USE THE TEFLON™ BRAND NAME WITH YOUR PRODUCT

Teflon™ is a registered trademark of Chemours for its brand of fluoroplastic resins, coatings, films, and dispersions. The Teflon™ brand name is licensed by Chemours in association with approved applications. Without a trademark license, customers may not identify their product with the Teflon™ brand name, as Chemours does not sell such offerings with the Teflon™ trademark. Unlicensed customers may refer to the Chemours product offering with only the Chemours name and product code number descriptor as Chemours sells its product offerings. There are no fair use rights or exhaustion of rights to use the Teflon™ trademark from buying from Chemours, a Chemours customer, or a distributor without a trademark license from Chemours.

If you are interested in applying for a trademark licensing agreement for the Teflon™ brand, please visit www.teflon.com/license

For more information, visit teflon.com/industrial
For sales and technical support contacts, visit teflon.com/industrialglobalsupport

Replaces: K-27853
C-10058 (7/15)

Appendix B

Data Manipulation

B.1 Near Infrared Spectroscopy

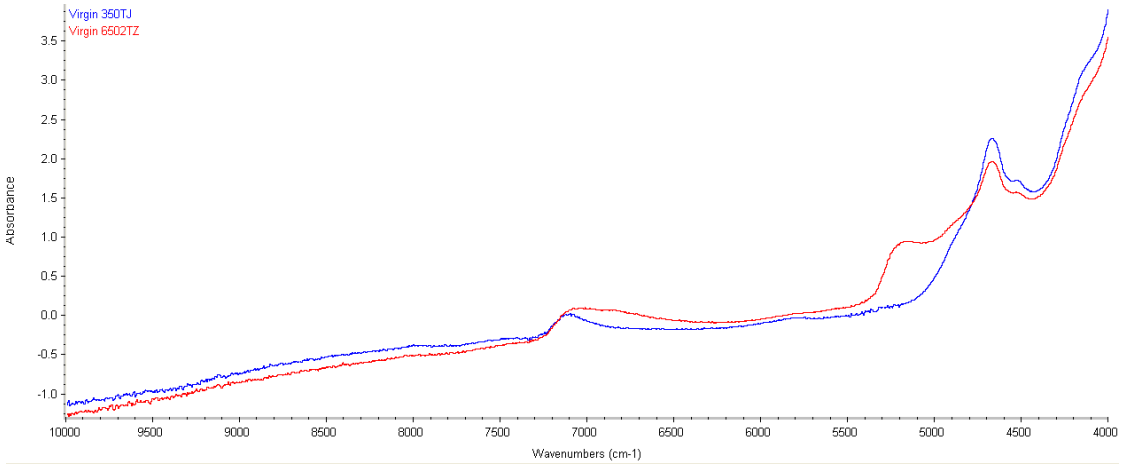

Figure B.1.1: Comparison of spectra obtained from the unprocessed virgin PFA material

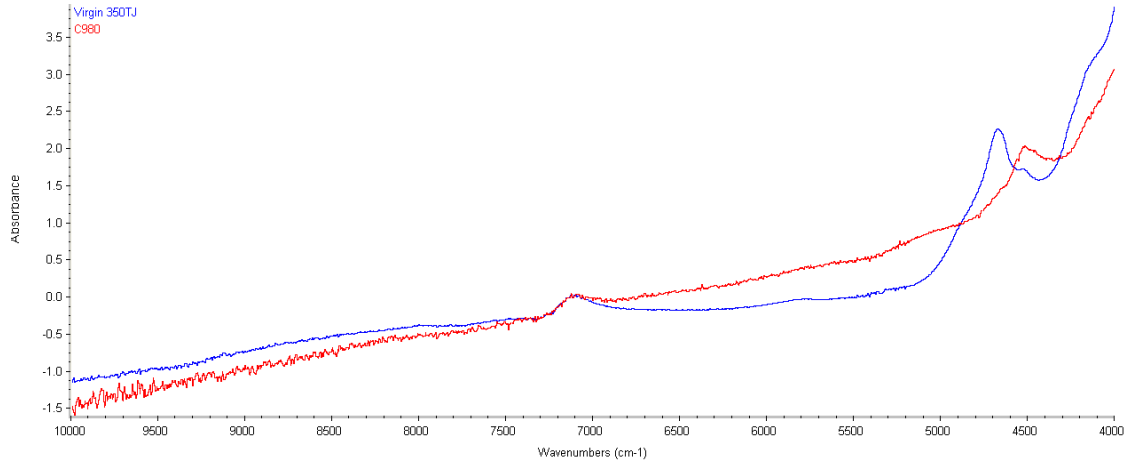

Figure B.1.2: Comparison of spectra obtained from unprocessed 350TJ to C980

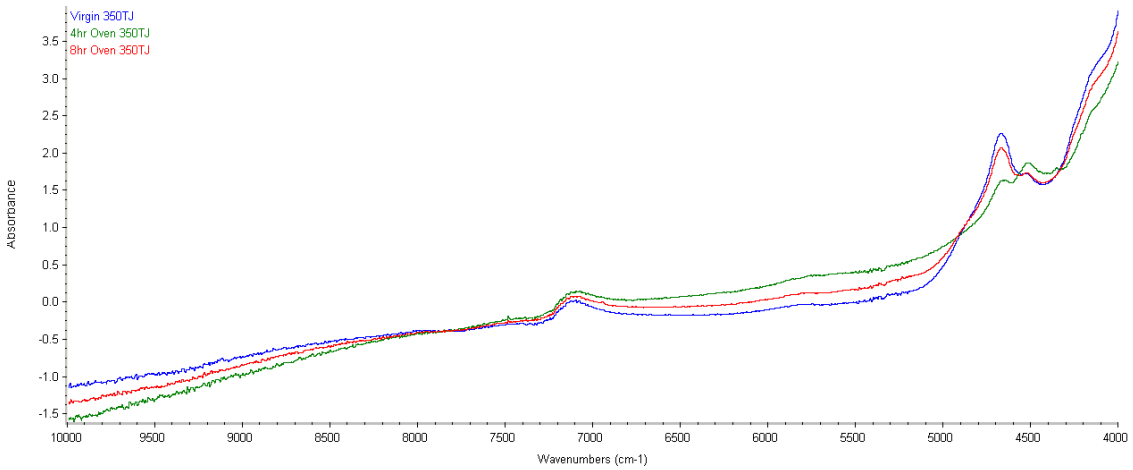

Figure B.1.3: Comparison of spectra obtained from the samples of 350TJ exposed to various residence times

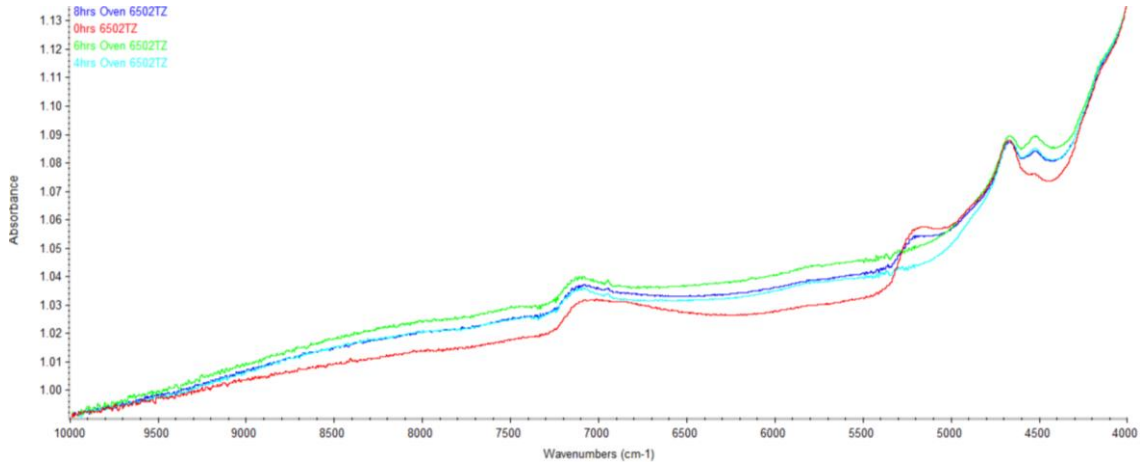

Figure B.1.4: Comparison of spectra obtained from the samples of 6502TZ exposed to various residence times

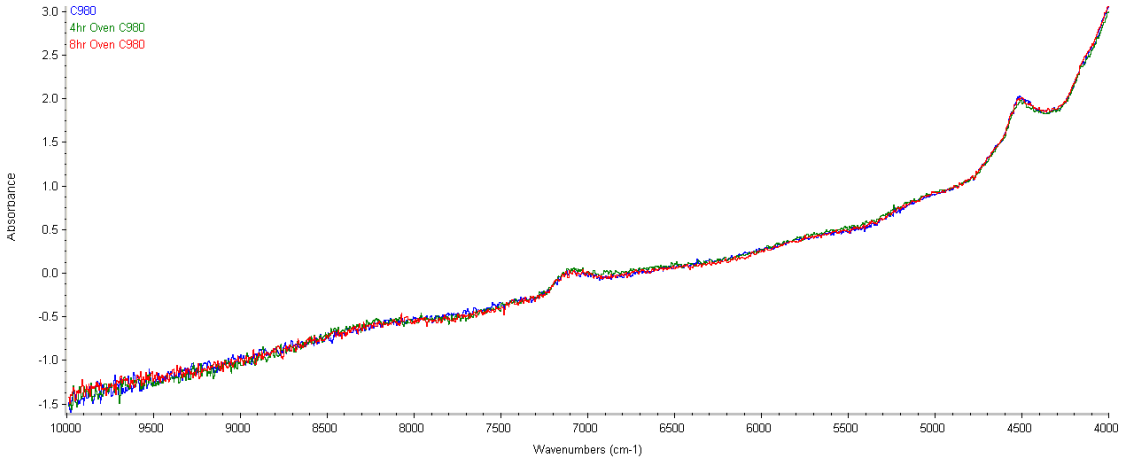

Figure B.1.5: Comparison of spectra obtained from the samples of C980 exposed to various residence times

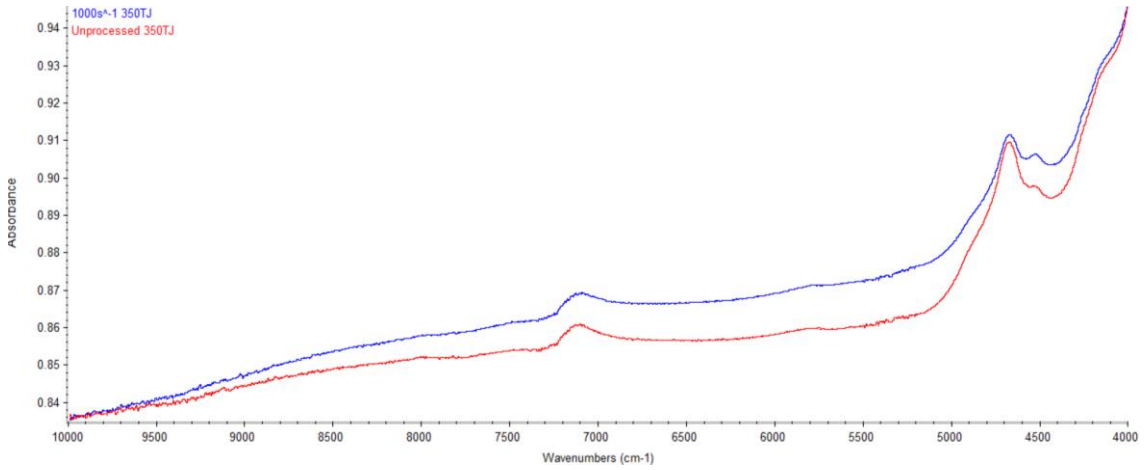

Figure B.1.6: Comparison of spectra obtained from unprocessed 350TJ and the material subjected to $1000s^{-1}$

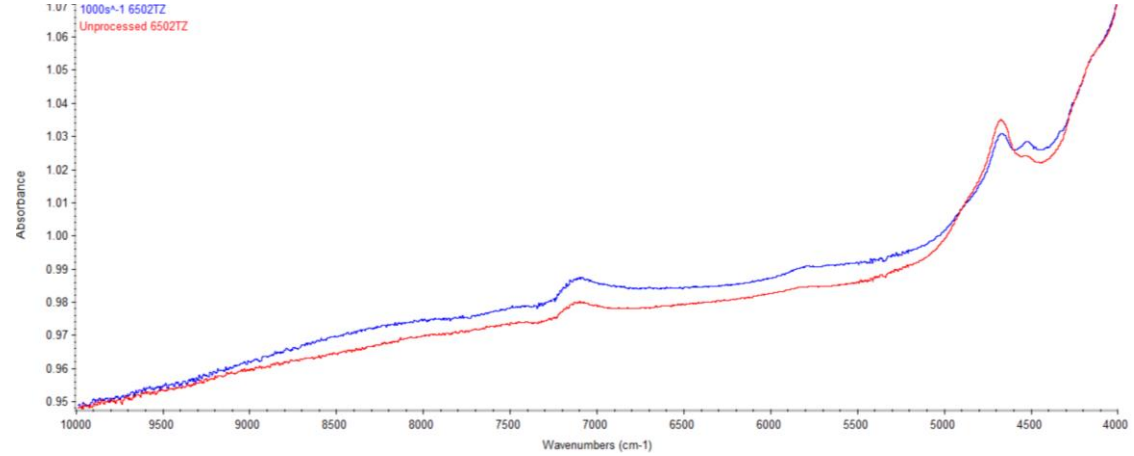

Figure B.1.7: Comparison of spectra obtained from unprocessed 6502TZ and the material subjected to $1000s^{-1}$

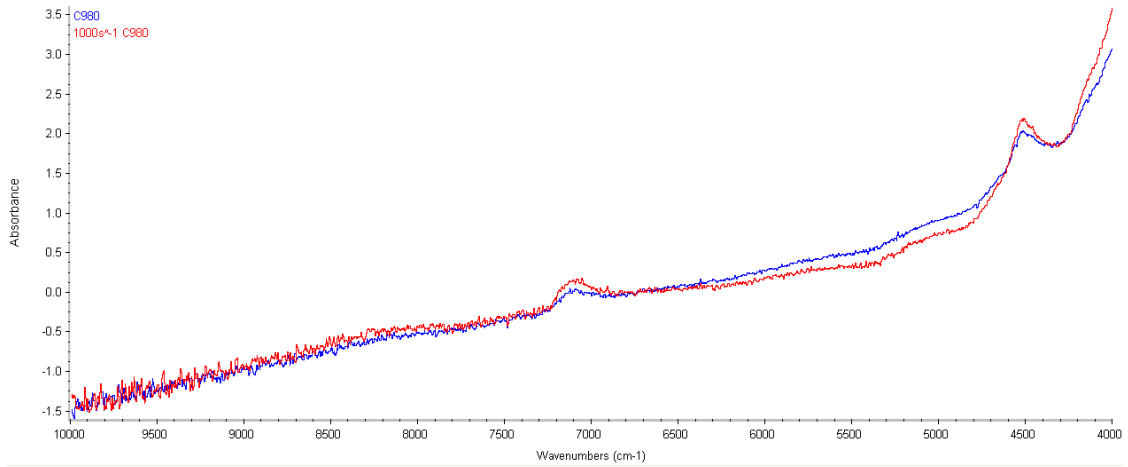

Figure B.1.8: Comparison of spectra obtained from unprocessed C980 and the material subjected to $1000s^{-1}$

Partial Least Squares (PLS) determines the differences in the intensity and wavelength of spectra and matches them to the specified component(s). PLS can quantify sample components when the correlation is complex due to various changes in the material.

In the TQ Analyst software classes were assigned to the spectra obtained from the different samples based on length of time at processing temperature or exposure to shear rate. The five spectra of each sample type were added as standards and labelled with the class to enable the software to calibrate the samples by looking at the differences in the spectra. The changes in the spectra were not always linear (as shown in Figures B.1.1 to B.1.8 above) so the second derivative of the spectra was used to enable the software to better model the relationships (an example of which is shown below in Figure B.1.9). The software was used to help determine the regions of interest, however with these materials the whole range of the spectrum was investigated.

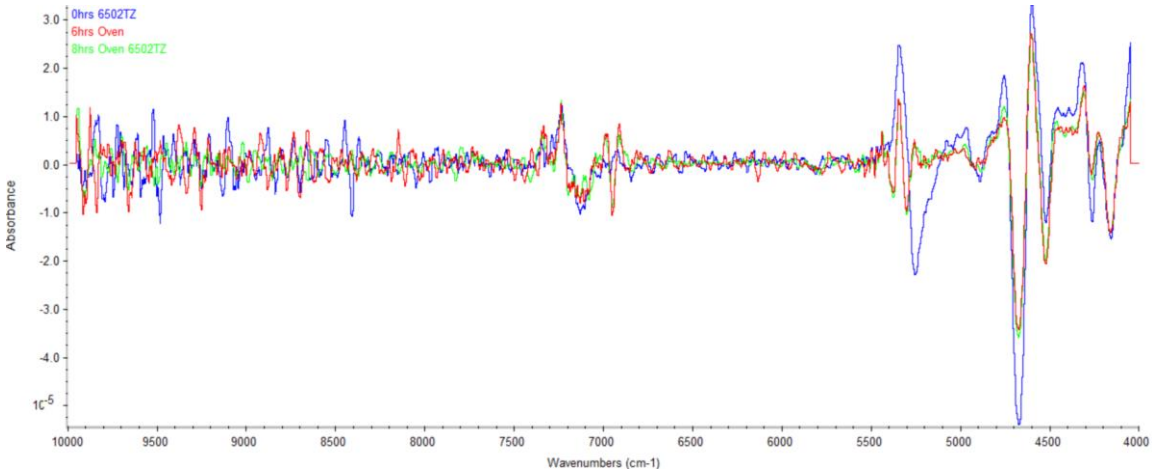

Figure B.1.9: Comparison of the second derivative of the spectra from the samples of 6502TZ exposed to various residence times

Partial Least Squares regression shows how well the standards are represented by determining the correlation between the value of the component assigned to the standard (actual value) and the value the software calculates (calculated value). A graph is generated showing the correlation, where the better the correlation the closer the correlation coefficient is to 1.

Principal components representing an independent source of variation in the spectra are determined using relevant parts of the spectra. Principal Component Scores show how well the standards used in PLS are represented

by the component that was used to calibrate the method. Principal Components Scores highlight trends in the data and represent the distance of a standard projected onto a principal components. Principal components are listed in order of the variance they represent, so the first one describes most of the common information in the data. Principal Component Scores 1 and 2 are plotted on a graph and show the “distance” between each standard.

B.2 Capillary Rheometry

The Yasuda Carreau model parameters were obtained using the Solver function in Microsoft Excel using the following equation:

$$\eta = \frac{\eta_0}{[1-(\lambda\dot{\gamma})^a]^{\frac{1-n}{a}}}$$

Where η_0 is the viscosity in at zero shear rate in Pa.s, λ is the relaxation time in s, n is the power law index, and a signifies the width of the transition from $0s^{-1}$ and the start of the power-law region.

The formula is inputted into the spreadsheet referencing cells containing the model parameters. The Solver function can then be set to minimise the sum of the squares of the errors between the viscosity data and the values predicted by the model.

The shear stress, shear rate and viscosity have been obtained from the raw pressure and piston speed data as follows.

The pressure data was plotted against time, with the pressure at each shear rate calculated by averaging the pressure readings once they had stabilised, as shown below with the vertical line annotations in Figure B.2.1.

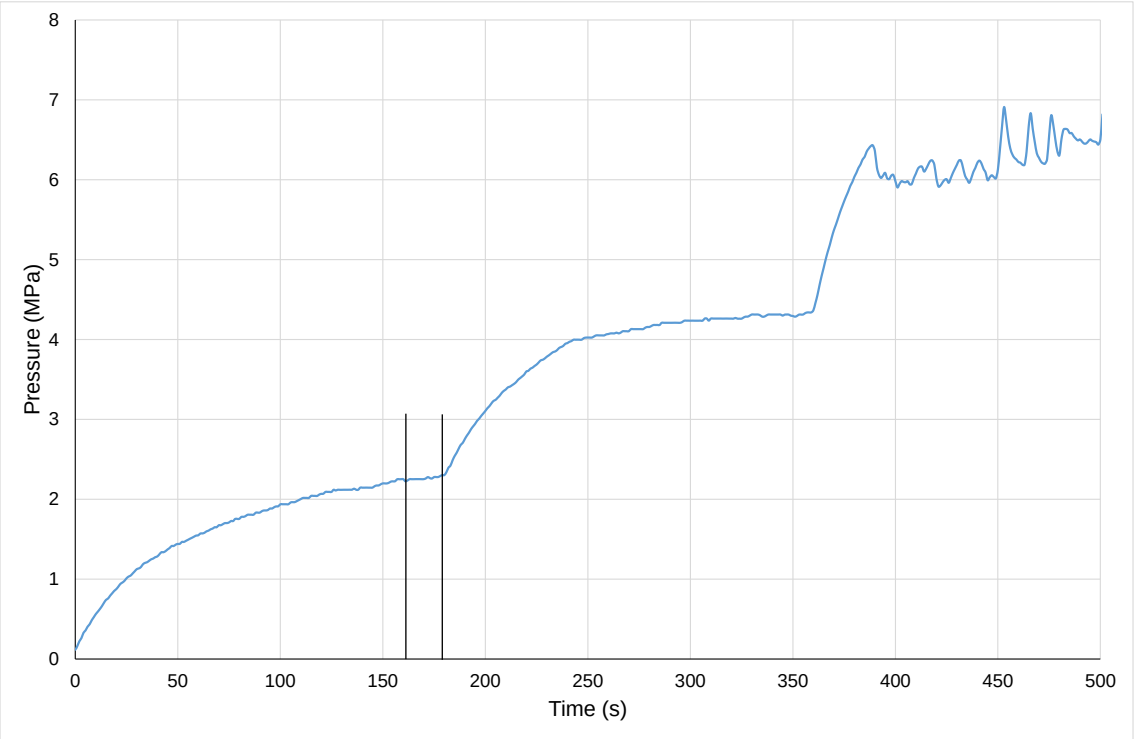

Figure B.2.1: Graph showing the raw pressure data generated during an eight step increasing shear test

The scale of the x axis of the graph was reduced to help identify the regions for calculating the average pressure, as the pressure took a shorter time to stabilise at higher shear rates (see Figure B.2.2 below). The timings entered in the blockprogramming software were used to judge the regions the average pressure should be calculated over as the instabilities made it difficult to identify them visually.

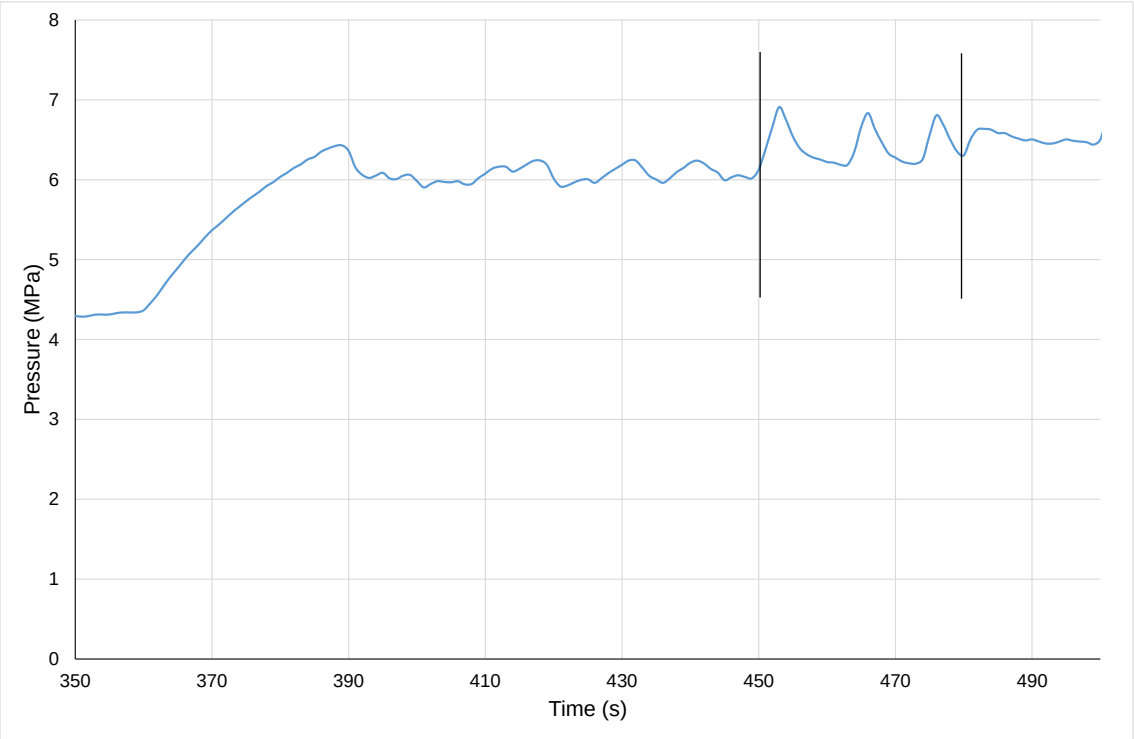

Figure B.2.2: Graph showing the raw pressure data generated during an eight step increasing shear test with a reduced scale on the x axis

Time	Pressure	Average Pressure	
Seconds	MPa	Formula	MPa
451	6.379719	=AVERAGE(E1207:E1236)	6.43143
452	6.660336		
453	6.908547		
454	6.747209		
455	6.541056		
456	6.394887		
457	6.319735		
458	6.275608		
459	6.252855		
460	6.22114		
461	6.212176		
462	6.185976		

463	6.185976		
464	6.352829		
465	6.660336		
466	6.832704		
467	6.634825		
468	6.469351		
469	6.328008		
470	6.276298		
471	6.226655		
472	6.204592		
473	6.200455		
474	6.256992		
475	6.556225		
476	6.805125		
477	6.687915		
478	6.505204		
479	6.355587		
480	6.304566		

Table B.2.1: Values of pressure corresponding the annotated section of the graph shown in Figure B.2.2

The Bagley correction was applied by taking the average pressure readings at each shear rate obtained from the short die away from the reading found using the long die (see example below).

$$\Delta P = (\Delta P_L - \Delta P_O)$$

Where ΔP_L is the long die pressure drop and ΔP_O is the orifice die pressure drop.

$$\Delta P = (6.034 - 0.240)$$

$$\Delta P = 5.794 \text{ MPa}$$

This was converted to a shear stress using the equation below:

$$\text{Wall Shear Stress, } \tau = \frac{R\Delta P}{2L}$$

where R and L are the radius and length of the capillary of the die, for example:

$$\tau = \frac{0.001 \times 5.794 \times 10^{6}}{2 \times 0.016}$$

$$\tau = 0.181 \text{MPa}$$

The shear rate was calculated the equation:

$$\text{Wall Shear Strain Rate, } \dot{\gamma} = \frac{4Q}{\pi R^{3}}$$

Where Q is the volumetric flow rate and is given by:

$$Q = AV$$

Where A is the cross sectional area of the capillary of the rheometer and V is the speed of the piston, for example with a piston speed of 4.67mm/min the flow rate is:

$$Q = \pi \times 0.0075^{2} \times \frac{4.67}{1000 \times 60}$$

$$Q = 1.38 \times 10^{-8} m^{3}/s$$

Which gives a shear rate of:

$$\dot{\gamma} = \frac{4 \times 1.38 \times 10^{-8}}{\pi \times 0.001^{3}}$$

$$\dot{\gamma} = 17.5 s^{-1}$$

The shear stress and shear rate enable the viscosity to be calculated using:

$$\text{Shear Viscosity, } \eta = \frac{\text{Shear Stress, } \tau}{\text{Shear Strain Rate, } \dot{\gamma}}$$

The viscosity using values generated in the examples above is as follows:

$$\eta = \frac{0.181 \times 10^6}{17.5}$$

$$\eta = 10339 \text{ Pa.s}$$

The viscosity and associated error have been generated at each shear rate using the mean and standard deviation of the three tests conducted under each set of conditions.

B.3 Differential Scanning Calorimetry

The values of enthalpy were determined as follows. The intersection of the gradients of the various sections of the curve were used to provide a baseline, as shown below in Figure B.3.1.

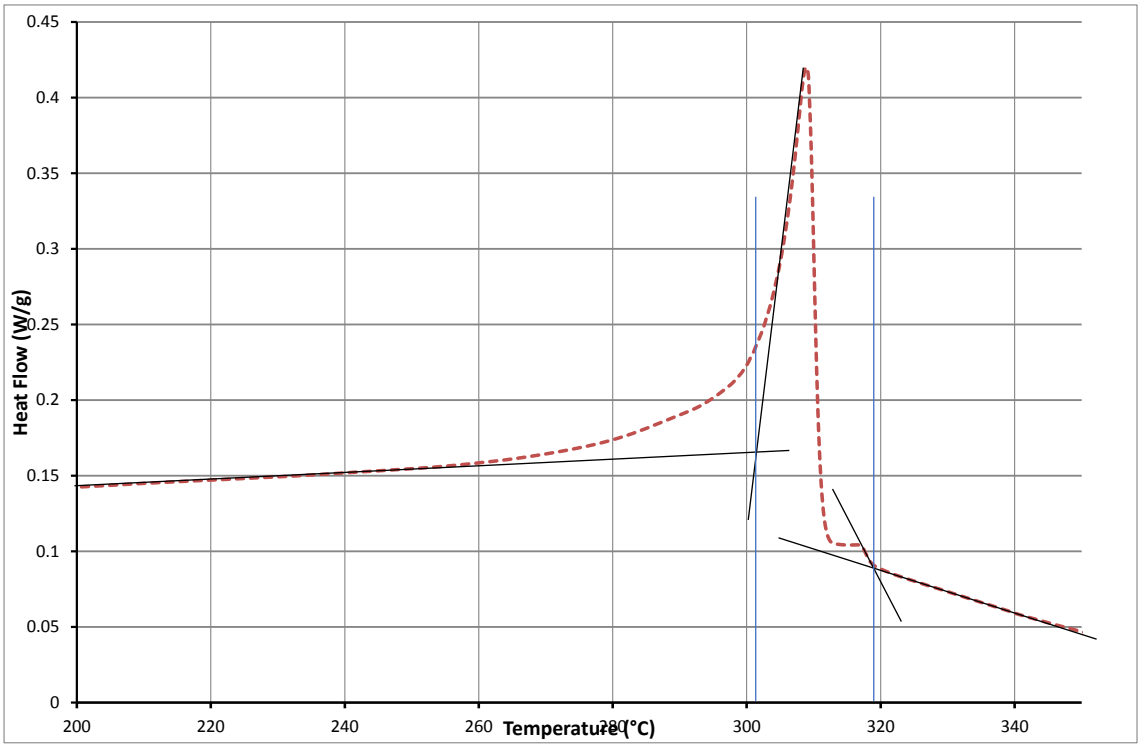

Figure B.3.1: Graph of the second heat of unprocessed virgin PFA with annotations showing the intersections of the gradients

Microsoft Excel does not have a function to enable the determination of areas under curves so the trapezium rule was used with each section calculated using the adjacent data points to give the largest number of sections possible with the limits determined by the intersection of the gradients as shown above. The sum of all the sections gives the whole area under the curve (A+B+C in Figure B.3.2 below), so the area under the baseline (A+B) was calculated and taken from the

total to leave the section of interest (C). This was converted into the enthalpy by dividing by the heating rate (in °C/s).

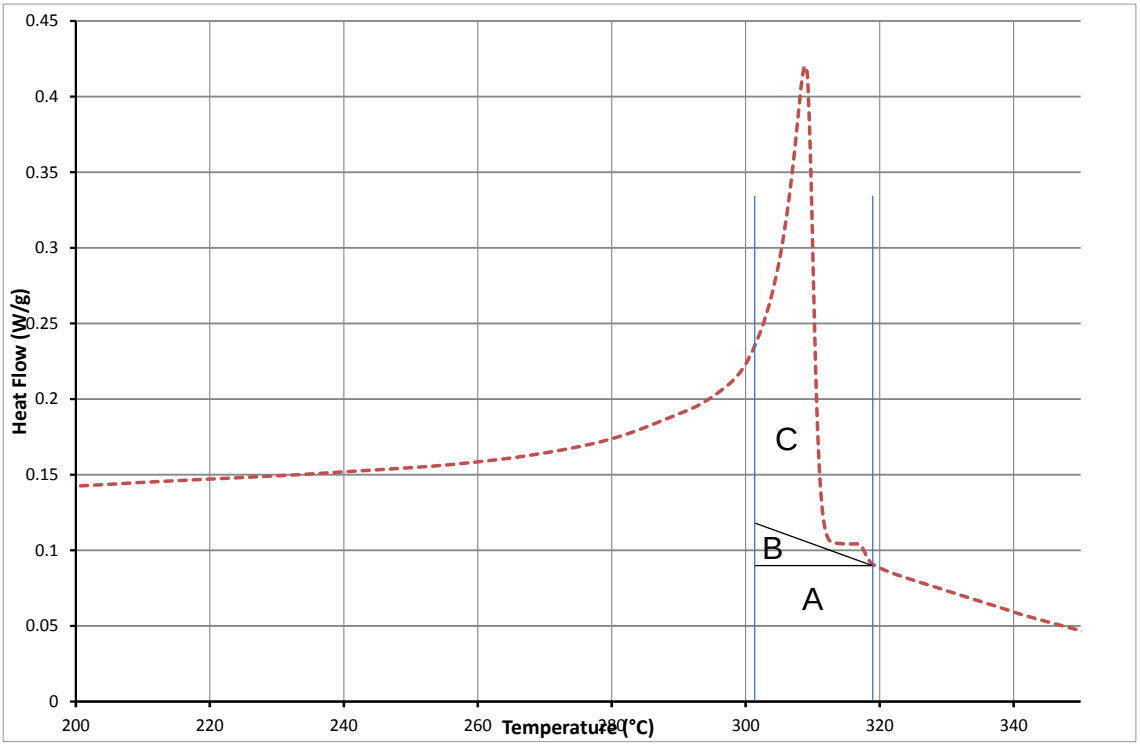

Figure B.3.2: Graph of the second heat of unprocessed virgin PFA with annotations showing the areas of the curve

The follows graphs in Figures B.3.3 to B.3.5 show the heat/cool/heat data where there have been notable changes worthy of further investigation.

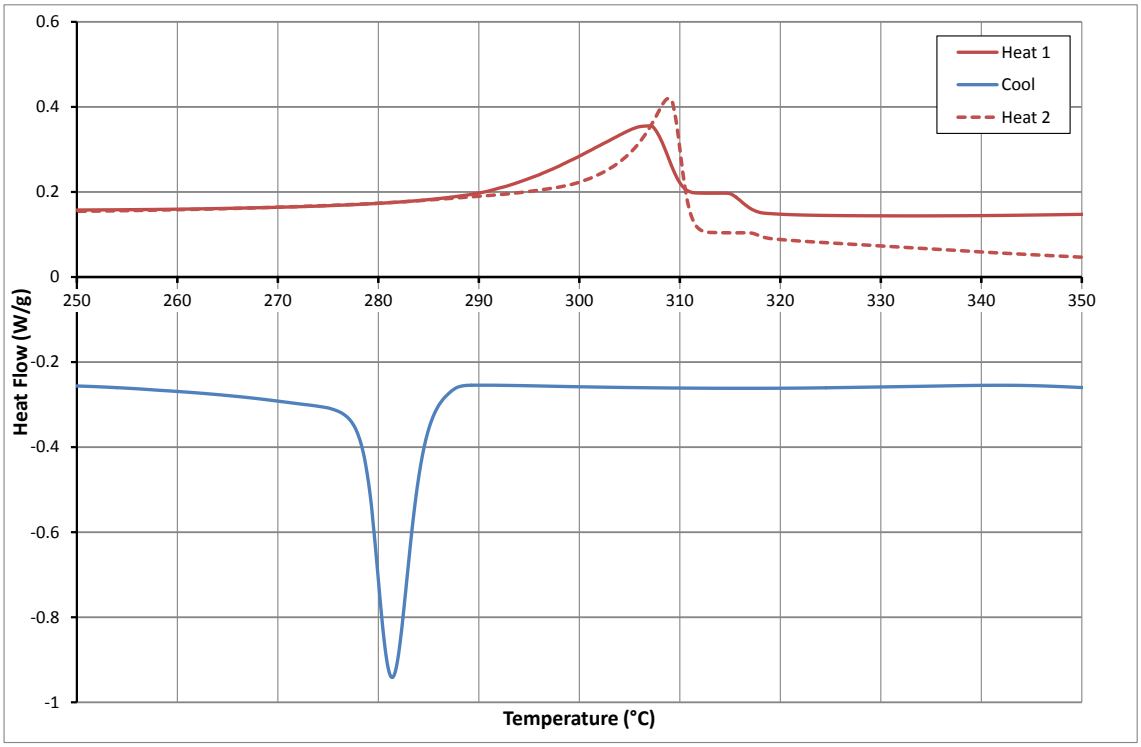

Figure B.3.3: Graph showing heat/cool/heat curves of unprocessed 350TJ PFA

The broad peak in the first heating curve shows there is a wide distribution of crystal sizes. The lower melt temperature of the material during its first heating shows the material is more amorphous, so is likely to have been cooled faster during manufacture than 10°C/min as this is the cooling rate used in the DSC run.

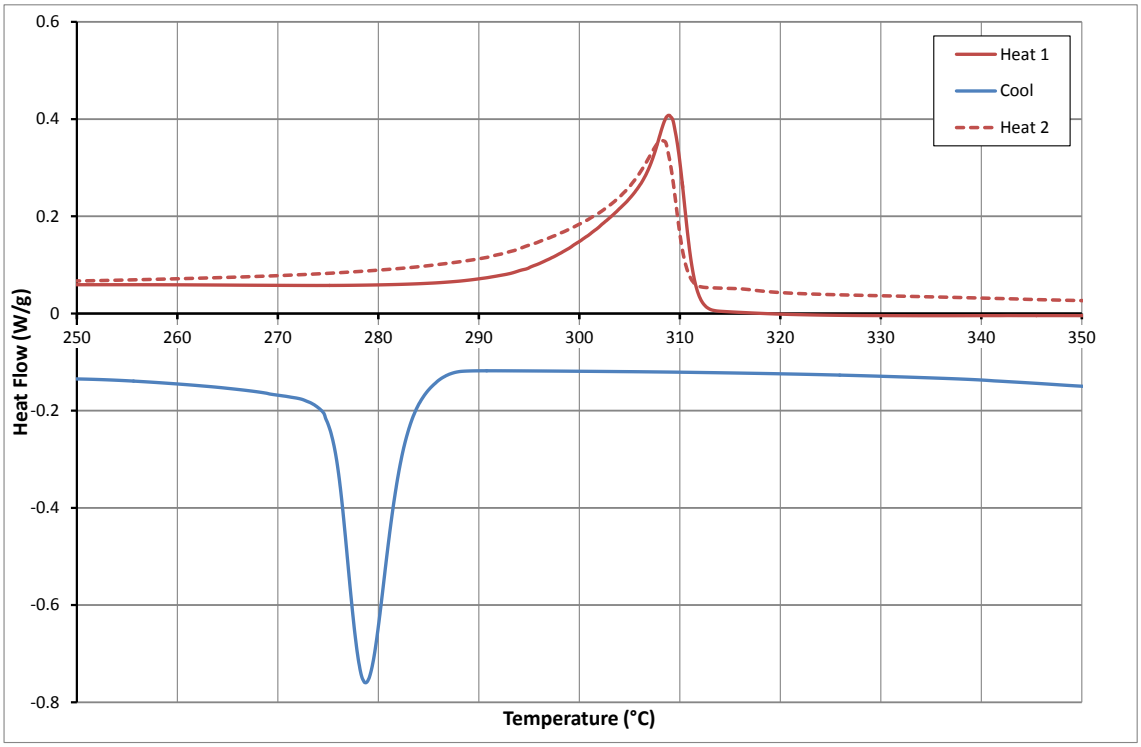

Figure B.3.4: Graph showing heat/cool/heat curves of 350TJ exposed to 8hrs at processing temperature

The width of the crystallisation peak of the 350TJ material aged for 8hrs is similar to that of the unprocessed PFA showing the crystalline size distribution has not changed much. However there has been a significant drop in the crystallisation temperature showing the crystallisation process has been able to continue for longer, possibly due to a change in the polymer morphology. There has been a slight decrease in the melt temperature of the polymer during the second heat compared to the first, whereas the unprocessed polymer showed a marked increase.

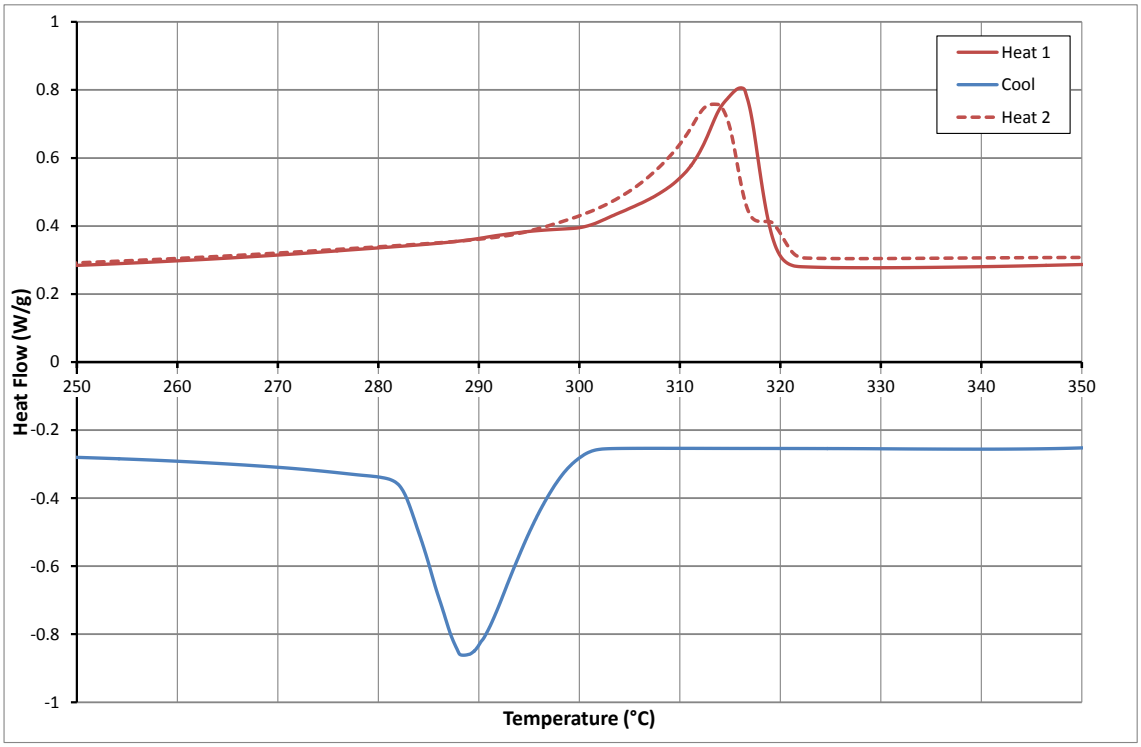

Figure B.3.5: Graph showing heat/cool/heat curves of severely damaged PFA

The second heating curve of the severely damaged PFA shows a decrease in the melt temperature compared to the first heat, however it remains significantly above that of the unprocessed polymer. The crystallisation peak is much broader than that of the unprocessed PFA, reflecting the broader distribution of crystal sizes. The crystallisation temperature of the severely damaged material is significantly higher than that of the unprocessed or the 8hr aged material, suggesting changes in polymer morphology that have led to a shorter crystallisation process.

B.4 Tensile Properties

The yield point on the stress strain curves of the samples was not well defined so the yield strength was taken as the stress at which the material begins to deviate from Hookean behaviour, whilst the modulus was calculated using the gradient of the linear region of the curve. Practically this was achieved by enlarging the linear section of the stress strain curve in Microsoft Excel and using a straight line to identify the points at which the data began to deviate (see Figure B.4.1 below).

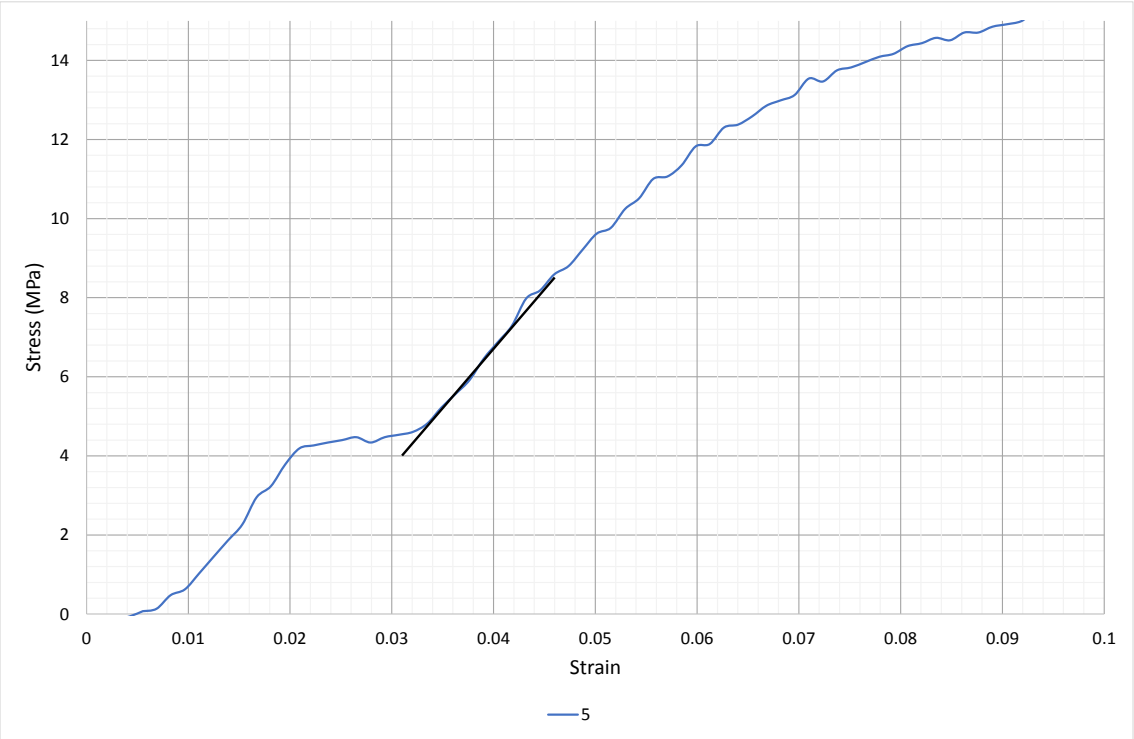

Figure B.4.1 Stress vs. strain data for one of the unprocessed virgin PFA samples

The limits of linearity in this example provided a yield strength of 7.98MPa, whilst the calculation to determine the modulus of 345MPa is shown below:

$$\text{Modulus (MPa)} = \frac{\text{Tensile Stress}}{\text{Tensile Strain}}$$

$$= \frac{7.98 - 5.22}{0.043 - 0.035}$$

$$= \frac{2.76}{0.008}$$

Appendix C

Fourier Transform Infrared Spectroscopy

C.1 Effect of Residence Time

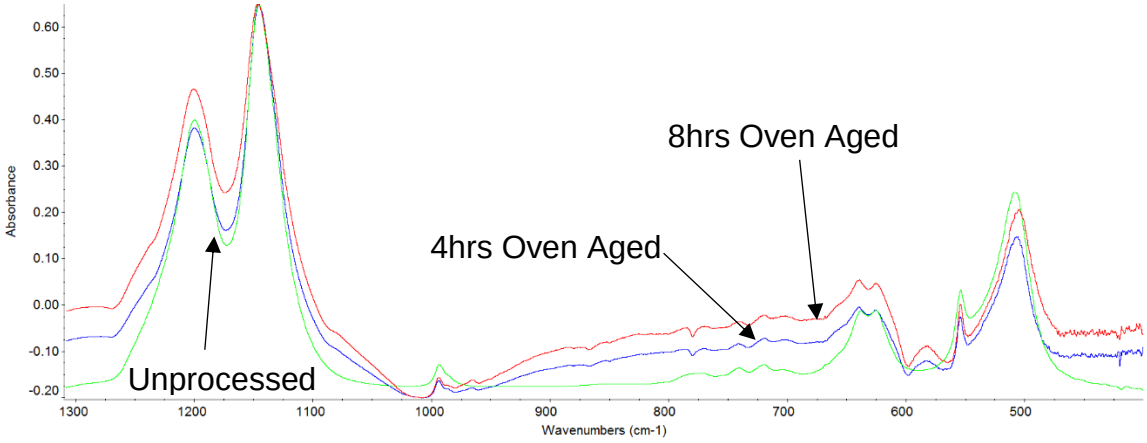

Figure C.1.1: Comparison of spectra obtained from the samples of 350TJ exposed to various residence times

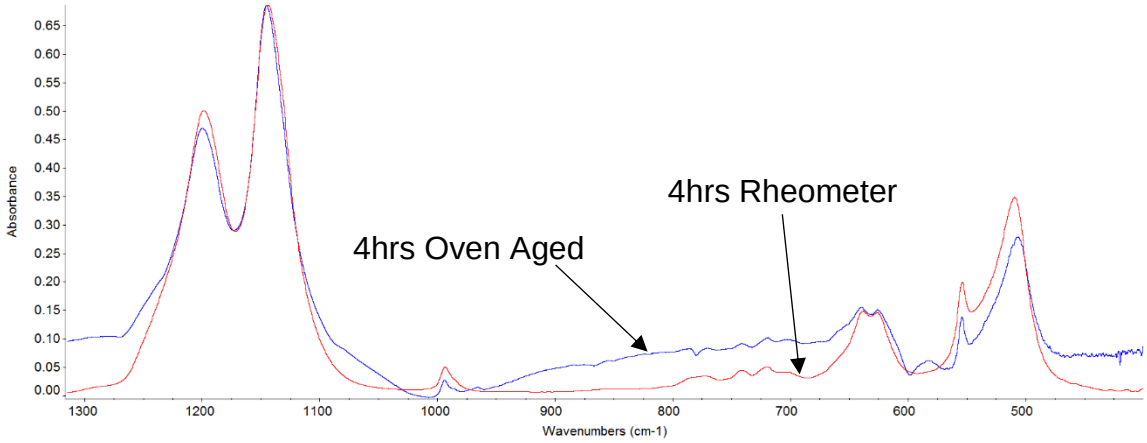

Figure C.1.2: Spectra obtained from the samples of 350TJ heat aged for 4hrs in the rheometer compared to the sample held in the oven

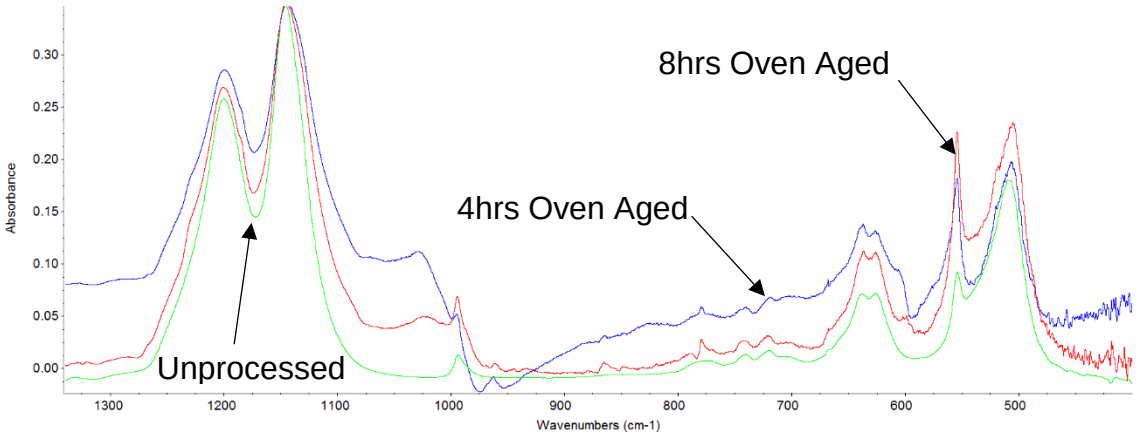

Figure C.1.3: Comparison of spectra obtained from the samples of 6502TZ exposed to various residence times

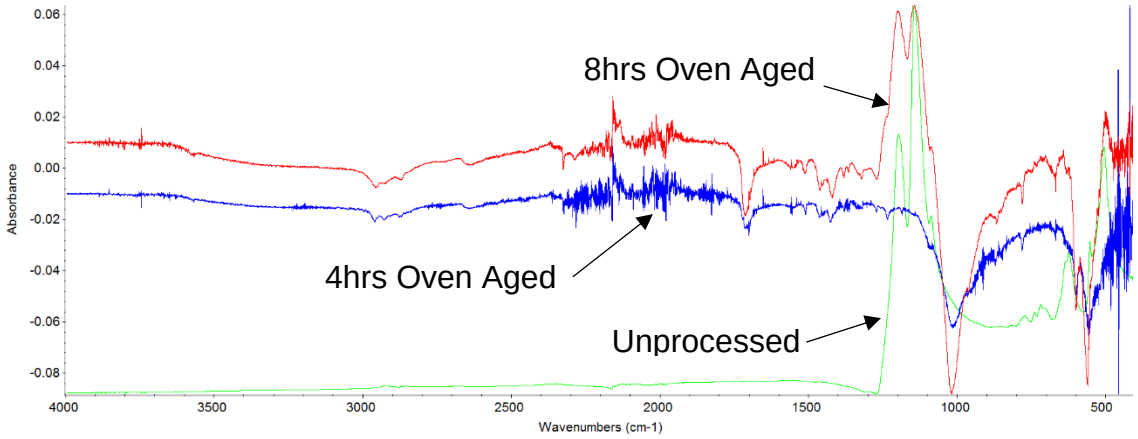

Figure C.1.4: Comparison of spectra obtained from the samples of C980 exposed to various residence times

	Unprocessed	4hrs Oven	4hrs Rheometer	8hrs
350TJ	1200.38	1200.03	1199.18	1200.33
	1146.25	1145.36	1144.71	1146.48
	993.70	-	993.82	-
	722.22	-	-	-
	639.30	639.73	638.38	639.14
	625.80	627.24	627.73	625.80
	553.96	554.24	554.02	554.20
	507.84	506.90	509.53	505.04
6502TZ	1200.51	1199.25	-	1200.41
	1146.51	1144.17	-	1145.33
	993.75	-	-	994.46
	639.30	637.02	-	636.93
	626.00	626.76	-	628.09
	554.06	554.51	-	552.99
	508.72	506.03	-	505.08
C980	1196.99	-	-	1197.68
	1143.28	-	-	1144.92
	718.33	-	-	-
	623.78	-	-	-
	552.99	-	-	-
	506.08	-	-	-

Table C.1.1: Wavenumbers of the peaks in the spectra of the PFA samples

The peak around 508cm^{-1} decreases with residence time for the virgin PFA samples, except for the 350TJ aged for 4hrs in the rheometer. The peak at approximately 626 cm^{-1} increases with residence time for the virgin polymers, however the 350TJ aged for 8hrs remains unchanged. The peak around 639 cm^{-1} decreases with residence time, apart from the 4hr oven aged 350TJ which increases. A decrease in the peak at 1146cm^{-1} is seen with residence time, but the wavenumber of the sample of 350TJ held for 8hrs in the oven increases. There is no clear trend from in the behaviour of the peak at approximately

1200cm^{-1}. Overall the changes seen do not form a coherent trend from which to base a conclusion. Figure C.1.4 shows the method is unsuitable for investigation of samples of C980.

C.2 Effect of Shear

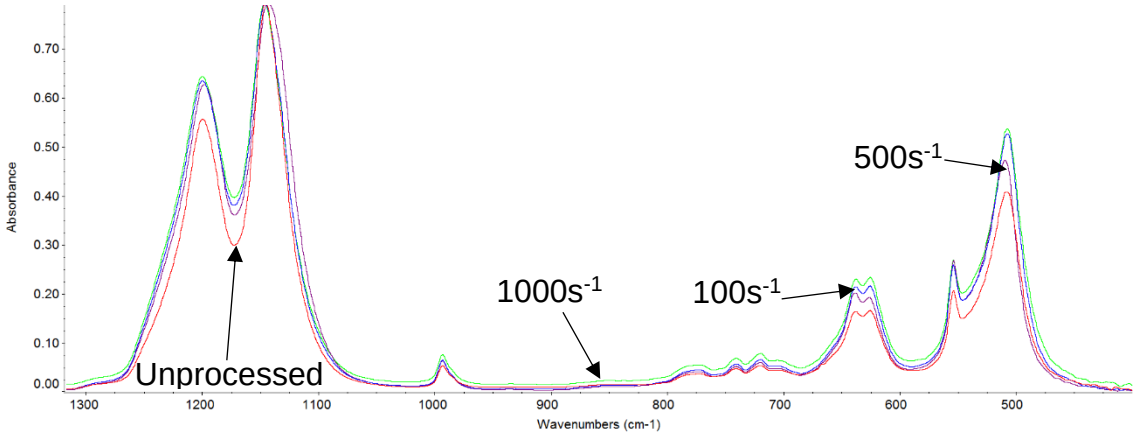

Figure C.2.1: Comparison of spectra obtained from unprocessed 350TJ and the samples exposed to various shear rates

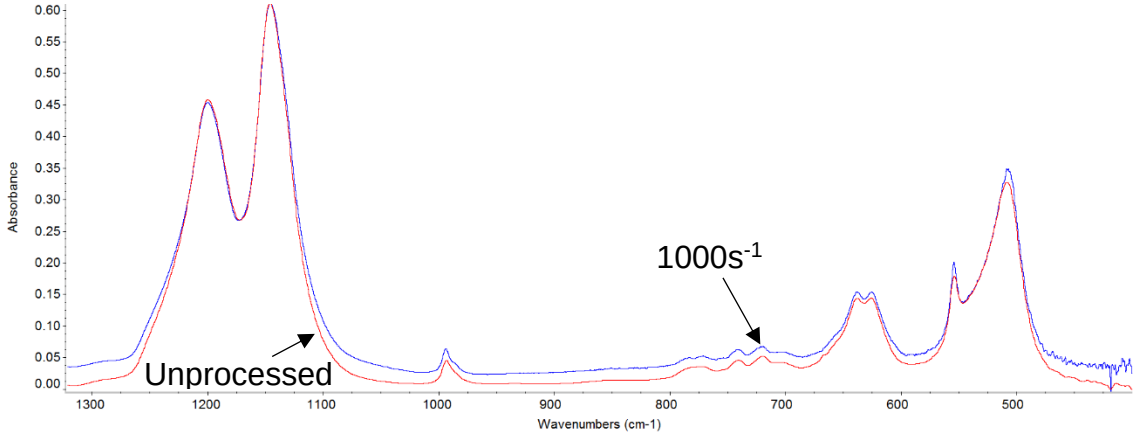

Figure C.2.2: Comparison of spectra obtained from unprocessed 6502TZ and the material subjected to 1000s^{-1}

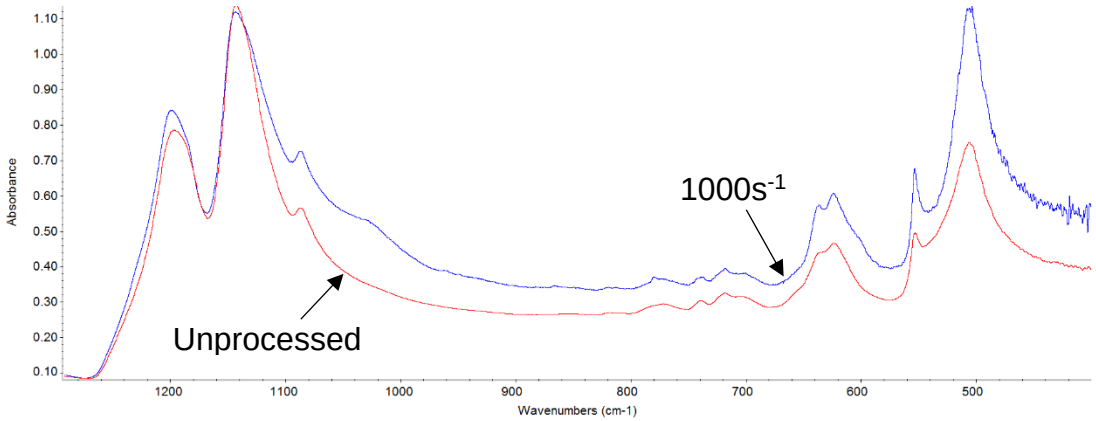

Figure C.2.3: Comparison of spectra obtained from unprocessed C980 and the material subjected to $1000s^{-1}$

	Unprocessed	**$100s^{-1}$**	**$500s^{-1}$**	**$1000s^{-1}$**
350TJ	1200.38	1200.45	1198.88	1200.69
	1146.25	1146.71	1143.50	1147.07
	993.70	993.82	993.82	993.83
	722.22	719.92	721.26	719.91
	639.30	639.30	638.71	638.33
	625.80	625.79	625.80	625.65
	553.96	553.98	553.84	553.99
	507.84	507.31	509.67	507.32
6502TZ	1200.51	-	-	1200.28
	1146.51	-	-	1145.74
	993.75	-	-	994.00
	639.30	-	-	638.19
	626.00	-	-	626.04
	554.06	-	-	554.31
C980	1196.99	-	-	1199.12
	1143.28	-	-	1143.52
	718.33	-	-	718.15
	623.78	-	-	624.00
	552.99	-	-	553.45
	506.08	-	-	503.75

Table C.2.1: Wavenumbers of the peaks in the spectra of the PFA samples

The peak around 508cm^{-1} increases for the sample of 350TJ exposed to 500s^{-1} and decreases for the sample of C980 exposed to 1000s^{-1}. The peak around 553cm^{-1} increases for the sample of C980 exposed to 1000s^{-1}, but remains the same for virgin PFA. The peak around 1146cm^{-1} decreases with shearing for 6502TZ and the sample of 350TJ exposed to 500s^{-1}. There is a significant increase in the peak at 1200cm^{-1} for sheared C980 material, and a decrease for the 350TJ subjected to 500s^{-1}.

C.3 Effect of Processing

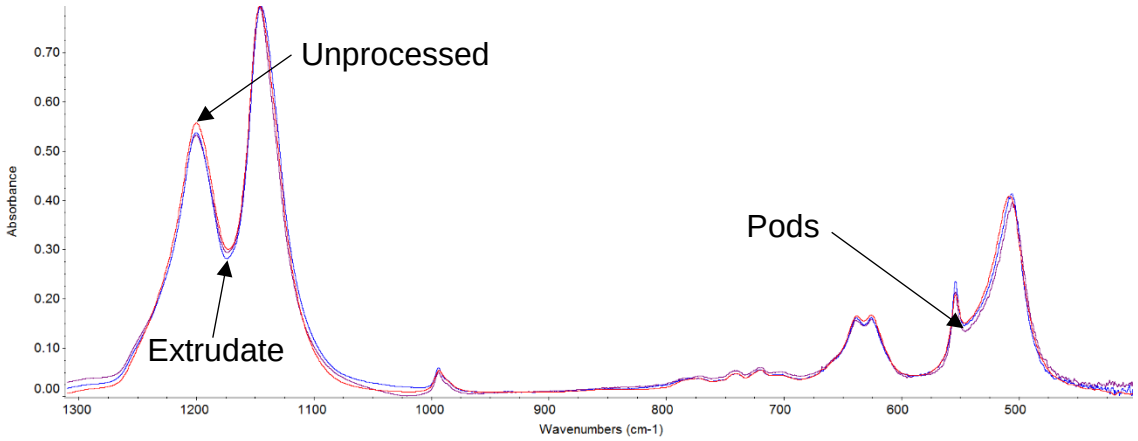

Figure C.3.1: Comparison of spectra obtained from unprocessed 350TJ and the samples exposed to transfer moulding conditions

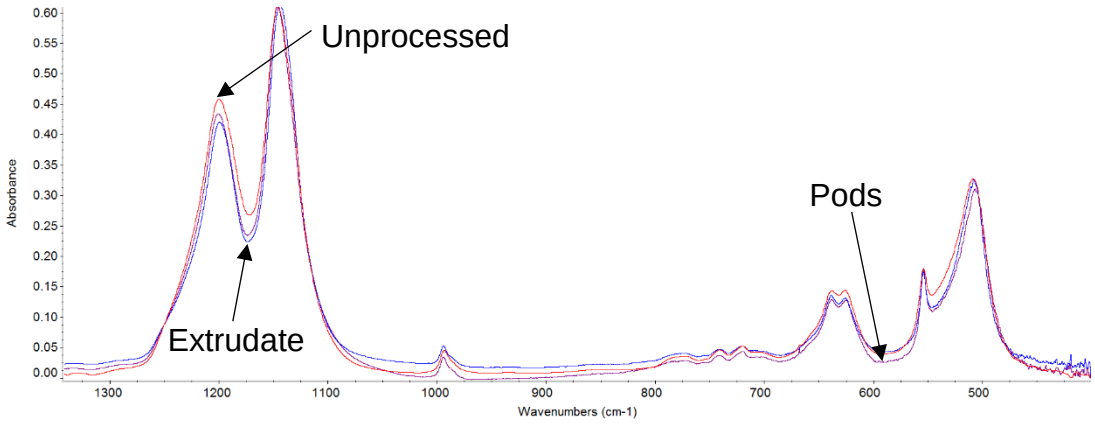

Figure C.3.2: Comparison of spectra obtained from unprocessed 6502TZ and the samples exposed to transfer moulding conditions

	Unprocessed	Extrudate	Pods
350TJ	1200.38	1200.31	1200.17
	1146.25	1145.24	1146.25
	993.70	994.11	994.12
	722.22	-	-
	639.30	639.90	639.54
	625.80	625.69	625.33
	553.96	554.16	554.23
	507.84	506.57	505.72
6502TZ	1200.51	1199.41	1200.39
	1146.51	1143.46	1146.3
	993.75	994.12	994.06
	639.30	638.78	638.34
	626.00	629.04	626.16
	554.06	554.23	554.10
	508.72	508.05	507.00

Table C.3.1: Wavenumbers of the peaks in the spectra of the PFA samples

The data shows a reduction in the wavenumber of the peak at 507cm^{-1} from unprocessed material to extrudate and pods for both the virgin materials. There is a reduction in the peak at 639cm^{-1} from unprocessed material to extrudate and pods for 6502TZ. The extrudate shows a decrease in the peak at 1146cm^{-1} for both materials. The peak at 1200cm^{-1} decreases for the 6502TZ extrudate, whilst the peak at 626cm^{-1} increases.

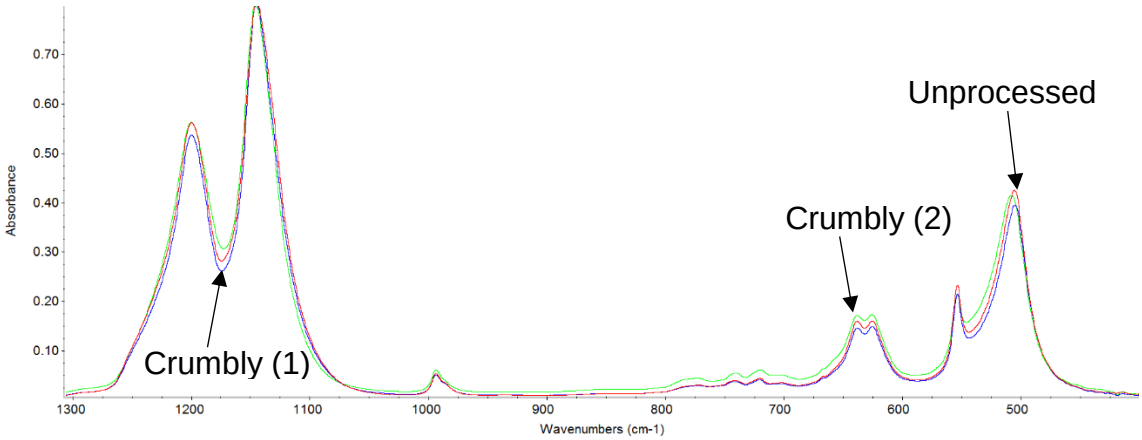

Figure C.3.3: Comparison of spectra obtained from unprocessed 350TJ and the severely damaged sample

Unprocessed	Crumbly (1)	Crumbly (2)
1200.38	1200.18	1200.11
1146.25	1145.45	1145.11
993.70	993.74	993.72
722.22	-	-
639.30	639.30	638.82
625.80	625.50	625.66
553.96	553.77	553.78
507.84	505.32	505.64

Table C.3.2: Wavenumbers of the peaks in the spectra of the PFA samples

The only significant change in the spectra of the damaged material was the shift of the peak at 507cm^{-1}.

C.4 Effect of Cooling Rate

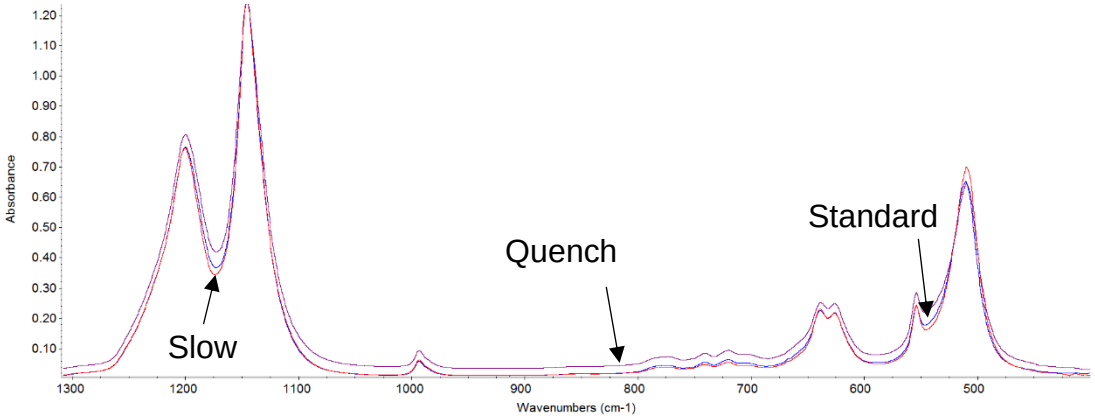

Figure C.4.1: Comparison of spectra obtained from the samples of 350TJ subjected to various cooling rates

Slow	Normal	Quench
1200.88	1200.61	1200.49
1146.2	1146.1	1146.19
993.69	993.70	993.69
639.01	638.92	638.48
553.78	553.85	553.84
509.52	510.27	509.62

Table C.4.1: Wavenumbers of the peaks in the spectra of the PFA samples

Other than slight reductions in the wavenumbers of the peaks at 1200cm^{-1} and 639cm^{-1} with an increase in the rate of cooling, there are no discernible changes in the peaks of the FTIR spectra of the samples subjected to different cooling rates.

Appendix D

5MPCA Melt Flow Rate Indexer Calibration Certificate

Calibration Certificate

RAY-RAN

COMPANY
CRP Ltd Todmorden Road Littleborough Lancaster OL15 9EG

RAY-RAN TEST EQUIPMENT LTD
Kelsey Close • Attleborough Fields Industrial Estate
Nuneaton • Warwickshire • CV11 6RS • United Kingdom
Tel : +44 (0)24 7634 2002 • Fax +44 (0)24 7664 1878
E-Mail : polytest@ray-ran.com
Web Site : http://www.ray-ran.com

CERTIFICATE	PAGE	DATE OF ISSUE	PURCHASE ORDER	IWO
6632	1 of 3	25/03/14	134024	S140314

ORDER CODE	PRODUCT	VOLTAGE	SERIAL NO
	Model 5MPCA Advanced Melt Flow System	220-240	**RR2900/035**

This certificate certifies that the equipment described has been calibrated in accordance with the required procedures and unless stated below conforms to **ISO 1133-1:2011.**

Equipment used to calibrate this apparatus is traceable in accordance with the companies **ISO 9001:2008** quality management system using UKAS calibrated measuring equipment.

0 – 1" Digital Micrometer	**UKAS Certificate Number : 1331360001**
2.0 – 2.5mm Internal Micrometer	**UKAS Certificate Number : 1331360003**
0.35 – 0.425" Internal Micrometer	**UKAS Certificate Number : 1331360004**
TTI6 True Temperature Indicator	**UKAS Certificate Number : 1079970001**
Pico Temperature Calibrator	**Certificate Number : 9729**
Measuring Slip Gauges	**UKAS Certificate Number : 1331360002**
Roughness Comparison Gauge	**SPI Model No : 30-695-1 (By Comparison)**

CALIBRATED BY	SIGNATURE
K MCWATT	

RAY-RAN TEST EQUIPMENT LTD

Microprocessor Serial No	Temperature Controller Serial No.
T990803	N / A

Cylinder				
Item Calibrated			Value	Actual
Length			115mm – 180mm	**162.61**
Item Calibrated			Tolerance	Value
Roughness by Comparison			≤ 0.25µm	0.05
Bore (mm)	Tolerance	Top	Middle	Bottom
9.550	± 0.007	**9.5542**	**9.5555**	**9.5524**

Standard Test Die			
Item Calibrated	Value	Tolerance	Actual
Bore (mm)	2.095	± 0.005	2.091
Diameter (mm)	9.474	± 0.025	9.480
Length (mm)	8.000	± 0.0250	8.018
Roughness by Comparison		≤ 0.25µm	0.05

Test Die Method C			
Item Calibrated	Value	Tolerance	Actual
Bore (mm)	1.050	± 0.0050	
Diameter (mm)	9.474	± 0.0070	
Length (mm)	4.000	± 0.0250	
Roughness by Comparison		≤ 0.25µm	

Piston with Brass Guide including 0.325 kg Test Weight			
Item Calibrated	Value	Tolerance	Actual
Weight (kg)	0.325	± 0.0016	0.3243
Tip Diameter (mm)	9.474	± 0.0070	9.4678
Tip Length (mm)	6.3500	± 0.1000	6.3754

Test Weights Excluding Weight of Piston			
Item Calibrated	Value	Tolerance	Actual
1.000 kg	0.675	± 0.0033	
1.050 kg	0.725	± 0.0036	
1.200 kg	0.875	± 0.0043	
2.160 kg	1.835	± 0.0091	1.8326
3.800 kg	3.475	± 0.0173	
5.000 kg	4.675	± 0.0233	4.6669
10.000 kg	9.675	± 0.0483	
12.500 kg	12.175	± 0.0613	
21.600 kg	21.275	± 0.1063	

Timer		
Value	Tolerance	Actual
15 Minutes	± 0.07 %	**15:00:94**

Encoder		
Value	Tolerance	Actual
25.4(mm)	± 0.100	**25.481**

RAY-*RAN* TEST EQUIPMENT LTD

Temperature Profile

Temperature at 10mm above Test Die		
Temperature °C	**Tolerance**	**Actual**
125	± 2.0	124.0
150	± 2.0	149.6
200	± 2.0	200.5
250	± 2.0	251.6
300	± 2.5	301.6
Temperature at 30mm above Test Die		
Temperature °C	**Tolerance**	**Actual**
125	± 2.0	124.0
150	± 2.0	149.5
200	± 2.0	200.3
250	± 2.0	251.5
300	± 2.5	301.9
Temperature at 50mm above Test Die		
Temperature °C	**Tolerance**	**Actual**
125	± 2.0	123.5
150	± 2.0	148.8
200	± 2.0	199.6
250	± 2.0	250.4
300	± 2.5	300.8
Temperature at 70mm above Test Die		
Temperature °C	**Tolerance**	**Actual**
125	± 2.0	123.1
150	± 2.0	148.2
200	± 2.0	198.6
250	± 2.0	249.1
300	± 2.5	297.6

See profile graph

Max Deviation of Temperature at 10mm above Test Die			
Temperature °C	**Tolerance °C**	**Time (mins)**	**Max Deviation °C**
125.00	± 1.0	10	0.0
150.00	± 1.0	10	0.0
200.00	± 1.0	10	0.1
250.00	± 1.0	10	0.2
300.00	± 1.0	10	0.1

See profile graph